Mitteilungen aus dem Institut für Mechanik

Christoph Müller

Thermodynamic modeling of polycrystalline shape memory alloys at finite strains

Heft Nr. 132

RUHR-UNIVERSITÄT BOCHUM

INSTITUT FÜR MECHANIK
RUHR-UNIVERSITÄT BOCHUM

Christoph Müller

Thermodynamic modeling of polycrystalline shape memory alloys at finite strains

MITTEILUNGEN AUS DEM INSTITUT FÜR MECHANIK NR. 132

August 2003

Herausgeber:

Institut für Mechanik
Ruhr-Universität Bochum
D-44780 Bochum

ISBN 3-935892-07-1

Printed in Germany

Zusammenfassung

In dieser Arbeit wird ein thermodynamisch konsistentes Modell zur Beschreibung pseudoelastischer Formgedächtnislegierungen vorgestellt.
Zur Beschreibung der Kinematik wird auf eine Eulersche Theorie endlicher Formänderungen zurückgegriffen. Der thermomechanische Zustand wird im Rahmen der Thermodynamik mit internen Zustandsvariablen anhand des Massengehaltes der martensitischen Phase als interner Zustandsvariable beschrieben. Die freie Helmholtz Energie wird als Funktion des elastischen Anteils der Hencky Dehnung, der Temperatur und des Martensitgehalts formuliert. Aus diesem Potential wird eine Evolutionsgleichung für den Martensitgehalt abgeleitet. Die während der Phasentransformation erzeugte Wärme schlägt sich infolge der thermomechanischen Kopplung unmittelbar im modellierten Materialverhalten nieder. Das Materialmodell kann um die Beschreibung von Ein- und Zweiwegeffekten sowie funktionaler Ermüdung erweitert werden.
Das Stoffgesetz ist zu Finite-Element Berechnungen im Rahmen einer Updated Lagrange Formulierung geeignet. Die Parameter des Modells werden anhand von Daten aus isothermen Versuchen identifiziert und durch thermische Parameter aus der Literatur ergänzt. Berechnungen mit dem implementierten Stoffgesetz auf Basis dieses Parametersatzes verdeutlichen den Einfluss der thermomechanischen Kopplung und zeigen die Eignung des Stoffgesetzes zur Analyse komplexer Bauteile aus Formgedächtnislegierungen.

Summary

In this treatise, a thermodynamically consistent material model for pseudoelastic shape memory alloys is proposed.
The kinematics are described based on a self-consistent Eulerian theory of finite deformations. Adopting a thermodynamic theory with internal state variables, the thermomechanical state is described choosing the mass fraction of martensite as internal state variable. The Helmholtz free energy is formulated as a function of elastic Hencky strain, temperature and mass fraction of martensite. A kinetic law governing the evolution of martensite is derived from this potential. Due to the thermomechanical coupling, the heat generated during phase transformation directly affects the material behavior modeled. The proposed material law may be extended to include additional effects such as one- and two-way shape memory effects and functional fatigue.
The material law is used in finite element analyses in an updated Lagrangian scheme. Its parameters are calibrated to isothermal experimental data. They are complemented by thermal parameters published in the literature. Calculations using the implemented material law based on this parameter set demonstrate the effects of the thermomechanical coupling and the suitability of the model to analyze complex shape memory structures.

"I do not know what I may appear to the world, but to myself I seem to have been only like a boy playing on the seashore, and diverting myself in now and then finding a smoother pebble or a prettier shell than ordinary, whilst the great ocean of truth lay all undiscovered before me."

Isaac Newton (Brewster 1965, S. 407).

Vorwort

Die vorliegende Arbeit entstand während meiner Tätigkeit als wissenschaftlicher Mitarbeiter am Institut für Mechanik der Ruhr-Universität Bochum. Sie wurde im Rahmen des Sonderforschungsbereiches 459 Formgedächtnistechnik von der Deutschen Forschungsgemeinschaft gefördert und von der Fakultät für Maschinenbau der Ruhr-Universität Bochum als Dissertation angenommen.

Mein Dank gilt Herrn Prof. Dr.-Ing. Otto T. Bruhns, der mir neben der Anregung zu dieser Arbeit und seiner Unterstützung bei ihrer Anfertigung den Freiraum für mein Zusatzstudium der Wirtschaftswissenschaft gab. Herrn Prof. Dr.-Ing. Gunther Eggeler danke ich für sein Interesse und für die Übernahme des Koreferates.

Bei allen Mitarbeitern des Lehrstuhls für Technische Mechanik möchte ich mich für die angenehme und freundliche Arbeitsatmosphäre bedanken. Von zahlreichen Diskussionen mit Herrn Dr.-Ing. Claus Oberste-Brandenburg und Herrn Dr.-Ing. Ndzi C. Bongmba sowie mit Prof. Bogdan Raniecki, Ph. D., D. Sc. am Institute of Fundamental Technological Research in Warschau habe ich sehr profitiert.

Schließlich danke ich meiner Familie für ihre Unterstützung und ihren Zuspruch.

Bochum, im August 2003 Christoph Müller

Referenten: Prof. Dr.-Ing. Otto T. Bruhns
Prof. Dr.-Ing. Gunther Eggeler

Tag der Einreichung: 03.06.2003
Tag der mündlichen Prüfung: 15.08.2003

Contents

List of Figures

List of Tables

Conventions and Notations

Scalars (italics)

A	Area
$A_s^{(\cdot)}$	Austenite start temperature
$A_f^{(\cdot)}$	Austenite finish temperature
B	Body
c_p	Specific heat at constant pressure
c_v	Specific heat at constant volume
D	Dissipation
da	Area element in the current configuration
dA	Area element in the reference configuration
dm	Mass element
$dx_{(i)}$	Component of line element in the current configuration
$dX_{(\alpha)}$	Component of line element in the reference configuration
dv	Volume element in the current configuration
dV	Volume element in the reference configuration
E	Young's modulus
f	Function for phase transformation
g	Specific Gibbs free energy
G	Shear modulus
h	Specific enthalpy
h	Spin function
h	Heat flux
h	Equivalent Hencky strain
$\dot{h}_{lat}$	Energy generation per unit volume
I, II, III	Principal invariants
I_1, I_2, I_3	Main invariants
J	Determinant of the deformation gradient
k	Thermal conductivity
k	Function for phase transformation
l	Arc length
K	Kinetic energy
m	Mass
M	Molar mass
$M_s^{(\cdot)}$	Martensite start temperature
$M_f^{(\cdot)}$	Martensite finish temperature
$M_d^{(\cdot)}$	Limiting temperature for martensitic transformation
n	Number of unique eigenvalues
P_a	External work
Q	Heat
$\bar{q}_{(\cdot)}$	Heat transfer rate
$q_{(\cdot)}$	Heat flux

r	Specific heat source, e.g. from radiation
R	Gas constant
R_m	Universal gas constant
s	Specific entropy
S	Entropy
T^0	Equilibrium temperature
t	Time
u	Specific internal energy
U	Internal energy
V	Volume
v_i	Component of velocity
w	Specific energy
W	Energy
X	Particle
x_i	Component of position in the current configuration
X_α	Component of position in the reference configuration
y	Value

Scalars (Greek characters)

α	Parameter
α	Coefficient of thermal expansion
α	Scalar in the current configuration
$\hat{\alpha}$	Scalar in the reference configuration
γ	Shear
$\dot{\gamma}$	Rate of entropy production
δ_{ij}	Kronecker symbol
η	Amplitude of pseudoelastic flow
η	Entropy due to structural rearrangement
Θ	Absolute temperature
Θ_0	Reference temperature
Θ_D	Debye temperature
κ	Bulk modulus
λ	Lamé constant
λ	Eigenvalue
μ	Lamé constant
ν	Poisson's ratio
ξ	Mass fraction of martensite
π_0^f	Phase chemical potential
π^f	Thermodynamic driving force
ρ	Current density
ρ_0	Referential density
Σ	Complementary hyperelastic potential
τ	Equivalent Kirchhoff stress

φ	Angle
χ	Eigenvalue
ψ	Specific Helmholtz free energy
ψ_{it}	Free energy of interaction

Vectors (boldface roman)

$\mathbf{a}$	Acceleration
$\mathbf{b}$	Force per volume in the current configuration
$\mathbf{b}_0$	Force per volume in the reference configuration
$\mathbf{dx}$	Line element in the current configuration
$\mathbf{dX}$	Line element in the reference configuration
$\mathbf{da}$	Area element in the current configuration
$\mathbf{dA}$	Area element in the reference configuration
$\mathbf{dl}$	Force element in the current configuration
$\mathbf{dL}$	Force element in the reference configuration
$\mathbf{e}_i$	Unit vector in the current configuration
$\mathbf{E}_\alpha$	Unit vector in the reference configuration
$\mathbf{J}$	Generalized irreversible flux
$\mathbf{n}$	Normal vector in the current configuration
$\mathbf{N}$	Normal vector in the reference configuration
$\mathbf{o}$	Origin in the current configuration
$\mathbf{O}$	Origin in the reference configuration
$\mathbf{q}$	Heat flow in the current configuration
$\mathbf{Q}$	Heat flow in the reference configuration
$\mathbf{t}$	Traction
$\mathbf{u}$	Displacement
$\mathbf{v}$	Velocity
$\mathbf{x}$	Parameter vector
$\mathbf{x}$	Position in the current configuration
$\mathbf{X}$	Position in the reference configuration
$\mathbf{X}$	Generalized irreversible force

Vectors (Greek characters)

$\boldsymbol{\alpha}$	Vector in the current configuration
$\hat{\boldsymbol{\alpha}}$	Vector in the reference configuration
$\boldsymbol{\eta}$	Virtual velocity field in the current configuration
$\boldsymbol{\eta}_0$	Virtual velocity field in the reference configuration
$\boldsymbol{\chi}$	Position vector
$\boldsymbol{\chi}$	Motion
$\boldsymbol{\chi}$	Current configuration
$\boldsymbol{\chi}_0$	Reference configuration
$\boldsymbol{\omega}$	Angular velocity

Second order tensors (boldface roman)

$\mathbf{1}$	Unit tensor
$\mathbf{a}$	Internal variables in the current configuration
$\mathbf{A}$	Internal variables in the reference configuration
$\mathbf{A}$	Eulerian tensor
$\tilde{\mathbf{A}}$	Two-point tensor
$\hat{\mathbf{A}}$	Lagrangian tensor
$\mathbf{B}$	Left Cauchy Green tensor
$\mathbf{B}_\sigma$	Eigenprojection of the left Cauchy Green tensor
$\mathbf{C}$	Right Cauchy Green tensor
$\mathbf{C}_\sigma$	Eigenprojection of the right Cauchy Green tensor
$\mathbf{D}$	Stretching tensor
$\mathbf{e}$	Euler-Almansi strain tensor
$\mathbf{E}$	Green-Lagrange strain tensor
$\mathbf{e}^{(m)}$	Eulerian strain tensor
$\mathbf{E}^{(m)}$	Lagrangian strain tensor
$\mathbf{F}$	Deformation gradient
$\mathbf{f}$	Relative deformation gradient
$\mathbf{h}$	Hencky strain in the current configuration
$\overset{\circ}{\mathbf{h}}^{\mathrm{Log}}$	Logarithmic rate of the Hencky strain tensor
$\mathbf{H}$	Hencky strain in the reference configuration
$\mathbf{L}$	Velocity gradient
$\mathbf{N}$	Spin
$\mathbf{P}$	Nominal stress tensor
$\mathbf{Q}$	Rotation tensor
$\mathbf{R}$	Rotation tensor (polar decomposition)
$\mathbf{R}^{\mathrm{Log}}$	Logarithmic rotation tensor
$\mathbf{r}^{\mathrm{Log}}$	Relative logarithmic rotation tensor
$\mathbf{S}$	Second Piola Kirchhoff stress tensor
$\mathbf{T}$	First Piola Kirchhoff stress tensor
$\mathbf{t}^{(m)}$	Eulerian stress tensor
$\mathbf{T}^{(m)}$	Lagrangian stress tensor
$\mathbf{U}$	Right stretching tensor
$\mathbf{V}$	Left stretching tensor
$\mathbf{W}$	Vorticity tensor

Second order tensors (Greek characters)

$\boldsymbol{\alpha}_0$	Tensor of thermal expansion coefficients
$\boldsymbol{\beta}_0$	Tensor of thermal expansion coefficients
$\boldsymbol{\varepsilon}$	Linearized (engineering) strain
$\boldsymbol{\kappa}$	Phase distortion
$\boldsymbol{\Lambda}$	Lagrange multiplier

$\boldsymbol{\sigma}$	Cauchy stress tensor
$\boldsymbol{\tau}$	Kirchhoff stress tensor
$\boldsymbol{\varphi}$	Quantity in the current configuration
$\boldsymbol{\Phi}$	Quantity in the reference configuration
$\boldsymbol{\Omega}$	Spin tensor
$\boldsymbol{\Omega}^{\mathrm{Log}}$	Logarithmic spin tensor

Fourth order tensors (boldface roman)

$\mathbb{B}$, $\mathbb{G}$, $\mathbb{X}$	Tensors associated with the logarithmic rate
$\mathbb{C}$	Tensor of elastic moduli
$\mathbb{D}$	Elastic compliance tensor
$\mathbb{I}$	Symmetric fourth order unit tensor

Other symbols

$\mathcal{B}$	Current configuration
$\bar{\mathcal{B}}$	Intermediate configuration
$\mathcal{B}_0$	Reference configuration
$\partial\mathcal{B}$	Surface in the current configuration
$\partial\mathcal{B}_0$	Surface in the reference configuration
$\partial_u\mathcal{B}$	Surface in the current configuration, displacements prescribed
$\partial_\sigma\mathcal{B}$	Surface in the current configuration, stresses prescribed
$\partial_v\mathcal{B}$	Surface in the current configuration, velocity prescribed
$\partial_u\mathcal{B}_0$	Surface in the reference configuration, displacements prescribed
$\partial_\sigma\mathcal{B}_0$	Surface in the reference configuration, stresses prescribed
$\partial_v\mathcal{B}_0$	Surface in the reference configuration, velocity prescribed
Δ	Increment
Δt	Time increment
$\mathrm{D}_{\mathbf{x}}$	Domain of parameter sets
$\mathbb{E}$	Euclidean vector space
$\mathcal{E}$	Euclidean point space
$\mathbb{N}$	Set of natural numbers
$\mathcal{O}$	Observer
$\mathbb{R}$	Set of real numbers
$\delta\mathbf{u}$	Virtual displacement

Special symbols & functions

$A \rightarrow M$	Austenite-Martensite transformation
$M \rightarrow A$	Martensite-Austenite transformation
$\mathcal{L}$	Lagrange functional
$D(\cdot)$	Debye function
$\nabla \cdot (\cdot)$	Divergence with respect to $\mathbf{x}$
$\nabla_0 \cdot (\cdot)$	Divergence with respect to $\mathbf{X}$

∇	Gradient with respect to $\mathbf{x}$
∇_0	Gradient with respect to $\mathbf{X}$
$f(\cdot)$	Scalar function
$g(\cdot)$	Scalar function
$\mathrm{skw}(\cdot)$	Skewsymmetric part of a tensor
$\mathrm{sym}(\cdot)$	Symmetric part of a tensor
$\mathrm{tr}\,(\cdot)$	Trace of a tensor
$(\cdot)^{\mathrm{T}}$	Transpose
$(\cdot)^{-1}$	Inverse
$\cdot$	Scalar product
:	Double contraction
$\star$	Rayleigh product
$\times$	Vector product
$\otimes$	Dyadic product
$\|\|(\cdot)\|\|$	Norm of a vector
$\dot{(\cdot)}$	Material time derivative
$(\cdot)'$	Derivative of $(\cdot)$
$\overset{\circ}{(\cdot)}^{*}$	Corotational time rate
$\overset{\circ}{(\cdot)}^{\mathrm{J}}$	Zaremba Jaumann time rate
$\overset{\circ}{(\cdot)}^{\mathrm{L}}$	Lie derivative
$\overset{\circ}{(\cdot)}^{\mathrm{Log}}$	Logarithmic time rate
$\overset{\circ}{(\cdot)}^{\mathrm{R}}$	Polar/Green-Naghdi time rate

Superscripts

$(\cdot)^{c}$	Consistent
$(\cdot)^{e}$	Elastic
$(\cdot)^{ei}$	Coupled elastic-inelastic
$(\cdot)^{etr}$	Coupled elastic-phase transformation
$(\cdot)^{geo}$	Geometric
$(\cdot)^{i}$	Inelastic
$(\cdot)^{mat}$	Material
$(\cdot)^{th}$	Thermal
$(\cdot)^{tr}$	Phase transformation
$(\cdot)^{\mathrm{Log}}$	Logarithmic
$(\cdot)^{A}$	Austenitic
$(\cdot)^{M}$	Martensitic
$(\cdot)^{A\rightarrow M}$	Austenite-Martensite transformation
$(\cdot)^{M\rightarrow A}$	Martensite-Austenite transformation
$(\cdot)^{\alpha}$	Phase specific
$(\cdot)^{*}$	Transformed

Subscripts

$(\cdot)_0$	Quantity associated with reference configuration
$(\cdot)_n$	Beginning of increment
$(\cdot)_{n+1}$	End of increment
$(\cdot)_{diss}$	Dissipated
$(\cdot)_{irr}$	Irreversible
$(\cdot)_{mech}$	Internal structure
$(\cdot)_{rev}$	Reversible
$(\cdot)_{st}$	Structural/Stored
$(\cdot)_{th}$	Thermal

1 Introduction

1.1 Introduction to shape memory alloys

Shape memory alloys are used in many applications, especially medical, where their use is superior to using conventional materials. The term *shape memory* refers to the ability of this class of materials to "remember" a shape assumed earlier, even after being deformed rather severely.
When a shape memory alloy is subjected to deformation at low temperature, where the material is in its martensitic state, the deformation is retained until the specimen is heated above a certain temperature, at which it will spontaneously return to its original shape prior to deformation. This effect is referred to as *shape memory effect.*
At more elevated temperatures, the material behavior changes to so-called *superelasticity*[1]. Characteristic for superelastic alloys is a hysteretic stress-strain response, where the original shape is recovered completely during unloading from the deformed state. The width of the hysteresis and the stress level at which it occurs depend on many parameters, such as the composition of the respective shape memory alloy, its thermomechanical treatment, temperature etc.
By subjecting shape memory alloys to external loads or to internal stresses, e.g. by introducing dislocations, the so-called *two-way shape memory effect* may be observed. Here, shape changes are observed by simply heating or cooling a specimen.
Today, shape memory alloys are chosen as couplings for aircraft hydraulic tubing because they are lightweight, easy to install and have a proven reliability. In this area, use is made of the one-way effect (Stöckel 1993, Melton 1998). Also, shape memory alloys are used as electrical connectors. Currently, several different designs compete on the market.
Applications of superelasticity are mostly in the medical industry, but they also include support wires in bras — the first widespread non-medical use of superelasticity, wires affixed to the heel of shoes to retain their shape, head bands of headphones, superelastic NiTi eyeglass frames, etc. In dental applications, orthodontic arch wires exhibiting superelastic behavior are superior to conventional materials as they supply a constant stress in a wide range of strains. Other applications are dental implants and attachments for partial dentures. In orthopedics, bone plates are attached with screws to secure bones, giving a compressive force on the fracture zones. U-shaped staples perform well in the same task (cf. Miyazaki 1998). However, while corrosion resistance of (NiTi) shape memory alloys is very good, biocompatibility is still an issue. For more than 20 years, Nitinol stents have been used in coronary, peripheral vascular and non-vascular applications. Today, many different designs are on

[1] The terminologies *pseudoelasticity*, *superelasticity* and *rubber-like behavior* are often used in an inconsistent manner, see Section 2.1.1 for a definition.

the market. Using shape memory alloys, self expanding stents can be designed that are delivered more easily. Some current stent designs are illustrated in Figure 1.1 (cf. Memry 2003).

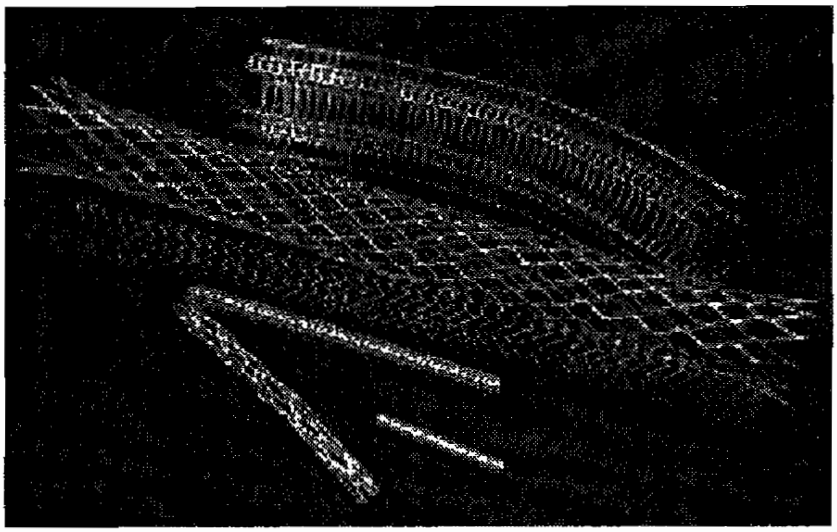

Figure 1.1: Stent designs

1.2 Motivation

In this treatise, a model for pseudoelastic or more precisely superelastic shape memory behavior is proposed, adopting the notions underlying an existing theory. To date, no thermodynamic theory for shape memory alloys within a self-consistent Eulerian scheme of finite deformations has been proposed, in spite of the large deformations observed in shape memory alloys and elaborate theories of kinematics available today.

Considering the applications presented in the previous section, there is demand for a three dimensional model of pseudoelastic material behavior. While applications such as orthodontic arch wires may be designed and simulated using one-dimensional models, the complex stress states in medical stents clearly require three-dimensional theories. In order to be employed as a simulation device, such a theory has to be adaptable to numerical solution procedures such as the finite element method. As the strains observed in shape memory alloys are in the range of 10 % for polycrystals (cf. Gadaj et al. 1999, Shaw 2000), a large deformation scheme should be used.

It has been established experimentally that phase transformation to martensite is a thermomechanically coupled process, with latent heat being generated during transformation to martensite. At the same time, the material behavior is strongly dependent on temperature. A model of shape memory alloys should account for that. For obvious reasons, the theory should be motivated by micromechanical observations to actually model physical effects. It should

be able to account for complex loading paths as well.
Hence, the task is as follows: Based on an evaluation of existing models, within a kinematically consistent framework of finite deformations a thermodynamically consistent model for pseudoelasticity is to be found. The model has to account for the thermomechanical coupling and is to be implemented into a finite element code. The formulation should be readily extendable to include additional effects such as one-way shape memory effect and tension-compression asymmetry at a later stage.

1.3 Outline

This dissertation is structured into eight chapters. Subsequent to this preface the properties of shape memory alloys and theories to their description are examined in detail. Micromechanical explanations for the behavior observed on the macroscale are given as modeling of shape memory alloys from a phenomenological point of view has to be motivated on physical grounds. For reference, literature covering a range of different experimental observations on shape memory alloys is cited.
Existing models describing shape memory alloy behavior may be categorized according to the technique applied. Theories representative of each class are presented and compared with regard to some features considered to be important here. Based on this discussion, the approach to modeling followed in this dissertation is outlined and justified.
In Chapter 3, the kinematical frame to be used is defined. Thorough derivations of the measures of deformation and strain needed give rise to the definition of objective rates, suitable for the formulation of material laws in a Eulerian frame.
Complementary to these kinematical considerations is the subsequent presentation of conservation equations and stress measures in Eulerian and Lagrangian formulations. Based on the definition of stress measures associated with both current and reference configurations, the stress power is derived. Subsequently, objective stress rates are introduced which may be used in the development of constitutive equations. Hill's notion of work conjugacy is introduced next. An extension of this concept to Eulerian quantities proposed by Xiao et al. (1998b) is used to define stresses and strains that form work conjugate pairs. This provides the foundation of the thermodynamical considerations in Chapter 5. However, first the weak form of the balance of momentum equation is formulated in rate form with regard to a subsequent numerical simulation.
The framework for phenomenological modeling is completed by defining the thermodynamic theory to be employed. Here, a theory with internal state variables is established based on a thermodynamic conjugate pair of stress and strain. The number and type of internal state variables is specified in Chap-

ter 6. In fact, criteria for thermodynamic consistency and thermomechanical coupling are derived for arbitrary sets of scalar or tensorial state variables.
Having elaborated the foundations to the constitutive theory, one of the models presented in Section 2.2, i.e. the R_L-model proposed by Raniecki et al. (1992), is reformulated on the grounds of a Eulerian theory based on the logarithmic rate, carefully choosing thermodynamically independent variables of state. First, a complementary hyperelastic potential for the elastic material response is defined. In order to describe the behavior of a solid in a two-phase state of constrained equilibrium, the Helmholtz free energy of the individual phases is derived. An averaging procedure based on the single internal variable of the model, the mass fraction of martensite, yields the Helmholtz free energy of the two-phase system, amended by a term accounting for the internal interaction in constrained equilibria. Adopting the concept of irreversible forces, the evolution of the thermodynamic driving force and subsequently a kinetic law for the mass fraction of martensite are obtained. The chapter is concluded by specifying the independent parameters of the model that need to be calibrated to experimental data for simulations. To this end, an isotropic material symmetry is proposed. By incorporating Fourier's law, the formulation of the model is concluded.
One of the objectives giving rise to the considerations in this treatise is the lack of a three-dimensional comprehensive theory readily adaptable to finite element methods. In Chapter 7, the implementation of the model into a finite element code is discussed. Care is exercised to retain objectivity during integration. The model is calibrated to experimental data. One-dimensional calculations in tension and simple shear are presented to characterize the material behavior predicted by the model. Finally, the model is successfully applied to the finite element simulation of fairly complex structures.
The dissertation is concluded by a summary of the treatise. Some remarks concerning possible modifications of the model to account for shape memory effects other than pseudoelasticity are given.

1.4 Mathematical notations

In addition to the conventions and notations defined on pages vi to xii, some mathematical notations of importance to the subsequent modeling are summarized here.
Tensor components are defined with respect to an orthogonal Cartesian coordinate system. The symmetric unit tensor of second order is given as

$$\mathbf{1} = \delta_{ij}\mathbf{e}_i \otimes \mathbf{e}_j \,, \tag{1.1}$$

while the symmetric unit tensor of fourth order has the form

$$\mathbb{I} = \frac{1}{2}\left(\delta_{im}\delta_{jn} + \delta_{in}\delta_{mj}\right)\mathbf{e}_i \otimes \mathbf{e}_j \otimes \mathbf{e}_m \otimes \mathbf{e}_n \,. \tag{1.2}$$

Contraction operations are defined by

$$\begin{aligned} \mathbf{a} \otimes \mathbf{b} &= a_i b_j \mathbf{e}_i \otimes \mathbf{e}_j \\ \mathbf{a} \cdot \mathbf{b} &= a_i b_i \\ \mathbf{AB} &= A_{ij} B_{jk} \mathbf{e}_i \otimes \mathbf{e}_k \\ \mathbf{A} : \mathbf{B} &= A_{ij} B_{ij} \end{aligned} \tag{1.3}$$

for $i, j, k = 1, 2, 3$. For trace, transpose, deviator and inverse, the following definitions hold

$$\begin{aligned} \mathrm{tr}\,(\mathbf{A}) &= A_{ii} \\ (\mathbf{A}^{\mathrm{T}})_{ij} &= A_{ji} \\ \mathrm{tr}\left(\mathbf{A}\mathbf{B}^{\mathrm{T}}\right) &= \mathbf{A} : \mathbf{B} \\ \mathbf{A}' &= \mathbf{A} - \frac{1}{3}\,\mathrm{tr}\,(\mathbf{A})\mathbf{1} \\ \mathbf{A}\mathbf{A}^{-1} &= \mathbf{1} \\ A_{ik} A_{kj}^{-1} &= \delta_{ij} = \begin{cases} 1 & i = j \\ 0 & i \neq j\,. \end{cases} \end{aligned} \tag{1.4}$$

For rotation tensors $\mathbf{Q}$ and $\mathbf{R}$ obeying

$$\mathbf{Q}\mathbf{Q}^{\mathrm{T}} = \mathbf{1} \qquad \det\mathbf{Q} = 1 \tag{1.5}$$

the *Rayleigh* product is defined by

$$\begin{aligned} \mathbf{Q} \star \boldsymbol{\alpha} &= \mathbf{Q}\boldsymbol{\alpha} \\ \mathbf{Q} \star \mathbf{A} &= \mathbf{Q}\mathbf{A}\mathbf{Q}^{\mathrm{T}} \\ (\mathbf{Q} \star \mathbb{H})_{ijkl} &= Q_{ip} Q_{jq} Q_{kr} Q_{ls} \mathbb{H}_{pqrs} \end{aligned} \tag{1.6}$$

for $i, j, k, \ldots = 1, 2, 3$. The following rules hold

$$\begin{aligned} \mathbf{Q} \star (\mathbb{H} : \mathbf{A}) &= (\mathbf{Q} \star \mathbb{H}) : (\mathbf{Q} \star \mathbf{A}) \\ \mathbf{Q} \star (\mathbf{R} \star \mathbf{A}) &= (\mathbf{Q}\mathbf{R}) \star \mathbf{A} \\ (\mathbf{Q} \star \mathbf{A}) : (\mathbf{Q} \star \mathbf{B}) &= \mathbf{A} : \mathbf{B} \\ \mathrm{tr}\,(\mathbf{A}\mathbf{B}\mathbf{C}) &= \mathrm{tr}\,(\mathbf{C}\mathbf{A}\mathbf{B})\,. \end{aligned} \tag{1.7}$$

2 Properties and description of shape memory alloys

The phenomenological description of shape memory alloys requires some basic knowledge of the underlying crystallographic effects. Thus, in this chapter the fundamental crystallographic properties responsible for shape memory behavior are presented. Micromechanical observations substantiate the stress-strain behavior macroscopically observed.
The characterization of different shape memory alloys from various perspectives is a matter of ongoing research. In Section 2.1.3, some references are made to experimental results giving rise to the assumptions necessary in formulating material laws.
Different models proposed to date were studied in the process of establishing the material law presented in Chapter 6. Their main features are summarized below.

2.1 Shape memory effects

2.1.1 Microscopic properties

Martensitic transformations are generally *displacive* or *diffusionless* transformations, characterized by a motion of the interface between the phases in the order of magnitude of the speed of sound. They are referred to as *athermal* transformations because the transformation to or from martensite is independent of time, but only dependent on temperature. Martensitic transformation is associated with latent heat, with heat being released during the transformation to martensite. Associated with the transformation is a hysteresis, and there is a temperature range where both phases coexist (cf. Wayman & Duerig 1990).
From a crystallographic point of view two mechanisms may be identified, the Bain strain and the lattice-invariant shear. The *Bain strain*, also referred to as *lattice deformation*, is the coordinated step-wise movement of the atoms of an initially austenitic structure, leading to a deformed martensitic structure. Depending on the alloy under consideration, there is a small volumetric change of about $-0.2\,\%$ to $-0.5\,\%$ during phase transformation from austenite to martensite (cf. Funakubo 1984).
The *lattice-invariant shear* is an accommodation step. While the shape of the martensitic structure produced by the Bain strain differs from the original shape, here the shape of the transformed structure is accommodated to its surroundings. Such an accommodation is possible either by irreversible *slip*, which can accommodate both volumetric and shape changes, or by *twinning*. Twinning is the dominant accommodation process in shape memory alloys as it can accommodate shape changes in a reversible way. The number of directions or *variants* required to restore the original shape of the matrix depends on the shape memory alloy.

Twin boundaries are of a very low energy and they are quite mobile. Under an applied stress, the twin boundaries, i.e. the boundaries between martensite plates as well as the boundaries within plates, will move to a resultant shape better accommodating the stress. The process of orientation due to the condensation of many twin variants into a single favored variant is called *detwinning.*

Shape memory alloys are frequently characterized by their *transformation temperatures.* These temperatures, usually denoted by M_s, M_f, A_s and A_f refer to the temperature at which the temperature induced transformation to martensite respectively austenite starts and finishes. As these transformation temperatures differ, a *hysteresis* of alloy-dependent width is associated with martensitic transformations. The notion of friction associated with the movement of twin-boundaries is often employed to explain the hysteresis.

Below M_f, temperature induced martensite is in a self-accommodated state. Application of an external load results in detwinning by lattice-invariant shear. Upon unloading, the stress-induced martensite is relaxed elastically without shape recovery. The remaining strain is not due to slip, therefore this effect is called *pseudoplasticity* or *one-way shape memory effect*, see Figure 2.1 (after Helm 2001). The remaining deformation may be removed by heating the specimen to a temperature above A_f. During this process, the oriented, stress-induced martensite transforms to austenite, hence the original shape is recovered. Subsequent cooling below the M_f temperature is associated with the formation of martensite twins, leading to both the original shape and the original crystallographic structure.

If the transformation back to martensite is prevented, either by application of external loads or by internal stresses, e.g. due to dislocations, the microstructure will change between austenite and martensite when the body is subjected to temperatures varying between M_f and A_f. This leads to shape changes due to variations in temperature only. This effect is called *two-way shape memory effect.*

If the specimen is loaded in its austenitic phase, stress-induced transformation to martensite sets in at a certain level of stress. The resulting oriented martensite is associated with significant strains, but may be completely recovered upon unloading. Therefore, such material behavior is called *superelasticity.* It must be distinguished between the terminologies *pseudoelasticity*, *superelasticity* and *rubber-like behavior.* Here, the definition given by Otsuka & Wayman (1998b) is adopted. When an apparently plastic deformation recovers by isothermal unloading, i.e. a closed hysteresis in stress-strain space is observed, the behavior is called *pseudoelasticity*, regardless of the origin of this behavior. The term pseudoelasticity comprises both superelasticity and rubber-like behavior. *Superelasticity* is characterized by a closed loop stress-strain curve due to stress-induced martensitic transformation during loading and reverse transformation during unloading. On the other hand, the latter

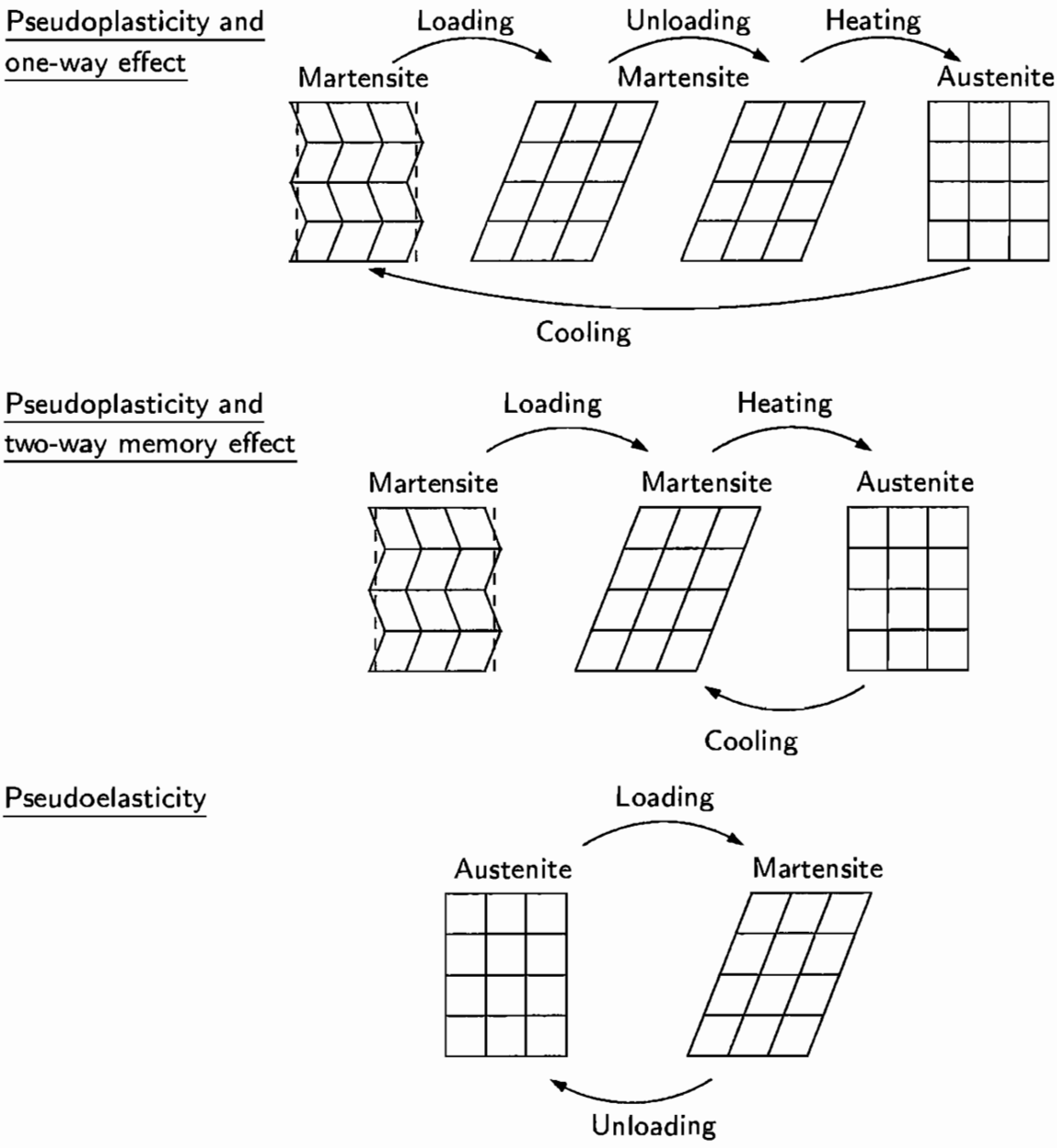

Figure 2.1: Shape memory effects

terminology, i.e. *rubber-like behavior*, refers to hysteretic behavior due to reversible movement of twin boundaries in the martensitic state. See Otsuka & Wayman (1998a) for a further discussion of microscopic properties.

2.1.2 Macroscopic properties

Macroscopically, the microscopic effects result in stress-strain responses which strongly depend on temperature. In Figure 2.2, the material response at temperatures above M_d, above A_f but below M_d and below M_f is depicted (see also 2.3). In the first case the material behavior is plastic because the energetic

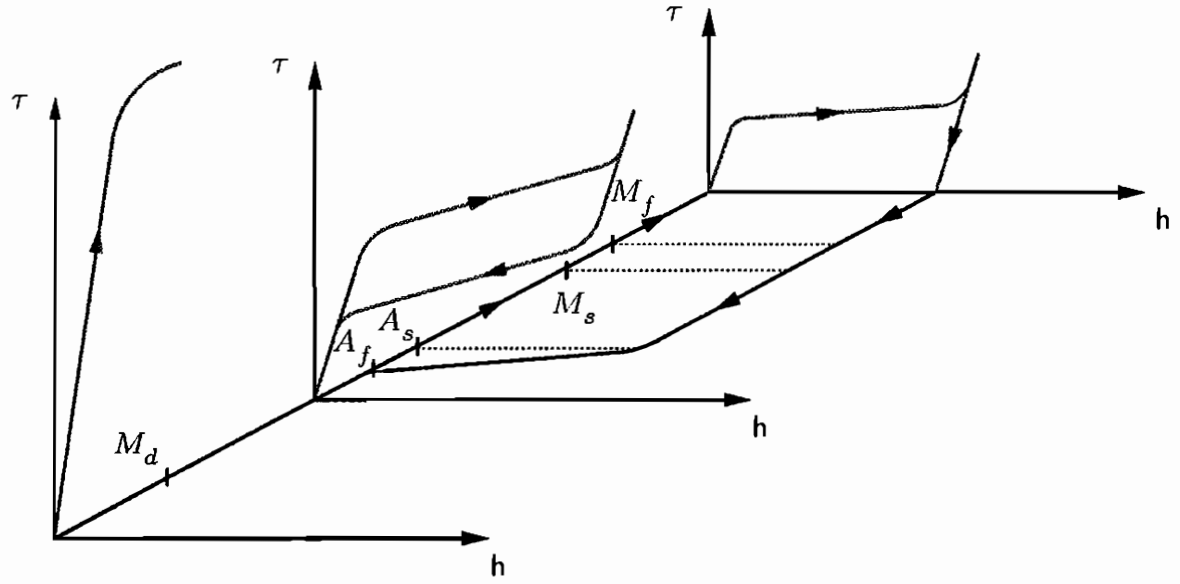

Figure 2.2: Plastic austenite, pseudoelasticity, shape memory effect (front to rear)

barrier to form martensite is so high at elevated temperatures that plastic slip occurs before stress-induced transformation sets in (cf. Hornbogen 1987).
Closer to the A_f-temperature, a pseudoelastic stress-strain hysteresis is observed. With varying temperature, this hysteresis may change its position, width and height (cf. Funakubo 1984). This is the temperature range under consideration here. Upon conclusion of the phase transformation, the material response is again elastic due to elastic deformation of stress-induced, oriented martensite.
Below M_f, one-way shape memory behavior is observed. Here, temperature-induced, accommodated martensite is converted into oriented martensite during deformation. There is no phase transformation involved in the process. However, in contrast to pseudoelasticity, where strains are recovered instantaneously upon unloading, the reverse transformation from oriented martensite below M_f must be initiated by heating above the A_s temperature first. As the material returns to a "remembered" previous configuration during shape recovery, the term *shape memory alloy* is motivated by the one-way effect.
Not shown in the diagram are two-way effect and rubber-like behavior. At temperatures well below M_f, rubber-like behavior due to movement of twin boundaries may be observed, leading to hysteretic behavior without phase transformation (cf. Otsuka & Wayman 1998b). Two-way shape memory effect is obtained by introducing dislocations to stabilize the configuration of martensite. The dislocations are not removed in the parent phase after reverse transformation and subsequent heating and are surrounded by a stress field which induces particular variants upon cooling. In two-way effect, contraction

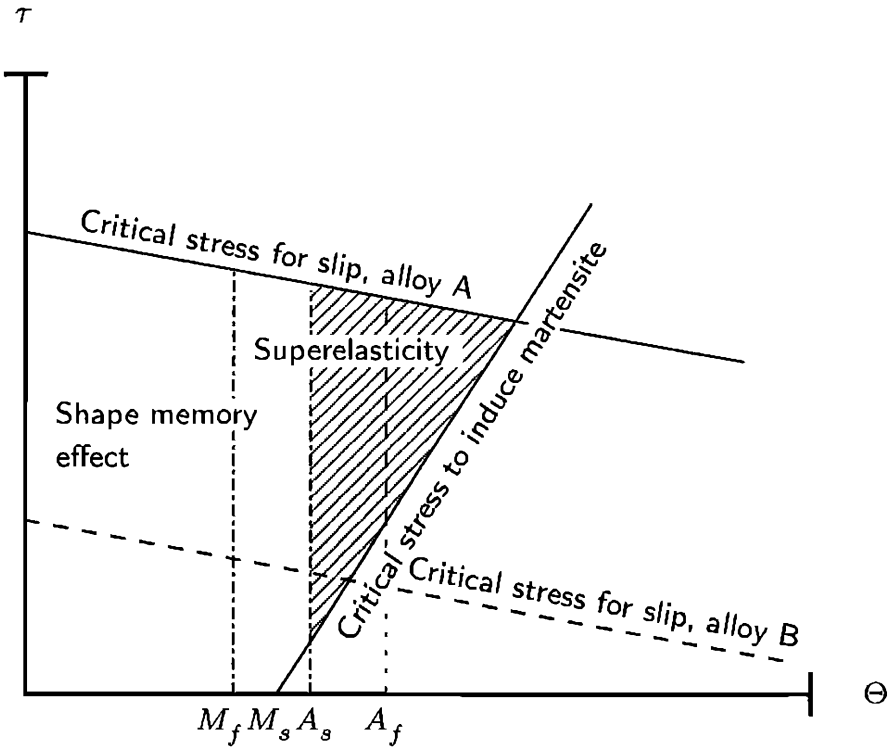

Figure 2.3: Regions of shape memory effect and superelasticity in stress temperature plane for alloys A and B

and elongation behavior can be observed when the specimen is subjected to thermal cycling. See Figure 2.3 (Otsuka & Wayman 1998b) for the different regions of shape memory effect in stress temperature plane. For alloy B, the slip stress is so low that superelasticity or shape memory effect are not permitted. These effects require that the stress must remain below the line for critical stress to avoid permanent deformation.
In TiNi shape memory alloys, the rhombohedral *R-phase* transformation occurs in a particular temperature range prior to the transformation to martensite (cf. Miyazaki & Otsuka 1986, Kawai et al. 1999). The R-phase shall not be discussed here explicitly.

2.1.3 Literature on shape memory alloys

In this section a short overview regarding the extensive literature on experimental results on shape memory behavior is given. It is by no means complete, but rather intended to provide a basis for further study and to motivate the modeling below.
A first impression of the stress strain response of NiTi at various temperatures is obtained from the work of Miyazaki et al. (1981) and Miyazaki et al. (1986), who study the effects associated with cyclic loading. Here, an evolving per-

manent set is observed.
The thermomechanical behavior of stress-induced martensitic transformation is investigated by Orgéas & Favier (1998). In their study, they observe a strong asymmetry between tension and compression. Kaack et al. (2002), Kaack (2002), Gibkes et al. (2002) study the influence of defects induced by mechanical and thermal cycling on the thermoelastic behavior of NiTi using frequency dependent photothermal radiometry. Based on this work, the temperature dependence of mechanical elasticity constants may be established.
Gadaj et al. (1999) determine the temperature evolution during tensile tests on TiNi specimens. They measure between 10 and 20 Kelvin temperature change while loading up to 4% true strain at different strain rates, which lead to different temperature evolutions. The effect of hydrostatic pressure is investigated by Kakeshita et al. (1992).
Under certain loading conditions, NiTi specimens may exhibit a macroscopic martensite band during superelastic deformation. Based on the work by Shaw & Kyriakides (1995), who study the uniaxial pseudoelastic response extensively to monitor and describe the evolution of phase boundaries, subsequent studies are conducted using flat strips (cf. Shaw & Kyriakides 1997) respectively microtubes (cf. Li & Sun 2002). It is observed that under combined tension and torsion the homogeneous torsional phase transformation is superposed by the initiation and growth of a macroscopic spiral martensite band appearing under tension. In this respect, a size effect is noticeable (cf. Sun et al. 2001).
The hysteretic behavior of NiTi is studied by Lin et al. (1994) and Tanaka et al. (1995a), who obtain results contradictory to those obtained by Müller & Xu (1991), Huo & Müller (1993) on a CuAlZn specimen. Evidently, the initiation of phase transformation within the bounding loop is not governed by a diagonal in NiTi as is the case for CuAlZn (see also the discussion of Müller & Xu 1991 below).
Phase transformation of SMAs is approximately isotropic. Orgéas & Favier (1998) study the isothermal behavior of stress induced martensitic transformations in an equiatomic NiTi alloy. Their shear specimens exhibit completely isotropic behavior both during initial loading, which is stress-induced martensitic transformation, and during subsequent cycling, which is a martensite reorientation process as they conduct their experiments below the A_f-temperature. Sittner & Novák (2000) arrive at the same conclusion by employing a constant stress averaging approach to model polycrystalline SMAs. Their calculations are based on experimental data obtained on CuAlNi single crystals.

2.2 Modeling of shape memory alloys

Common approaches to modeling of shape memory alloys may be classified according to the applied technique, differentiating between

- theories based on statistical mechanics
- models based on Landau theory
- micromechanical models and
- phenomenological theories.

Some concepts developed within these categories are presented below. As the focus is on phenomenological theories here, no in-depth discussion of other techniques but rather a general overview is given. Theories of particular interest to the phenomenological modeling in Chapter 6 are described in more detail.

2.2.1 Statistical mechanics

Within the framework of statistical mechanics, it is postulated that the rate of transformation between constituents is proportional to the net probability that one phase will overcome the energetic barrier required to transform to a second phase. Several theories have been established on these grounds to characterize and model the behavior of shape memory alloys.
A very popular model is proposed by Achenbach and Müller (see Achenbach 1989 and the references therein). They consider a lattice body which may be austenitic or in one of two martensitic configurations. The energetic state of the system depends on temperature, the load applied, and on the interfacial energy. The latter is a function of the number of interfaces. By means of statistical mechanics the free energy at equilibrium and constitutive equations are obtained.
Based on this model, Seelecke studies the torsional vibration of a shape memory wire by subjecting a rigid mass suspended by the wire to a rotational motion (cf. Seelecke 1997). As the wire behaves as a torsion spring, the mass oscillates, its motion being damped by the dissipation of energy during martensitic transformation. Since this effect is temperature dependent, the system may be actively controlled by heating of the wire. Similar experiments by Seelecke (2002) using a tubular specimen lead to an amended version of the model to study the damping behavior. In Govindjee & Hall (2000), computational aspects regarding the implementation of the model by Achenbach (1989) are considered. Numerical simulations on a structural system yield realistic and promising results.
The notions introduced by Müller (1989) in his study on the size and temperature dependence of the pseudoelastic hysteresis under one-dimensional tension

and his definition of an interfacial energy between martensitic and austenitic domains in the body have inspired many other theories. They were subsequently generalized to three dimensions, see the discussion of Raniecki et al. (1992) below. According to Müller (1989), the interfacial energy includes phenomena such as the elastic misfit of the individual phases and the energy of elastic interaction of neighboring domains. It is the determinant for the size of the pseudoelastic hysteresis.
Later, Müller & Xu (1991) give further experimental results on the hysteretic behavior of CuZnAl single crystals to determine the width of the pseudoelastic hysteresis, if and how the width of the hysteresis changes with temperature and what kind of processes are admissible within the bounding loop. They conclude that the width is determined by the interfacial energy including elastic misfit of the phases and elastic interaction of neighboring domains. Revising some of their previous arguments concerning inner loops (cf. Müller 1989), they find that phase transformation is initiated at states of unstable equilibria, which may be represented by a diagonal in the stress-strain hysteresis. Based on these observations, they develop a one-dimensional theory that is in good agreement with their experimental data. A more phenomenological approach by Fu et al. (1993), approximating a non-convex free energy curve by two intersecting parabolas and a non-monotone load by a straight line in a load-deflection diagram, leads to a qualitative description of pseudoelasticity, reproducing the experimentally observed characteristics of inner cycles. The theory is elaborated further based on additional data measured on an CuAlZn specimen by Huo & Müller (1993), reviewing other concepts of statistical mechanics as well. Again, emphasis is on the description of the behavior observed within the bounding loop of the hysteresis.

2.2.2 Landau theory and relaxation of free energy

Within the framework of Landau theory, Falk proposes a one-dimensional model capable of a qualitative description of the material behavior of shape memory alloys (cf. Falk 1983). Considering a single crystal, the temperature dependent (one-dimensional Landau) Helmholtz free energy density is derived. All thermodynamical functions are derived from this potential. To account for the interfacial energy, a Ginzburg-Landau theory is adopted. The concept is extended to three dimensions by Falk & Konopka (1990). Based on a modified version of the original model developed by Falk (1983), Bubner (1996) simulates the behavior of CuZnAl single crystals. His model reproduces experimental observations except for the diagonal of unstable equilibria, identified by Müller (1989) as the criterion for initiation of phase transformation.
Recently, relaxation methods have been becoming increasingly popular. They are motivated by the common problem of microstructural approaches, that a given material can form many different microstructures, which are difficult

to construct collectively. Also, numerical computations are elusive, as discrete schemes develop oscillations on the scale of the grid. Hence, it has been proposed to relax the problem and to minimize a relaxed energy function instead of the free energy determined using e.g. Landau theory (Bhattacharya & Dolzmann 2000). Adopting the model by Achenbach (1989), Govindjee et al. (2002) examine the free energy of mixing for the case of n variants. Based on a quasi-convex analysis, the free energy is relaxed yielding a lower bound that gives rise to practical evolutionary computations.

2.2.3 Micromechanical models

A micromechanical model for superelasticity is proposed by Patoor et al. (1996). Here, the micromechanical analysis is based on a kinematical description of the physical strain mechanisms and a definition of a local thermodynamical potential. The volume fractions of the different variants of martensite are chosen as internal variables describing the evolution of the microstructural state of the material. Using a self-consistent scheme, global relationships are obtained. Calculations performed based on the constitutive equation derived in this manner are in good agreement with experimental data on Cu-based shape memory alloys.
Within the model, the internal stresses are presumed to originate from martensitic interactions. Hence, an interaction matrix is introduced to account for these microstructural aspects.
This concept has been refined continuously. Niclaeys et al. (2002) modify the interaction matrix to obtain a more realistic description of the interaction energy, which is influenced by the fact that martensitic variants tend to form in self-accommodated groups to minimize the energy associated with their formation. So far, this effect had been considered only within micromechanical models (cf. Gao et al. 2000, Huang et al. 2000).
Adopting a self-consistent model to calculate the transformation surfaces for different textures, Chirani et al. (2003) observe that the normality rule known from plasticity is obeyed. This property indicates that the phenomenological description of superelasticity may be possible with plasticity type models.
Other micromechanical models regard the martensite generated during $A \rightarrow M$ phase transformation as a spherical inclusion in the austenitic matrix which is subject to interactions with the matrix (cf. Sun & Hwang 1993). Application of Eshelby or Mori-Tanaka (self-consistent) methods (cf. Mori & Tanaka 1973), commonly under the assumption of isotropic elasticity for matrix and inclusion, leads to descriptions on the macroscopic scale.
Other micromechanical approaches are concerned with the kinetics of phase boundary movement. Based on thermodynamic principles at the material microlevel, Fischer & Oberaigner (2001) derive a jump condition and ther-

modynamic force at the interface and eventually obtain two coupled relations describing the kinetics of the phase boundary and heat conduction. A micromechanical model proposed by Sun & Lexcellent (1996) based on Sun & Hwang (1993) describes the two-way shape memory effect during cooling and heating after initial training of the material. The model may be used as a theoretical basis to predict the two-way shape memory effect of polycrystals. Sittner & Novák (2000) study the anisotropy behavior of martensitic transformation in tension/compression experiments with oriented CuAlNi single crystals. Application of a constant stress averaging procedure to model the behavior of the polycrystal shows the impact of crystallographic properties and material attributes associated with martensitic transformations on the macroscopic behavior of shape memory alloy polycrystals. The link between micromechanical and phenomenological theories is investigated by Fischer & Tanaka (1992), who give a review of various approaches, equations and general results on conditions for the development and growth of transformed regions on a microscale (cf. Fischer et al. 1994).

2.2.4 Phenomenological models

Many phenomenological models are based on plasticity theories or on extensions thereof. Within an extended classical theory of plasticity, Bertram (1982) proposes a model based on two temperature dependent yield functions in stress space. A criterion for the conclusion of phase transformation, called plastic limit deformation, is defined in strain space. A one-dimensional theory to describe the thermomechanical behavior during processes of stress-induced martensitic transformation is developed by Tanaka et al. (1986). As no reorientation of martensite is considered, the theory is limited to pseudoelasticity, defining the mass fraction of martensite as an internal variable determining the constitutive equation. The evolution of martensite is described using an exponential function proposed by Koistinen & Marburger (1959). Delobelle & Lexcellent (1996) define an internal variable similar to the kinematic hardening variables of plasticity theories to describe the pseudoelastic hysteresis. Using a viscoplasticity-type flow rule, internal loops under isothermal conditions are described in reasonable agreement with experimental data. By treating the continuum as a three-phase body, Lexcellent et al. (2000) differentiate between both self-accommodating, thermally induced martensite and detwinned or oriented, stress induced martensite, leading to an amended definition of the Helmholtz free energy. Two internal variables, the volume fraction of self-accommodating martensite and the volume fraction of stress induced martensite, are used. By accounting for the thermomechanical procedure of training of the material by a term in the free energy function, i.e. the applied stress during thermal cycling, the two-way shape memory effect is accounted for.

Raniecki et al. (1992) propose a three-dimensional thermodynamic theory, elaborated further by Raniecki & Lexcellent (1994, 1998), to describe pseudoelasticity. The model is based on a specific Helmholtz free energy function for a two-phase solid in a state of constrained equilibrium. Introducing the mass fraction of martensite as an internal state variable, all states on and within the stress-strain hysteresis are accounted for. Hence, adopting the concept of generalized irreversible forces, the thermodynamic force driving martensitic phase transformation can be identified. Considerations concerning active and neutral processes lead to a rate-equation for the mass fraction of martensite, uniquely determining the inelastic strain rate and thereby the stress. As this model is based on thermodynamical considerations, thermodynamical consistency is automatically ensured.
The model may be interpreted as an extension of the one-dimensional theories proposed by Müller (1989) and Müller & Xu (1991) to three dimensions. The description of transformation kinetics is based on Tanaka (1990), who adopts the argumentation of Magee (1970). The model has been shown to be readily implemented into finite element codes and may be calibrated to various shape memory alloys (cf. Raniecki & Lexcellent 1994, Ziólkowski 2001, Müller & Bruhns 2002a). As the model proposed in Chapter 6 is an extension of Raniecki et al. (1992), a more detailed discussion is given below.
A model for both pseudoelasticity and one-way shape memory effect is subsequently proposed by Boyd & Lagoudas (1996a, 1996b). By accounting for the reorientation of martensite, the description of one-way shape memory effect becomes possible. However, reorientation of martensite is disregarded later in a theory extending the earlier concepts by Lagoudas and coworkers (cf. Qidwai & Lagoudas 2000). The latter theory is based on an additive decomposition of the Green-Lagrange strain tensor to account for motions characterized by small strains but large rotations.
Within the framework of *generalized plasticity* (cf. Lubliner 1984), Auricchio & Lubliner (1995) and Lubliner & Auricchio (1996) propose a model to describe pseudoelasticity and one-way shape memory effect. Based on the definition of an inelastic potential of Drucker-Prager type, inelastic domains for $A \rightarrow M$ and $M \rightarrow A$ transformations are defined. In conjunction with a flow rule for the Drucker-Prager potential, a rate equation for the mass fraction of martensite is postulated. For the dependence on the inelastic potential chosen, a closed-form solution for the mass fraction of martensite exists, giving rise to an explicit equation for the inelastic strain rate associated with forward and reverse phase transformations, respectively. However, while the underlying generalized plasticity theory incorporates thermodynamic fundamentals, such as the Clausius-Duhem inequality, the model is not embedded in a thermomechanical frame in the sense that no definition of a free energy function is included. This is a drawback shared by most plasticity-type models of shape memory behavior.

Even though the model is intended to be used for the description of both pseudoelasticity and one-way shape memory effect, it is in fact limited to the former as no reorientation of martensite is considered. Also, without a sound thermodynamic framework incorporating the latent heat of phase transformation, the thermomechanically coupled process of temperature-induced shape recovery cannot be modeled adequately. While subsequent developments (cf. Auricchio & Taylor 1997, Auricchio et al. 1997, Auricchio 2001) do not overcome the shortcomings mentioned, they show the efficient implementability of the model into the finite element method (see also Rebelo et al. 2001a, Rebelo et al. 2001b).

A very comprehensive model to describe pseudoelasticity as well as one- and two-way shape memory effects is developed by Bo & Lagoudas (1999a, 1999b, 1999c, 1999d). Based on a micromechanical analysis over a representative volume element (RVE) they first obtain a generic form of the Gibbs free energy for polycrystalline shape memory alloys. Except for the term accounting for plasticity effects, their Gibbs free energy function is equivalent to the formulation by Raniecki & Lexcellent (1994), which in turn is closely related to the Helmholtz free energy as derived in Raniecki & Bruhns (1991) that is adopted below.

Bo & Lagoudas introduce a set of four internal state variables, i.e. the volume fraction of martensite, a macroscopic transformation strain, and back and drag stresses due to both martensitic phase transformation and its interaction with eigenstrains. In addition, they consider plastic strains as the microstructural change responsible for the two-way shape memory effect. While the fraction of martensite and the drag stress are scalars, the remaining three internal variables are second-order tensors.

The definition of both a volume fraction of martensite and a transformation strain tensor is motivated by the necessity to differentiate between twinned and detwinned martensite, which is of fundamental importance to model both temperature- and stress-induced transformations. Still, calibrating the model by thermal cycling at different prescribed levels of stress yields a parameter set unable to describe both types of transformations quantitatively. In addition, the manner in which the accumulation of plastic eigenstrains in terms of the loading history is accounted for cannot be readily adapted to numerical solution procedures. Only under certain assumptions, e.g. requiring the proportionality of loading paths and disregarding the evolution of plastic eigenstrains, but at the same time abandoning the characteristics which distinguish the model from other approaches, the model is suited for numerical implementations. However, the underlying concepts are valuable in developing material laws accounting for all three shape memory effects.

A few models such as Lexcellent et al. (1994) are specifically proposed for R-phase transformations. However, on the macroscopic scale it may be admissible to employ existing phenomenological theories for austenite-martensite

transformations in a analogous manner to R-phase transformations.
There is only a very limited number of theories of shape memory behavior within large deformation schemes. Auricchio & Taylor (1997) propose a finite deformation theory based on the multiplicative decomposition of the deformation gradient into an elastic part and a part associated with phase transformation. Disregarding martensitic reorientation, only pseudoelasticity is within the scope of the model. The theory is based on the notions of plasticity and not embedded in a thermodynamic frame. Pethö (2000, 2001) decomposes the total deformation gradient into elastic, plastic, and phase transformation parts, describing elasticity using an integrable hypoelastic model based on the logarithmic rate proposed recently, see below. A multiplicative decomposition of the deformation gradient is proposed by Helm as well (cf. Helm 2001, Helm & Haupt 2001, 2003). He extends a geometrically linear theory intended for the description of pseudoelasticity and both one- and two-way shape memory effects to finite deformations.

2.3 Motivation

Studying the extensive literature on models for shape memory alloys, it may seem that there is no need for another phenomenological model. In fact, the question arises why so many different theories coexist.
As all models are based on simplifications of observed phenomena, the suitability of one model or another sometimes is a matter of priorities. A model not appropriate in one particular case may be very well suited in another situation, where different phenomena are under consideration.
The majority of existing models is based on an assumption that is regarded as an oversimplification here: the assumption of small strains. In view of the magnitude of the strains observed in pseudoelasticity and one-way shape memory effect, which may exceed 15 % for monocrystals (cf. Sittner & Novák 2000, Miyazaki et al. 1984) and is close to 10 % for polycrystals (cf. Gadaj et al. 1999, Shaw 2000), the assumption of small strains is a rather strong restriction. Hence, in contrast to many researchers regarding the error due to the small strain-assumption as irrelevant in comparison to other simplifications of their models, here the focus is on providing a sound thermomechanical basis for models of shape memory alloy behavior, comprising a Eulerian theory of finite deformations based on the logarithmic rate (cf. Xiao et al. 1997a, 1997b, 1998c, 1998d) and a thermodynamic theory with internal state variables (cf. Truesdell & Toupin 1960, Coleman & Gurtin 1967, Malvern 1969, Truesdell & Noll 1992), regarding only the *reversible* strain as thermodynamic state variable (cf. Lehmann 1974, 1984).
The phenomenological model proposed is limited to the description of pseudoelasticity. However, it will be illustrated how the model may be extended to include one- and two-way shape memory effects and other phenomena ex-

perimentally observed. It seems that this approach is advantageous to first proposing an extensive model and then attempting to reestablish this theory within a different kinematical setting.

3 Deformation and motion

3.1 Introduction

In this chapter the kinematics of non-linear continuum mechanics are presented. The kinematic relations relevant to subsequent considerations and the respective Eulerian and Lagrangian[2] strain measures are given. Based on the notion of objectivity, the corotational rate adopted later for the formulation of constitutive equations describing pseudoelastic material behavior is introduced. The theory consistently combines the additive and multiplicative decompositions discussed in the literature.
This chapter is based mainly on the monograph by Ogden (1984) and the work of Xiao et al. (1997a, 1997b, 1998c, 1998d, 2000b) and Bruhns et al. (2001). Some references are made to the monographs of Truesdell & Noll (1992), Malvern (1969), Chadwick (1976) and Marsden & Hughes (1983), who treat the subject in more detail.

3.2 Kinematics

3.2.1 The notion of observers

The concept of an *observer* provides the framework necessary for the description of the phenomena that occur in the physical world. An observer is introduced in order to provide a means of measuring physical quantities and to monitor the relative positions of points in space and the progress of time (cf. Ogden 1984).
In continuum mechanics, the space under consideration generally is the three-dimensional Euclidean point space $\mathcal{E}$, and the times observed are elements of the set of real numbers $\mathbb{R}$. Events are recorded by an observer $\mathcal{O}$ as a pair $(\mathbf{x}, t)$ in the Cartesian product $\mathcal{E} \times \mathbb{R}$, where $\mathbf{x} \in \mathcal{E}$ is a point of $\mathcal{E}$ and $t \in \mathbb{R}$ is a time in $\mathbb{R}$.
Two events perceived by $\mathcal{O}$ at distinct points $\mathbf{x}_1$ and $\mathbf{x}_2$ at times t_1 and t_2 are separated by distances $|\mathbf{x}_2 - \mathbf{x}_1|$ in $\mathcal{E}$ and $|t_2 - t_1|$ in $\mathbb{R}$. The most general one-to-one mapping of $\mathcal{E} \times \mathbb{R}$ onto itself that preserves both these distances in space and time and the order in which events occur is given by

$$\mathbf{x}_2^* - \mathbf{x}_1^* = \mathbf{Q}(t)(\mathbf{x}_2 - \mathbf{x}_1) \quad \text{with} \quad t^* = t - a\,. \tag{3.1}$$

Here, the tensor $\mathbf{Q}$ is a time dependent second-order orthogonal tensor and $a \in \mathbb{R}$ a constant. Stipulating that different observers should agree about distance and time intervals of events, (3.1) may be referred to as an *observer transformation.* Adopting this concept, the mapping

$$(\mathbf{x}, t) \rightarrow (\mathbf{x}^*, t^*) \tag{3.2}$$

[2] Ogden (1984) uses the term *Lagrangean* strain measure instead of *Lagrangian* strain measure.

is a change of observer from $\mathcal{O}$, who records the event at place $\mathbf{x}$ and time t, to $\mathcal{O}^*$, who observes the same event at place $\mathbf{x}^*$ and time t^*.
The tensor $\mathbf{Q}$ introduced above is specified to be proper orthogonal. Hence, transformation (3.1) is interpreted as a rotation of vectors in $\mathbb{E}$ which preserves orientation. With the additional notational change $\mathbf{c}(t) = \mathbf{x}_1^* - \mathbf{Q}(t)\mathbf{x}_1$, a change of observer according to (3.1) is given by the well-known equation

$$\mathbf{x}^* = \mathbf{Q}(t)\mathbf{x} + \mathbf{c}(t) \quad \text{with} \quad t^* = t - a\,, \tag{3.3}$$

where the index 2 is omitted.
It should be noted that the definitions of an observer and of an observer transformation are independent of the choice of basis for the vector space $\mathbb{E}$.
The notion of an observer is of fundamental importance. For example, for the same moving point, two observers in relative motion will record different values of speed. Evidently, measurements of physical quantities generally depend on the choice of observer. On the other hand, in contrast to their kinematical descriptions do physical phenomena not depend on the choice of observer. This must be reflected by the mathematical formulation of physical laws such as the constitutive model developed below.
In the following, the distinction between t and t^*, which separates the recording of events between $\mathcal{O}$ and $\mathcal{O}^*$, is of no relevance, and for simplicity it is assumed that $t^* = t$ or equivalently $a = 0$.
The definition of an observer is independent of a choice of origin. However, if observers $\mathcal{O}$ and $\mathcal{O}^*$ choose origins $\mathbf{o}$ and $\mathbf{o}^*$ in $\mathcal{E}$, respectively, $\mathbf{x}$ and $\mathbf{x}^*$ may be interpreted as the respective position vectors of the points $\mathbf{x}$ and $\mathbf{x}^*$ relative to $\mathbf{o}$ and $\mathbf{o}^*$.

3.2.2 Configurations and motions of bodies

A body B is a set of (material) points or particles which can be put into one-to-one correspondence with some region $\mathcal{B}$ of the Euclidean point space $\mathcal{E}$. As the body moves, the region $\mathcal{B}$ it occupies in $\mathcal{E}$ changes constantly.
The one-to-one mapping

$$\chi : B \to \mathcal{E} \tag{3.4}$$

of the particles of B to the places they occupy in $\mathcal{E}$ is termed a *configuration* of B. The configuration χ of the body and its inverse χ^{-1} are taken to be twice continuously differentiable (cf. Ogden 1984). For a generic particle X of B, the place $\mathbf{x}$ occupied by $X \in B$ in the configuration χ is

$$\mathbf{x} = \chi(X, t)\,. \tag{3.5}$$

Inversely, a particle X of B may be found for known, observer-dependent configuration χ, given the position $\mathbf{x}$

$$X = \chi^{-1}(\mathbf{x}, t)\,. \tag{3.6}$$

The set of places $\mathcal{B}$ occupied by all particles of the body B in the configuration χ is

$$\chi(B) = \{\chi(X), X \in B\} \,. \tag{3.7}$$

A one-parameter set of configurations $\chi_t : B \to \mathcal{E}$ depending on the parameter t is termed a *motion* of the body B. For fixed X corresponding to a given particle, the equation

$$\mathbf{x} = \chi_t(X) = \chi(X, t) \tag{3.8}$$

describes a curve in $\mathcal{E}$ called the *path* of X in the motion.

3.2.3 Reference configurations and deformations

The domain of a body in the initial state at a time $t = 0$ is called the *initial configuration*. Physical observations of the body B are made in specific configurations. Therefore, in describing the motion and deformation of the body, a *reference configuration* is needed. During the motion, the particles of B may be labeled by their places in this fixed, but arbitrarily chosen reference configuration. It is not required that the reference configuration corresponds to the initial configuration, in fact, it does not have to be a configuration actually occupied by B at any point in time at all. The significance of the reference configuration lies in the fact that motion is defined with respect to this configuration. However, here it is assumed that initial and reference configuration are identical.
For given position $\mathbf{X}$ of the particle X in the reference configuration, the time-independent configuration χ_0 specified by

$$\mathbf{X} = \chi_0(X) \,, \quad X = \chi_0^{-1}(\mathbf{x}, t) \tag{3.9}$$

is the reference configuration. The region of $\mathcal{E}$ occupied by B in the reference configuration is denoted by $\mathcal{B}_0$. The current configuration is denoted by χ_t with $\chi_t(B) = \mathcal{B}_t$.
Ignoring the distinction between the particle X and the place $\mathbf{X}$ used to identify it for practical purposes, from the last two equations the current place $\mathbf{x}$ of the particle with the position $\mathbf{X}$ in the reference configuration is

$$\mathbf{x} = \chi(\mathbf{X}, t) \,. \tag{3.10}$$

The mapping χ from $\mathcal{B}_0$ to $\mathcal{B}_t$ defined by (3.10) depends implicitly on the reference configuration chosen. For any fixed time t, χ is called a *deformation* from the reference configuration, and for arbitrary time t, equation (3.10) specifies a one-parameter family of such deformations. Clearly, a deformation can be defined only for a given reference configuration. While different observers may choose different reference configurations, any choice of reference

configuration is independent of observer.
The places $\mathbf{X}$ and $\mathbf{x}$ occupied by the particle X of B in the reference and current configurations may also be regarded as position vectors in $\mathbb{E}$ relative to the respective fixed origins $\mathbf{O}$ and $\mathbf{o}$ in $\mathcal{E}$. For the general case of non-coinciding origins, the body with the particle X is depicted in its reference and current configurations in Figure 3.1 (see Ogden 1984).

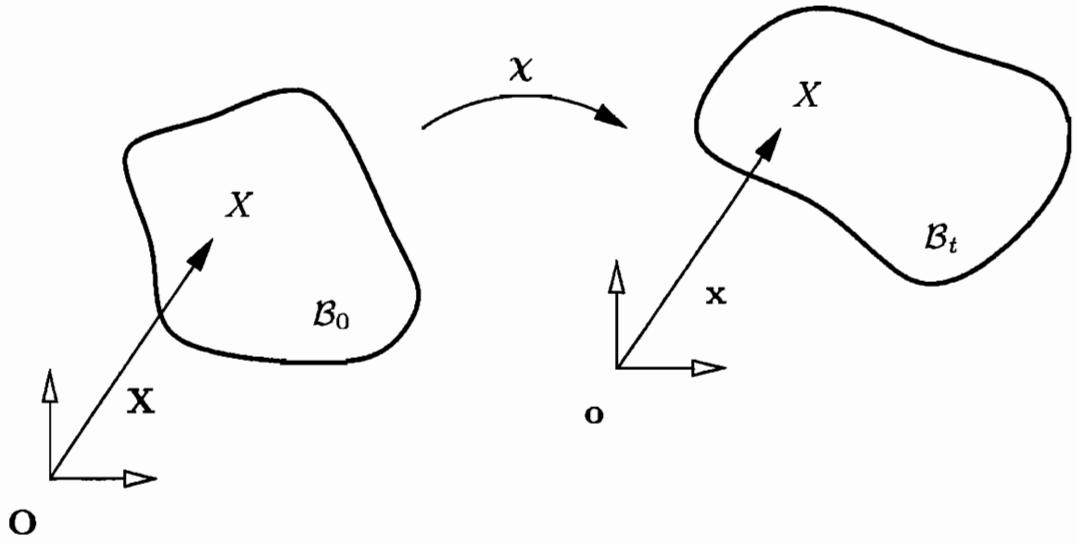

Figure 3.1: Body and particle in reference and current configurations

Rigid-body motions

A *rigid-body motion* of a body B recorded by a single observer $\mathcal{O}$ is a motion during which the distance between arbitrary pairs of particles of B is preserved. Formally, the motion

$$\mathbf{x} = \chi(\mathbf{X}, t) \tag{3.11}$$

observed by $\mathcal{O}$ is rigid if and only if

$$\mathbf{x} = \mathbf{c}(t) + \mathbf{Q}(t)\mathbf{X}\,, \tag{3.12}$$

where $\mathbf{x} \in \mathcal{B}_0$.

Notation

Components of vectors and tensors associated with a basis $\{\mathbf{E}_\alpha\}$ in the reference configuration $\mathcal{B}_0$ will be denoted by Greek character indices

$$\mathbf{X} = X_\alpha \mathbf{E}_\alpha\,. \tag{3.13}$$

The coordinates X_α are called *referential* or *Lagrangian* coordinates of the particle X. Italic indices will be used for components of vectors and tensors associated with a basis $\{\mathbf{e}_i\}$ in the current configuration $\mathcal{B}_t$. The corresponding coordinates in the current configuration x_i

$$\mathbf{x} = x_i \mathbf{e}_i \tag{3.14}$$

are called *current* or *Eulerian* coordinates of X.
Scalar, vector or tensor fields may be defined over either the reference configuration $\mathcal{B}_0$ or the current configuration $\mathcal{B}_t$. If φ is a scalar, vector or tensor field defined over $\mathcal{B}_t$, using (3.10) the corresponding field $\mathbf{\Phi}$ over $\mathcal{B}_0$ is

$$\mathbf{\Phi}(\mathbf{X}, t) = \varphi(\mathbf{x}, t) = \varphi(\chi(\mathbf{X}, t), t)\,. \tag{3.15}$$

Inversely, for $\mathbf{\Phi}$ defined over $\mathcal{B}_0$, the equivalent scalar, vector or tensor field over $\mathcal{B}_t$ is defined by the inverse of the deformation (3.10)

$$\mathbf{X} = \chi^{-1}(\mathbf{x}, t) \tag{3.16}$$

which yields

$$\varphi(\mathbf{x}, t) = \mathbf{\Phi}(\mathbf{X}, t) = \mathbf{\Phi}(\chi^{-1}(\mathbf{x}, t), t)\,. \tag{3.17}$$

Physical phenomena associated with the deformation (3.10) of a body B may be described using fields defined over $\mathcal{B}_0$ in the so-called *Lagrangian* or *referential* (*material*) description, or using fields defined over $\mathcal{B}_t$ in the *Eulerian* or *spatial* description.
The notation of upper-case letters for Lagrangian and of lower-case letters for Eulerian fields introduced here sometimes conflicts with the notation using bold-face, lower-case letters for vectors and bold-face, upper-case letters for tensors. In these cases, the latter convention overrides the former and it will be stated explicitly over which configuration the respective field is defined.

3.2.4 Velocity and acceleration

The velocity $\mathbf{v}(\mathbf{X}, t)$ defined over the reference configuration $\mathcal{B}_0$ of a material particle occupying the position $\mathbf{X}$ in $\mathcal{B}_0$ is given by

$$\mathbf{v}(\mathbf{X}, t) = \frac{\mathrm{d}\chi}{\mathrm{dt}}(\mathbf{X}, t) = \dot{\chi}(\mathbf{X}, t)\,. \tag{3.18}$$

The velocity represents the rate of change of the position vector for a material point, i.e. the time derivative with $\mathbf{X}$ held constant. The acceleration $\mathbf{a}(\mathbf{X}, t)$ is the rate of change of velocity of a material point. Defined over $\mathcal{B}_0$ the acceleration is

$$\mathbf{a}(\mathbf{X}, t) = \frac{\mathrm{d}\mathbf{v}}{\mathrm{dt}}(\mathbf{X}, t) = \frac{\mathrm{d}^2\chi}{\mathrm{dt}^2}(\mathbf{X}, t)\,. \tag{3.19}$$

The derivative $\mathrm{d}(\cdot)/\mathrm{dt}$ at fixed $\mathbf{X}$ is called the *Lagrangian time derivative*, while the derivative with respect to time at fixed $\mathbf{x}$ is referred to as the *Eulerian time derivative*. The Eulerian time derivative follows from the Lagrangian or *material* time derivative using the chain rule for partial derivatives

$$\left.\frac{\mathrm{d}(\cdot)}{\mathrm{dt}}\right|_{\mathbf{X}} = \left.\frac{\partial(\cdot)}{\partial t}\right|_{\mathbf{x}} + (\nabla \otimes (\cdot)) \cdot \mathbf{v}(\mathbf{x}, t)\,. \tag{3.20}$$

The term $(\partial(\cdot)/\partial t)|_{\mathbf{x}}$ is called the *spatial time derivative*; the second term on the right-hand side of (3.20) is the *convective* or *transport* term (cf. Belytschko et al. 2000).
Hence, in the Eulerian description the acceleration is

$$\mathbf{a}(\mathbf{x}, t) = \frac{\partial \mathbf{v}}{\partial t}(\mathbf{x}, t) + \mathbf{L} \cdot \mathbf{v}(\mathbf{x}, t)\,, \tag{3.21}$$

where the *velocity gradient* tensor $\mathbf{L}$, a Eulerian tensor, is introduced

$$\mathbf{L} = \nabla \otimes \mathbf{v}(\mathbf{x}, t) = \frac{\partial \mathbf{v}(\mathbf{x}, t)}{\partial \mathbf{x}}\,. \tag{3.22}$$

Under an observer transformation as defined by equation (3.3), the motion is perceived by the observer $\mathcal{O}^*$ as

$$\boldsymbol{\chi}^*(\mathbf{X}, t) = \mathbf{Q}(t)\boldsymbol{\chi}(\mathbf{X}, t) + \mathbf{c}(t)\,. \tag{3.23}$$

Introducing the *axial* vector $\boldsymbol{\omega}$ associated with the skew-symmetric spin tensor $\boldsymbol{\Omega} = \dot{\mathbf{Q}}\mathbf{Q}^{\mathrm{T}}$

$$\boldsymbol{\Omega} \cdot \boldsymbol{\alpha} = \boldsymbol{\omega} \times \boldsymbol{\alpha} \quad \forall\, \boldsymbol{\alpha} \in \mathbb{E}\,, \tag{3.24}$$

the velocity observed by $\mathcal{O}^*$ is calculated using (3.10) as

$$\begin{aligned} \mathbf{v}^*(\mathbf{X}, t) &= \mathbf{Q}\mathbf{v} + \dot{\mathbf{c}}(t) + \dot{\mathbf{Q}}\boldsymbol{\chi}(\mathbf{X}, t) \\ &= \mathbf{Q}\mathbf{v} + \dot{\mathbf{c}}(t) + \boldsymbol{\omega} \times (\mathbf{x}^* - \mathbf{c})\,. \end{aligned} \tag{3.25}$$

In the same manner, the acceleration observed by $\mathcal{O}^*$, who is in relative motion to $\mathcal{O}$, is found to be

$$\begin{aligned} \mathbf{a}^*(\mathbf{X}, t) &= \mathbf{Q}\mathbf{a} + \ddot{\mathbf{c}}(t) + \ddot{\mathbf{Q}}\boldsymbol{\chi}(\mathbf{X}, t) + 2\dot{\mathbf{Q}}\mathbf{v} \\ &= \mathbf{Q}\mathbf{a} + \ddot{\mathbf{c}}(t) + \dot{\boldsymbol{\omega}} \times (\mathbf{x}^* - \mathbf{c}) - \|\boldsymbol{\omega}\|^2(\mathbf{x}^* - \mathbf{c}) + 2\boldsymbol{\omega} \times \mathbf{Q}\mathbf{v}\,. \end{aligned} \tag{3.26}$$

Here, $\|(\cdot)\|$ is the norm of the vector $(\cdot)$.

3.3 Analysis of deformation

In this section, the quantities and relations required to analyze a deformation of a body B from a reference configuration $\mathcal{B}_0$ to a current configuration $\mathcal{B}_t$ are presented. Since the comparison of reference and current configuration does not require the knowledge of intermediate stages in the motion, in (3.10) the explicit dependence on time is suppressed

$$\mathbf{x} = \chi(\mathbf{X}), \tag{3.27}$$

and the current configuration is now denoted by $\mathcal{B}$. In component form with respect to an orthogonal Cartesian basis $\{\mathbf{E}_\alpha\}$ respectively $\{\mathbf{e}_i\}$ and origin $\mathbf{O}$ respectively $\mathbf{o}$ chosen by $\mathcal{O}$ in the reference (current) configuration, the deformation from $\mathcal{B}_0$ to $\mathcal{B}$ may be written as

$$x_i = \chi_i(X_\alpha). \tag{3.28}$$

3.3.1 Deformation gradient

In the neighborhood of a material particle X, the derivatives $\partial x_i/\partial X_\alpha$ are continuous and the differential of (3.28) is

$$dx_i = \frac{\partial x_i}{\partial X_\alpha}\, dX_\alpha \tag{3.29}$$

or in tensorial notation

$$\mathbf{dx} = \mathbf{F}\mathbf{dX}. \tag{3.30}$$

The tensor $\mathbf{F}$ given by (3.30) is called the *deformation gradient*. It is defined by

$$\mathbf{F} = \nabla_0 \otimes \chi(\mathbf{X}) = \frac{\partial \mathbf{x}}{\partial \mathbf{X}}. \tag{3.31}$$

The deformation gradient lives partially in the reference configuration and partially in the current configuration. For this reason, it is often referred to as a *two-point* (or *mixed Eulerian-Lagrangian*) tensor, with one leg or index in each configuration, the reference configuration and the current configuration. With respect to bases $\{\mathbf{E}_\alpha\}$ and $\{\mathbf{e}_i\}$ the deformation gradient reads

$$\mathbf{F} = \frac{\partial x_i}{\partial X_\alpha}\, \mathbf{e}_i \otimes \mathbf{E}_\alpha. \tag{3.32}$$

According to (3.30), a *material line element* $\mathbf{dX}$, i.e. a vector $\mathbf{dX}$ at the point $\mathbf{X}$ in $\mathcal{B}_0$, is transformed by $\mathbf{F}$ to the line element $\mathbf{dx}$ at the point $\mathbf{x}$ in $\mathcal{B}$. To rule out the physically unrealistic case where the deformation reduces the

length of line elements to zero, $\mathbf{F}$ is required to be a *non-singular* tensor. This can be assured if its determinant fulfills the inequality

$$J = \det(\mathbf{F}) > 0\,. \tag{3.33}$$

The inverse $\mathbf{F}^{-1}$ of the deformation gradient exists and may be used to invert (3.30)

$$\mathbf{dX} = \mathbf{F}^{-1}\mathbf{dx}\,. \tag{3.34}$$

3.3.2 Deformation of volume and surface

The *Jacobian determinant* J is the local ratio of current to reference volume of a material volume element

$$dv = J\,dV\,. \tag{3.35}$$

This is observed by considering the non-coplanar line elements $\mathbf{dX}^{(i)}$ transforming according to

$$\mathbf{dx}^{(i)} = \mathbf{F}\mathbf{dX}^{(i)}\,. \tag{3.36}$$

At a point $\mathbf{X}$ in the reference configuration, these line elements define the infinitesimal volume element dV

$$dV = \mathbf{dX}^{(1)} \cdot (\mathbf{dX}^{(2)} \times \mathbf{dX}^{(3)}) = \det(\mathbf{dX}^{(1)}, \mathbf{dX}^{(2)}, \mathbf{dX}^{(3)})\,, \tag{3.37}$$

while their Eulerian counterparts define the infinitesimal volume element dv

$$dv = \det(\mathbf{dx}^{(1)}, \mathbf{dx}^{(2)}, \mathbf{dx}^{(3)}) \tag{3.38}$$

at the place $\mathbf{x}$. These two equations in conjunction with (3.30) and (3.33) yield equation (3.35).
The material time derivative of the Jacobian determinant J is given by

$$\dot{J} = J\,\nabla \cdot \mathbf{v}\,. \tag{3.39}$$

Deformations with

$$J = \det(\mathbf{F}) = 1 \tag{3.40}$$

are said to be *isochoric* or volume preserving at $\mathbf{X}$.
The infinitesimal vector element of material surface $\mathbf{dA}$ defined by $\mathbf{dX}^{(2)}$ and $\mathbf{dX}^{(3)}$ transforms to $\mathbf{da}$ defined by $\mathbf{dx}^{(2)}$ and $\mathbf{dx}^{(3)}$. By virtue of (3.35) it follows

$$\mathbf{dx}^{(1)} \cdot \mathbf{da} = J\mathbf{dX}^{(1)} \cdot \mathbf{dA}\,. \tag{3.41}$$

Then, substitution of (3.30) yields *Nanson's formula* (cf. Ogden 1984)

$$\mathbf{da} = J\mathbf{F}^{-\mathrm{T}}\mathbf{dA} \tag{3.42}$$

with $\mathbf{da} = \mathbf{n}\,da$ and $\mathbf{dA} = \mathbf{N}\,dA$, respectively. The positive unit normals $\mathbf{n}$ and $\mathbf{N}$ to the surfaces $\mathbf{da}$ of $\mathcal{B}$ and $\mathbf{dA}$ of $\mathcal{B}_0$, respectively, are pointing away from the respective surfaces. As these vectors are not embedded in the material, they do not transform according to transformation rule (3.30).

3.3.3 Polar decomposition

According to the polar decomposition theorem, any non-singular second-order tensor $\mathbf{A}$ can be decomposed uniquely into positive definite symmetric second-order tensors $\mathbf{V}$ and $\mathbf{U}$, and an orthogonal second-order tensor $\mathbf{R}$ such that (cf. Malvern 1969)

$$\mathbf{A} = \mathbf{VR} = \mathbf{RU}\,. \tag{3.43}$$

Specifically, the deformation gradient $\mathbf{F}$ may be decomposed into its left and right multiplicative decompositions

$$\mathbf{F} = \mathbf{VR} = \mathbf{RU}\,, \tag{3.44}$$

where, owing to (3.33), the *rotation* tensor $\mathbf{R}$ is *proper* orthogonal

$$\mathbf{R}^{\mathrm{T}}\mathbf{R} = \mathbf{R}\mathbf{R}^{\mathrm{T}} = \mathbf{1} \quad \text{with} \quad \det(\mathbf{R}) = 1\,. \tag{3.45}$$

Here, $\mathbf{1}$ is the second-order identity tensor. From (3.45) it follows that

$$\det(\mathbf{F}) = \det(\mathbf{V}) = \det(\mathbf{U})\,. \tag{3.46}$$

The positive definite symmetric second-order tensors $\mathbf{V}$ and $\mathbf{U}$ are called the *left* and *right stretch* tensors, respectively. $\mathbf{V}$ is a Eulerian quantity and $\mathbf{U}$ a Lagrangian tensor.
The polar decomposition theorem may be illustrated graphically as shown in Figure 3.2 (cf. Macvean 1968). Note that the orientation of arbitrary line-elements is not preserved by $\mathbf{V}$ or $\mathbf{U}$. As a consequence, even for $\mathbf{R} = \mathbf{1}$ the orientation of a line element transformed according to (3.30) generally changes during deformation.
The left stretch tensor $\mathbf{V}$ is obtained from the right stretch tensor $\mathbf{U}$ by forward-rotating with $\mathbf{R}$ and vice versa

$$\mathbf{V} = \mathbf{R} \star \mathbf{U} \qquad\qquad \mathbf{U} = \mathbf{R}^{\mathrm{T}} \star \mathbf{V}\,. \tag{3.47}$$

For $\mathbf{R} = \mathbf{1}$, the deformation is said to be a *pure strain* and $\mathbf{V} = \mathbf{U} = \mathbf{F}$. The deformation gradient $\mathbf{F}$ represents a rigid rotation if and only if $\mathbf{V} = \mathbf{U} = \mathbf{1}$. However, in general the deformation is decomposed into a rotation $\mathbf{R}$ followed

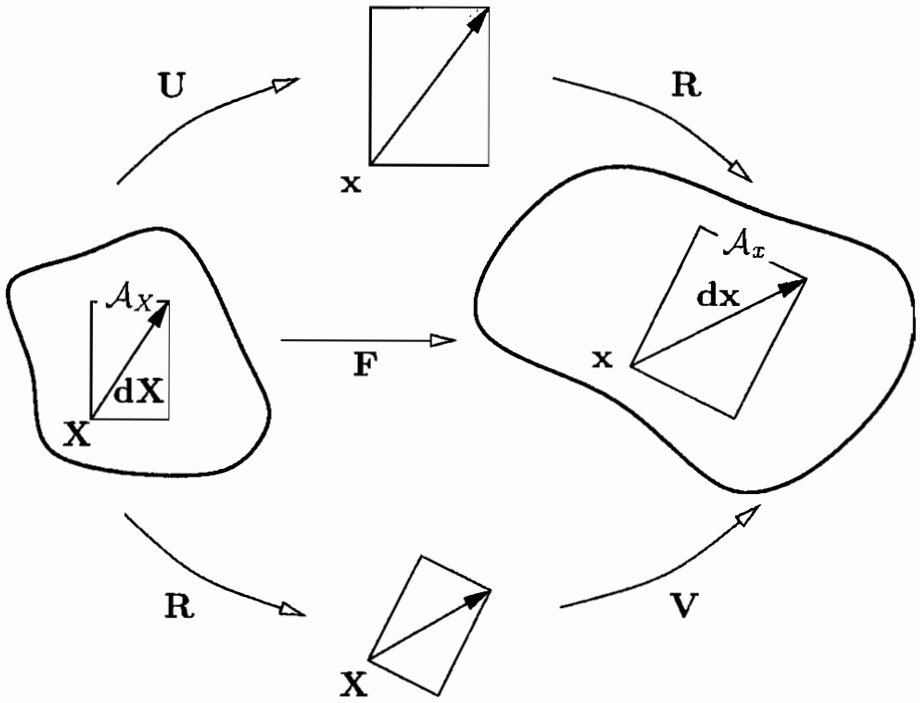

Figure 3.2: Polar decomposition

by a stretch $\mathbf{V}$ (left polar decomposition), or using the right polar decomposition, into a stretch $\mathbf{U}$ succeeded by a rotation $\mathbf{R}$.
The symmetric and positive definite tensors $\mathbf{F}\mathbf{F}^{\mathrm{T}}$ and $\mathbf{F}^{\mathrm{T}}\mathbf{F}$ respectively are called the *left* and *right Cauchy-Green* tensors

$$\mathbf{B} = \mathbf{V}^2 = \mathbf{F}\mathbf{F}^{\mathrm{T}} \qquad \mathbf{C} = \mathbf{U}^2 = \mathbf{F}^{\mathrm{T}}\mathbf{F}\,. \tag{3.48}$$

The following rotated correspondence between the Eulerian tensor $\mathbf{B}$ and the Lagrangian tensor $\mathbf{C}$ holds

$$\mathbf{B} = \mathbf{R} \star \mathbf{C} \qquad \mathbf{C} = \mathbf{R}^{\mathrm{T}} \star \mathbf{B}\,. \tag{3.49}$$

Spectral representation

In a *spectral representation*, a second-order tensor $\mathbf{A}$ is expressed in terms of its *eigenvalues* or *principal values* λ and its *eigenvectors* $\mathbf{a}$, which are commonly referred to as *principal axes* or *principal directions* as well. The eigenvalues and -vectors of $\mathbf{A}$ satisfy the relation

$$\mathbf{A}\mathbf{a} = \lambda\mathbf{a}\,. \tag{3.50}$$

The eigenvalues λ_i of $\mathbf{A}$ are obtained by solving the *characteristic equation*

$$\det(\mathbf{A} - \lambda\mathbf{1}) = 0\,, \tag{3.51}$$

which can be expanded in terms of the principal invariants of $\mathbf{A}$

$$\lambda^3 - I(\mathbf{A})\lambda^2 + II(\mathbf{A})\lambda - III(\mathbf{A}) = 0\,, \tag{3.52}$$

where

$$I = \mathrm{tr}\,(\mathbf{A}) \tag{3.53}$$

$$II = \frac{1}{2}\left(\mathrm{tr}\,(\mathbf{A})^2 - \mathrm{tr}\,(\mathbf{A}^2)\right) \tag{3.54}$$

$$III = \det(\mathbf{A})\,. \tag{3.55}$$

In addition to the principal invariants I, II and III, the main invariants I_1, I_2 and I_3 are defined for later use

$$I_1 = \mathrm{tr}\,(\mathbf{A}) \tag{3.56}$$

$$I_2 = \mathrm{tr}\,(\mathbf{A}^2) \tag{3.57}$$

$$I_3 = \mathrm{tr}\,(\mathbf{A}^3)\,. \tag{3.58}$$

They are related to the principal invariants by

$$I = I_1 \tag{3.59}$$

$$II = \frac{1}{2}\left(I_1^2 - I_2\right) \tag{3.60}$$

$$III = \frac{1}{6}\left(I_1^3 - 3I_1I_2 + 2I_3\right)\,. \tag{3.61}$$

For symmetric second-order tensors $\mathbf{A} = \mathbf{A}^{\mathrm{T}}$, the eigenvectors are mutually orthogonal and the eigenvalues λ are real (cf. Basar & Weichert 2000). Then, a closed-form solution is available (cf. Hoger & Carlson 1984, Sawyers 1986)

$$\lambda_i = \frac{1}{3}\left(I + 2\sqrt{I^2 - 3II}\cos\left(\frac{1}{3}(\varphi - 2\pi i)\right)\right)$$

$$\varphi = \cos^{-1}\left(\frac{2I^3 - 9I\cdot II + 27III}{2(I^2 - 3II)^{\frac{3}{2}}}\right) \tag{3.62}$$

$$i = 1, 2, 3\,.$$

Denoting the eigenvalues of the right stretch tensor $\mathbf{U}$ by λ_i and the corresponding orthonormal unit eigenvectors by $\mathbf{N}^i$, $\|\mathbf{N}^i\| = 1$, gives the spectral representation

$$\mathbf{U} = \sum_{i=1}^{3} \lambda_i\, \mathbf{N}^i \otimes \mathbf{N}^i\,. \tag{3.63}$$

The unit eigenvectors $\mathbf{N}^i$ are termed *Lagrangian principal axes*. They can be rotated forward into the current configuration to yield the *Eulerian principal*

axes $\mathbf{n}^i = \mathbf{R} \star \mathbf{N}^i$ with $\|\mathbf{n}^i\| = 1$. By virtue of (3.47), $\mathbf{U}$ and $\mathbf{V}$ have the same eigenvalues λ_i. Hence,

$$\mathbf{V} = \sum_{i=1}^{3} \lambda_i \, \mathbf{n}^i \otimes \mathbf{n}^i \,. \tag{3.64}$$

Noting (3.46) it is observed that the eigenvalues of $\mathbf{F}$ correspond to those of $\mathbf{V}$ and $\mathbf{U}$. Owing to the fact that $\mathbf{F}$ and $\mathbf{R}$ are two-point tensors, in their spectral representation the first eigenvector lives in the current configuration and the second lives in the reference configuration. All eigenvalues of $\mathbf{R}$ are equal to 1. Of particular interest to the subsequent considerations are the eigenvalues of $\mathbf{B}$. The spectral representations of the left and right Cauchy-Green tensors follow from their definitions (3.48) together with (3.64) and (3.63)

$$\mathbf{B} = \sum_{i=1}^{3} \chi_i \mathbf{n}^i \otimes \mathbf{n}^i \qquad \mathbf{C} = \sum_{i=1}^{3} \chi_i \mathbf{N}^i \otimes \mathbf{N}^i \,, \tag{3.65}$$

where $\chi_i = {\lambda_i}^2$ are the eigenvalues of $\mathbf{B}$ and $\mathbf{C}$.
For multiple eigenvalues, the eigenvectors of the corresponding tensor are no longer unique. Using eigenprojections (cf. Xiao et al. 1998b, 1998d, Hoger 1986, Carlson & Hoger 1986), uniqueness can be established, and basis-free forms of the considered tensors can be derived with the aid of equation (3.70) given below. For example, the left Cauchy-Green tensor may be expressed in terms of its eigenprojections $\mathbf{B}_\sigma$ as

$$\mathbf{B} = \sum_{\sigma=1}^{n} \chi_\sigma \mathbf{B}_\sigma \,. \tag{3.66}$$

Here, the number of unique eigenvalues is denoted by n. The following simple manipulation relations hold

$$\mathbf{B}_\sigma \mathbf{B}_\tau = \delta_{\sigma\tau} \mathbf{B}_\tau \tag{3.67}$$

$$\sum_{\sigma=1}^{n} \mathbf{B}_\sigma = \mathbf{1} \tag{3.68}$$

$$\mathbf{B}_\sigma \mathbf{B} = \chi_\sigma \mathbf{B}_\sigma \,, \tag{3.69}$$

where the *Kronecker delta* symbol δ_{ij} has been introduced. The eigenprojections may be calculated by means of *Sylvester's formula* (cf. Xiao et al. 1998d)

$$\mathbf{B}_\sigma = \delta_{n1}\mathbf{1} + \prod_{\tau\neq\sigma}^{n} \frac{\mathbf{B} - \chi_\tau \mathbf{1}}{\chi_\sigma - \chi_\tau} \,. \tag{3.70}$$

Here and henceforth, the notation $\prod_{\tau\neq\sigma}^{n}(\cdot)$ represents the continued product for all $\sigma, \tau = 1, \ldots, n$ with $\tau \neq \sigma$. The product vanishes for $n = 1$.

3.4 Analysis of strain

3.4.1 The notion of strain

To define the notion of *strain*, the deformation of an arbitrary line element $\mathbf{dX}$ at the point $\mathbf{X}$ is considered. During deformation, its length changes to $\mathbf{dx}$, and the difference between the squared lengths of the line element in $\mathcal{B}$ and $\mathcal{B}_0$ can be calculated from (3.30)

$$|\mathbf{dx}|^2 - |\mathbf{dX}|^2 = \mathbf{dX}(\mathbf{F}^T\mathbf{F} - \mathbf{1})\mathbf{dX}\,. \tag{3.71}$$

If the length of the line element is unchanged after deformation, the material is *unstrained.* In this case, the right-hand side of equation (3.71) must vanish for arbitrary $\mathbf{dX}$, hence the tensorial restriction

$$\mathbf{F}^T\mathbf{F} = \mathbf{1} \tag{3.72}$$

must hold true. Evidently, noting (3.33), the most general deformation yielding zero strain is a rigid translation combined with a rigid rotation. If (3.72) is fulfilled, the deformation gradient $\mathbf{F}$ is a proper orthogonal tensor $\mathbf{Q}$.
The material is said to be *strained* at $\mathbf{X}$ if (3.72) is violated. Relation (3.71) for the change in length of an arbitrary line element of material may then be used to define a strain tensor called *Green-Lagrangian* strain tensor $\mathbf{E}$

$$\mathbf{E} = \frac{1}{2}(\mathbf{F}^T\mathbf{F} - \mathbf{1}) = \frac{1}{2}(\mathbf{U}^2 - \mathbf{1})\,. \tag{3.73}$$

The factor $\frac{1}{2}$ is a normalization factor whose significance follows from the discussion of general measures of strain in Section 3.4.2.
If equation (3.71) is not written in the referential configuration, but instead in terms of $\mathbf{dx}$ in the current configuration

$$|\mathbf{dx}|^2 - |\mathbf{dX}|^2 = \mathbf{dx}(\mathbf{1} - (\mathbf{F}\mathbf{F}^T)^{-1})\mathbf{dx}\,, \tag{3.74}$$

the *Almansi-Eulerian* strain tensor may be defined

$$\mathbf{e} = \frac{1}{2}(\mathbf{1} - (\mathbf{F}\mathbf{F}^T)^{-1}) = \frac{1}{2}(\mathbf{1} - \mathbf{V}^{-2})\,. \tag{3.75}$$

The Green-Lagrangian and Almansi-Eulerian strain tensors are related not only by a rotated correspondence as stated in the next section for arbitrary strain measures, but specifically the Green-Lagrangian strain tensor can be obtained as one — of four possible — induced Lagrangian tensors (cf. Ogden 1984)

$$\mathbf{E} = \mathbf{F}^T\mathbf{e}\mathbf{F}\,. \tag{3.76}$$

Although formally not quite correct (cf. Bongmba 2001), this operation is often referred to as the *pull-back* of the Almansi-Eulerian strain tensor to the

reference configuration. Equivalently, by an operation frequently termed *push-forward*, the Almansi-Eulerian strain measure may be derived as an induced Eulerian tensor from the Green-Lagrangian strain tensor

$$\mathbf{e} = \mathbf{F}^{-\mathrm{T}}\mathbf{E}\mathbf{F}^{-1}. \tag{3.77}$$

Linearization

Considering the displacement $\mathbf{u}$ of a material particle X from its position in the reference configuration $\mathcal{B}_0$ to its position in the current configuration $\mathcal{B}$

$$\mathbf{u} = \chi(\mathbf{X}, t) - \mathbf{X}, \tag{3.78}$$

the *displacement gradient* is

$$\nabla_0 \otimes \mathbf{u} = \mathbf{F} - \mathbf{1}. \tag{3.79}$$

Substitution into the definition of the Green-Lagrangian strain tensor (3.73) gives

$$\mathbf{E} = \frac{1}{2}\left(\nabla_0 \otimes \mathbf{u} + (\nabla_0 \otimes \mathbf{u})^{\mathrm{T}} + (\nabla_0 \otimes \mathbf{u})^{\mathrm{T}} \nabla_0 \otimes \mathbf{u}\right). \tag{3.80}$$

Adopting the assumption of small displacements underlying the theory of small strains, the quadratic term of $\mathbf{u}$ is negligible in comparison to the other terms in (3.80). Then, Lagrangian and Eulerian descriptions coincide and as $\mathbf{F} \approx \mathbf{1}$, the gradient with respect to $\mathbf{X}$ approximately equals that with respect to $\mathbf{x}$. Therefore, for small displacements the linearized strain

$$\mathbf{E} \approx \boldsymbol{\varepsilon} = \frac{1}{2}(\nabla \otimes \mathbf{u} + (\nabla^{\mathrm{T}} \otimes \mathbf{u})) \tag{3.81}$$

can be derived from (3.80). As the assumption of small displacements is not assumed to be fulfilled here, this relation is only given for the sake of completeness. All derivations in succeeding chapters are based on finite measures of strain.

3.4.2 Strain measures

Strain measures such as the Green-Lagrangian and Almansi-Eulerian strain tensors have to fulfill certain criteria. They have to be objective[3] and isotropic[4] tensor functions. Also, they have to be monotonically increasing when the

[3] See Section 3.5.

[4] A tensor function is a function whose arguments are (second order) tensors and whose values are scalars or tensors. A scalar valued tensor function $f(\mathbf{A}_1, \ldots, \mathbf{A}_n)$ is said to be *isotropic* if the relation $\mathbf{Q} \star f(\mathbf{A}_1, \ldots, \mathbf{A}_n) = f(\mathbf{Q} \star \mathbf{A}_1, \ldots, \mathbf{Q} \star \mathbf{A}_n)$ is satisfied for all orthogonal tensors $\mathbf{Q}$ and all $\mathbf{A}_i$ in the domain of definition of f. In particular, f is isotropic if and only if the forms of its component functions are the same for all orthonormal bases (cf. Macvean 1968, Truesdell & Noll 1992).

length of a line element of material increases. For small strains, all strain measures are to be equivalent to the first order in some suitable measure of 'smallness' (cf. Ogden 1984). For rigid body motions, a measure of strain has to vanish.
As has been shown in the previous section, the material is unstrained if and only if $\mathbf{V} = \mathbf{U} = \mathbf{1}$. Therefore, according to Hill (1968), the criteria

$$\mathbf{e}^{(m)}(\mathbf{V} = \mathbf{1}) = \mathbf{E}^{(m)}(\mathbf{U} = \mathbf{1}) = \mathbf{0} \tag{3.82}$$

and

$$\left(\mathbf{e}^{(m)}\right)'\Big|_{\mathbf{V}=\mathbf{1}} = \left(\mathbf{E}^{(m)}\right)'\Big|_{\mathbf{U}=\mathbf{1}} = \mathbb{I} \tag{3.83}$$

may be postulated for positive or negative integers m. $\mathbb{I}$ is the symmetric fourth-order identity tensor and $(\cdot)'$ denotes the gradient of $(\cdot)$ with respect to $\mathbf{V}$ on the left-hand side of (3.83) respectively the gradient with respect to $\mathbf{U}$ in the middle term of (3.83). Then, in addition to the Green-Lagrangian and Almansi-Eulerian strain tensors defined above, the following strain tensors may be defined (cf. Ogden 1984)

$\mathbf{e}^{(m)}(\mathbf{V})$	$\mathbf{E}^{(m)}(\mathbf{U})$	
$\frac{1}{m}(\mathbf{V}^m - \mathbf{1})$	$\frac{1}{m}(\mathbf{U}^m - \mathbf{1})$	$(m \neq 0)$
$\ln\mathbf{V}$	$\ln\mathbf{U}$	$(m = 0)$.

(3.84)

They can be transformed between the current and reference configurations in the same way as the stretch and the Cauchy-Green tensors by the rotated correspondence

$$\mathbf{e}^{(m)} = \mathbf{R} \star \mathbf{E}^{(m)} \qquad \mathbf{E}^{(m)} = \mathbf{R}^{\mathrm{T}} \star \mathbf{e}^{(m)}. \tag{3.85}$$

Using the notion of eigenprojections introduced in Section 3.3.3, a general class of Eulerian and Lagrangian strain measures can be defined through one single scalar function, the *scale function* $f(\lambda_\sigma)$ (cf. Hill 1978, Xiao et al. 1998b), in the form

$$\begin{aligned} \mathbf{e}^{(m)} &= \sum_{\sigma=1}^{n} f(\lambda_\sigma)\mathbf{V}_\sigma & \mathbf{E}^{(m)} &= \sum_{\sigma=1}^{n} f(\lambda_\sigma)\mathbf{U}_\sigma \\ &= \sum_{\sigma=1}^{n} g(\chi_\sigma)\mathbf{B}_\sigma & &= \sum_{\sigma=1}^{n} g(\chi_\sigma)\mathbf{C}_\sigma \end{aligned} \tag{3.86}$$

with

$$f(\lambda_\sigma) = \frac{1}{m}(\lambda_\sigma^m - 1). \tag{3.87}$$

Here, the eigenprojections $\mathbf{V}_\sigma$, $\mathbf{U}_\sigma$ and $\mathbf{C}_\sigma$ of the left and right stretch tensors and the right Cauchy-Green Tensor, respectively, are introduced. They may be calculated using Sylvester's formula (3.70). Conditions (3.82) and (3.83) are then expressed as (cf. Hill 1978)

$$f(1) = 0 \qquad f'(1) = 1\,. \tag{3.88}$$

The Almansi-Eulerian strain tensor $\mathbf{e}$ defined over $\mathcal{B}$ and the Green-Lagrangian strain tensor $\mathbf{E}$ defined over $\mathcal{B}_0$ may be derived from (3.86_1) respectively (3.86_2) and (3.87) for $m = -2$ respectively $m = 2$

$$\mathbf{e} = \sum_{\sigma=1}^{n} \frac{1}{2}(1 - \lambda_\sigma^{-2})\mathbf{V}_\sigma = \frac{1}{2}(\mathbf{1} - \mathbf{V}^{-2}) \tag{3.89}$$

$$\mathbf{E} = \sum_{\sigma=1}^{n} \frac{1}{2}(\lambda_\sigma^{2} - 1)\mathbf{U}_\sigma = \frac{1}{2}(\mathbf{U}^{2} - \mathbf{1})\,. \tag{3.90}$$

Using the natural logarithmic scale function $g(\chi) = \frac{1}{2}\ln\chi$, Hencky's logarithmic strain measure can be found (Hencky 1928, Xiao et al. 1997b)

$$\mathbf{h} = \sum_{\sigma=1}^{n} \frac{1}{2}\ln\chi_\sigma \mathbf{B}_\sigma = \frac{1}{2}\ln\mathbf{B} \tag{3.91}$$

$$\mathbf{H} = \sum_{\sigma=1}^{n} \frac{1}{2}\ln\chi_\sigma \mathbf{C}_\sigma = \frac{1}{2}\ln\mathbf{C}\,. \tag{3.92}$$

The logarithmic strains $\mathbf{h}$ respectively $\mathbf{H}$ are of particular importance for the constitutive model proposed below. They possess some intrinsic advantages in contrast to other measures of strain, i.e. the property of additivity, readily observed in one-dimensional loading (cf. Ogden 1984, Xiao et al. 1998b). However, due to the transcendental form of logarithmic strain measures, their use was often limited to particular cases. Recently, it was shown by Xiao et al. that there exists an objective corotational rate of Hencky's Eulerian logarithmic strain measure $\mathbf{h}$ that is identical to the Eulerian stretching tensor $\mathbf{D}$, see Section 3.6.2.

For $m = 1$, the *Biot* strain tensor can be derived

$$\mathbf{E}^{(1)}(\mathbf{U}) = \sum_{\sigma=1}^{n}(\lambda_\sigma - 1)\mathbf{C}_\sigma = \mathbf{U} - \mathbf{1}\,. \tag{3.93}$$

The Biot tensor is used frequently for developing constitutive equations as the principal values of $\mathbf{U}$ are the elongations of line segments in the principal directions of $\mathbf{U}$ (Belytschko et al. 2000).

In the succeeding chapters, the focus will be on the Eulerian logarithmic strain $\mathbf{h}$ and an appropriate rate.

3.5 Objectivity

As has been pointed out before, the description of a physical quantity associated with the motion of a body generally depends on the choice of observer. However, in contrast to their kinematical descriptions, physical phenomena are independent of the choice of observer. In this section, an approach to determine the *objectivity*, i.e. the observer-independence of scalar, vector and tensor fields, is presented.
Given the observer transformation $(\mathbf{x}, t) \rightarrow (\mathbf{x}^*, t^*)$ as specified in (3.3)

$$\mathbf{x}^* = \mathbf{Q}(t)\mathbf{x} + \mathbf{c}(t) \quad \text{with} \quad t^* = t - a\,, \tag{3.94}$$

the motion (3.11) transforms to

$$\boldsymbol{\chi}^*(\mathbf{X}, t^*) = \mathbf{Q}(t)\boldsymbol{\chi}(\mathbf{X}, t) + \mathbf{c}(t) \quad \text{with} \quad t^* = t - a\,. \tag{3.95}$$

The definitions of velocity (3.18) and acceleration (3.19) are relative. Hence, they are linked to kinematics through the relative motion of the observers. This is reflected by the quantities $\dot{\mathbf{c}}(t)$, $\ddot{\mathbf{c}}(t)$, $\dot{\mathbf{Q}}(t)$ and $\ddot{\mathbf{Q}}(t)$ occurring in (3.25) and (3.26).
It has to be distinguished between the transformation rules for Eulerian tensors, Lagrangian tensors and two-point tensors, i.e. the transformation rule a tensor has to satisfy in order to be objective depends on the configuration it lives in.
Following Ogden (1984), Lagrangian scalars $\hat{\alpha}$, vectors $\hat{\boldsymbol{\alpha}}$ and tensors $\hat{\mathbf{A}}$ are objective if they are unaffected by an observer transformation

$$\hat{\alpha}^*(\mathbf{X}, t^*) = \hat{\alpha}(\mathbf{X}, t) \tag{3.96}$$

$$\hat{\boldsymbol{\alpha}}^*(\mathbf{X}, t^*) = \hat{\boldsymbol{\alpha}}(\mathbf{X}, t) \tag{3.97}$$

$$\hat{\mathbf{A}}^*(\mathbf{X}, t^*) = \hat{\mathbf{A}}(\mathbf{X}, t)\,. \tag{3.98}$$

On the other hand, Eulerian scalars α, vectors $\boldsymbol{\alpha}$ and tensors $\mathbf{A}$ are objective if they obey the transformation rules

$$\alpha^*(\mathbf{x}^*, t^*) = \alpha(\mathbf{x}, t) \tag{3.99}$$

$$\boldsymbol{\alpha}^*(\mathbf{x}^*, t^*) = \mathbf{Q}(t)\boldsymbol{\alpha}(\mathbf{x}, t) = \mathbf{Q}(t) \star \boldsymbol{\alpha}(\mathbf{x}, t) \tag{3.100}$$

$$\mathbf{A}^*(\mathbf{x}^*, t^*) = \mathbf{Q}(t)\mathbf{A}(\mathbf{x}, t)\mathbf{Q}(t)^{\mathrm{T}} = \mathbf{Q}(t) \star \mathbf{A}(\mathbf{x}, t)\,. \tag{3.101}$$

For second-order two-point tensors, Ogden (1984) defines the objectivity criterion

$$\tilde{\mathbf{A}}^*(\mathbf{X}, t^*) = \mathbf{Q}(t)\tilde{\mathbf{A}}(\mathbf{X}, t)\,. \tag{3.102}$$

Based on these definitions, the objectivity of the kinematical quantities introduced above may be examined. It should be noted that no distinction between

the terms *(observer) frame indifferent* and *objective* is made here.
Under a change of observer, for an observer-independent reference configuration the deformation gradient transforms to

$$\mathbf{F}^* = \mathbf{Q}\mathbf{F}\,. \tag{3.103}$$

Therefore, the deformation gradient $\mathbf{F}$ is an objective two-point tensor.
Its determinant, the Jacobian J, is unaffected by an observer transformation, i.e. the local volume ratio does not depend on its kinematical description

$$J^* = \det(\mathbf{F}^*) = \det(\mathbf{F}) = J\,. \tag{3.104}$$

The tensors $\mathbf{V}$ and $\mathbf{B}$ are objective Eulerian tensors

$$\mathbf{V}^* = \mathbf{Q} \star \mathbf{V} \qquad \mathbf{B}^* = \mathbf{Q} \star \mathbf{B} \tag{3.105}$$

and $\mathbf{U}$ and $\mathbf{C}$ are objective Lagrangian tensors

$$\mathbf{U}^* = \mathbf{U} \qquad \mathbf{C}^* = \mathbf{C}\,. \tag{3.106}$$

The rotation tensor $\mathbf{R}$ is an objective two-point tensor

$$\mathbf{R}^* = \mathbf{Q}\mathbf{R}\,. \tag{3.107}$$

It should be noted that if an Eulerian tensor is objective, then its Lagrangian counterpart via the rotated correspondence (3.85) is also objective, and vice versa (cf. Xiao et al. 1998b).
The transformation behavior under a change of observer exhibited by other relevant quantities will be examined as the respective quantities are introduced.

3.6 Analysis of motion

3.6.1 Deformation and strain rates

For the discussion of deformation and strain rates, the time dependence in the description of deformation (3.10) that was suppressed in (3.27) is included again

$$\mathbf{x} = \boldsymbol{\chi}(\mathbf{X}, t)\,. \tag{3.108}$$

Then, taking the material time derivative of the deformation gradient (3.31) and making use of the commutativity of the partial derivatives with respect to t and $\mathbf{X}$ resulting from the independence of these variables gives

$$\dot{\mathbf{F}} = \nabla_0 \otimes \dot{\boldsymbol{\chi}}(\mathbf{X}) = (\nabla \otimes \mathbf{v}(\mathbf{x}, t))\mathbf{F} = \mathbf{L}\mathbf{F}\,. \tag{3.109}$$

In this way, an alternative definition of the velocity gradient tensor $\mathbf{L}$ first introduced in (3.22) is obtained

$$\mathbf{L} = \frac{\partial \dot{\mathbf{x}}}{\partial \mathbf{x}} = \dot{\mathbf{F}}\mathbf{F}^{-1}. \tag{3.110}$$

The velocity gradient may be used to relate the material line element $\mathbf{dx}$ in $\mathcal{B}$ to its material time derivative

$$\mathbf{d}\dot{\mathbf{x}} = \mathbf{L}\mathbf{dx}, \tag{3.111}$$

which is derived by taking the material time derivative of equation (3.30) and using definition (3.110). Relative to a rectangular Cartesian basis, the velocity gradient has the components

$$L_{ij} = \frac{\partial v_i}{\partial x_j}. \tag{3.112}$$

Taking the material time derivative of definition (3.73_1) of the Green-Lagrangian strain tensor and applying (3.110) yields

$$\dot{\mathbf{E}} = \frac{1}{2}\mathbf{F}^{\mathrm{T}}\left(\mathbf{L} + \mathbf{L}^{\mathrm{T}}\right)\mathbf{F} = \mathbf{F}^{\mathrm{T}}\mathbf{D}\mathbf{F}, \tag{3.113}$$

where the *Eulerian strain rate* tensor or *stretching* tensor $\mathbf{D}$ is defined

$$\mathbf{D} = \frac{1}{2}\left(\mathbf{L} + \mathbf{L}^{\mathrm{T}}\right). \tag{3.114}$$

Until recently it was believed that the stretching tensor $\mathbf{D}$ is not in general expressible as either the Lagrangian or Eulerian time derivative of a strain tensor, so it was not considered a rate of strain (cf. Ogden 1984). However, Xiao et al. (1997b, 1998d) showed that the stretching is in fact integrable to deliver the Eulerian Hencky strain tensor $\mathbf{h}$ defined in (3.91), see the discussion below.

The stretching is a measure of the rate at which line elements of material are changing their length. Hence, a rigid-body motion requires $\mathbf{D} = \mathbf{0}$. In addition, $\mathbf{D}$ is also a measure of the rate of change of the angle of shear between line elements.

From (3.114) it follows that $\mathbf{D}$ is the symmetric part of the velocity gradient $\mathbf{L}$. The antisymmetric part of the additive decomposition

$$\mathbf{L} = \mathbf{D} + \mathbf{W} \tag{3.115}$$

is called the *vorticity* or *body spin* tensor $\mathbf{W}$

$$\mathbf{W} = \frac{1}{2}(\mathbf{L} - \mathbf{L}^{\mathrm{T}}). \tag{3.116}$$

If a motion is rigid, it represents a rigid-body rotation or spin with angular velocity $\boldsymbol{\omega}$, where $\boldsymbol{\omega}$ is the axial vector of $\mathbf{W}$; otherwise, the vorticity tensor contributes a rigid-body spin to the motion, and an additional component in terms of the stretching $\mathbf{D}$ describes the rotation of line elements superposed on the rigid body spin.
The following relations hold (cf. Ogden 1984)

$$\frac{\partial J}{\partial \mathbf{F}} = J\mathbf{F}^{-1} \qquad \dot{\mathbf{F}}\frac{\partial J}{\partial \mathbf{F}} = J\mathbf{L} \qquad \frac{\dot{J}}{J} = \operatorname{tr}(\mathbf{L}) = \operatorname{tr}(\mathbf{D})\,. \tag{3.117}$$

Under a change of observer, the velocity gradient transforms to

$$\mathbf{L}^* = \mathbf{Q} \star \mathbf{L} + \dot{\mathbf{Q}}\mathbf{Q}^{\mathrm{T}}\,. \tag{3.118}$$

It is therefore not an objective tensor. On the other hand, its additive decomposition $\mathbf{D}$ transforms objectively

$$\mathbf{D}^* = \mathbf{Q} \star \mathbf{D}\,, \tag{3.119}$$

while the vorticity tensor $\mathbf{W}$, as a measure of the rigid rotation of a triad of line elements, is influenced by the rotation of observers and is not an objective Eulerian tensor

$$\mathbf{W}^* = \mathbf{Q} \star \mathbf{W} + \dot{\mathbf{Q}}\mathbf{Q}^{\mathrm{T}}\,. \tag{3.120}$$

3.6.2 Spins and corotational rates

Under a change of observer or *change of frame*[5] as given by equation (3.3), the deformation $\boldsymbol{\chi}(\mathbf{X}, t)$ transforms to

$$\boldsymbol{\chi}^*(\mathbf{X}, t^*) = \mathbf{Q}(t)\boldsymbol{\chi}(\mathbf{X}, t) + \mathbf{c}(t) \quad \text{with} \quad t^* = t - a\,. \tag{3.121}$$

To simplify matters, in the following it is assumed that $a = 0$, i.e. a possible difference in time between the two frames is ignored.
In equation (3.121), the rotating frame $(\cdot)^*$ is defined by the skew-symmetric second-order Eulerian tensor $\mathbf{Q} = \mathbf{Q}(t)$. Alternatively, the rotating frame $(\cdot)^*$ may be defined by its spin $\boldsymbol{\Omega}^*$, which determines $\mathbf{Q}$ to within a constant proper orthogonal tensor through the linear tensorial differential equation (cf. Xiao et al. 1998b)

$$\boldsymbol{\Omega}^* = \dot{\mathbf{Q}}^{\mathrm{T}}\mathbf{Q} = -\mathbf{Q}^{\mathrm{T}}\dot{\mathbf{Q}}\,. \tag{3.122}$$

[5]The phrases *frame of reference* and *change of frame (of reference)* are used here as equivalents of *observer* and *change of observer*, although formally for an arbitrarily chosen observer, the assigned coordinate system for that observer represents the *frame of reference of the particular observer*. According to this definition, a change of frame of reference does not involve a change of observer.

This second definition of a rotating frame by its spin $\boldsymbol{\Omega}^*$, an Eulerian time-dependent skew-symmetric tensor, will be adopted here.
In the transformed ($\boldsymbol{\Omega}^*$-)frame, the objective symmetric time-dependent second-order Eulerian tensor $\mathbf{A}$ has the representation

$$\mathbf{A}^* = \mathbf{Q} \star \mathbf{A} = \mathbf{Q}\mathbf{A}\mathbf{Q}^{\mathrm{T}} . \tag{3.123}$$

The material time derivative of (3.123) then gives

$$\dot{\mathbf{A}}^* = \mathbf{Q}\dot{\mathbf{A}}\mathbf{Q}^{\mathrm{T}} + \dot{\mathbf{Q}}\mathbf{A}\mathbf{Q}^{\mathrm{T}} + \mathbf{Q}\mathbf{A}\dot{\mathbf{Q}}^{\mathrm{T}} = \mathbf{Q} \star \overset{\circ}{\mathbf{A}}{}^* , \tag{3.124}$$

where the *corotational rate* of the Eulerian tensor $\mathbf{A}$ defined by the Eulerian spin $\boldsymbol{\Omega}^*$ has been defined

$$\overset{\circ}{\mathbf{A}}{}^* = \dot{\mathbf{A}} + \mathbf{A}\boldsymbol{\Omega}^* - \boldsymbol{\Omega}^*\mathbf{A} . \tag{3.125}$$

Substituting (3.123) into (3.124), it is evident that the corotational rate of an objective Eulerian tensor defined by an Eulerian spin $\boldsymbol{\Omega}^*$ is a material time derivative in an $\boldsymbol{\Omega}^*$-frame

$$\mathbf{Q} \star \overset{\circ}{\mathbf{A}}{}^* = \overset{\cdot}{\overline{\mathbf{Q} \star \mathbf{A}}} . \tag{3.126}$$

This interpretation does not hold for tensors $\bar{\mathbf{A}}$ that are not objective.
Corotational rates of objective Eulerian and Lagrangian tensors must be objective rate measures to ensure that any superimposed rigid rotation motion has no effect on them (cf. Truesdell & Noll 1992). This condition is essential to the notion of work-conjugacy which will be presented in Section 4.4. However, of the infinitely many corotational rates possible, not every rate $\overset{\circ}{\mathbf{A}}{}^*$ of the objective Eulerian tensor $\mathbf{A}$ is objective. Generally, whether the corotational rate $\overset{\circ}{\mathbf{A}}{}^*$ is objective or not depends on its defining spin $\boldsymbol{\Omega}^*$, which should be associated with the deformation and motion of the deforming body in an appropriate manner (cf. Bruhns 2003).
The local deformation state and the rate-of-change of the local deformation state are characterized by the deformation gradient $\mathbf{F}$ and the velocity gradient $\mathbf{L}$. Therefore, the most general form of a spin tensor $\boldsymbol{\Omega}^*$ associated with the deformation and rotation of a deforming body is assumed by Xiao et al. (1998b) as

$$\boldsymbol{\Omega}^* = \boldsymbol{\Omega}^*(\mathbf{F}, \mathbf{L}) . \tag{3.127}$$

They specify necessary requirements that have to be fulfilled by the spin $\boldsymbol{\Omega}^*$ to ensure that it defines a reasonable objective rate. Based on these requirements, a general form of spins $\boldsymbol{\Omega}^*$ may be derived (cf. Xiao et al. 1998c)

$$\boldsymbol{\Omega}^* = \mathbf{W} + \sum_{\sigma \neq \tau}^{n} \bar{h}\left(\frac{\chi_\sigma}{\operatorname{tr}(\mathbf{B})}, \frac{\chi_\tau}{\operatorname{tr}(\mathbf{B})}\right) \mathbf{B}_\sigma \mathbf{D} \mathbf{B}_\tau . \tag{3.128}$$

Here and henceforth, the notation $\sum_{\sigma\neq\tau}^{n}(\cdot)$ represents the summation for all $\sigma,\tau = 1,\ldots,n$ with $\sigma \neq \tau$. The sum vanishes for $n = 1$.
All commonly known spins can be obtained from a subclass of these material spins

$$\mathbf{\Omega}^{*} = \mathbf{W} + \sum_{\sigma\neq\tau}^{n} h\left(\frac{\chi_\sigma}{\chi_\tau}\right)\mathbf{B}_\sigma\mathbf{D}\mathbf{B}_\tau\,, \tag{3.129}$$

where the simplified spin function $h(z^{-1})$ has the property

$$h(z^{-1}) = -h(z) \quad \forall\ z > 0\,. \tag{3.130}$$

A rotating frame which is defined by a material spin of the form (3.128) respectively (3.129) is called a corotating material frame. The time rate of an objective Eulerian tensor in a corotating material frame is an objective corotational rate and vice versa (Xiao et al. 1998b).
For example, $h^{\mathrm{J}}(z) = 0$ yields the vorticity tensor $\mathbf{W}$

$$\mathbf{\Omega}^{\mathrm{J}} = \mathbf{W}\,, \tag{3.131}$$

which by substitution into (3.125) defines the *Zaremba-Jaumann* rate

$$\overset{\circ}{\mathbf{A}}{}^{\mathrm{J}} = \dot{\mathbf{A}} + \mathbf{A}\mathbf{W} - \mathbf{W}\mathbf{A}\,. \tag{3.132}$$

The Zaremba-Jaumann rate is used frequently as an introductory example of objective corotational rates. However, in developing constitutive equations it should be used with care as it predicts oscillatory stresses under plane shear loading (cf. Lehmann 1972, Dienes 1979, Khan & Huang 1995).
For

$$h^{\mathrm{R}}(z) = \frac{1-\sqrt{z}}{1+\sqrt{z}}\,, \tag{3.133}$$

the *polar* spin $\mathbf{\Omega}^{\mathrm{R}}$ is obtained

$$\mathbf{\Omega}^{\mathrm{R}} = \dot{\mathbf{R}}\mathbf{R}^{\mathrm{T}} = \mathbf{W} + \sum_{\sigma\neq\tau}^{n} \frac{\sqrt{\chi_\tau}-\sqrt{\chi_\sigma}}{\sqrt{\chi_\tau}+\sqrt{\chi_\sigma}}\mathbf{B}_\sigma\mathbf{D}\mathbf{B}_\tau\,, \tag{3.134}$$

which defines the so-called *polar* or *Green-Naghdi* rate

$$\overset{\circ}{\mathbf{A}}{}^{\mathrm{R}} = \mathbf{R}\star\dot{\overline{\mathbf{R}^{\mathrm{T}}\star\mathbf{A}}} = \dot{\mathbf{A}} + \mathbf{A}\mathbf{\Omega}^{\mathrm{R}} - \mathbf{\Omega}^{\mathrm{R}}\mathbf{A}\,. \tag{3.135}$$

Evidently, the Eulerian counterpart of the material time rate of an objective Lagrangian tensor is the polar rate of the Eulerian counterpart of this tensor. This indicates that the material time rate of an objective Lagrangian tensor is a particular kind of corotational rate of this tensor, which is defined by the

Lagrangian spin $\mathbf{R}^{\mathrm{T}}\boldsymbol{\Omega}^{\mathrm{R}}\mathbf{R}$.
It has been shown that several widely used Eulerian rate type equations intended for characterizing elastic response cannot be integrated to yield an elastic relation (cf. Simo & Pister 1984). Both the Zaremba-Jaumann rate and the polar rate do not fulfill the *self-consistency condition* stating that, for each process of purely elastic deformation, a constitutive formulation of $\mathbf{D}^e$ intended for characterizing elastic response must be exactly-integrable to yield an elastic, in particular, a hyperelastic relation between an elastic strain measure and a stress measure. In this sense they are *self-inconsistent* (cf. Bruhns et al. 1999, Xiao et al. 2000b).
On the other hand, the Eulerian rate type formulation based on the stretching $\mathbf{D}$ as suggested by Xiao et al. (1997a, 1997b, 1998c, 1998d) has been shown to be self-consistent. It is based on the *logarithmic* spin

$$\boldsymbol{\Omega}^{\mathrm{Log}} = \mathbf{W} + \sum_{\sigma\neq\tau}^{n} \left(\frac{1+(\chi_\sigma/\chi_\tau)}{1-(\chi_\sigma/\chi_\tau)} + \frac{2}{\ln(\chi_\sigma/\chi_\tau)} \right) \mathbf{B}_\sigma \mathbf{D} \mathbf{B}_\tau \,, \tag{3.136}$$

which follows from (3.129) by substitution of the logarithmic spin function

$$h^{\mathrm{Log}}(z) = \frac{1+z}{1-z} + \frac{2}{\ln z} \,. \tag{3.137}$$

Adopting the logarithmic spin $\boldsymbol{\Omega}^{\mathrm{Log}}$, equation (3.125) takes the form

$$\overset{\circ}{\mathbf{A}}{}^{\mathrm{Log}} = \dot{\mathbf{A}} + \mathbf{A}\boldsymbol{\Omega}^{\mathrm{Log}} - \boldsymbol{\Omega}^{\mathrm{Log}}\mathbf{A} \,. \tag{3.138}$$

The objective corotational rate $\overset{\circ}{\mathbf{A}}{}^{\mathrm{Log}}$ is called the *logarithmic rate* of $\mathbf{A}$.
For a long time it was believed that the stretching tensor $\mathbf{D}$ cannot be written as a direct flux of a strain measure (cf. Ogden 1984), in spite of the names *rate of deformation* or *Eulerian strain rate* given to $\mathbf{D}$. Recently, it was proved that for the logarithmic rate of the Eulerian Hencky strain $\mathbf{h}$ the relation

$$\overset{\circ}{\mathbf{h}}{}^{\mathrm{Log}} = \dot{\mathbf{h}} + \mathbf{h}\boldsymbol{\Omega}^{\mathrm{Log}} - \boldsymbol{\Omega}^{\mathrm{Log}}\mathbf{h} = \mathbf{D} \tag{3.139}$$

holds (cf. Xiao et al. 1997b, 1998c, 1998d; see also Reinhardt & Dubey 1995, 1996): The objective corotational rate of Hencky's Eulerian logarithmic strain measure defined by the logarithmic spin $\boldsymbol{\Omega}^{\mathrm{Log}}$ (3.136) is identical to the Eulerian stretching tensor $\mathbf{D}$, i.e. in a corotating material frame $\mathbf{D}$ is a *true* time rate of $\mathbf{h}$, and $\mathbf{h}$ is the only strain measure enjoying this property.
The proper orthogonal tensor $\mathbf{R}^{\mathrm{Log}}$ defined by the linear tensorial differential equation

$$\dot{\mathbf{R}}^{\mathrm{Log}} = -\mathbf{R}^{\mathrm{Log}}\boldsymbol{\Omega}^{\mathrm{Log}} \qquad \mathbf{R}^{\mathrm{Log}}\big|_{t=0} = \mathbf{1} \tag{3.140}$$

is called *logarithmic rotation*. Using $\mathbf{R}^{\mathrm{Log}}$, the rotated correspondence

$$\overline{\mathbf{R}^{\mathrm{Log}} \star \mathbf{A}}^{\cdot} = \mathbf{R}^{\mathrm{Log}} \star \overset{\circ}{\mathbf{A}}{}^{\mathrm{Log}} \tag{3.141}$$

holds true, which is of particular interest when it is applied to $\mathbf{h}$ using the kinematical relation (3.139)

$$\overline{\mathbf{R}^{\mathrm{Log}} \star \mathbf{h}}^{\cdot} = \mathbf{R}^{\mathrm{Log}} \star \mathbf{D}\,. \tag{3.142}$$

The left-hand side of (3.141) represents the material time rate of a Lagrangian tensor. This measure can be integrated with respect to time and rotated forward into the current configuration to give

$$\mathbf{A} = (\mathbf{R}^{\mathrm{Log}})^{\mathrm{T}} \star \int_0^t \mathbf{R}^{\mathrm{Log}} \star \overset{\circ}{\mathbf{A}}{}^{\mathrm{Log}} \mathrm{d}s\,. \tag{3.143}$$

This technique is called *corotational integration* (cf. Khan & Huang 1995). Corotational integration of the stretching $\mathbf{D}$ gives the Eulerian Hencky strain $\mathbf{h}$. The logarithmic rate is the rate-of-change observed in a rotating frame with the logarithmic spin $\boldsymbol{\Omega}^{\mathrm{Log}}$, which does not coincide with a rotating frame with the polar spin $\boldsymbol{\Omega}^{\mathrm{R}}$. In a rotating frame with the polar spin $\boldsymbol{\Omega}^{\mathrm{R}}$, each $\mathbf{R}$-rotated material symmetry axis keeps unchanged. Therefore, for an initially anisotropic material, the contribution of the rates of the $\mathbf{R}$-rotated material symmetry axes must be incorporated in a rate equation for $\mathbf{D}^e$. The resulting relationship between the logarithmic rate (3.138) and the polar rate (3.135) is

$$\overset{\circ}{\mathbf{A}}{}^{\mathrm{Log}} = \overset{\circ}{\mathbf{A}}{}^{\mathrm{R}} + \mathbf{A}\boldsymbol{\Omega}^{\mathrm{LR}} - \boldsymbol{\Omega}^{\mathrm{LR}}\mathbf{A}\,. \tag{3.144}$$

Here, the spin tensor

$$\boldsymbol{\Omega}^{\mathrm{LR}} = \boldsymbol{\Omega}^{\mathrm{Log}} - \boldsymbol{\Omega}^{\mathrm{R}} = \sum_{\sigma \neq \tau}^{n} \left(\frac{2\sqrt{\chi_\sigma/\chi_\tau}}{1 - (\chi_\sigma/\chi_\tau)} + \frac{2}{\ln(\chi_\sigma/\chi_\tau)} \right) \mathbf{B}_\sigma \mathbf{D} \mathbf{B}_\tau \tag{3.145}$$

was defined from (3.136) and (3.134) (cf. Xiao et al. 2000b).

3.7 Decomposition of finite deformation

For processes of combined elastic and inelastic material behavior, the respective elastic and inelastic components of the deformation have to be determined. In a linear theory of small strains, the additive decomposition

$$\dot{\boldsymbol{\varepsilon}} = \dot{\boldsymbol{\varepsilon}}^e + \dot{\boldsymbol{\varepsilon}}^i \tag{3.146}$$

of the total strain rate $\dot{\boldsymbol{\varepsilon}}$ into its elastic component $\dot{\boldsymbol{\varepsilon}}^e$ and its inelastic component $\dot{\boldsymbol{\varepsilon}}^i$ is frequently used. For the general case of finite deformations, there

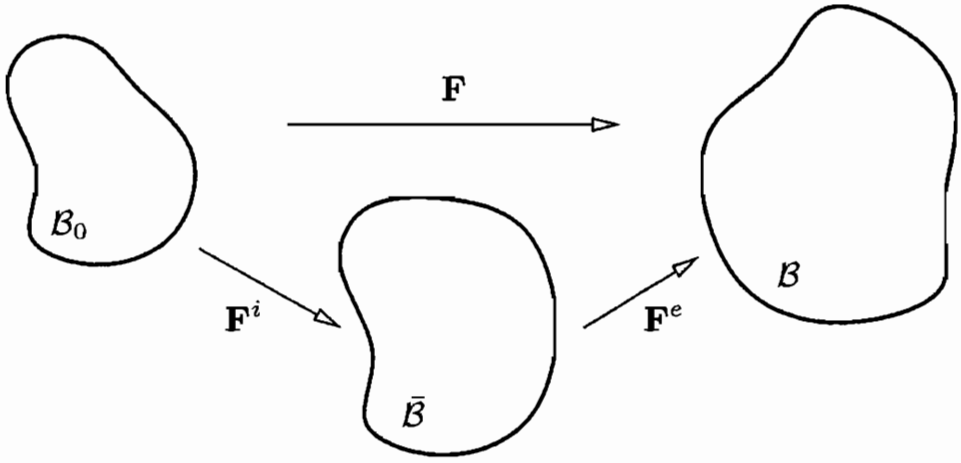

Figure 3.3: Multiplicative decomposition of the deformation gradient

has been some debate on the appropriate decomposition (cf. Naghdi 1990, Xiao et al. 2000b).
Here, for each process of elastic-inelastic deformation the additive decomposition of the total stretching $\mathbf{D}$ into an elastic part $\mathbf{D}^e$ and a coupled elastic-inelastic part $\mathbf{D}^{ei}$ is assumed (cf. Xiao et al. 2000b)

$$\mathbf{D} = \mathbf{D}^e + \mathbf{D}^{ei}. \tag{3.147}$$

The additive decomposition was successfully applied to small and finite deformation elastoplasticity theories (cf. Drucker 1988, Nemat-Nasser 1983, 1992). In a natural and direct manner, the elastic part $\mathbf{D}^e$ may be interpreted as the deformation rate related to the elastic deformation $\mathbf{F}^e$ in equation (3.148) below. The coupled elastic-inelastic part $\mathbf{D}^{ei}$ is associated with both the elastic deformation $\mathbf{F}^e$ and the inelastic deformation $\mathbf{F}^i$. When there is no change in the microstructure responsible for inelastic deformation[6], the deformation is purely elastic and the elastic part $\mathbf{D}^e$ corresponds to the total stretching $\mathbf{D}$. From the decomposition (3.147), it is not possible to determine which part of the total deformation $\mathbf{F}$ is inelastic. However, in general there is no a priori definition of the elastic and the inelastic deformations, either. To appropriately relate $\mathbf{D}^e$ and $\mathbf{D}^{ei}$ to *elastic deformation* and *inelastic deformation*, the multiplicative decomposition of the deformation gradient $\mathbf{F}$ into its elastic and inelastic parts $\mathbf{F}^e$ respectively $\mathbf{F}^i$ as depicted in Figure 3.3 is considered

$$\mathbf{F} = \mathbf{F}^e\mathbf{F}^i. \tag{3.148}$$

This decomposition is attributed to Lee (1969), but it was first introduced by

[6]The general term of *inelastic* deformation will be specified to include only deformation due to martensitic phase transformation in Chapter 6.

Kröner (1960) with reference to linear theory. Applying the polar decomposition theorem (3.44) to $\mathbf{F}^e$ and $\mathbf{F}^i$ gives

$$\mathbf{F}^e = \mathbf{V}^e\mathbf{R}^e = \mathbf{R}^e\mathbf{U}^e \tag{3.149}$$

respectively

$$\mathbf{F}^i = \mathbf{V}^i\mathbf{R}^i = \mathbf{R}^i\mathbf{U}^i\,. \tag{3.150}$$

For each process of purely elastic deformation, $\mathbf{F}^e$ equals $\mathbf{F}$.
The determinants of both the elastic and the inelastic parts of the deformation are required to be non-negative

$$\det(\mathbf{F}^e) > 0 \qquad \det(\mathbf{F}^i) > 0\,. \tag{3.151}$$

Inelastic deformations due to plasticity are generally treated as volume preserving. Then, changes in volume are associated with elastic deformation alone, $J = \det(\mathbf{F}^e)$.
By decomposition (3.148), an additional configuration, the stress-free *intermediate configuration* $\bar{\mathcal{B}}$ is introduced. At each moment in time, $\bar{\mathcal{B}}$ is reached by elastic unloading from $\mathcal{B}$. The elastic part of the deformation $\mathbf{F}^e$ is associated with a motion from the intermediate configuration $\bar{\mathcal{B}}$ to the current configuration $\mathcal{B}$, while the inelastic part of the deformation relates the reference configuration $\mathcal{B}_0$ with the intermediate configuration $\bar{\mathcal{B}}$.
Taking the initial, natural state of the material as the reference configuration, the initial condition for the deformation gradient is

$$\mathbf{F}|_{t=0} = \mathbf{1}\,. \tag{3.152}$$

From this, it is evident that the three configurations $\mathcal{B}_0$, $\mathcal{B}$ and $\bar{\mathcal{B}}$ coincide at the initial instant $t = 0$. However, an arbitrary rigid body rotation superposed on the intermediate configuration has no effect on decomposition (3.148)

$$\mathbf{F} = \mathbf{F}^e\mathbf{F}^i = \bar{\mathbf{F}}^e\bar{\mathbf{F}}^i\,, \tag{3.153}$$

where

$$\bar{\mathbf{F}}^e = \mathbf{F}^e\mathbf{Q} \qquad \bar{\mathbf{F}}^i = \mathbf{Q}^{\mathrm{T}}\mathbf{F}^i\,. \tag{3.154}$$

As a consequence, $\mathbf{F}^e$ and $\mathbf{F}^i$ can be determined only to within an arbitrary rotation $\mathbf{Q}$. Due to this fact, the initial conditions for the intermediate and the reference configurations may differ by a rigid body rotation.
However, the stated indeterminacy is of greater consequence if it is removed in constitutive modeling by adopting an additional assumption, i.e. choosing $\mathbf{F}^e = \mathbf{V}^e$ and thus ignoring the elastic rotation $\mathbf{R}^e$. This widely used assumption is inconsistent with the invariance requirement under a change of observer in a general sense (cf. Casey & Naghdi 1981, Naghdi 1990), and

no use of it will be made here. Instead, a relationship between decompositions (3.147) and (3.148) will be established.
With (3.148), from definition (3.110) and the material time derivative of the deformation gradient

$$\dot{\mathbf{F}} = \dot{\mathbf{F}}^e\mathbf{F}^i + \mathbf{F}^e\dot{\mathbf{F}}^i \tag{3.155}$$

the decomposition

$$\mathbf{L} = \dot{\mathbf{F}}\mathbf{F}^{-1} = \mathbf{L}^e + \mathbf{F}^e\mathbf{L}^i\mathbf{F}^{-e} \tag{3.156}$$

may be derived. Here, the elastic and inelastic parts of the velocity gradient, $\mathbf{L}^e$ respectively $\mathbf{L}^i$, are defined as

$$\mathbf{L}^e = \dot{\mathbf{F}}^e\mathbf{F}^{-e} \qquad \mathbf{L}^i = \dot{\mathbf{F}}^i\mathbf{F}^{-i}. \tag{3.157}$$

Substitution into (3.114) and (3.116) gives

$$\mathbf{D} = \mathrm{sym}(\mathbf{L}^e) + \mathrm{sym}(\mathbf{F}^e\mathbf{L}^i\mathbf{F}^{-e}) \tag{3.158}$$

$$\mathbf{W} = \mathrm{skw}(\mathbf{L}^e) + \mathrm{skw}(\mathbf{F}^e\mathbf{L}^i\mathbf{F}^{-e}). \tag{3.159}$$

By comparison of (3.147) and (3.158), a natural and direct relationship between the decompositions (3.147) and (3.148) is obtained

$$\mathbf{D}^e = \mathrm{sym}(\dot{\mathbf{F}}^e\mathbf{F}^{-e}) \qquad \mathbf{D}^{ei} = \mathrm{sym}(\mathbf{F}^e\dot{\mathbf{F}}^i\mathbf{F}^{-i}\mathbf{F}^{-e}). \tag{3.160}$$

The result explains the name *coupled elastic-inelastic part* of $\mathbf{D}$ previously assigned to $\mathbf{D}^{ei}$.
Adopting the relationship supplied by equation (3.160) between the decompositions (3.147) and (3.148), without any assumptions relating to $\mathbf{F}^e$ or $\mathbf{F}^i$, the elastic and inelastic parts $\mathbf{F}^e$ respectively $\mathbf{F}^i$ in the decomposition (3.148), as well as all their related kinematical quantities, can be determined consistently and uniquely by (3.160) in conjunction with an appropriate elastic equation for the elastic part of the left stretch tensor $\mathbf{V}^e$ (cf. Xiao et al. 2000b). In addition, it was shown by Xiao et al. (2000b) that the invariance requirement stated by Casey & Naghdi (1981) and Naghdi (1990) is obeyed in a full sense, as the transformation rules

$$\mathbf{F}^{e*} = \mathbf{Q}\mathbf{F}^e\bar{\mathbf{Q}}^T \qquad \mathbf{F}^{i*} = \bar{\mathbf{Q}}\mathbf{F}^i \tag{3.161}$$

hold. Here, the rotation $\bar{\mathbf{Q}}$ is the rotation of the initial intermediate configuration in the transformed frame $\bar{\mathcal{B}}^*|_{t=0}$ relative to the initial configuration in the transformed frame $\mathcal{B}_0^*$.
Due to these properties, the presented theory is used as kinematical framework underlying finite elastoplasticity models with and without damage (cf. Xiao et al. 2000b, Bruhns et al. 2001, Bongmba & Bruhns 2001). It will be adopted to the formulation of a constitutive law describing pseudoelastic material behavior in the following chapters.

4 Conservation equations and stress measures

4.1 Introduction

The kinematical relations given in the previous chapter have to be complemented by appropriate balance laws. In this chapter, the principles of conservation of mass, linear and angular momentum as well as the conservation of mechanical energy are presented both in Eulerian and Lagrangian formulations.
The formulation of constitutive equations has to be preceded by the definition of appropriate stress measures and stress rates which obey the principle of frame indifference introduced above. Hence, the stress tensors and stress rates underlying the subsequent considerations are specified and interpreted.
In Section 4.4, the notion of work conjugacy attributed to Hill (1968, 1978) and recently extended to Eulerian measures of stress and strain by Xiao et al. (1998b) is introduced. The chapter is completed by specifying the weak form of the balance of momentum equation in a Eulerian and a Lagrangian formulation. The rate form of this equation plays a fundamental role in the numerical solution of elastic-inelastic material laws.
The subsequent derivations are based in part on the monographs by Ogden (1984) and Simo & Hughes (1998) and complemented by the books of Chadwick (1976) and Belytschko et al. (2000).

4.2 Conservation laws

4.2.1 Conservation of mass

For arbitrary bodies B, the *mass* is defined by the function

$$m(B) \geq 0\,. \tag{4.1}$$

The mass $m(B)$ is inherent to the body B and independent of its motion. It is an objective scalar, independent of the configuration occupied by B as perceived by an arbitrary observer

$$\dot{m}(B) = 0\,. \tag{4.2}$$

Equation (4.2) is an expression for the principle of *conservation of mass* (cf. Ogden 1984). It is also referred to as *continuity equation.* For each configuration $\mathcal{B}$ of the body B, there exists a scalar field called the mass *density* $\rho(\mathbf{x}, t) \geq 0$ of the material of B in $\mathcal{B}$. In the reference configuration $\mathcal{B}_0$, the density is denoted by ρ_0. Thus, for a volume element dv for $\mathcal{B}$ and a volume element dV for $\mathcal{B}_0$, the mass is given by

$$m = \int_{\mathcal{B}} \rho \, \mathrm{d}v = \int_{\mathcal{B}_0} \rho_0 \, \mathrm{d}V\,. \tag{4.3}$$

Using (3.35), invoking the smoothness of the integrand yields the following local form of the principle of conservation of mass

$$\rho = J^{-1}\rho_0 \,. \tag{4.4}$$

Noting (3.39) in conjunction with (3.110) and (3.115), the material time derivative of (4.4) may be written as

$$\dot{J} = J\,\nabla \cdot \mathbf{v} = J\mathrm{tr}\,(\mathbf{D})\,. \tag{4.5}$$

Hence, the usual dynamic form of mass conservation is obtained

$$\dot{\rho} + \rho\nabla \cdot \mathbf{v} = 0\,, \tag{4.6}$$

or equivalently, using $\nabla \cdot (\rho\mathbf{v}) = \nabla\rho \cdot \mathbf{v} + \rho\nabla \cdot \mathbf{v}$,

$$\frac{\partial \rho}{\partial t} + \nabla \cdot (\rho\mathbf{v}) = 0\,. \tag{4.7}$$

The corresponding global form of the continuity equation is

$$\int_{\mathcal{B}} [\dot{\rho} + \rho\nabla \cdot (\mathbf{v})]\,\mathrm{d}v = 0\,. \tag{4.8}$$

4.2.2 Conservation of linear momentum

In the Eulerian configuration, the *linear momentum* of the body B is defined as

$$\int_{\mathcal{B}} \rho\mathbf{v}\,\mathrm{d}v\,. \tag{4.9}$$

Newton's second law of motion, the principle of *conservation of linear momentum* or simply *momentum conservation* principle, is obtained by considering an arbitrary configuration $\mathcal{B}$ of B with boundary $\partial\mathcal{B}$, subjected to *body forces* and to *contact forces*

$$\int_{\mathcal{B}} \rho\mathbf{b}\,\mathrm{d}v + \int_{\partial\mathcal{B}} \mathbf{t}\,\mathrm{d}a\,. \tag{4.10}$$

Here, the *body-force density* $\mathbf{b}$ acting over $\mathcal{B}$ is a force per unit mass and the *contact-force density* $\mathbf{t}$ acting over $\partial\mathcal{B}$ is a force per unit area, with $\mathbf{b} = \mathbf{b}(\mathbf{x}, t)$ and $\mathbf{t} = \mathbf{t}(\partial\mathcal{B}, \mathbf{x}, t)$.

The forces on a given body which arise from external influences are independent of the observer or frame of reference. Hence, it must be distinguished between these *applied* forces and *inertial* forces, which depend fundamentally

on the choice of observer and his frame of reference. Both the body-force density $\mathbf{b}$ and the contact-force density $\mathbf{t}$, also called *traction* or *stress vector*, are objective Eulerian vector fields and transform according to rule (3.100).
Newton's second law of motion states that the material time derivative of the linear momentum defined in (4.9) equals the resultant applied force (4.10)

$$\frac{\mathrm{d}}{\mathrm{dt}} \int_{\mathcal{B}} \rho \mathbf{v} \, \mathrm{d}v = \int_{\mathcal{B}} \rho \mathbf{b} \, \mathrm{d}v + \int_{\partial \mathcal{B}} \mathbf{t} \, \mathrm{d}a \,. \tag{4.11}$$

4.2.3 Conservation of angular momentum

The *rotational momentum* of B with respect to a point $\mathbf{x}_0$ is defined as

$$\int_{\mathcal{B}} \rho(\mathbf{x} - \mathbf{x}_0) \times \mathbf{v} \, \mathrm{d}v \,. \tag{4.12}$$

Here, the point $\mathbf{x}_0$ of $\mathcal{E}$ is not required to be a point of $\mathcal{B}$. However, the value of the rotational momentum, sometimes called *moment of momentum*, depends on the choice of $\mathbf{x}_0$.
The resultant moment or *torque* of the applied forces about $\mathbf{x}_0$ is

$$\int_{\mathcal{B}} \rho(\mathbf{x} - \mathbf{x}_0) \times \mathbf{b} \, \mathrm{d}v + \int_{\partial \mathcal{B}} (\mathbf{x} - \mathbf{x}_0) \times \mathbf{t} \, \mathrm{d}a \,. \tag{4.13}$$

As the moment of the applied forces depends on the choice of the point $\mathbf{x}_0$, it is not objective.
Similarly to the balance of linear momentum, there is a balance between the resultant moment of the applied forces and the rate of change of the rotational momentum of the body, the *balance of rotational momentum*

$$\frac{\mathrm{d}}{\mathrm{dt}} \int_{\mathcal{B}} \rho(\mathbf{x} - \mathbf{x}_0) \times \mathbf{v} \, \mathrm{d}v = \int_{\mathcal{B}} \rho(\mathbf{x} - \mathbf{x}_0) \times \mathbf{b} \, \mathrm{d}v + \int_{\partial \mathcal{B}} (\mathbf{x} - \mathbf{x}_0) \times \mathbf{t} \, \mathrm{d}a \,. \tag{4.14}$$

Balances (4.11) and (4.14) are independent of each other and known as *Euler's laws of motion.*

4.2.4 Cauchy's laws of motion

According to *Cauchy's fundamental postulate*, the traction $\mathbf{t}$ at a position $\mathbf{x}$ depends on the surface through the unit normal $\mathbf{n}$ to the considered surface at $\mathbf{x}$, and on the time t. If the stress vector is continuous in $\mathbf{x}$, the dependence on $\mathbf{n}$ is linear

$$\mathbf{t}(\mathbf{x}, \mathbf{n}, t) = \boldsymbol{\sigma}(\mathbf{x}, t)\mathbf{n} \,. \tag{4.15}$$

This relation is known as *Cauchy's theorem.* The objective Eulerian second-order tensor field $\boldsymbol{\sigma}$ independent of $\mathbf{n}$ is the *Cauchy stress* tensor, also referred to as *true stress* tensor.
In component notation with respect to a rectangular Cartesian basis, equation (4.15) reads

$$t_i = \sigma_{ij} n_j \,. \tag{4.16}$$

Hence, σ_{ij} may be interpreted as the $\mathbf{e}_i$-component of the force per unit area on an element of surface in $\mathcal{B}$ whose unit normal is in the $\mathbf{e}_j$-direction.
Using Cauchy's theorem, the balance of momentum equation (4.11) is written in the form

$$\frac{\mathrm{d}}{\mathrm{dt}} \int_{\mathcal{B}} \rho \mathbf{v} \, \mathrm{d}v = \int_{\mathcal{B}} \rho \mathbf{b} \, \mathrm{d}v + \int_{\partial \mathcal{B}} \boldsymbol{\sigma} \mathbf{n} \, \mathrm{d}a \,. \tag{4.17}$$

Application of the divergence theorem to the surface integral on the right-hand side gives

$$\int_{\mathcal{B}} \left[\rho \dot{\mathbf{v}} - \rho \mathbf{b} - \nabla \cdot \boldsymbol{\sigma}^{\mathrm{T}} \right] \mathrm{d}v = \mathbf{0} \,. \tag{4.18}$$

Then invoking the arbitrariness of the domain for continuous ρ, $\mathbf{b}$ and $\dot{\mathbf{v}}$, and for $\boldsymbol{\sigma}$ once continuously differentiable, the local form known as *Cauchy's first law of motion*

$$\nabla \cdot \boldsymbol{\sigma}^{\mathrm{T}} + \rho \mathbf{b} = \rho \dot{\mathbf{v}} \tag{4.19}$$

is obtained. Here, the relation

$$\frac{\mathrm{d}}{\mathrm{dt}} \int_{\mathcal{B}} \rho \boldsymbol{\varphi} \, \mathrm{d}v = \int_{\mathcal{B}} \rho \dot{\boldsymbol{\varphi}} \, \mathrm{d}v \,, \tag{4.20}$$

valid for arbitrary scalar, vector or tensor fields $\boldsymbol{\varphi}$ defined over $\mathcal{B}$, is used.
In terms of rectangular Cartesian components, Cauchy's first law of motion (4.19) reads

$$\frac{\partial \sigma_{ij}}{\partial x_j} + \rho b_i = \rho \dot{v}_i \,. \tag{4.21}$$

Substitution of (4.19) into the balance of rotational momentum (4.14) gives

$$\int_{\mathcal{B}} (\mathbf{x} - \mathbf{x}_0) \times \nabla \cdot \boldsymbol{\sigma}^{\mathrm{T}} \, \mathrm{d}v = \int_{\partial \mathcal{B}} (\mathbf{x} - \mathbf{x}_0) \times \boldsymbol{\sigma} \mathbf{n} \, \mathrm{d}a \,. \tag{4.22}$$

Noting that $\mathbf{u} \times \mathbf{v}$ is the axial vector of the antisymmetric second-order tensor $\mathbf{v} \otimes \mathbf{u} - \mathbf{u} \otimes \mathbf{v}$ for arbitrary vectors $\mathbf{u}$ and $\mathbf{v}$, the rotational momentum balance may be written in the form (cf. Chadwick 1976, Ogden 1984)

$$\int_{\mathcal{B}} \{(\mathbf{x} - \mathbf{x}_0) \otimes (\nabla \cdot \boldsymbol{\sigma}^{\mathrm{T}}) - (\nabla \cdot \boldsymbol{\sigma}^{\mathrm{T}}) \otimes (\mathbf{x} - \mathbf{x}_0)\} \, \mathrm{d}v = \int_{\partial\mathcal{B}} \{(\mathbf{x} - \mathbf{x}_0) \otimes (\boldsymbol{\sigma}\mathbf{n}) - (\boldsymbol{\sigma}\mathbf{n}) \otimes (\mathbf{x} - \mathbf{x}_0)\} \, \mathrm{d}a \,. \quad (4.23)$$

Application of the divergence theorem to the surface integral on the right-hand side and the relation

$$\nabla \cdot (\boldsymbol{\sigma}^{\mathrm{T}} \otimes (\mathbf{x} - \mathbf{x}_0)) = (\nabla \cdot \boldsymbol{\sigma}^{\mathrm{T}}) \otimes (\mathbf{x} - \mathbf{x}_0) + \boldsymbol{\sigma} \quad (4.24)$$

lead to

$$\int_{\mathcal{B}} (\boldsymbol{\sigma} - \boldsymbol{\sigma}^{\mathrm{T}}) \, \mathrm{d}v = \mathbf{0} \,. \quad (4.25)$$

Invoking the arbitrariness of $\mathcal{B}$ for continuous $\boldsymbol{\sigma}$ yields *Cauchy's second law of motion*

$$\boldsymbol{\sigma}^{\mathrm{T}} = \boldsymbol{\sigma} \,. \quad (4.26)$$

By virtue of (4.19), the balance of rotational momentum is equivalent to Cauchy's second law of motion (4.26), which may be expressed in rectangular Cartesian components to give

$$\sigma_{ij} = \sigma_{ji} \,. \quad (4.27)$$

As a consequence of symmetry (4.26), the Cauchy stress tensor $\boldsymbol{\sigma}$ is expressible in the spectral representation defined in Section 3.3.3. However, in general the eigenvectors of $\boldsymbol{\sigma}$ do not coincide with the directions of the Eulerian principal axes $\mathbf{n}^i$ introduced in (3.64). This is true for isotropic elastic solids only.
The *Eulerian field equations*, i.e. the equation of mass conservation (4.6), and Cauchy's laws of motions (4.19) and (4.26), are summarized in Figure 4.1.

Conservation of mass	$\dot{\rho} + \rho \nabla \cdot \mathbf{v} = 0$
Cauchy's first law of motion	$\nabla \cdot \boldsymbol{\sigma}^{\mathrm{T}} + \rho \mathbf{b} = \rho \dot{\mathbf{v}}$
Cauchy's second law of motion	$\boldsymbol{\sigma}^{\mathrm{T}} = \boldsymbol{\sigma}$

Figure 4.1: Eulerian field equations

4.3 Stress measures and stress rates

4.3.1 Lagrangian and two-point stress measures

The description of nonlinear problems requires the definition of additional stress measures that are related to the reference configuration.
The Cauchy stress tensor $\boldsymbol{\sigma}$ is a Eulerian stress measure. Using Nanson's formula (3.42)

$$\mathbf{da} = J\mathbf{F}^{-\mathrm{T}}\mathbf{dA} \tag{4.28}$$

to express the resultant contact force on the boundary $\partial\mathcal{B}$ of the current configuration $\mathcal{B}$ in terms of the force on the referential boundary $\partial\mathcal{B}_0$ of $\mathcal{B}_0$ gives

$$\int_{\partial\mathcal{B}} \boldsymbol{\sigma}\mathbf{n}\,\mathrm{d}a = \int_{\partial\mathcal{B}_0} J\boldsymbol{\sigma}\mathbf{F}^{-\mathrm{T}}\mathbf{N}\,\mathrm{d}A\,, \tag{4.29}$$

where the unit normal to the boundary $\partial\mathcal{B}_0$ is denoted by $\mathbf{N}$ and the element of surface in the reference configuration by dA.
With the definition of the *first Piola-Kirchhoff stress* tensor $\mathbf{T}$

$$\mathbf{T} = J\boldsymbol{\sigma}\mathbf{F}^{-\mathrm{T}}\,, \tag{4.30}$$

the resultant force on the boundary $\partial\mathcal{B}_0$ may also be written as

$$\int_{\partial\mathcal{B}_0} J\boldsymbol{\sigma}\mathbf{F}^{-\mathrm{T}}\mathbf{N}\,\mathrm{d}A = \int_{\partial\mathcal{B}_0} \mathbf{T}\mathbf{N}\,\mathrm{d}A\,. \tag{4.31}$$

The first Piola-Kirchhoff stress is an objective two-point tensor which is induced from $J\boldsymbol{\sigma}$. Its transpose is called the *nominal stress* tensor[7] $\mathbf{P}$

$$\mathbf{P} = \mathbf{T}^{\mathrm{T}} = J\mathbf{F}^{-1}\boldsymbol{\sigma}\,. \tag{4.32}$$

With respect to rectangular Cartesian Lagrangian and Eulerian bases, $\{\mathbf{E}_\alpha\}$ of $\mathcal{B}_0$ and $\{\mathbf{e}_i\}$ of $\mathcal{B}$, the components of the first Piola-Kirchhoff stress and the nominal stress tensor are

$$\mathbf{T} = T_{i\alpha}\mathbf{e}_i \otimes \mathbf{E}_\alpha \qquad \mathbf{P} = P_{\alpha i}\mathbf{E}_\alpha \otimes \mathbf{e}_i\,. \tag{4.33}$$

The Eulerian load vector $\mathbf{dl} = \mathbf{t}\,da$ on an element of surface da in $\mathcal{B}$ can be expressed as

$$\mathbf{dl} = \boldsymbol{\sigma}\mathbf{da} = \mathbf{TdA}\,. \tag{4.34}$$

[7] The nomenclature used by different authors is contradictory. The definition adopted here is given by Ogden (1984) and Truesdell & Noll (1992). However, Malvern (1969) and Simo & Hughes (1998) call $\mathbf{P}$ the first Piola-Kirchhoff stress.

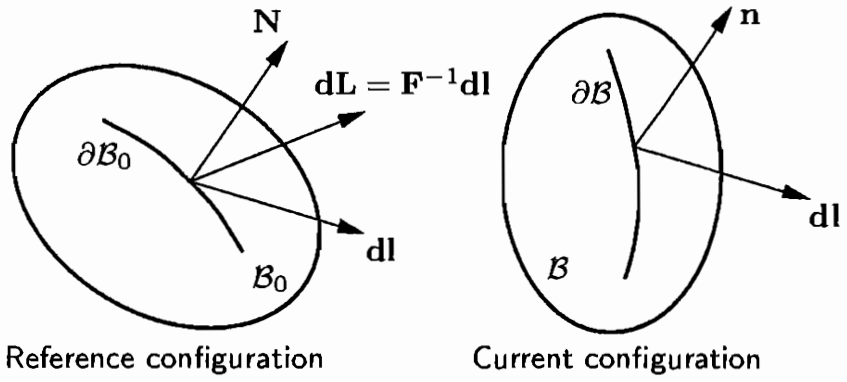

Cauchy stress	$\mathbf{dl} = \boldsymbol{\sigma}\mathbf{da}$
First Piola-Kirchhoff stress	$\mathbf{dl} = \mathbf{TdA}$
Second Piola-Kirchhoff stress	$\mathbf{dL} = \mathbf{SdA}$

Figure 4.2: Definition of stress measures

Hence, component $T_{i\alpha}$ of $\mathbf{T}$ is the $\mathbf{e}_i$-component of force per unit reference area on an element of surface in the current configuration, whose normal was in the $\mathbf{E}_\alpha$-direction in the reference configuration (see Figure 4.2, after Belytschko et al. 2000).
By multiplying with $\mathbf{F}^{-1}$, a Lagrangian stress measure may be derived from relation (4.34), yielding the Lagrangian load vector $\mathbf{dL}$

$$\mathbf{dL} = \mathbf{F}^{-1}\mathbf{dl} = \mathbf{F}^{-1}\mathbf{TdA} = \mathbf{SdA}\,. \tag{4.35}$$

The objective second-order Lagrangian tensor $\mathbf{S}$ is called the *second Piola-Kirchhoff stress* tensor. The second Piola-Kirchhoff stress is symmetric

$$\mathbf{S} = J\mathbf{F}^{-1}\boldsymbol{\sigma}\mathbf{F}^{-\mathrm{T}} = \mathbf{F}^{-1}\mathbf{T} = \mathbf{P}\mathbf{F}^{-\mathrm{T}}\,. \tag{4.36}$$

Frequently, the *weighted* Cauchy stress $J\boldsymbol{\sigma}$ is referred to as the *Kirchhoff stress* $\boldsymbol{\tau}$

$$\boldsymbol{\tau} = J\boldsymbol{\sigma}\,. \tag{4.37}$$

The second Piola-Kirchhoff stress may be interpreted as a Lagrangian tensor induced from the Eulerian tensor $\boldsymbol{\tau}$

$$\mathbf{S} = \mathbf{F}^{-1}\boldsymbol{\tau}\mathbf{F}^{-\mathrm{T}} \qquad \boldsymbol{\tau} = \mathbf{F}\mathbf{S}\mathbf{F}^{\mathrm{T}}\,. \tag{4.38}$$

4.3.2 Lagrangian field equations

The stress measures defined in the previous section can be used to derive a Lagrangian set of field equations. Using the nominal stress tensor $\mathbf{P}$, the balance of linear momentum in form of equation (4.11) is rewritten in the reference configuration $\mathcal{B}_0$

$$\int_{\mathcal{B}_0} \rho_0 \ddot{\boldsymbol{\chi}} \, \mathrm{d}V = \int_{\mathcal{B}_0} \rho_0 \mathbf{b}_0 \, \mathrm{d}V + \int_{\partial\mathcal{B}_0} \mathbf{P}^{\mathrm{T}} \mathbf{N} \, \mathrm{d}A \,. \tag{4.39}$$

Here, the referential body-force density is given by $\mathbf{b}_0(\mathbf{X}, t) = \mathbf{b}(\boldsymbol{\chi}(\mathbf{X}, t), t)$. Invoking the divergence theorem, the Lagrangian representation of Cauchy's first law of motion, the so-called *Lagrangian equation of motion*

$$\nabla_0 \cdot \mathbf{P} + \rho_0 \mathbf{b}_0 = \rho_0 \ddot{\boldsymbol{\chi}} \qquad \frac{\partial P_{\alpha i}}{\partial X_\alpha} + \rho_0 b_{0i} = \rho_0 \ddot{\chi}_i \tag{4.40}$$

is obtained. It is given here both in tensorial notation and in component notation with respect to a rectangular Cartesian basis.
To complete the set of Lagrangian field equations, the symmetry of $\boldsymbol{\sigma}$ is expressed as

$$\mathbf{F}\mathbf{P} = \mathbf{P}^{\mathrm{T}}\mathbf{F}^{\mathrm{T}} \qquad \mathbf{P}\mathbf{F}^{-\mathrm{T}} = \mathbf{F}^{-1}\mathbf{P}^{\mathrm{T}} \,, \tag{4.41}$$

and the mass conservation equation is written in the form

$$\frac{\rho_0}{\rho} = J \,. \tag{4.42}$$

The Lagrangian field equations are summarized in Figure 4.3.

Conservation of mass	ρ_0	$= J\rho$
Cauchy's first law of motion	$\nabla_0 \cdot \mathbf{P} + \rho_0 \mathbf{b}_0$	$= \rho_0 \ddot{\boldsymbol{\chi}}$
Cauchy's second law of motion	$\mathbf{F}\mathbf{P}$	$= \mathbf{P}^{\mathrm{T}}\mathbf{F}^{\mathrm{T}}$

Figure 4.3: Lagrangian field equations

4.3.3 Work rate and conservation of energy

From Cauchy's first law of motion, the mechanical conservation of energy equation may be obtained. In particular, the mechanical stress power describing the work done during deformation can be defined.

Noting the symmetry of $\boldsymbol{\sigma}$ by virtue of Cauchy's second law of motion, the scalar product of (4.19) with the velocity $\mathbf{v}$ gives

$$(\nabla \cdot \boldsymbol{\sigma}) \cdot \mathbf{v} + \rho \mathbf{b} \cdot \mathbf{v} = \rho \dot{\mathbf{v}} \cdot \mathbf{v} \,. \tag{4.43}$$

This may be rearranged to yield

$$\nabla \cdot (\boldsymbol{\sigma} \mathbf{v}) - \operatorname{tr} (\boldsymbol{\sigma} (\nabla \otimes \mathbf{v})) + \rho \mathbf{b} \cdot \mathbf{v} = \rho \mathbf{v} \cdot \dot{\mathbf{v}} \,. \tag{4.44}$$

Integration over the domain $\mathcal{B}$ and subsequent use of the divergence theorem and the conservation of mass leads to the *mechanical energy balance equation*

$$\int_{\mathcal{B}} \rho \mathbf{b} \cdot \mathbf{v} \, \mathrm{d}v + \int_{\partial \mathcal{B}} \mathbf{t} \cdot \mathbf{v} \, \mathrm{d}a = \frac{\mathrm{d}}{\mathrm{dt}} \int_{\mathcal{B}} \frac{1}{2} \rho \mathbf{v} \cdot \mathbf{v} \, \mathrm{d}v + \int_{\mathcal{B}} \operatorname{tr} (\boldsymbol{\sigma} \mathbf{D}) \, \mathrm{d}v \,. \tag{4.45}$$

Here, the definition of the stretching tensor (3.114) in combination with (3.22)

$$\mathbf{D} = \operatorname{sym}(\nabla \otimes \mathbf{v}) \tag{4.46}$$

is used in conjunction with the symmetry of $\boldsymbol{\sigma}$, which gives rise to the relation

$$\operatorname{tr} (\boldsymbol{\sigma} \mathbf{L}) = \operatorname{tr} (\boldsymbol{\sigma} \mathbf{D}) \,. \tag{4.47}$$

The left-hand side of the equation of mechanical energy conservation (4.45) represents the *rate of work of the applied forces* on the body B in configuration $\mathcal{B}$. The first addendum on the right-hand side of equation (4.45) comprising the kinetic energy density $\frac{1}{2} \rho \mathbf{v} \cdot \mathbf{v}$ is the *rate of change of the kinetic energy* of B

$$\frac{\mathrm{d}}{\mathrm{dt}} \int_{\mathcal{B}} \frac{1}{2} \rho \mathbf{v} \cdot \mathbf{v} \, \mathrm{d}v \,. \tag{4.48}$$

The second part, which may be written in the form

$$\int_{\mathcal{B}} \boldsymbol{\sigma} : \mathbf{D} \, \mathrm{d}v = \int_{\mathcal{B}} \boldsymbol{\sigma} : \mathbf{L} \, \mathrm{d}v \,, \tag{4.49}$$

is the *rate of work of the stresses* on the body, also referred to as *stress power*. By virtue of definitions (4.32) and (3.110) and noting (4.47), the stress power per unit volume of $\mathcal{B}_0$ is derived

$$\dot{w} = \operatorname{tr} \left(\mathbf{P} \dot{\mathbf{F}} \right) = \operatorname{tr} (\mathbf{P} (\mathbf{L} \mathbf{F})) = J \boldsymbol{\sigma} : \mathbf{D} = \boldsymbol{\tau} : \mathbf{D} \,. \tag{4.50}$$

Due to the objectivity of J, $\boldsymbol{\sigma}$ and $\mathbf{D}$, the stress power is objective. Still, individual terms in the above equation, such as $\dot{\mathbf{F}}$, do not transform objectively. Alternatively to deriving the Lagrangian form of the conservation of mechanical energy equation from (4.40) by repeating the method outlined above,

equation (4.50) may be inserted directly into equation (4.45). Then, the Eulerian balance of mechanical energy equation may be reformulated with respect to the Lagrangian configuration $\mathcal{B}_0$ to yield

$$\int_{\mathcal{B}_0} \rho_0 \mathbf{b}_0 \cdot \dot{\boldsymbol{\chi}} \, \mathrm{d}V + \int_{\partial\mathcal{B}_0} (\mathbf{P}^{\mathrm{T}}\mathbf{N}) \cdot \dot{\boldsymbol{\chi}} \, \mathrm{d}A = \frac{\mathrm{d}}{\mathrm{d}t} \int_{\mathcal{B}_0} \frac{1}{2} \rho_0 \dot{\boldsymbol{\chi}} \cdot \dot{\boldsymbol{\chi}} \, \mathrm{d}V + \int_{\mathcal{B}_0} \mathrm{tr}\left(\mathbf{P}\dot{\mathbf{F}}\right) \mathrm{d}V \,. \quad (4.51)$$

4.3.4 Stress rates

In Section 4.2.4, the Cauchy stress $\boldsymbol{\sigma}$ was defined as an objective Eulerian tensor field. Hence, it transforms according to rule (3.101)

$$\boldsymbol{\sigma}^*(\mathbf{x}^*, t^*) = \mathbf{Q}(t) \star \boldsymbol{\sigma}(\mathbf{x}, t) \,. \quad (4.52)$$

Yet, the material time derivative of $\boldsymbol{\sigma}$ given by

$$\dot{\boldsymbol{\sigma}} = \frac{\partial \boldsymbol{\sigma}}{\partial t} + \mathbf{v} \cdot (\nabla \otimes \boldsymbol{\sigma}) \quad (4.53)$$

is not objective, as follows by combination of the equations above

$$\dot{\boldsymbol{\sigma}}^*(\mathbf{x}^*, t^*) = \mathbf{Q}(t) \star \dot{\boldsymbol{\sigma}} + \left(\dot{\mathbf{Q}}(t)\mathbf{Q}^{\mathrm{T}}(t)\right) \boldsymbol{\sigma}^* - \boldsymbol{\sigma}^* \left(\dot{\mathbf{Q}}(t)\mathbf{Q}^{\mathrm{T}}(t)\right) \,. \quad (4.54)$$

However, while the kinematical description of the material behavior may be dependent on the choice of observer, the material behavior itself is a physical phenomenon independent of the choice of observer. Hence, constitutive models must be based on objective quantities, i.e. on an objective stress rate.
Considering (4.54), one particular objective corotational stress rate, the so-called *Jaumann* rate of the stress $\boldsymbol{\sigma}$, may be derived

$$\overset{\circ}{\boldsymbol{\sigma}}{}^{\mathrm{J}} = \dot{\boldsymbol{\sigma}} + \boldsymbol{\sigma}\mathbf{W} - \mathbf{W}\boldsymbol{\sigma} \,. \quad (4.55)$$

As outlined in Section 3.6.2, other objective corotational rates are defined by a general class of spin tensors $\boldsymbol{\Omega}^*$. Here, the Green-Naghdi and the logarithmic rate of the weighted Cauchy or Kirchhoff stress $\boldsymbol{\tau}$ will be of importance

$$\overset{\circ}{\boldsymbol{\tau}}{}^{\mathrm{R}} = \dot{\boldsymbol{\tau}} + \boldsymbol{\tau}\boldsymbol{\Omega}^{\mathrm{R}} - \boldsymbol{\Omega}^{\mathrm{R}}\boldsymbol{\tau} \quad (4.56)$$

$$\overset{\circ}{\boldsymbol{\tau}}{}^{\mathrm{Log}} = \dot{\boldsymbol{\tau}} + \boldsymbol{\tau}\boldsymbol{\Omega}^{\mathrm{Log}} - \boldsymbol{\Omega}^{\mathrm{Log}}\boldsymbol{\tau} \,. \quad (4.57)$$

The concepts of pull-back and push-forward (see also Section 3.4.1) provide a mathematically consistent method for defining time derivatives of tensors, called *Lie derivatives*. The Lie derivative of the Kirchhoff stress, which is essentially the push-forward of the material time derivative of the pull-back of

the Kirchhoff stress, plays a crucial role in the rate-incremental version of the weak form of the balance of momentum equation. The Lie derivative may be derived considering the identity

$$\frac{\mathrm{d}}{\mathrm{dt}}\left(\mathbf{F}^{-1}\right) = -\mathbf{F}^{-1}\frac{\mathrm{d}}{\mathrm{dt}}(\mathbf{F})\mathbf{F}^{-1}, \tag{4.58}$$

which is an immediate consequence of $\mathbf{F}\mathbf{F}^{-1} = \mathbf{1}$. Taking the material time derivative of the second Piola-Kirchhoff stress (4.38_1) leads to

$$\dot{\mathbf{S}} = \mathbf{F}^{-1}\overset{\circ}{\boldsymbol{\tau}}{}^{\mathrm{L}}\mathbf{F}^{-\mathrm{T}} \qquad \overset{\circ}{\boldsymbol{\tau}}{}^{\mathrm{L}} = \mathbf{F}\dot{\mathbf{S}}\mathbf{F}^{\mathrm{T}}, \tag{4.59}$$

where the Lie derivative of $\boldsymbol{\tau}$ is given by

$$\overset{\circ}{\boldsymbol{\tau}}{}^{\mathrm{L}} = \mathbf{F}\frac{\mathrm{d}}{\mathrm{dt}}\left(\mathbf{F}^{-1}\boldsymbol{\tau}\mathbf{F}^{-\mathrm{T}}\right)\mathbf{F}^{\mathrm{T}} = \dot{\boldsymbol{\tau}} - \boldsymbol{\tau}\mathbf{L}^{\mathrm{T}} - \mathbf{L}\boldsymbol{\tau}\,. \tag{4.60}$$

For subsequent considerations, the Lie derivative has to be related to the logarithmic rate of the Kirchhoff stress. Following Simo & Pister (1984), the Lie derivative is expressed in terms of the Jaumann rate by virtue of relations (3.115) and (4.55)

$$\begin{aligned}\overset{\circ}{\boldsymbol{\tau}}{}^{\mathrm{L}} &= \dot{\boldsymbol{\tau}} - \boldsymbol{\tau}\mathbf{L}^{\mathrm{T}} - \mathbf{L}\boldsymbol{\tau}\\ &= \dot{\boldsymbol{\tau}} - \boldsymbol{\tau}(\mathbf{W}+\mathbf{D})^{\mathrm{T}} - (\mathbf{W}+\mathbf{D})\boldsymbol{\tau}\\ &= \overset{\circ}{\boldsymbol{\tau}}{}^{\mathrm{J}} - \boldsymbol{\tau}\mathbf{D} - \mathbf{D}\boldsymbol{\tau}\,.\end{aligned} \tag{4.61}$$

Then, noting the relationship between the logarithmic spin $\boldsymbol{\Omega}^{\mathrm{Log}}$ and the vorticity $\mathbf{W}$ (cf. Xiao et al. 1997b)

$$\boldsymbol{\Omega}^{\mathrm{Log}} = \mathbf{W} + \mathbf{N}^{\mathrm{Log}}, \tag{4.62}$$

the logarithmic rate of the Kirchhoff stress is written as

$$\overset{\circ}{\boldsymbol{\tau}}{}^{\mathrm{Log}} = \overset{\circ}{\boldsymbol{\tau}}{}^{\mathrm{J}} + \boldsymbol{\tau}\mathbf{N}^{\mathrm{Log}} - \mathbf{N}^{\mathrm{Log}}\boldsymbol{\tau}\,. \tag{4.63}$$

Thus, substitution into (4.61) yields the required relationship between the logarithmic rate of $\boldsymbol{\tau}$ and the Lie derivative of $\boldsymbol{\tau}$

$$\begin{aligned}\overset{\circ}{\boldsymbol{\tau}}{}^{\mathrm{L}} &= \overset{\circ}{\boldsymbol{\tau}}{}^{\mathrm{Log}} - \boldsymbol{\tau}\mathbf{N}^{\mathrm{Log}} + \mathbf{N}^{\mathrm{Log}}\boldsymbol{\tau} - \boldsymbol{\tau}\mathbf{D} - \mathbf{D}\boldsymbol{\tau}\\ &= \overset{\circ}{\boldsymbol{\tau}}{}^{\mathrm{Log}} - \boldsymbol{\tau}(\mathbb{B}:\mathbf{D}) + (\mathbb{B}:\mathbf{D})\boldsymbol{\tau} - \boldsymbol{\tau}\mathbf{D} - \mathbf{D}\boldsymbol{\tau}\\ &= \overset{\circ}{\boldsymbol{\tau}}{}^{\mathrm{Log}} + \mathbb{G}:\mathbf{D}\,.\end{aligned} \tag{4.64}$$

The spin $\mathbf{N}^{\mathrm{Log}}$ is given by equation (A.16) in Appendix A.2. The respective definitions of $\mathbb{B}$ and $\mathbb{G}$ are presented in Appendix A.2 and Appendix A.3.

4.4 Conjugate stress analysis

In Section 4.3.3, the stress power per unit volume was derived

$$\dot{w} = \boldsymbol{\tau} : \mathbf{D} \,. \tag{4.65}$$

Equation (4.65) describes a physical quantity, the rate of work of the stresses on the body. However, this expression for stress power is difficult to incorporate in the formulation of constitutive laws as it is based on the stretching tensor $\mathbf{D}$, which cannot be written as the direct flux of any strain tensor. Hence, to fulfill the conservation of energy requirement in the formulation of constitutive laws, an appropriate alternative relation is needed. The *work conjugacy* relation

$$\dot{w} = \mathbf{T}^{(m)} : \dot{\mathbf{E}}^{(m)} = \boldsymbol{\tau} : \mathbf{D} \,, \tag{4.66}$$

defined by Hill (1968, 1978), is a notion to overcome this difficulty. It states that the Lagrangian measure of stress $\mathbf{T}^{(m)}$ and the Lagrangian measure of strain $\mathbf{E}^{(m)}$ form a conjugate pair if the inner product of $\mathbf{T}^{(m)}$ and $\dot{\mathbf{E}}^{(m)}$ equals the stress power $\dot{w}$ specified by equation (4.66).
For example, according to Hill's work conjugacy relation (4.66), the second Piola-Kirchhoff stress tensor $\mathbf{S}$ and the Green-Lagrange strain tensor $\mathbf{E}$ are conjugate stress and strain tensors as well as the nominal stress tensor $\mathbf{P}$ and the deformation gradient $\mathbf{F}$. For other measures of stress and strain, such as the rotated Kirchhoff stress $\mathbf{R}^{\mathrm{T}} \star \boldsymbol{\tau}$ and the referential Hencky strain $\mathbf{H}$, the work conjugacy relation holds for coaxial $\mathbf{R}^{\mathrm{T}} \star \boldsymbol{\tau}$ and $\mathbf{H}$ only.
Due to the limitation of Hill's work conjugacy notion to Lagrangian measures only, an extension of (4.66) to Eulerian measures of stress and strain may be considered. For example, for a conjugate pair of Lagrangian stress and strain tensors, the rotated correspondences defined by (3.85) should be work conjugate as well.
A relation to formalize this argument is proposed by Xiao et al. (1998b). They consider a pair of symmetric Eulerian tensors (t,e), where $\mathbf{t}$ is an objective stress measure and $\mathbf{e}$ an objective measure of strain.[8] In a frame defined by the spin $\boldsymbol{\Omega}^*$ relative to a fixed background frame, this pair is observed by an observer $\mathcal{O}^*$ as $(\mathbf{Q} \star \mathbf{t},\ \mathbf{Q} \star \mathbf{e})$.

Hence, for the observer $\mathcal{O}^*$ taking the inner product $(\mathbf{Q} \star \mathbf{t}) : \overline{(\mathbf{Q} \star \mathbf{e})}^{\cdot}$, the pair (t,e) is work conjugate if the relation

$$\dot{w} = (\mathbf{Q} \star \mathbf{t}) : \overline{(\mathbf{Q} \star \mathbf{e})}^{\cdot} = \mathbf{t} : \overset{\circ}{\mathbf{e}}{}^{*} \tag{4.67}$$

is satisfied. Here, $\overset{\circ}{\mathbf{e}}{}^{*}$ is a corotating time derivative of the strain tensor $\mathbf{e}$, defined by the spin $\boldsymbol{\Omega}^{*\mathrm{T}} = \dot{\mathbf{Q}}^{\mathrm{T}}\mathbf{Q}$, as introduced in relation (3.122)

$$\overset{\circ}{\mathbf{e}}{}^{*} = \mathbf{Q}^{\mathrm{T}} \star \frac{\mathrm{d}}{\mathrm{d}t} (\mathbf{Q} \star \mathbf{e}) = \dot{\mathbf{e}} + \mathbf{e}\boldsymbol{\Omega}^* - \boldsymbol{\Omega}^*\mathbf{e} \,. \tag{4.68}$$

[8] The Eulerian stress tensor $\mathbf{t}$ is not to be mistaken for the traction $\mathbf{t}$ used in the previous sections.

From the symmetry requirement of $\mathbf{t}$ and $\mathbf{e}$, and the objectivity of $\mathbf{t}$ and $\dot{w}$, it is concluded that the extended work conjugacy relation (4.67) holds true only for objective corotational rates $\overset{\circ}{\mathbf{e}}{}^*$ (cf. Xiao et al. 1998b).
Using the spectral decomposition of $\mathbf{e}$

$$\mathbf{e} = \sum_{\alpha=1}^{n} g(\chi_\alpha)\mathbf{B}_\alpha \qquad g(\chi_\alpha) = f(\sqrt{\chi_\alpha})\,, \tag{4.69}$$

the following expression for $\overset{\circ}{\mathbf{e}}{}^*$ is obtained

$$\overset{\circ}{\mathbf{e}}{}^* = \sum_{\alpha,\beta=1}^{n} \rho(\chi_\alpha, \chi_\beta)\mathbf{B}_\alpha \mathbf{D}\mathbf{B}_\beta\,. \tag{4.70}$$

Here, the eigenvalues and eigenprojections of the left Cauchy-Green tensor $\mathbf{B}$ are denoted by χ_α and $\mathbf{B}_\alpha$, respectively. The functional

$$\rho(\chi_\alpha, \chi_\beta) = [(\chi_\alpha + \chi_\beta) + (\chi_\alpha - \chi_\beta)h(\chi_\alpha/\chi_\beta)]\, g_{\alpha\beta}\,, \tag{4.71}$$

with

$$g_{\alpha\beta} = \begin{cases} g'(\chi_\alpha) & \text{for} \quad \alpha = \beta \\ \dfrac{g(\chi_\alpha) - g(\chi_\beta)}{\chi_\alpha - \chi_\beta} & \text{for} \quad \alpha \neq \beta \end{cases} \tag{4.72}$$

depends on the eigenvalues of $\mathbf{B}$ and on the spin function h, see Section 3.6.2. Hence, the objective corotational rate $\overset{\circ}{\mathbf{e}}{}^*$ is determined by specifying the Eulerian measure of strain through the scale function $f(\sqrt{\chi_\alpha})$, and by the choice of rate through the spin function h.
The $\boldsymbol{\Omega}^*$-work conjugate stress measure $\mathbf{t}$ of an arbitrary Eulerian strain measure $\mathbf{e}$ is given by

$$\mathbf{t} = \sum_{\alpha,\beta=1}^{n} \rho^{-1}(\chi_\alpha, \chi_\beta)\mathbf{B}_\alpha \boldsymbol{\tau} \mathbf{B}_\beta\,. \tag{4.73}$$

In particular, the polar spin function (3.133), for which $\mathbf{Q}^{\mathrm{T}} = \mathbf{R}$ in (4.67) and (4.68), yields the work conjugate stress

$$\mathbf{t} = \sum_{\alpha,\beta=1}^{n} \left(2\sqrt{\chi_\alpha \chi_\beta}\right)^{-1} \left(\frac{\chi_\alpha - \chi_\beta}{g(\chi_\alpha) - g(\chi_\beta)}\right) \mathbf{B}_\alpha \boldsymbol{\tau} \mathbf{B}_\beta\,. \tag{4.74}$$

Specifying the Eulerian measure of strain to correspond to the Hencky strain $\mathbf{h}$

$$g(\chi_\alpha) = \frac{1}{2}\ln\chi_\alpha\,, \tag{4.75}$$

the $\boldsymbol{\Omega}^{\mathrm{R}}$-conjugate stress to $\mathbf{h}$ is obtained. It is denoted by $\boldsymbol{\pi}$

$$\boldsymbol{\pi} = \sum_{\alpha,\beta=1}^{n} \sqrt{\chi_\alpha^{-1}\chi_\beta^{-1}} \left(\frac{\chi_\alpha - \chi_\beta}{\ln\chi_\alpha - \ln\chi_\beta} \right) \mathbf{B}_\alpha \boldsymbol{\tau} \mathbf{B}_\beta . \tag{4.76}$$

Note that for the polar spin $\boldsymbol{\Omega}^{\mathrm{R}}$, the extended work conjugacy relation (4.67) corresponds to Hill's work conjugacy relation (4.66), since by virtue of (3.135_1) and (1.7_3)

$$\dot{w} = \boldsymbol{\pi} : \overset{\circ}{\mathbf{h}}{}^{\mathrm{R}} = (\mathbf{R}^{\mathrm{T}} \star \boldsymbol{\pi}) : (\mathbf{R}^{\mathrm{T}} \star \overset{\circ}{\mathbf{h}}{}^{\mathrm{R}}) = \boldsymbol{\Pi} : \dot{\mathbf{H}} . \tag{4.77}$$

Here, use is made of the rotated correspondences (3.85)

$$\boldsymbol{\Pi} = \mathbf{R}^{\mathrm{T}} \star \boldsymbol{\pi} \qquad \boldsymbol{\pi} = \mathbf{R} \star \boldsymbol{\Pi} , \tag{4.78}$$

and of the definition of the Lagrangian stress $\boldsymbol{\Pi}$ from the rotated Kirchhoff stress $\tilde{\boldsymbol{\tau}} = \mathbf{R}^{\mathrm{T}} \star \boldsymbol{\tau}$

$$\boldsymbol{\Pi} = \sum_{\alpha,\beta=1}^{n} \sqrt{\chi_\alpha^{-1}\chi_\beta^{-1}} \left(\frac{\chi_\alpha - \chi_\beta}{\ln\chi_\alpha - \ln\chi_\beta} \right) \mathbf{C}_\alpha \tilde{\boldsymbol{\tau}} \mathbf{C}_\beta . \tag{4.79}$$

Hence, relations (4.76) and (4.79) are independent of the material symmetry. In particular, the Eulerian stress $\boldsymbol{\pi}$ defined in equation (4.76) and the Lagrangian stress $\boldsymbol{\Pi}$ given by (4.79) hold for isotropic and anisotropic material symmetries.

For isotropic materials, the Kirchhoff stress $\boldsymbol{\tau}$ and the left Cauchy-Green tensor $\mathbf{B}$ are coaxial. Hence, $\boldsymbol{\tau}$ and $\mathbf{B}_\alpha$ commute in (4.76). Noting manipulation rules (A.1) to (A.7) for eigenprojections and $\lim_{\alpha\to\beta}(\chi_\alpha - \chi_\beta)/(\ln\chi_\alpha - \ln\chi_\beta) = \chi_\alpha$ then gives

$$\boldsymbol{\pi} = \sum_{\alpha}^{n} \tau_\alpha \mathbf{B}_\alpha = \boldsymbol{\tau} \qquad \boldsymbol{\Pi} = \sum_{\alpha}^{n} \tau_\alpha \mathbf{C}_\alpha = \tilde{\boldsymbol{\tau}} . \tag{4.80}$$

The Kirchhoff stress $\boldsymbol{\tau}$ and the Hencky strain $\mathbf{h}$ form a work conjugate pair according to Hill's definition (4.66) under isotropy only. Basis-free expressions for $\mathbf{t}$ and $\boldsymbol{\tau}$ are given in Appendix A.4.

From equation (4.73), stress measures work conjugate to any given Eulerian or Lagrangian strain measure $\mathbf{e}$ respectively $\mathbf{E}$ with regard to material spins defined by the spin function h may be obtained. Specifically, substituting the logarithmic spin function (3.137) gives the stress

$$\boldsymbol{\pi} = \boldsymbol{\tau} . \tag{4.81}$$

Thus, extension (4.67) of Hill's work conjugacy relation implies that the Kirchhoff stress $\boldsymbol{\tau}$ is the stress measure that is $\boldsymbol{\Omega}^{\mathrm{Log}}$-conjugate to the Eulerian

Hencky strain. Invoking equation (3.139), stating that the stretching $\mathbf{D}$ equals the logarithmic rate of $\mathbf{h}$, by virtue of (4.67) the Kirchhoff stress $\boldsymbol{\tau}$ and the Hencky strain $\mathbf{h}$ form a work conjugate pair

$$\dot{w} = \mathbf{t} : \overset{\circ}{\mathbf{e}}{}^{*} = \boldsymbol{\tau} : \mathbf{D} \,. \tag{4.82}$$

4.5 Weak form of balance of momentum

4.5.1 Principle of virtual work

The numerical solution of the balance of momentum equations (4.19) or (4.40), e.g. by the finite element method, is based on the weak form, often called the *variational form*, of the momentum equation (cf. Belytschko et al. 2000). The principle of virtual work to be derived in this section is equivalent to the momentum equation and the traction boundary conditions. Collectively, the latter are called the classical *strong form*.
The boundary $\partial\mathcal{B}_0$ of the body B in $\mathcal{B}_0$ is subject to displacement boundary conditions $\partial_u\mathcal{B}_0$, and traction boundary conditions $\partial_\sigma\mathcal{B}_0$. At each element of the boundary, either displacements or tractions are prescribed

$$\partial_u\mathcal{B}_0 \cap \partial_\sigma\mathcal{B}_0 = \varnothing \qquad \partial\mathcal{B}_0 = \partial_u\mathcal{B}_0 \cup \partial_\sigma\mathcal{B}_0 \,. \tag{4.83}$$

The traction boundary conditions are given by

$$\mathbf{P}^{\mathrm{T}}\mathbf{N} = \bar{\mathbf{t}}_0 \quad \text{on} \quad \partial_\sigma\mathcal{B}_0 \,, \tag{4.84}$$

and the displacement boundary conditions are

$$\mathbf{u} = \bar{\mathbf{u}} \qquad \text{on} \quad \partial_u\mathcal{B}_0 \,. \tag{4.85}$$

In order to be kinematically admissible, the displacements $\mathbf{u}(\mathbf{X}, t)$ have to satisfy the displacement boundary conditions on $\partial_u\mathcal{B}_0$. Therefore, the test function

$$\delta\mathbf{u}(\mathbf{X}, t) = \mathbf{u}^{*}(\mathbf{X}, t) - \mathbf{u}(\mathbf{X}, t) \,, \tag{4.86}$$

relating kinematically admissible displacements $\mathbf{u}(\mathbf{X}, t)$ and $\mathbf{u}^{*}(\mathbf{X}, t)$, is required to vanish on $\partial_u\mathcal{B}_0$

$$\delta\mathbf{u}(\mathbf{X}, t) = \mathbf{0} \quad \text{on} \quad \partial_u\mathcal{B}_0 \,. \tag{4.87}$$

The test function $\delta\mathbf{u}(\mathbf{X}, t)$ is called the *virtual displacement*.
With these definitions, taking the dot product of Cauchy's first law of motion in its Lagrangian description (4.40) with any admissible virtual displacement $\delta\mathbf{u}$ and subsequent integration over the reference volume leads to

$$\int_{\mathcal{B}_0} \nabla_0 \cdot \mathbf{P} \cdot \delta\mathbf{u} \, \mathrm{d}V + \int_{\mathcal{B}_0} \rho_0 \mathbf{b}_0 \cdot \delta\mathbf{u} \, \mathrm{d}V = \int_{\mathcal{B}_0} \rho_0 \ddot{\boldsymbol{\chi}} \cdot \delta\mathbf{u} \, \mathrm{d}V \,. \tag{4.88}$$

Restricting attention to quasi-static processes, inertial forces are neglected. Then, applying the divergence theorem and rearranging of terms gives

$$\int_{\mathcal{B}_0} \mathbf{P}^{\mathrm{T}} : (\nabla_0 \otimes \delta\mathbf{u})\,\mathrm{d}V = \int_{\partial\mathcal{B}_0} \mathbf{P}^{\mathrm{T}}\mathbf{N} \cdot \delta\mathbf{u}\,\mathrm{d}A + \int_{\mathcal{B}_0} \rho_0 \mathbf{b}_0 \cdot \delta\mathbf{u}\,\mathrm{d}V\,. \tag{4.89}$$

Defining the test function $\delta\mathbf{u}(\mathbf{X}, t)$ according to (4.86) as the difference of two kinematically admissible displacement fields, the integral over the kinematic boundary vanishes and the only boundary integral in the weak form is over the traction boundary. Designating the virtual displacement gradient $(\nabla_0 \otimes \delta\mathbf{u})$ by $\delta\mathbf{F}$ yields the *principle of virtual work* in Lagrangian form

$$\int_{\mathcal{B}_0} \mathbf{P}^{\mathrm{T}} : \delta\mathbf{F}\,\mathrm{d}V = \int_{\partial\mathcal{B}_0} \bar{\mathbf{t}}_0 \cdot \delta\mathbf{u}\,\mathrm{d}A + \int_{\mathcal{B}_0} \rho_0 \mathbf{b}_0 \cdot \delta\mathbf{u}\,\mathrm{d}V\,. \tag{4.90}$$

By the same method, a Eulerian formulation of the principle of virtual work may be derived. Defining the Eulerian gradient of the virtual displacement as

$$\nabla \otimes \delta\mathbf{u} = (\nabla_0 \otimes \delta\mathbf{u})\mathbf{F}^{-1}\,, \tag{4.91}$$

and noting the change of variable formula (3.17), application of Nanson's formula (3.42) and definition (3.35) of the Jacobian determinant J lead to

$$\int_{\mathcal{B}} \boldsymbol{\sigma} \vdots (\nabla \otimes \delta\mathbf{u})\,\mathrm{d}v = \int_{\partial\mathcal{B}} \bar{\mathbf{t}} \cdot \delta\mathbf{u}\,\mathrm{d}a + \int_{\mathcal{B}} \rho\mathbf{b} \cdot \delta\mathbf{u}\,\mathrm{d}v\,, \tag{4.92}$$

with the traction and displacement boundary conditions

$$\boldsymbol{\sigma}\mathbf{n} = \bar{\mathbf{t}} \qquad \text{on} \qquad \partial_\sigma\mathcal{B} \tag{4.93}$$

respectively

$$\mathbf{u} = \bar{\mathbf{u}} \qquad \text{on} \qquad \partial_u\mathcal{B}\,. \tag{4.94}$$

4.5.2 Rate of the weak form of balance of momentum

Based on the considerations in the previous section, the rate form of the weak form of momentum balance can be derived. It plays an important role in the incremental solution of quasi-static elastic-inelastic processes (cf. Simo & Hughes 1998). As will be seen below, it leads to the continuum tangent stiffness matrix. Hence, it is closely associated with the numerical implementation of hypoelastic models.

In a manner similar to the definition of admissible virtual displacements, the spatial velocity field $\boldsymbol{\eta}(\mathbf{x}, t)$ is defined as an admissible spatial variation. The test function $\boldsymbol{\eta}$ is sometimes called a *virtual velocity*. It has properties equivalent to those of $\delta\mathbf{u}$. In particular, $\boldsymbol{\eta}$ vanishes on the prescribed boundary $\partial_v\mathcal{B}$.

Neglecting inertial contributions, for a rate of change in loading given by $\dot{\mathbf{b}}_0$ and $\dot{\bar{\mathbf{t}}}_0$, equilibrium condition (4.40) takes the form

$$\nabla_0 \cdot \dot{\mathbf{P}} + \rho_0 \dot{\mathbf{b}}_0 = \mathbf{0} \,. \tag{4.95}$$

Denoting the admissible material velocity field corresponding to the Eulerian quantity η by $\eta_0(\mathbf{X}, t)$, application of the divergence theorem to the above yields

$$\int_{\mathcal{B}_0} \dot{\mathbf{P}}^{\mathrm{T}} : (\nabla_0 \otimes \boldsymbol{\eta}_0) \, \mathrm{d}V - \int_{\partial \mathcal{B}_0} \dot{\bar{\mathbf{t}}}_0 \cdot \boldsymbol{\eta}_0 \, \mathrm{d}A - \int_{\mathcal{B}_0} \rho_0 \dot{\mathbf{b}}_0 \cdot \boldsymbol{\eta}_0 \, \mathrm{d}V = 0 \,. \tag{4.96}$$

This is the rate-incremental version of the Lagrangian weak form of momentum equation (4.90). The corresponding Eulerian counterpart is derived by considering relations (4.32) and (4.36) between the nominal stress $\mathbf{P}$ and the second Piola-Kirchhoff stress $\mathbf{S}$

$$\mathbf{P} = \mathbf{S}\mathbf{F}^{\mathrm{T}} = \mathbf{F}^{-1}\boldsymbol{\tau} \,. \tag{4.97}$$

With the definition

$$\nabla \otimes \boldsymbol{\eta} = (\nabla_0 \otimes \boldsymbol{\eta}_0)\mathbf{F}^{-1} \,, \tag{4.98}$$

equivalent to (4.91), by virtue of (3.110) and (1.7_4) the virtual power density on the left-hand side of (4.96) is expressed in the form

$$\begin{aligned} \dot{\mathbf{P}}^{\mathrm{T}} : (\nabla_0 \otimes \boldsymbol{\eta}_0) &= \left(\dot{\mathbf{F}}\mathbf{S} + \mathbf{F}\dot{\mathbf{S}}\right) : (\nabla_0 \otimes \boldsymbol{\eta}_0) \\ &= \left(\mathbf{L}\mathbf{F}\mathbf{S} + \mathbf{F}\dot{\mathbf{S}}\right) : (\nabla_0 \otimes \boldsymbol{\eta}_0) \\ &= \left(\mathbf{L}\mathbf{F}\mathbf{S}\mathbf{F}^{\mathrm{T}} + \mathbf{F}\dot{\mathbf{S}}\mathbf{F}^{\mathrm{T}}\right)\mathbf{F}^{-\mathrm{T}} : (\nabla_0 \otimes \boldsymbol{\eta}_0) \\ &= \left(\mathbf{L}\boldsymbol{\tau} + \overset{\circ}{\boldsymbol{\tau}}{}^{\mathrm{L}}\right) : (\nabla_0 \otimes \boldsymbol{\eta}_0)\mathbf{F}^{-1} \\ &= \left(\mathbf{L}\boldsymbol{\tau} + \overset{\circ}{\boldsymbol{\tau}}{}^{\mathrm{L}}\right) : (\nabla \otimes \boldsymbol{\eta}) \,. \end{aligned} \tag{4.99}$$

Hence

$$\int_{\mathcal{B}_0} \left(\mathbf{L}\boldsymbol{\tau} + \overset{\circ}{\boldsymbol{\tau}}{}^{\mathrm{L}}\right) : (\nabla \otimes \boldsymbol{\eta}) \, \mathrm{d}V = \int_{\partial \mathcal{B}_0} \dot{\bar{\mathbf{t}}}_0 \cdot \boldsymbol{\eta}_0 \, \mathrm{d}A + \int_{\mathcal{B}_0} \rho_0 \dot{\mathbf{b}}_0 \cdot \boldsymbol{\eta}_0 \, \mathrm{d}V \,. \tag{4.100}$$

Substituting the logarithmic rate of the Kirchhoff stress (4.64) as well as formulas (3.35) and (3.42), the Eulerian rate formulation of the weak form of momentum balance is obtained

$$\begin{aligned} \int_{\mathcal{B}} \frac{1}{J} \left(\mathbf{L}\boldsymbol{\tau} + \overset{\circ}{\boldsymbol{\tau}}{}^{\mathrm{Log}} + \mathbb{G} : \mathbf{D}\right) : (\nabla \otimes \boldsymbol{\eta}) \, \mathrm{d}v \\ = \int_{\partial \mathcal{B}} \dot{\bar{\mathbf{t}}} \cdot \boldsymbol{\eta} \, \mathrm{d}a + \int_{\mathcal{B}} \rho \dot{\mathbf{b}} \cdot \boldsymbol{\eta} \, \mathrm{d}v \,. \end{aligned} \tag{4.101}$$

The tensor $\mathbf{G}$ first introduced in equation (4.64) is specified in Appendix A.3. The rate-incremental version (4.101) of the weak form of the balance of momentum equation provides the basis for the finite element implementation of the material law proposed.

5 Thermodynamics

Processes of phase transformation in solids are characterized by a strong thermomechanical coupling. In order to phenomenologically describe thermomechanical processes, not only a kinematical, but also a thermodynamic framework is needed.
In this chapter, criteria for thermodynamically admissible processes are derived within an internal-variable theory based on the work of Lehmann (1974, 1984, 1989b) and Coleman & Gurtin (1967) as well as the monographs by Truesdell & Toupin (1960), Malvern (1969), Truesdell & Noll (1992) and Belytschko et al. (2000). Starting from the principle of conservation of energy and the second law of thermodynamics, the notion of decomposition of stress power into an elastic and an inelastic part is introduced. For irreversible thermodynamical processes of constrained equilibria, the internal entropy production rate is expressed in terms of generalized irreversible forces. The thermomechanical coupling is governed by a heat conduction equation in combination with a suitable relation for the rate at which energy is generated.

5.1 Introduction

The phase transforming body B under consideration is treated as a classical continuum. This implies that a macroscopic description of microscopic effects such as the nucleation and evolution of austenite and martensite may be obtained by employing suitable averaging procedures. As a consequence, the kinematical framework presented in Chapter 3 may be used.
It is assumed that the thermodynamical state of each material element is determined uniquely by the values of a set of external and internal state variables, even when the body is not in thermodynamical equilibrium. Thus, the dissipative effects are accounted for by postulating the existence of *internal state variables* which influence the free energy of the body. Their evolution is governed by differential equations in terms of the strain (cf. Coleman & Gurtin 1967).[9] For known current values of the external and internal state variables, the response of the respective material element may be determined for arbitrary stages of any admissible thermomechanical process without knowledge of the history of the process prior to the current state (cf. Lehmann 1989c). Of course, as required by the *principle of determinism*, the current state is determined by the current deformation and the history of the motion of the body as reflected by the values of the internal variables (cf. Truesdell & Noll 1992).

[9] This is only one of several ways to account for the dissipative effects which, in addition to heat conduction, accompany deformation. Alternatively, a viscous stress depending on the rate of strain could be introduced, or it could be assumed that the entire past history of the strain influences the stress in a manner compatible with a *principle of fading memory* (cf. Coleman & Noll 1960, 1961, 1964).

The thermodynamical state is described based on the assumption that each particle of the body has the properties of a local thermodynamical system whose state is uniquely determined by the values of a suitable set of well defined external and internal state variables. By imposing appropriate constraints, the internal variables can be held at any definite set of values, with the material sample attaining an equilibrium state corresponding to the prescribed external state variables. The body is then said to be in a state of *constrained equilibrium* (cf. Rice 1971).
External state variables are the stress $\boldsymbol{\sigma}$ and the temperature Θ or their conjugated state variables, i.e. the reversible strain $\mathbf{h}^e$ and the entropy S, respectively.[10] These external state variables suffice to describe reversible processes only. Hence, to represent states of changing internal structure due to irreversible processes, such as the evolution of the local fraction of the austenitic and martensitic phases, additional internal state variables $\mathbf{a}$ have to be introduced. The additional state variables may differ from internal process variables intended to characterize the irreversible process. However, process and state variables must be equivalent quantities. Here, they are assumed to be equal, hence they are referred to as *internal state variables.* In general, an infinite set of internal state variables is required

$$\mathbf{a} = \{\mathbf{a}_1, \dots, \mathbf{a}_\infty\} . \tag{5.1}$$

However, within phenomenological theories only finite sets of scalar or tensor-valued internal state variables of even rank may be considered. In fact, the phenomenological model presented in Chapter 6 is based on only one scalar internal variable, the mass fraction of martensite ξ

$$\mathbf{a} = \{\xi\} . \tag{5.2}$$

The evolution of the internal variables is governed by rate-equations in terms of the independent external state variables and the set of all internal variables. For prescribed deformation $\mathbf{h}^e$ and temperature Θ, the general form of an evolution equation of the internal variable $\mathbf{a}_i$ then is

$$\overset{\circ}{\mathbf{a}}{}_i^* = \overset{\circ}{\mathbf{a}}{}_i^*(\Theta, \mathbf{h}^e, \mathbf{a}) , \tag{5.3}$$

where $\overset{\circ}{(\cdot)}{}^*$ is a suitable time rate.
Note that no distinction is made between the terms *elastic* and *reversible* here. Thus, reversible effects of thermal expansion are included in $\mathbf{h}^e$, which represents the elastic part of the strain $\mathbf{h}$.[11]

[10] For an analysis of stress and strain measures that are conjugate in power, see Section 4.4.
[11] See Section 5.4.2 for arguments on choosing $\mathbf{h}^e$ instead of $\mathbf{h}$ as state variable.

5.2 Thermomechanical processes

A *thermomechanical process* takes a body from its initial state $\mathcal{B}_0$ to its current state $\mathcal{B}$. All external and internal state variables and kinematical quantities related to $\mathcal{B}_0$ are assumed to be given. The process is initiated by prescribing a set of independent process variables consisting of thermomechanical boundary conditions as well as body forces and sources of energy. All dependent process variables in the thermomechanically deformed state $\mathcal{B}$ are obtained from the description of this process. Among these variables are the thermomechanical quantities at the boundaries of the body, the displacement, stress and temperature fields as well as the specific body forces and sources of energy inside the body wherever they are not prescribed. In addition, the internal state variables and all other quantities of interest, such as the heat flux $\mathbf{q}$, follow from the description of the thermomechanical process (cf. Lehmann 1984).
Following Coleman & Gurtin (1967), a thermomechanical process for B may be described by a set of nine functions depending on the time t and the particle X, which is identified by its position $\mathbf{X}$ in the reference configuration on the grounds of the discussion in Section 3.2.3:

Spatial position in the motion χ	$\mathbf{x} = \chi(\mathbf{X}, t)$	
Stress tensor	$\boldsymbol{\pi} = \boldsymbol{\pi}(\mathbf{X}, t)$	
Specific body force per unit mass	$\mathbf{b} = \mathbf{b}(\mathbf{X}, t)$	
Specific internal energy per unit mass	$u = u(\mathbf{X}, t)$	
Heat flux vector	$\mathbf{q} = \mathbf{q}(\mathbf{X}, t)$	(5.4)
Heat source (incident radiation absorbed by B)	$r = r(\mathbf{X}, t)$	
Specific entropy per unit mass	$s = s(\mathbf{X}, t)$	
Absolute temperature	$\Theta = \Theta(\mathbf{X}, t)$	
Set of internal state variables	$\mathbf{a} = \mathbf{a}(\mathbf{X}, t)$	

The initial and current states of the body are linked by general, material independent field equations and a constitutive law. Some material independent relations have already been presented, i.e. the kinematics in Chapter 3 and the balance equations for mass, linear and angular momentum, and mechanical energy in Section 4.2. The set is completed in this chapter by the thermodynamical conservation of energy equation frequently called first law of thermodynamics, and the second law of thermodynamics, a relation in terms of the entropy S. The set of nine functions (5.4) is called a *thermomechanical process*[12] in B if and only if it is compatible with the balance of linear and angular momentum, see Figures 4.1 and 4.3, and the balance of energy (5.13) (cf. Coleman & Gurtin 1967).
In order to uniquely define a *reversible energy*, an imaginary reference state $\mathcal{B}_0^*$

[12]The term *thermomechanical processes* for the processes under consideration is used here in agreement with Lehmann (1984), while Coleman & Gurtin (1967) refer to *thermodynamic processes*.

and the decomposition of mechanical work are introduced. The thermodynamical reference state is not part of the history of thermomechanical deformations of the body B, but quantities such as the reference temperature Θ_0 are defined with reference to $\mathcal{B}_0^*$. It is not possible to define a process leading from the initial state $\mathcal{B}_0$ to the imaginary reference state $\mathcal{B}_0^*$. On the other hand, an imaginary reversible process between the current state and the imaginary state exists, during which the internal variables remain constant. Such a reversible process in combination with a unique decomposition of mechanical work into a reversible and an irreversible part serves to define a reversible energy, which may be determined from a unique measure of reversible strain. Here, the elastic logarithmic strain $\mathbf{h}^e$ is chosen to define the reversible energy of the body.

5.3 Conservation of energy

The *total energy* W stored in a body B consists of its *internal energy* U and its *kinetic energy* K

$$W = U + K\,. \tag{5.5}$$

The internal energy is obtained by integration of the specific internal energy u over the mass of the body

$$U = \int_m u\, dm = \int_{\mathcal{B}} \rho u \,\mathrm{d}v\,, \tag{5.6}$$

and its kinetic energy by integration of the square of the velocity of the body over its domain

$$K = \frac{1}{2}\int_{\mathcal{B}} \rho \mathbf{v}\cdot\mathbf{v}\,\mathrm{d}v\,. \tag{5.7}$$

Here, ρ is the current density and $\mathbf{v}$ is the velocity of the body.
In a thermomechanical process where mechanical work and heat are the only sources of energy, the principle of conservation of energy states that the rate of change in total energy $\dot{W}$ is equal to the work done by the body forces and surface tractions plus the heat energy delivered to the body by the heat flux and other sources of heat

$$\dot{W} = P_a + Q\,. \tag{5.8}$$

The external work P_a done by the body forces $\rho\mathbf{b}$ and surface tractions $\mathbf{t}$ is given by

$$P_a = \int_{\mathcal{B}} \rho\mathbf{b}\cdot\mathbf{v}\,\mathrm{d}v + \int_{\partial\mathcal{B}} \mathbf{t}\cdot\mathbf{v}\,da\,, \tag{5.9}$$

where **b** is a force per unit mass and **t** is a force per unit area.
The power Q consists of the rate of change in the energy of *heat sources* r and the *heat flux* h

$$Q = \int_{\mathcal{B}} \rho r \, \mathrm{d}v + \int_{\partial\mathcal{B}} h \, da \,, \tag{5.10}$$

where the heat flux h is obtained from

$$h = -\mathbf{n} \cdot \mathbf{q} \,. \tag{5.11}$$

Here, **q** is the *heat flux vector* and **n** the vector normal to the surface element **da** pointing away from the body. In order to associate heat flows into the body with increasing energy, the sign of the heat flux term (5.11) is negative, since positive heat flow is out of the body.
The *first law of thermodynamics* states that the rate of change in the total energy in the body is equal to the rate of work by the external forces and rate of work provided by heat flux and energy sources (cf. Belytschko et al. 2000, Altenbach & Altenbach 1994). The weak form of the first law of thermodynamics is obtained using (4.15) and (4.43) by substitution of the rate form of (5.5) with (5.6) – (5.7) and (5.9) – (5.11) into (5.8)

$$\int_{\mathcal{B}} \rho \dot{u} \, \mathrm{d}v = \int_{\mathcal{B}} (\boldsymbol{\sigma} : \mathbf{D} - \nabla \cdot \mathbf{q} + \rho r) \, \mathrm{d}v \,. \tag{5.12}$$

Then invoking the arbitrariness of the domain gives the partial differential equation of energy conservation

$$\rho \dot{u} = \boldsymbol{\sigma} : \mathbf{D} - \nabla \cdot \mathbf{q} + \rho r \,. \tag{5.13}$$

For vanishing heat flux and heat sources, the differential equation for a purely mechanical process is obtained from the strong form of the first law

$$\rho \dot{u} = \boldsymbol{\sigma} : \mathbf{D} \,. \tag{5.14}$$

The above is called the *internal energy rate* or *internal power*. It defines the rate of energy imparted to a unit volume of the body in terms of the measures of stress and strain. Since according to (5.14) the internal power is obtained by contraction of the Cauchy stress $\boldsymbol{\sigma}$ and the stretching **D**, it is evident that the Cauchy stress and the stretching are conjugate in power.[13] Equivalent Lagrangian descriptions to the Eulerian formulation of the first law of thermodynamics (5.12) and (5.13) can be derived using (3.35) and (3.42). With (4.42) and the referential heat flux vector

$$\mathbf{Q} = J\mathbf{F}^{-1}\mathbf{q} \,, \tag{5.15}$$

[13] Alternatively, the phrase *conjugate in work or energy* is used, but the phrase *conjugate in power* is more accurate.

the Lagrangian description of the weak form of the first law (5.12) is obtained

$$\int_{\mathcal{B}_0} \rho_0 \dot{u} \, \mathrm{d}V = \int_{\mathcal{B}_0} \left(\mathrm{tr}\left(\mathbf{P}\dot{\mathbf{F}}\right) - \nabla_0 \cdot \mathbf{Q} + \rho_0 r \right) \mathrm{d}V \,. \tag{5.16}$$

Here, equation (4.50) for the energy rate was used to express the internal power in terms of the nominal stress tensor $\mathbf{P}$ and the rate of the deformation gradient $\mathbf{F}$.
The Lagrangian counterpart to (5.13) is

$$\rho_0 \dot{u} = \mathrm{tr}\left(\mathbf{P}\dot{\mathbf{F}}\right) - \nabla_0 \cdot \mathbf{Q} + \rho_0 r \,. \tag{5.17}$$

5.4 Second law of thermodynamics

5.4.1 Entropy

The first law of thermodynamics is an expression of the interconvertibility of heat and work and imposes no restrictions on the direction of processes. Based on the concept of entropy, the second law of thermodynamics puts limits on the direction of irreversible processes. It therefore poses certain restrictions on constitutive relations (cf. Belytschko et al. 2000).
The entropy S of a body B is obtained by integration of the specific entropy s over the domain of the body

$$S = \int_{\mathcal{B}} \rho s \, \mathrm{d}v \,. \tag{5.18}$$

Entropy is a measure for the amount of energy irreversibly transformed into forms of energy such as heat that cannot be transformed into mechanical work. Irreversible processes are always associated with the production of entropy and vice versa. A process of constant entropy is called an *isentropic* process.

5.4.2 Thermodynamic potentials and Maxwell relations

Continuum thermodynamics with internal state variables based on a caloric equation of state assumes that the local specific internal energy u is determined by the thermodynamic state, specified by external and internal state variables (cf. Malvern 1969, Coleman & Gurtin 1967). For the material under consideration, which may be treated as homogeneous as no changes in its components are considered, the *caloric equation of state*

$$u = u(s, \mathbf{h}^e, \mathbf{a}) \tag{5.19}$$

is postulated, the dependence on $\mathbf{X}$ being implicit. Note that, in accordance with Lehmann (1974, 1984), only the *reversible* strain $\mathbf{h}^e$ is introduced as

thermodynamic state variable. Specifically, the inelastic part of the deformation gradient $\mathbf{F}^i$ is no state variable, since there are processes associated with inelastic deformation that do not result in a change of state, and processes without residual inelastic deformation may be associated with a change of state. Therefore, the elastic-inelastic part of the strain $\mathbf{h}^{ei}$ (compare equation (3.147)) is no state variable either. However, the concept is not unique to the reversible Hencky strain. On the contrary, arbitrary reversible measures of strain are admissible. Of course, different measures of strain are conjugated in power to different stress measures.

Thermodynamic temperature Θ and thermodynamic tension $\boldsymbol{\pi}$ are defined by

$$\Theta = \left.\frac{\partial u}{\partial s}\right|_{\mathbf{h}^e} \qquad \boldsymbol{\pi} = \rho_0 \left.\frac{\partial u}{\partial \mathbf{h}^e}\right|_s , \tag{5.20}$$

where the subscripts indicate variables held constant. Due to the assumed dependence of u on $\mathbf{h}^e$, the stress $\boldsymbol{\pi}$ is obtained as thermodynamic tension. The specific internal energy can thus be regarded as a potential for the thermodynamic tension $\boldsymbol{\pi}$.[14]

Holding the set of internal variables $\mathbf{a}$ intended to describe irreversible processes constant momentarily, in the Lagrangian configuration the rate of change in the thermodynamic state of a given particle $\mathbf{X}$ is

$$\dot{u} = \frac{\partial u}{\partial s}\,\dot{s} + \frac{\partial u}{\partial \mathbf{H}^e} : \dot{\mathbf{H}}^e . \tag{5.21}$$

By virtue of (1.7), (3.125) and (3.126), for the current configuration the rate of the internal energy is

$$\dot{u} = \frac{\partial u}{\partial s}\,\dot{s} + \frac{\partial u}{\partial \mathbf{h}^e} : \overset{\circ}{\mathbf{h}}{}^{e\,\mathrm{R}} . \tag{5.22}$$

By comparison with (5.20) it follows

$$\dot{u} = \Theta\,\dot{s} + \frac{1}{\rho_0}\,\boldsymbol{\pi} : \overset{\circ}{\mathbf{h}}{}^{e\,\mathrm{R}} . \tag{5.23}$$

This equation is called *Gibbs relation.*

In addition to the specific internal energy u, Malvern (1969) introduces three other thermodynamic potentials: the specific Helmholtz free energy, specific enthalpy and specific Gibbs energy. The specific *Helmholtz free energy* ψ is the portion of the specific internal energy u available for doing work in an *isothermal* process (Θ = *const*). It is defined from u by a single *Legendre transformation* (cf. Oberste-Brandenburg 1999)

$$\psi = u - \frac{\partial u}{\partial s}\,s . \tag{5.24}$$

[14] As mentioned above, the energy of the body is influenced by the internal state variables $\mathbf{a}$. These parts of the internal energy do not contribute to the stress defined by equation (5.20_2).

This is combined with the definition of the thermodynamic temperature (5.20). Then, replacing the specific entropy s by its conjugate variable Θ gives

$$\begin{aligned} \psi &= \psi(\mathbf{h}^e, \Theta, \mathbf{a}) \\ &= u - \Theta s \,. \end{aligned} \tag{5.25}$$

Elimination of the reversible Hencky strain $\mathbf{h}^e$ from (5.25) by another Legendre transformation yields the specific *Gibbs energy* or *free enthalpy* g

$$g = \psi - \frac{\partial \psi}{\partial \mathbf{h}^e} : \mathbf{h}^e \,. \tag{5.26}$$

The specific Gibbs energy depends on the thermodynamic temperature Θ and on the stress $\boldsymbol{\pi}$

$$g = g(\Theta, \boldsymbol{\pi}, \mathbf{a}) \,. \tag{5.27}$$

Substitution of the time rate of (5.25) into (5.23) gives

$$\begin{aligned} \dot{\psi} &= \frac{\partial \psi}{\partial \Theta} \dot{\Theta} + \frac{\partial \psi}{\partial \mathbf{h}^e} : \overset{\circ}{\mathbf{h}}{}^{e\,\mathrm{R}} \\ &= -s\dot{\Theta} + \frac{1}{\rho_0} \boldsymbol{\pi} : \overset{\circ}{\mathbf{h}}{}^{e\,\mathrm{R}} . \end{aligned} \tag{5.28}$$

Evidently,

$$s = -\left. \frac{\partial \psi}{\partial \Theta} \right|_{\mathbf{h}^e} \qquad \boldsymbol{\pi} = \rho_0 \left. \frac{\partial \psi}{\partial \mathbf{h}^e} \right|_{\Theta} . \tag{5.29}$$

Thus, the specific Gibbs energy may be obtained from the specific free energy

$$g = \psi - \frac{1}{\rho_0} \boldsymbol{\pi} : \mathbf{h}^e \,. \tag{5.30}$$

The specific *enthalpy* h is defined as the portion of internal energy that can be released as heat when the thermodynamic tensions are held constant

$$\begin{aligned} h &= h(\boldsymbol{\pi}, s, \mathbf{a}) \\ &= g - \frac{\partial g}{\partial \Theta} \Theta \,. \end{aligned} \tag{5.31}$$

Employing the same procedure as above, rate equations for g are obtained

$$\begin{aligned} \dot{g} &= \frac{\partial g}{\partial \Theta} \dot{\Theta} + \frac{\partial g}{\partial \boldsymbol{\pi}} : \overset{\circ}{\boldsymbol{\pi}}{}^{\mathrm{R}} \\ &= -s\dot{\Theta} - \frac{1}{\rho_0} \mathbf{h}^e : \overset{\circ}{\boldsymbol{\pi}}{}^{\mathrm{R}} . \end{aligned} \tag{5.32}$$

Potential	Partial Derivatives
Internal energy u	$\Theta = \left.\frac{\partial u}{\partial s}\right\|_{\mathbf{h}^e} \quad \boldsymbol{\pi} = \rho_0 \left.\frac{\partial u}{\partial \mathbf{h}^e}\right\|_s$
Helmholtz free energy ψ	$s = -\left.\frac{\partial \psi}{\partial \Theta}\right\|_{\mathbf{h}^e} \quad \boldsymbol{\pi} = \rho_0 \left.\frac{\partial \psi}{\partial \mathbf{h}^e}\right\|_\Theta$
Gibbs energy g	$s = -\left.\frac{\partial g}{\partial \Theta}\right\|_{\boldsymbol{\pi}} \quad \mathbf{h}^e = -\rho_0 \left.\frac{\partial g}{\partial \boldsymbol{\pi}}\right\|_\Theta$
Enthalpy h	$\Theta = \left.\frac{\partial h}{\partial s}\right\|_{\boldsymbol{\pi}} \quad \mathbf{h}^e = -\rho_0 \left.\frac{\partial h}{\partial \boldsymbol{\pi}}\right\|_s$

Table 5.1: Definitions of thermodynamic variables based on their potentials

This defines

$$s = -\left.\frac{\partial g}{\partial \Theta}\right|_{\boldsymbol{\pi}} \qquad \mathbf{h}^e = -\rho_0 \left.\frac{\partial g}{\partial \boldsymbol{\pi}}\right|_\Theta , \tag{5.33}$$

and therefore

$$h = g + s\Theta . \tag{5.34}$$

Substitution of (5.34) into rate equation (5.32) yields

$$\begin{aligned} \dot{h} &= \frac{\partial h}{\partial s}\dot{s} + \frac{\partial h}{\partial \boldsymbol{\pi}} : \overset{\circ}{\boldsymbol{\pi}}{}^{\mathrm{R}} \\ &= \Theta\dot{s} - \frac{1}{\rho_0}\mathbf{h}^e : \overset{\circ}{\boldsymbol{\pi}}{}^{\mathrm{R}} , \end{aligned} \tag{5.35}$$

and temperature and elastic strain are found from the partial derivatives

$$\Theta = \left.\frac{\partial h}{\partial s}\right|_{\boldsymbol{\pi}} \qquad \mathbf{h}^e = -\rho_0 \left.\frac{\partial h}{\partial \boldsymbol{\pi}}\right|_s . \tag{5.36}$$

Using this result, another Legendre transformation may be used to obtain the specific internal energy u

$$\begin{aligned} u &= h - \frac{\partial h}{\partial \boldsymbol{\pi}} : \boldsymbol{\pi} \\ &= h + \frac{1}{\rho_0}\mathbf{h}^e : \boldsymbol{\pi} . \end{aligned} \tag{5.37}$$

The foregoing results are summarized in Table 5.1. From the first two rows it can be seen that the internal energy density u is a potential for the thermodynamic tension π in an isentropic process ($s = const$), while the specific Helmholtz free energy ψ is a potential for the tension in an isothermal process.
From these potentials the *Maxwell relations* may be derived by calculating their mixed second derivatives. For example, the specific Gibbs energy (5.27)

$$g = g(\Theta, \pi, \mathbf{a}) \tag{5.38}$$

depends on the temperature Θ and on the stress π. Hence from (5.34) it follows

$$\frac{\partial^2 g}{\partial \Theta \partial \pi} = \frac{\partial^2 h}{\partial \Theta \partial \pi} - \frac{\partial^2 (s\Theta)}{\partial \Theta \partial \pi} = - \left. \frac{\partial s}{\partial \pi} \right|_{\Theta} . \tag{5.39}$$

Equivalently, (5.30) gives

$$\frac{\partial^2 g}{\partial \Theta \partial \pi} = - \left. \frac{1}{\rho_0} \frac{\partial \mathbf{h}^e}{\partial \Theta} \right|_{\pi} , \tag{5.40}$$

where it is assumed that the derivatives with respect to Θ and π commute. Equating (5.39) with (5.40) yields one of four Maxwell relations. Application of this procedure to the specific internal energy, Helmholtz free energy and enthalpy then gives the set of Maxwell relations summarized in Table 5.2.

Potential	Maxwell relation
$u(s, \mathbf{h}^e, \mathbf{a})$	$\left. \frac{\partial \Theta}{\partial \mathbf{h}^e} \right\|_s = \left. \frac{1}{\rho_0} \frac{\partial \pi}{\partial s} \right\|_{\mathbf{h}^e}$
$\psi(\mathbf{h}^e, \Theta, \mathbf{a})$	$- \left. \frac{\partial s}{\partial \mathbf{h}^e} \right\|_{\Theta} = \left. \frac{1}{\rho_0} \frac{\partial \pi}{\partial \Theta} \right\|_{\mathbf{h}^e}$
$g(\Theta, \pi, \mathbf{a})$	$- \left. \frac{\partial s}{\partial \pi} \right\|_{\Theta} = - \left. \frac{1}{\rho_0} \frac{\partial \mathbf{h}^e}{\partial \Theta} \right\|_{\pi}$
$h(\pi, s, \mathbf{a})$	$\left. \frac{\partial \Theta}{\partial \pi} \right\|_s = - \left. \frac{1}{\rho_0} \frac{\partial \mathbf{h}^e}{\partial s} \right\|_{\pi}$

Table 5.2: Maxwell relations

5.4.3 Clausius-Duhem inequality

The *second law of thermodynamics* is based on the notion of entropy and states that the total rate of increase of entropy in a body B cannot be smaller than the entropy input supplied to the body from the outside

$$\frac{\mathrm{d}}{\mathrm{d}t}\int_{\mathcal{B}} \rho s \,\mathrm{d}v \geq \int_{\mathcal{B}} \frac{\rho r}{\Theta}\,\mathrm{d}v - \int_{\partial\mathcal{B}} \frac{\mathbf{q}\cdot\mathbf{n}}{\Theta}\,da\,. \tag{5.41}$$

Applying the divergence theorem to the surface integral gives

$$\int_{\mathcal{B}} \left(\rho\dot{s} - \frac{\rho r}{\Theta} + \nabla\cdot\left(\frac{\mathbf{q}}{\Theta}\right)\right)\mathrm{d}v \geq 0\,, \tag{5.42}$$

and noting that the inequality is valid for arbitrary volumes yields

$$\rho\dot{s} - \frac{\rho r}{\Theta} + \nabla\cdot\left(\frac{\mathbf{q}}{\Theta}\right) \geq 0\,. \tag{5.43}$$

This inequality is known as *Clausius-Duhem inequality*. The Lagrangian formulation of (5.43) is

$$\rho_0\dot{s} - \frac{\rho_0 r}{\Theta} + \nabla_0\cdot\left(\frac{\mathbf{Q}}{\Theta}\right) \geq 0\,. \tag{5.44}$$

In (5.43) and (5.44), the inequality implies internal entropy production in an irreversible process; the equality holds for reversible processes.
Decomposing the rate $\dot{s}$ in (5.43) as suggested by Lehmann (1984)

$$\dot{s} = \dot{s}_{rev} + \dot{s}_{irr} \tag{5.45}$$

into a reversible part

$$\dot{s}_{rev} - \frac{r}{\Theta} + \frac{1}{\rho}\nabla\cdot\left(\frac{\mathbf{q}}{\Theta}\right) = 0 \tag{5.46}$$

and an irreversible part $\dot{s}_{irr}$ gives

$$\rho\dot{\gamma} = \rho\dot{s}_{irr} = \rho\dot{s} - \frac{\rho r}{\Theta} + \nabla\cdot\left(\frac{\mathbf{q}}{\Theta}\right). \tag{5.47}$$

Here, $\dot{s}_{irr}$ is identified as the *internal entropy production rate* per unit mass $\dot{\gamma}$. Hence, in a Eulerian respectively Lagrangian description the Clausius-Duhem inequality (5.43) respectively (5.44) is written as[15]

$$\rho\dot{\gamma} \geq 0 \qquad \rho_0\dot{\gamma} \geq 0\,. \tag{5.48}$$

[15] Originally, Clausius formulated the second law for cyclic processes $\oint \rho\dot{\gamma} \geq 0$ only. He arrived at relations of the form of (5.48) by the additional assumption that two arbitrary states within the cyclic process must be linked by a reversible path (cf. Ziegler 1970).

The first law of thermodynamics (5.13) and the Clausius-Duhem inequality (5.48) may be combined by elimination of the heat source r to give

$$\rho\dot{s} + \nabla\cdot\left(\frac{\mathbf{q}}{\Theta}\right) - \frac{1}{\Theta}\left(\rho\dot{u} - \boldsymbol{\sigma} : \mathbf{D} + \nabla\cdot\mathbf{q}\right) \geq 0\,. \tag{5.49}$$

Using

$$\nabla\cdot\left(\frac{\mathbf{q}}{\Theta}\right) = \frac{1}{\Theta}\nabla\cdot\mathbf{q} - \frac{1}{\Theta^2}\,\mathbf{q}\cdot\nabla\Theta\,, \tag{5.50}$$

the term $\nabla\cdot\mathbf{q}/\Theta$ is eliminated and (5.49) can be rearranged to yield

$$\Theta\rho\dot{\gamma} = \rho\left(\Theta\dot{s} - \dot{u}\right) + \boldsymbol{\sigma} : \mathbf{D} - \Theta^{-1}\mathbf{q}\cdot\nabla\Theta \geq 0\,. \tag{5.51}$$

Substitution of the time derivative of (5.25)

$$\Theta\dot{s} - \dot{u} = -\dot{\Theta}s - \dot{\psi} \tag{5.52}$$

into (5.51) eliminates the rate of the specific internal energy and yields the Clausius-Duhem inequality in terms of the specific Helmholtz free energy

$$\Theta\rho\dot{\gamma} = \boldsymbol{\sigma} : \mathbf{D} - \rho\left(\dot{\psi} + s\dot{\Theta}\right) - \Theta^{-1}\mathbf{q}\cdot\nabla\Theta \geq 0\,. \tag{5.53}$$

This formulation of the Clausius-Duhem inequality will be used subsequently. With respect to the Lagrangian configuration, the Clausius-Duhem inequality reads

$$\Theta\rho_0\dot{\gamma} = \mathrm{tr}\left(\mathbf{P}\dot{\mathbf{F}}\right) - \rho_0\left(\dot{\psi} + s\dot{\Theta}\right) - \Theta^{-1}\mathbf{Q}\cdot\nabla_0\Theta \geq 0\,. \tag{5.54}$$

5.5 Decomposition of stress power

Based on the multiplicative decomposition (3.148) of the deformation gradient into an elastic and an inelastic part

$$\mathbf{F} = \mathbf{F}^e\mathbf{F}^i\,, \tag{5.55}$$

and the corresponding relation (3.155) for the rate of the deformation gradient

$$\dot{\mathbf{F}} = \dot{\mathbf{F}}^e\mathbf{F}^i + \mathbf{F}^e\dot{\mathbf{F}}^i\,, \tag{5.56}$$

the stress power $\boldsymbol{\sigma} : \mathbf{D}$ in (5.53) may be decomposed additively into a reversible (elastic) and an irreversible (inelastic) part

$$J\boldsymbol{\sigma} : \mathbf{D} = \dot{w} = \dot{w}^e + \dot{w}^i\,. \tag{5.57}$$

The elastic part of the stress power is denoted by $\dot{w}^e$ and defined as

$$\dot{w}^e = \boldsymbol{\tau} : \mathbf{D}^e = \frac{1}{2}\,\boldsymbol{\tau} : \left(\dot{\mathbf{F}}^e\mathbf{F}^{-e} + \mathbf{F}^{-e\mathrm{T}}\dot{\mathbf{F}}^{e\mathrm{T}}\right)\,, \tag{5.58}$$

and the inelastic part $\dot{w}^i$ as

$$\dot{w}^i = \boldsymbol{\tau} : \mathbf{D}^{ei} = \frac{1}{2}\boldsymbol{\tau} : \left(\mathbf{F}^e\dot{\mathbf{F}}^i\mathbf{F}^{-i}\mathbf{F}^{-e} + \mathbf{F}^{-e\mathrm{T}}\mathbf{F}^{-i\mathrm{T}}\dot{\mathbf{F}}^{i\mathrm{T}}\mathbf{F}^{e\mathrm{T}}\right) . \tag{5.59}$$

Here and henceforth the Kirchhoff stress $\boldsymbol{\tau} = J\boldsymbol{\sigma} = (\rho_0/\rho)\,\boldsymbol{\sigma}$ is used.
Substitution of the decomposition of power into the Clausius-Duhem inequality (5.53) gives

$$\Theta\rho\dot{\gamma} = \frac{\rho}{\rho_0}\boldsymbol{\tau} : \mathbf{D}^e + \frac{\rho}{\rho_0}\dot{w}^i - \rho\left(\dot{\psi} + s\dot{\Theta}\right) - \Theta^{-1}\mathbf{q}\cdot\nabla\Theta \geq 0 . \tag{5.60}$$

Using (3.139)

$$\overset{\circ}{\mathbf{h}}{}^{\mathrm{Log}} = \mathbf{D} , \tag{5.61}$$

the inelastic part of the specific energy rate (5.59) may be written in terms of the logarithmic rate of the Hencky strain[16]

$$\dot{w}^i = \boldsymbol{\tau} : \overset{\circ}{\mathbf{h}}{}^{ei\,\mathrm{Log}} . \tag{5.62}$$

5.6 Thermodynamic consistency

The constitutive theory to be developed can only be a valid description of the thermomechanical process considered if it obeys the restrictions posed by the first and second laws of thermodynamics. Specifically, the second law in form of the Clausius-Duhem inequality puts limits on the direction of irreversible processes. Using the relations presented in the previous sections, a criterion for thermomechanical constitutive theories ensuring agreement with the laws of thermodynamics can be derived. Theories obeying this criterion are called *thermodynamically consistent.*
Based on the postulated caloric equation of state (5.19)

$$u = u(s, \mathbf{h}^e, \mathbf{a}) , \tag{5.63}$$

constitutive equations for temperature Θ, stress $\boldsymbol{\pi}$ and heat flux $\mathbf{q}$ of the form

$$\begin{aligned} \Theta &= \Theta(s, \mathbf{h}^e, \mathbf{a}) \\ \boldsymbol{\pi} &= \boldsymbol{\pi}(s, \mathbf{h}^e, \mathbf{a}) \\ \mathbf{q} &= \mathbf{q}(s, \mathbf{h}^e, \mathbf{a}) \end{aligned} \tag{5.64}$$

may be established (cf. Malvern 1969). In accordance with Lehmann (1989c), it is presumed that the specific internal energy is uniquely determined by the external and internal state variables s, $\mathbf{h}^e$, and $\mathbf{a}$. The choice of internal variables $\mathbf{a}$ is specific to the respective phenomenological model.

[16] Note that motivated by (4.50), $\dot{w}^i$ is defined as an energy density here.

Legendre transformation (5.25) introduces the absolute temperature as a state variable

$$\psi = \psi(\mathbf{h}^e, \Theta, \mathbf{a}) . \tag{5.65}$$

Consequently, the constitutive equations are of the form

$$\begin{aligned} \boldsymbol{\pi} &= \boldsymbol{\pi}(\mathbf{h}^e, \Theta, \mathbf{a}) \\ s &= s(\mathbf{h}^e, \Theta, \mathbf{a}) \\ \mathbf{q} &= \mathbf{q}(\mathbf{h}^e, \Theta, \mathbf{a}) . \end{aligned} \tag{5.66}$$

Here, the *principle of equipresence* attributed to Truesdell (1951) is used, which states that "a variable present as an independent variable in one constitutive equation should be so present in all" (Truesdell & Toupin 1960), unless its presence is contradictory to a general law of physics or the assumed symmetry of the material. Processes defined by (5.66) have to obey the *principle of material frame indifference* or *principle of objectivity of material properties*, which asserts that an admissible process must remain admissible after a change of frame (cf. Coleman & Gurtin 1967). Hence, constitutive equations (5.66) must be isotropic tensor functions.
There are several other principles governing the mechanical behavior of materials, thus posing restrictions on constitutive equations to ensure mathematical and physical compliance. Some of them, such as the choice of independent and dependent variables according to the *principle of causality*, have been obeyed implicitly. Equations (5.66) were formulated based on the *principle of local action*, asserting that the state at a given particle $\mathbf{X}$ may be determined without regard to the motion outside an arbitrary neighborhood of $\mathbf{X}$ (cf. Truesdell & Noll 1992). Finally, *physical consistency* must be achieved by ensuring that the constitutive equations do not contradict the balance equations derived in Section 4.2 and the first and second laws of thermodynamics (cf. Altenbach & Altenbach 1994). In the following, appropriate criteria for thermodynamical consistency are derived.
The total differential of the specific Helmholtz free energy $\psi = \psi(\mathbf{h}^e, \Theta, \mathbf{a})$ reads[17]

$$\dot{\psi} = \frac{\partial \psi}{\partial \mathbf{h}^e} : \overset{\circ}{\mathbf{h}}{}^{e\,\mathrm{R}} + \frac{\partial \psi}{\partial \Theta}\dot{\Theta} + \frac{\partial \psi}{\partial \mathbf{a}} \cdot \overset{\circ}{\mathbf{a}}{}^{\mathrm{R}} . \tag{5.67}$$

By virtue of (3.144), the polar rate is eliminated from (5.67)

$$\begin{aligned} \overset{\circ}{\mathbf{h}}{}^{e\,\mathrm{R}} &= \overset{\circ}{\mathbf{h}}{}^{e\,\mathrm{Log}} - \mathbf{h}^e\boldsymbol{\Omega}^{\mathrm{LR}} + \boldsymbol{\Omega}^{\mathrm{LR}}\mathbf{h}^e \\ \overset{\circ}{\mathbf{a}}{}^{\mathrm{R}} &= \overset{\circ}{\mathbf{a}}{}^{\mathrm{Log}} - \mathbf{a}\boldsymbol{\Omega}^{\mathrm{LR}} + \boldsymbol{\Omega}^{\mathrm{LR}}\mathbf{a} . \end{aligned} \tag{5.68}$$

[17] The appropriate type of contraction of the partial derivative of the free energy with respect to the internal variables and the rate of the internal variables as well as the appropriate time rate depend on the type of the respective internal variable.

Here, a notion by Hill (1978) may be introduced (cf. Bongmba 2001). For moderate deformations, the material time derivative of $\mathbf{H}$ is approximated by

$$\dot{\mathbf{H}} \approx \mathbf{R} \star \mathbf{D} . \tag{5.69}$$

Hence, for moderate deformations the stress $\boldsymbol{\pi}$ may be approximated by the Kirchhoff stress $\boldsymbol{\tau}$. In addition, for the logarithmic rotation it follows that

$$(\mathbf{R}^{\mathrm{Log}})^{\mathrm{T}} \approx \mathbf{R} , \tag{5.70}$$

giving

$$\boldsymbol{\Omega}^{\mathrm{LR}} \approx \mathbf{0} . \tag{5.71}$$

Hence, (5.67) takes the form

$$\dot{\psi} = \frac{\partial \psi}{\partial \mathbf{h}^e} : \overset{\circ}{\mathbf{h}}{}^{e\,\mathrm{Log}} + \frac{\partial \psi}{\partial \Theta} \dot{\Theta} + \frac{\partial \psi}{\partial \mathbf{a}} \cdot \mathring{\mathbf{a}}^{\mathrm{Log}} . \tag{5.72}$$

Combination of the Clausius-Duhem inequality (5.60) with (5.72) then gives

$$\Theta \rho \dot{\gamma} = \frac{\rho}{\rho_0} \dot{w}^i + \left(\frac{\rho}{\rho_0} \boldsymbol{\tau} - \rho \frac{\partial \psi}{\partial \mathbf{h}^e} \right) : \overset{\circ}{\mathbf{h}}{}^{e\,\mathrm{Log}} - \rho \left(\frac{\partial \psi}{\partial \Theta} + s \right) \dot{\Theta} - \rho \frac{\partial \psi}{\partial \mathbf{a}} \cdot \mathring{\mathbf{a}}^{\mathrm{Log}} - \Theta^{-1} \mathbf{q} \cdot \nabla \Theta \geq 0 . \tag{5.73}$$

To ensure thermodynamic consistency, all admissible processes have to comply with (5.73) for all particles $\mathbf{X}$ of B at any time t. This is guaranteed for arbitrary $\overset{\circ}{\mathbf{h}}{}^{e\,\mathrm{Log}}$ and $\dot{\Theta}$ if the *thermal equation of state* introduced in equation (5.29_2) (cf. Lehmann 1984)

$$\boldsymbol{\tau} = \rho_0 \frac{\partial \psi}{\partial \mathbf{h}^e} \tag{5.74}$$

and the caloric equation of state (5.29_1) (cf. Coleman & Noll 1963, Malvern 1969)

$$s = -\frac{\partial \psi}{\partial \Theta} \tag{5.75}$$

hold true (see also Schmidt et al. 1984). In addition, the remaining part called *internal entropy production rate* $\dot{\gamma}$ must be non-negative (cf. Kestin & Rice 1970)

$$\Theta \rho \dot{\gamma} = \frac{\rho}{\rho_0} \dot{w}^i - \rho \frac{\partial \psi}{\partial \mathbf{a}} \cdot \mathring{\mathbf{a}}^{\mathrm{Log}} - \Theta^{-1} \mathbf{q} \cdot \nabla \Theta \geq 0 . \tag{5.76}$$

Generally, the inelastic mechanical work $\dot{w}^i$ is only dissipated in part: Depending on the material under consideration, a significant amount of inelastic work

may be stored in the body due to changes in its internal structure. Therefore, Lehmann (1984) proposed the decomposition

$$\dot{w}^i = \dot{w}_{diss} + \dot{w}_{st} \tag{5.77}$$

with

$$\dot{w}_{diss} \geq 0\,. \tag{5.78}$$

Here, $\dot{w}_{diss}$ is the dissipative part of $\dot{w}^i$ as indicated by inequality (5.78). The remaining part $\dot{w}_{st}$ of inelastic mechanical work is mechanical work associated with changes in the internal structure of the material. Introducing the entropy change η due to the interaction between these structural changes and the external energy supplied to the body, and recognizing that such structural changes will be accompanied by the evolution of a set of internal variables, the stored mechanical work may be written in the form

$$\dot{w}_{st} = \rho_0 \Theta \dot{\eta} + \rho_0 \frac{\partial \psi}{\partial \mathbf{a}_{mech}} \cdot \mathring{\mathbf{a}}_{mech}{}^{\mathrm{Log}}\,. \tag{5.79}$$

Here, the internal variables representing the changes in internal structure $\mathbf{a}_{mech}$ are introduced. The remaining internal variables of the set $\mathbf{a}$ are denoted by $\mathbf{a}_{th}$, hence

$$\mathbf{a} = \{\mathbf{a}_{mech}, \mathbf{a}_{th}\}\,. \tag{5.80}$$

Substitution of (5.79) into (5.76) using (5.80) then gives

$$\Theta \rho \dot{\gamma} = \frac{\rho}{\rho_0}\, \dot{w}_{diss} + \rho \Theta \dot{\eta} - \rho \frac{\partial \psi}{\partial \mathbf{a}_{th}} \cdot \mathring{\mathbf{a}}_{th}{}^{\mathrm{Log}} - \Theta^{-1}\mathbf{q} \cdot \nabla \Theta \geq 0\,. \tag{5.81}$$

It is not generally possible to resolve the inequality $\dot{\gamma} \geq 0$ into an internal dissipation term holding for nonzero $\nabla\Theta$ and a heat conduction inequality $-\Theta^{-1}\mathbf{q} \cdot \nabla\Theta \geq 0$ holding for nonzero $\mathring{\mathbf{a}}_{th}{}^{\mathrm{R}}$ (cf. Coleman & Gurtin 1967, Kestin & Rice 1970). However, such a resolution is valid if the time rate of the internal variables is independent of $\nabla\Theta$.
In the following, the set of internal state variables is chosen to include only $\mathbf{a}_{mech}$ describing internal changes in structure. Then, in conjunction with the reasoning above, the strong form of the Clausius-Duhem inequality requires that

$$\Theta \rho \dot{\gamma}_{th} = -\Theta^{-1}\mathbf{q} \cdot \nabla \Theta \geq 0 \tag{5.82}$$

and

$$\Theta \rho \dot{\gamma}_{mech} = \frac{\rho}{\rho_0}\, \dot{w}_{diss} + \rho \Theta \dot{\eta} \geq 0 \tag{5.83}$$

must hold, singly.
Recognizing the assumption $\mathbf{a} = \mathbf{a}_{mech}$, substitution of (5.77) and (5.79) into

the latter inequality gives the internal entropy production rate due to dissipative power in the form

$$\Theta\rho\dot{\gamma}_{mech} = \frac{\rho}{\rho_0}\,\dot{w}^i - \rho\,\frac{\partial\psi}{\partial\mathbf{a}}\cdot\overset{\circ}{\mathbf{a}}^{\mathrm{Log}} \geq 0\,. \tag{5.84}$$

The quantities entering the expression for internal entropy production are often designated as *generalized irreversible forces* or *affinities* $\mathbf{X}^i$ and *fluxes* $\mathbf{J}$ (Truesdell & Toupin 1960, Kestin & Rice 1970). In the formulation above, by virtue of (5.62) a possible choice for the generalized irreversible forces is

$$\mathbf{X}^i = \left\{\frac{\rho}{\rho_0}\,\boldsymbol{\tau}, -\rho\left(\frac{\partial\psi}{\partial\mathbf{a}}\right), -\Theta^{-1}\nabla\Theta\right\}, \tag{5.85}$$

giving the fluxes

$$\mathbf{J} = \left\{\overset{\circ}{\mathbf{h}}^{ei\,\mathrm{Log}}, \overset{\circ}{\mathbf{a}}^{\mathrm{Log}}, \mathbf{q}\right\}. \tag{5.86}$$

While the choice of which factor is flux and which factor is force is somewhat arbitrary, they have to be chosen in such a manner that the contraction of the generalized irreversible force vector $\mathbf{X}^i$ and the fluxes $\mathbf{J}$ gives the mechanical and thermal dissipation power

$$\Theta\rho\dot{\gamma} = \mathbf{X}^i\cdot\mathbf{J} \geq 0\,. \tag{5.87}$$

Based on these considerations, in irreversible thermodynamics it is usually assumed that the fluxes are determined by phenomenological equations as functions of all generalized irreversible forces

$$(\mathbf{J})_k = L_{kj}(\mathbf{X}^i)_j\,, \tag{5.88}$$

or inversely

$$(\mathbf{X}^i)_k = a_{kj}(\mathbf{J})_j\,, \tag{5.89}$$

where according to the *Onsager reciprocal relations* the coefficient matrices L_{kj} and a_{kj} are assumed to be symmetric (cf. Malvern 1969).
Substitution of the phenomenological equations into (5.87) gives the quadratic forms

$$\Theta\rho\dot{\gamma} = L_{kj}(\mathbf{X}^i)_k(\mathbf{X}^i)_j \geq 0 \tag{5.90}$$

and

$$\Theta\rho\dot{\gamma} = a_{kj}(\mathbf{J})_k(\mathbf{J})_j \geq 0\,. \tag{5.91}$$

Equation (5.91) is called a *dissipation function*

$$D = D(\mathbf{J}) = a_{kj}(\mathbf{J})_k(\mathbf{J})_j\,. \tag{5.92}$$

In agreement with the phenomenological equation (5.89) this definition yields

$$(\mathbf{X}^i)_k = \frac{1}{2}\frac{\partial D}{\partial (\mathbf{J})_k}\,. \tag{5.93}$$

Again, it should be noted that in general the dissipation function (5.92) does not separate into the sum of two or more parts as it was assumed in (5.84) and (5.82), where thermal and mechanical generalized forces were considered uncoupled.
The constitutive relations derived in Chapter 6 will be based on the preceding considerations to ensure thermodynamic consistency.

5.7 Thermomechanical coupling

A thermomechanical process is characterized by a strong interaction between thermal and mechanical effects. The evolution of temperature depends on heat conduction to be described by an appropriate law, e.g. Fourier's law, and on the rate at which energy is generated during deformation.
To obtain a rate equation for the generated energy, first the total differential of the specific Helmholtz free energy (5.67) is substituted into (5.52)

$$\Theta\dot{s} = \dot{u} - \dot{\Theta}s - \left(\frac{\partial\psi}{\partial\mathbf{h}^e} : \overset{\circ}{\mathbf{h}}{}^{e\,\mathrm{R}} + \frac{\partial\psi}{\partial\Theta}\dot{\Theta} + \frac{\partial\psi}{\partial\mathbf{a}}\cdot\overset{\circ}{\mathbf{a}}{}^{\mathrm{R}}\right)\,. \tag{5.94}$$

Adopting (5.68) and (5.71), (5.94) may be rewritten

$$\Theta\dot{s} = \dot{u} - \dot{\Theta}s - \left(\frac{\partial\psi}{\partial\mathbf{h}^e} : \overset{\circ}{\mathbf{h}}{}^{e\,\mathrm{Log}} + \frac{\partial\psi}{\partial\Theta}\dot{\Theta} + \frac{\partial\psi}{\partial\mathbf{a}}\cdot\overset{\circ}{\mathbf{a}}{}^{\mathrm{Log}}\right)\,, \tag{5.95}$$

which, in conjunction with the thermal and caloric equations of state (5.74) and (5.75), gives

$$\Theta\dot{s} = \dot{u} - \frac{1}{\rho_0}\boldsymbol{\tau} : \overset{\circ}{\mathbf{h}}{}^{e\,\mathrm{Log}} - \frac{\partial\psi}{\partial\mathbf{a}}\cdot\overset{\circ}{\mathbf{a}}{}^{\mathrm{Log}}\,. \tag{5.96}$$

Eliminating the rate of the specific internal energy (5.13)

$$\dot{u} = \frac{1}{\rho}\boldsymbol{\sigma} : \mathbf{D} - \frac{1}{\rho}\nabla\cdot\mathbf{q} + r \tag{5.97}$$

and replacing the Cauchy stress by the Kirchhoff stress $\boldsymbol{\tau} = J\boldsymbol{\sigma}$ yields

$$\Theta\dot{s} = \frac{1}{\rho_0}\boldsymbol{\tau} : \mathbf{D}^{ei} - \frac{1}{\rho}\nabla\cdot\mathbf{q} + r - \frac{\partial\psi}{\partial\mathbf{a}}\cdot\overset{\circ}{\mathbf{a}}{}^{\mathrm{Log}}\,. \tag{5.98}$$

Furthermore, an additional equation for the rate of the specific entropy may be obtained from the caloric equation of state in terms of the specific Gibbs free energy g (5.33_1)

$$s = -\frac{\partial g}{\partial\Theta}\,. \tag{5.99}$$

The definition of the specific heat at constant pressure c_p with $\boldsymbol{\pi} = \boldsymbol{\tau}$

$$c_p = \left.\frac{\partial h}{\partial \Theta}\right|_{\boldsymbol{\tau}}, \tag{5.100}$$

combined with Legendre transformation (5.31) of the specific Gibbs energy $g = g(\Theta, \boldsymbol{\tau}, \mathbf{a})$ to the specific enthalpy $h = h(\boldsymbol{\tau}, s, \mathbf{a})$

$$h = g - \frac{\partial g}{\partial \Theta}\,\Theta \tag{5.101}$$

gives

$$c_p = -\Theta \left.\frac{\partial^2 g}{\partial \Theta^2}\right|_{\boldsymbol{\tau}}. \tag{5.102}$$

Rearranging the time rate obtained from the total differential of equation (5.99)

$$-\dot{s} = \frac{\partial^2 g}{\partial \Theta \partial \boldsymbol{\tau}} : \overset{\circ}{\boldsymbol{\tau}}{}^{\mathrm{Log}} + \frac{\partial^2 g}{\partial \Theta^2}\dot{\Theta} + \frac{\partial^2 g}{\partial \Theta \partial \mathbf{a}} : \overset{\circ}{\mathbf{a}}{}^{\mathrm{Log}} \tag{5.103}$$

and substitution of (5.102) yields

$$c_p \dot{\Theta} = \Theta \dot{s} + \Theta \frac{\partial^2 g}{\partial \Theta \partial \boldsymbol{\tau}} : \overset{\circ}{\boldsymbol{\tau}}{}^{\mathrm{Log}} + \Theta \frac{\partial^2 g}{\partial \Theta \partial \mathbf{a}} : \overset{\circ}{\mathbf{a}}{}^{\mathrm{Log}}. \tag{5.104}$$

Using (5.98) and noting that

$$\frac{\partial g}{\partial \mathbf{a}} = \frac{\partial \psi}{\partial \mathbf{a}}, \tag{5.105}$$

rearranging of terms gives

$$c_p \dot{\Theta} = -\frac{1}{\rho} \nabla \cdot \mathbf{q} + \frac{1}{\rho_0} \boldsymbol{\tau} : \mathbf{D}^{ei} + r - \frac{\partial g}{\partial \mathbf{a}} \cdot \overset{\circ}{\mathbf{a}}{}^{\mathrm{Log}} + \Theta \frac{\partial^2 g}{\partial \Theta \partial \boldsymbol{\tau}} : \overset{\circ}{\boldsymbol{\tau}}{}^{\mathrm{Log}} + \Theta \frac{\partial^2 g}{\partial \Theta \partial \mathbf{a}} : \overset{\circ}{\mathbf{a}}{}^{\mathrm{Log}}. \tag{5.106}$$

The sum of the last five terms on the right-hand side of this equation equals the rate at which energy is generated per unit mass

$$\frac{1}{\rho}\dot{h}_{lat} = \frac{1}{\rho_0} \boldsymbol{\tau} : \mathbf{D}^{ei} + r - \frac{\partial g}{\partial \mathbf{a}} \cdot \overset{\circ}{\mathbf{a}}{}^{\mathrm{Log}} + \Theta \frac{\partial^2 g}{\partial \Theta \partial \boldsymbol{\tau}} : \overset{\circ}{\boldsymbol{\tau}}{}^{\mathrm{Log}} + \Theta \frac{\partial^2 g}{\partial \Theta \partial \mathbf{a}} : \overset{\circ}{\mathbf{a}}{}^{\mathrm{Log}}. \tag{5.107}$$

Here, the rate $\dot{h}_{lat}$ at which energy is generated per unit volume is defined. Using (5.107), equation (5.106) reduces to

$$c_p \dot{\Theta} = -\frac{1}{\rho} \nabla \cdot \mathbf{q} + \frac{1}{\rho}\dot{h}_{lat}. \tag{5.108}$$

6 Phenomenological model

6.1 Introduction

Based on the one-dimensional theory for pseudoelasticity developed by Müller (1989, 1991), within a small deformation theory Raniecki et al. (1992) propose a three-dimensional thermodynamic model to describe materials undergoing pseudoelastic phase transformations. They call their model R_L-model since in its original form it is a rather general *reference* model that can be specified to correspond to a number of material models known in the literature (see Section 2.2.4 in this context).
In this chapter, an extension of the R_L-model to finite deformations is proposed. While the fundamental ideas of the R_L-model are accepted and will be adopted consequently, the thermodynamic framework is reformulated in agreement with the considerations given in Chapter 5.
Constitutive relations are developed based on the kinematic theory presented in Chapter 3. The derivations originate from the specific Helmholtz free energy of constrained equilibria. Hence, after a few remarks on the description of the purely elastic response of the pseudoelastic body considered here, this potential is formulated in terms of the external and internal state variables. The general set of internal variables defined in Chapter 5 is specified to include one scalar internal variable, the mass fraction of martensite ξ. This limits the applicability of the phenomenological model to pseudoelasticity; however, it is possible to extend the framework given to include shape-memory and two-way effects. Some remarks regarding possible modifications are given in Section 8.2.
In agreement with the thermodynamic considerations presented in Chapter 5, thermal and caloric equations of state are derived. Equations governing the evolution of ξ during forward and reverse phase transformations are specified in agreement with the requirements posed by the Clausius-Duhem inequality. Based on these relations, rate equations for the elastic-phase transformation part of the strain and in turn for the elastic part of the strain are derived to permit the calculation of stress.

6.2 Elastic material response

The elastic response of the phase transforming body has to be characterized in order to derive the specific Helmholtz free energy function. In Section 3.7, the decomposition of the stretching into an elastic and an elastic-inelastic part was introduced. Here, the only type of inelastic material response under consideration is inelasticity due to phase transformation. Hence, equation (3.147) may be written as

$$\mathbf{D} = \mathbf{D}^e + \mathbf{D}^{etr} . \tag{6.1}$$

The elastic-phase transformation part of the stretching denoted by $\mathbf{D}^{etr}$ follows from the description of the transformation kinetics in Section 6.4.
On the other hand, the purely elastic response depends on the elastic part of the stretching $\mathbf{D}^e$. In this section, a rate type equation for $\mathbf{D}^e$ is derived based on a hyperelasticity theory developed by Xiao et al. (1999a, 2000b). In its general form, this theory is applicable to both isotropic and anisotropic material symmetries.

6.2.1 Complementary hyperelastic potential

In Section 5.4.2, the thermodynamic potential $g(\Theta, \pi, \mathbf{a})$ called Gibbs free energy was introduced. The Gibbs free energy may be interpreted as the *complementary hyperelastic potential* Σ of the elastic-phase transforming body. In the reference configuration, this potential is defined as

$$\Sigma(\Theta, \mathbf{R}^{\mathrm{T}} \star \pi, \mathbf{R}^{\mathrm{T}} \star \mathbf{a}) = -\rho_0 g(\Theta, \mathbf{\Pi}, \mathbf{A}) \,. \tag{6.2}$$

Here, the Lagrangian stress measure that is work-conjugated to the Lagrangian logarithmic strain measure $\mathbf{H}$ is designated by $\mathbf{\Pi}$. $\mathbf{A}$ is the Lagrangian representation of the Eulerian internal variables $\mathbf{a}$. For processes of purely elastic deformation, where $\mathbf{a} = const$, the elastic part of the Lagrangian Hencky strain is obtained from the complementary hyperelastic potential (6.2) by virtue of the thermal equation of state

$$\mathbf{H}^e = \frac{\partial \Sigma}{\partial \mathbf{\Pi}} \,. \tag{6.3}$$

Following Xiao et al. (2000b), the complementary potential may equivalently be written in terms of temperature Θ, Eulerian stress π and internal variables $\mathbf{a}$

$$\Sigma = \Sigma(\Theta, \pi, \mathbf{a}) \tag{6.4}$$

with

$$\frac{\partial \Sigma}{\partial \pi} = \mathbf{R} \star \frac{\partial \Sigma}{\partial \mathbf{\Pi}} \,. \tag{6.5}$$

Noting the rotated correspondence (3.85), the Eulerian thermal equation of state (5.33_2) defining the elastic part of the Eulerian Hencky strain $\mathbf{h}$ is obtained

$$\mathbf{h}^e = \frac{\partial \Sigma}{\partial \pi} \,. \tag{6.6}$$

The complementary hyperelastic potential $\Sigma(\Theta, \mathbf{\Pi})$ is invariant under the initial material symmetry group $\mathcal{G}_0$. Hence

$$\Sigma(\Theta, \mathbf{Q}_0 \star \mathbf{\Pi}) = \Sigma(\Theta, \mathbf{\Pi}) \tag{6.7}$$

for arbitrary rotation tensors $\mathbf{Q}_0 \in \mathcal{G}_0$. As a consequence, its Eulerian counterpart $\Sigma(\Theta, \boldsymbol{\pi})$ obeys the invariance requirement

$$\Sigma(\Theta, \mathbf{Q} \star \boldsymbol{\pi}) = \Sigma(\Theta, \boldsymbol{\pi}) \tag{6.8}$$

for rotation tensors $\mathbf{Q} \in \mathbf{R} \star \mathcal{G}_0$. Therefore, the complementary potential Σ is a tensor function representable by the main invariants given in (3.56) to (3.58) and vectors $\boldsymbol{\alpha}_i$ characterizing the structure of the $\mathbf{R}$-rotated group $\mathbf{R} \star \mathcal{G}_0$. This is a consequence of the dependence of $\Sigma(\Theta, \boldsymbol{\Pi})$ on the initial material symmetry axes that characterize the structure of the group $\mathcal{G}_0$. Denoting the vectors representing the initial material symmetry axes by $\hat{\boldsymbol{\alpha}}_i$, their Eulerian counterparts are given by $\boldsymbol{\alpha}_i = \mathbf{R}\hat{\boldsymbol{\alpha}}_i$.

6.2.2 Eulerian rate type formulation of hyperelastic response

Based on the hyperelastic potential $\Sigma(\Theta, \boldsymbol{\pi})$ discussed in the previous section, rate type constitutive equations applicable to arbitrary material symmetries may be derived.
It is assumed that the rate equation

$$\mathbf{D}^e = \overset{\circ}{\overline{\partial\Sigma/\partial\boldsymbol{\pi}}}^{\,\mathrm{Log}} \tag{6.9}$$

holds true. This expression is based on the self-consistency condition introduced in Section 3.6.2, requiring that for each process of purely elastic deformation, a constitutive formulation of $\mathbf{D}^e$ must be exactly-integrable to yield a hyperelastic relation between an elastic strain measure and a stress measure (cf. Bruhns et al. 1999, Xiao et al. 2000b). Here, this concept is extended to the non-isothermal case.
In evaluating (6.9), the dependency of the gradient $\partial\Sigma/\partial\boldsymbol{\pi}$ on the $\mathbf{R}$-rotated material symmetry axes must be noted. The logarithmic rate is the rate-of-change observed in a frame rotating with the spin $\boldsymbol{\Omega}^{\mathrm{Log}}$. The material axes, however, rotate with the spin $\boldsymbol{\Omega}^{\mathrm{R}}$. The contribution of this relative rotation must be taken into account in (6.9)

$$\mathbf{D}^e = \frac{\partial^2\Sigma}{\partial\boldsymbol{\pi}^2} : \overset{\circ}{\boldsymbol{\pi}}{}^{\mathrm{R}} + \left(\frac{\partial\Sigma}{\partial\boldsymbol{\pi}}\right)\boldsymbol{\Omega}^{\mathrm{LR}} - \boldsymbol{\Omega}^{\mathrm{LR}}\left(\frac{\partial\Sigma}{\partial\boldsymbol{\pi}}\right) + \boldsymbol{\alpha}\dot{\Theta}\,. \tag{6.10}$$

Here, definition (3.145) and

$$\overset{\circ}{\overline{\partial\Sigma/\partial\boldsymbol{\pi}}}^{\,\mathrm{R}} = \frac{\partial^2\Sigma}{\partial\boldsymbol{\pi}^2} : \overset{\circ}{\boldsymbol{\pi}}{}^{\mathrm{R}} \tag{6.11}$$

are used. The tensor of thermal expansion $\boldsymbol{\alpha}$, see Section 6.3.1 below, is given by

$$\boldsymbol{\alpha} = \frac{\partial^2\Sigma}{\partial\boldsymbol{\pi}\partial\Theta}\,. \tag{6.12}$$

The latter equality in (6.10) is established on the grounds that **R**-rotated material symmetry axes remain unchanged in a frame defined by the polar spin $\boldsymbol{\Omega}^{\mathrm{R}}$.
If the material behavior is isotropic, the chain rule

$$\overset{\circ}{\overline{\alpha(\boldsymbol{\pi})}}^{\mathrm{Log}} = \frac{\partial \alpha}{\partial \boldsymbol{\pi}} : \overset{\circ}{\boldsymbol{\pi}}{}^{\mathrm{Log}} \tag{6.13}$$

holds and the elastic part of the stretching is given by (cf. Xiao et al. 1999a, Bruhns et al. 1999)

$$\mathbf{D}^e = \frac{\partial^2 \Sigma}{\partial \boldsymbol{\pi}^2} : \overset{\circ}{\boldsymbol{\pi}}{}^{\mathrm{Log}} + \boldsymbol{\alpha}\dot{\Theta}\,. \tag{6.14}$$

Note that for arbitrary material symmetries, chain rule (6.13) does not hold and the elastic part of the stretching cannot be described by a relation of the form

$$\mathbf{D}^e = \overset{\circ}{\overline{\partial \Sigma / \partial \boldsymbol{\pi}}}^{\mathrm{Log}} \neq \frac{\partial^2 \Sigma}{\partial \boldsymbol{\pi}^2} : \overset{\circ}{\boldsymbol{\pi}}{}^{\mathrm{Log}}\,. \tag{6.15}$$

Hence, in general equation (6.10) must be used instead of (6.14) (cf. Xiao et al. 2000b).
Later, attention will be restricted to isotropic elasticity. Then, the Eulerian stress measure $\boldsymbol{\pi}$ is coaxial to $\mathbf{h}^e$ and coincides with the Kirchhoff stress $\boldsymbol{\tau}$. For now, no restrictions regarding material symmetries shall be imposed. It is assumed that the complementary hyperelastic potential Σ is of the form

$$\Sigma(\boldsymbol{\pi}) = \frac{1}{2}\,\boldsymbol{\pi} : \mathbb{D} : \boldsymbol{\pi} + (\Theta - \Theta_0)\boldsymbol{\alpha} : \boldsymbol{\pi}\,, \tag{6.16}$$

where the *elastic compliance* tensor $\mathbb{D}$ is introduced. A linear dependence on Θ is assumed here in agreement with the considerations in Section 6.3.1. Using equation (6.6), the elastic Hencky strain is specified in terms of $\boldsymbol{\pi}$ and $\mathbb{D}$

$$\mathbf{h}^e = \boldsymbol{\pi} : \mathbb{D} + (\Theta - \Theta_0)\boldsymbol{\alpha}\,. \tag{6.17}$$

Introducing the tensor of *elastic moduli* $\mathbb{C}$, also called *elastic stiffness* tensor, the foregoing equation may be inverted to give

$$\boldsymbol{\pi} = \mathbf{h}^e : \mathbb{C} - (\Theta - \Theta_0)\boldsymbol{\alpha} : \mathbb{C}\,. \tag{6.18}$$

6.3 Helmholtz free energy of constrained equilibria

In a state of constrained equilibrium, the material sample attains an equilibrium state corresponding to the prescribed external state variables, i.e. reversible Hencky strain $\mathbf{h}^e$ and temperature Θ, when the internal variables are taken to be held fixed at any definite set of values by imposition of appropriate

constraints. Under constant external loads, a two-phase solid body B will thus remain at complete rest, even though in general B will not be in a state of absolute equilibrium.

The rate of progression of any local microstructural rearrangement within the material is dependent on the current stress state only through the thermodynamic force conjugate to the extent of that rearrangement (cf. Rice 1971). However, considerations concerning this kinetic aspect must be preceded by a characterization of the state of constrained equilibrium that is postulated here.

Specifically, the existence of the specific Helmholtz free energy ψ depending on the external state variables $\mathbf{h}^e$ and Θ and the internal state variables $\mathbf{a}$ is presumed. This thermodynamic potential was defined in equation (5.25)

$$\psi = \psi(\mathbf{h}^e, \Theta, \mathbf{a}) . \tag{6.19}$$

Note that, in accordance with Lehmann (1989c), a dependence of ψ on the elastic-inelastic part of the strain measure is excluded in contrast to the theory of Raniecki et al. (1992), see Section 5.4.2.

In order to describe pseudoelasticity, the general set of internal variables defined in Chapter 5 may be specified to include only one scalar internal variable

$$\mathbf{a} = \{\xi\} . \tag{6.20}$$

Here, the *mass fraction of martensite* ξ is defined

$$\xi = \frac{m^M}{m} \qquad m = m^A + m^M . \tag{6.21}$$

The total mass of the phase transforming body B is denoted by m, and m^A respectively m^M are the mass of the austenitic respectively martensitic phase of B. Here and henceforth, quantities associated with the individual phases α will be denoted by

$$\alpha = \begin{cases} A & \text{(Austenite)} \\ M & \text{(Martensite)} . \end{cases}$$

It is assumed that the current state of B is uniquely determined for prescribed ξ, given the external state variables $\mathbf{h}^e$ and Θ. Since the chemical composition of the phases does not change during processes of diffusionless martensitic transformation, no internal variable accounting for such effects is necessary. However, the scope of the theory developed here is confined to pseudoelasticity as a consequence of considering only one scalar internal variable. To accurately model one-way and two-way shape memory effects, additional variables are required, i.e. to represent the orientation of stress induced martensite or to capture the evolution of plastic eigenstrains.

The specific Helmholtz free energy of B in states of equilibrium may be written as the weighted sum of the specific Helmholtz free energies of both phases

$$\psi = (1 - \xi)\psi^A + \xi\psi^M \,. \tag{6.22}$$

In constrained equilibria, physical events such as the interaction of different martensitic systems and the elastic misfit of differently oriented phase domains within the single crystal have to be accounted for (cf. Raniecki et al. 1992). Hence, equation (6.22) has to be supplemented by a an additional term to allow for these effects, see Section 6.3.2.

6.3.1 Helmholtz free energy of a single phase

To derive the specific Helmholtz free energies of the individual phases, the *specific heat at constant volume* c_v is introduced. Its dependence upon the temperature Θ may be obtained by studying an idealized model of a crystal, such as the Einstein crystal or the Debye crystal (cf. Morrill 1972). The very simple *Einstein crystal* gives a reasonably good description of the specific heat for solids. However, only at very high temperatures it agrees with data established experimentally, while for lower temperatures it underestimates the values of c_v. Debye used a more complicated model known as the *Debye crystal*, which gives a better approximation of the specific heat c_v

$$c_v = 3R\left(4D\left(\frac{\Theta_D}{\Theta}\right) - \frac{3\,\Theta_D/\Theta}{\exp(\Theta_D/\Theta) - 1}\right) , \tag{6.23}$$

where the *Debye temperature* Θ_D and *Debye function* D are introduced

$$D(y) = \frac{3}{y^3}\int_0^y \frac{x^3}{\exp(x) - 1}\,\mathrm{d}x \,. \tag{6.24}$$

Specific heat (6.23) depends on the gas constant constant R, which is obtained from the universal gas constant $R_m = 8.315\,^{\mathrm{kJ}}/_{\mathrm{kmol\,K}}$ and the molecular mass M of the solid body B through

$$R = \frac{R_m}{M} \,. \tag{6.25}$$

For temperatures close to or above the Debye temperature, c_v is almost constant (cf. Raniecki & Bruhns 1991). This is illustrated graphically in Figure 6.1 (cf. Morrill 1972, Oberste-Brandenburg 1999). For stoichiometric NiTi, Kuentzler (1992) measured a Debye temperature of about $\Theta_D = 340\,\mathrm{K}$, while Lee et al. (2001) experimentally obtained an effective Debye temperature of $\Theta_D = 370\,\mathrm{K}$. These values are considered to be sufficiently close to the

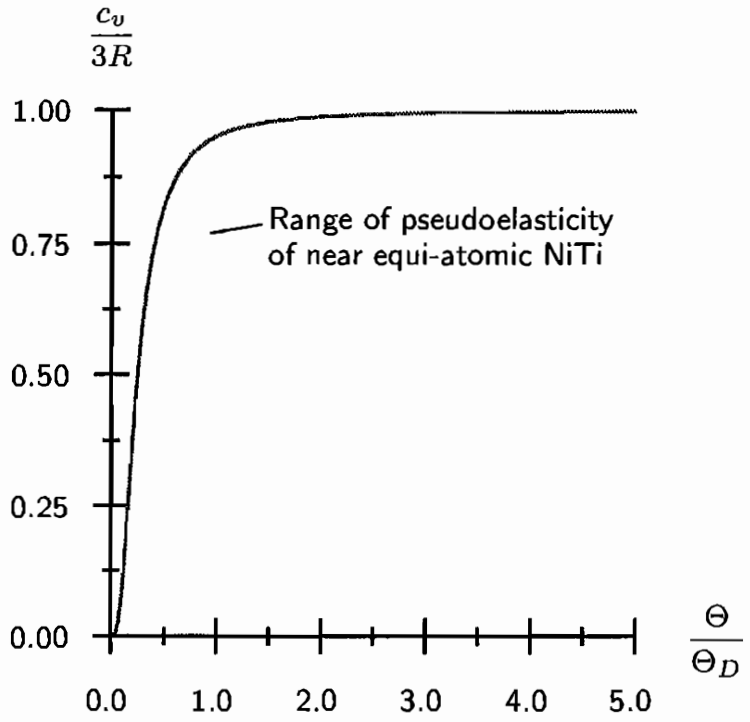

Figure 6.1: Dependence of specific heat at constant volume on temperature

temperature range where Nickel-Titanium SMAs behave pseudoelastically.[18] Hence, in the following the dependence of the specific heat at constant volume c_v upon temperature is neglected. However, a fairly accurate, but much simpler expression for c_v than given in equation (6.23) would be available from a series expansion in Θ/Θ_D at low temperatures and in Θ_D/Θ at high temperatures (cf. Callen 1970).
The specific internal energy u defines c_v through

$$c_v = \left.\frac{\partial u}{\partial \Theta}\right|_v . \tag{6.26}$$

Taking the derivative of Legendre transformation (5.25_2)

$$\psi = u - \Theta s \tag{6.27}$$

[18]The pseudoelastic temperature range depends on several parameters such as chemical composition and thermomechanical treatment (cf. Hodgson & Brown 2000). Therefore, an exact specification of the pseudoelastic temperature range is not possible even for NiTi SMAs. The region depicted in Figure 6.1 is based on transformation temperatures given in Funakubo (1984) and Saburi (1998).

with respect to temperature, and substituting (6.26) as well as the equation of state (5.29_1)

$$s = -\left.\frac{\partial \psi}{\partial \Theta}\right|_{\mathbf{h}^e} \tag{6.28}$$

gives

$$c_v = \Theta \frac{\partial s}{\partial \Theta} \,. \tag{6.29}$$

Martensitic phase transformation in SMAs, characterized here by the mass fraction of martensite ξ, is approximately isochoric (cf. Funakubo 1984). Therefore, the definition of c_v at constant volume may equivalently be expressed as the specific heat at constant reversible strain (cf. Oberste-Brandenburg 1999)

$$c_v = \Theta \left.\frac{\partial s}{\partial \Theta}\right|_{\mathbf{h}^e} \,. \tag{6.30}$$

Integration then gives

$$s = c_v \ln\left(\frac{\Theta}{\Theta_0}\right) + s_0 \,. \tag{6.31}$$

The constant of integration s_0, possibly dependent on reversible strain and mass fraction of martensite

$$s_0 = s_0(\mathbf{h}^e, \xi) \,, \tag{6.32}$$

is left to be determined. Substitution of (6.28) into (6.31) and subsequent integration yield

$$\psi = c_v \left(\Theta - \Theta_0 - \Theta \ln\left(\frac{\Theta}{\Theta_0}\right)\right) - s_0 \left(\Theta - \Theta_0\right) + \psi_0 \,, \tag{6.33}$$

where the constant of integration

$$\psi_0 = \psi_0(\mathbf{h}^e, \xi) \tag{6.34}$$

is introduced.
To determine the constants of integration s_0 and ψ_0, elasticity as specified in (6.18) is adopted

$$\frac{\partial \boldsymbol{\pi}}{\partial \mathbf{h}^e} = \mathbf{C} \,. \tag{6.35}$$

Then, following the considerations of Oberste-Brandenburg (1999), an expansion of the temperature dependent tensor of elastic moduli $\mathbb{C}$ into a Taylor series about Θ_0 gives

$$\mathbb{C} = \mathbb{C}_0 - \sum_{i=1}^{\infty} \frac{1}{i!} (\Theta - \Theta_0)^i \mathbb{C}_\Theta^{(i)} , \tag{6.36}$$

where the stiffness tensor at reference temperature $\mathbb{C}_0$

$$\mathbb{C}_0 = \mathbb{C}(\Theta = \Theta_0) \tag{6.37}$$

and the partial derivatives of the stiffness tensor

$$\mathbb{C}_\Theta^{(i)} = -\frac{\partial^i \mathbb{C}}{\partial \Theta^i}\bigg|_{\Theta=\Theta_0} \tag{6.38}$$

are introduced. Taking the second derivative of (6.31) with respect to $\mathbf{h}^e$ and using the Maxwell relations summarized in Table 5.2, substitution of (6.35) yields a differential equation for s_0

$$\frac{\partial^2 s_0}{\partial \mathbf{h}^{e\,2}} = \frac{1}{\rho_0} \sum_{i=1}^{\infty} \frac{1}{(i-1)!} (\Theta - \Theta_0)^{i-1} \mathbb{C}_\Theta^{(i)} . \tag{6.39}$$

Integrating twice with respect to $\mathbf{h}^e$ and denoting the constants of integration by $\boldsymbol{\beta}_0 = \boldsymbol{\beta}_0(\xi)$ and $s_0^* = s_0^*(\xi)$, respectively, gives

$$s_0(\mathbf{h}^e, \xi) = \frac{1}{2\rho_0} \mathbf{h}^e : \left(\sum_{i=1}^{\infty} \frac{1}{(i-1)!} (\Theta - \Theta_0)^{i-1} \mathbb{C}_\Theta^{(i)} \right) : \mathbf{h}^e + \boldsymbol{\beta}_0 : \mathbf{h}^e + s_0^* . \tag{6.40}$$

Since s_0 is independent of temperature, this relation may be simplified to yield

$$s_0(\mathbf{h}^e, \xi) = \frac{1}{2\rho_0} \mathbf{h}^e : \mathbb{C}_\Theta : \mathbf{h}^e + \boldsymbol{\beta}_0 : \mathbf{h}^e + s_0^* , \tag{6.41}$$

where the first derivative of $\mathbb{C}$ with respect to Θ is written as

$$\mathbb{C}_\Theta = \mathbb{C}_\Theta^{(1)} . \tag{6.42}$$

Due to the independence of s_0 on temperature, all higher order derivatives must vanish. Therefore, the dependence of $\mathbb{C}$ on temperature is at most linear

$$\mathbb{C} = \mathbb{C}_0 - (\Theta - \Theta_0)\mathbb{C}_\Theta . \tag{6.43}$$

Using equation (6.41), the second constant of integration ψ_0 introduced in equation (6.33) can be determined. Substitution of (6.33) into the thermal

equation of state (5.29_2), and noting that (6.41) is a function of $\mathbf{h}^e$ and that $s_0^* = s_0^*(\xi)$, gives

$$\boldsymbol{\pi} = \rho_0 \frac{\partial \psi_0}{\partial \mathbf{h}^e} - (\Theta - \Theta_0)\left(\mathbf{h}^e : \mathbb{C}_\Theta + \rho_0 \boldsymbol{\beta}_0\right) . \tag{6.44}$$

Combination of this preliminary result with (6.43) and (6.35) yields the differential equation

$$\rho_0 \frac{\partial^2 \psi_0}{\partial \mathbf{h}^{e\,2}} = \mathbb{C}_0 , \tag{6.45}$$

which may be integrated twice to give

$$\psi_0 = \frac{1}{2\rho_0} \mathbf{h}^e : \mathbb{C}_0 : \mathbf{h}^e . \tag{6.46}$$

In deriving (6.46), use was made of the initial conditions

$$\begin{aligned} \psi_0(\mathbf{h}^e = \mathbf{0}) \quad &= 0 \\ \frac{\partial \psi_0}{\partial \mathbf{h}^e}(\mathbf{h}^e = \mathbf{0}) &= \mathbf{0} . \end{aligned} \tag{6.47}$$

The constants of integration $\boldsymbol{\beta}_0$ and s_0^* are possibly dependent on the internal state variable ξ. However, assuming that this influence is negligible, they are treated as constant parameters here. Then, based on the definition of the elastic compliance tensor (6.17)

$$\frac{\partial \mathbf{h}^e}{\partial \boldsymbol{\pi}} = \mathbb{D} , \tag{6.48}$$

the tensor of *thermal expansion* $\boldsymbol{\alpha}$ may be introduced

$$\boldsymbol{\alpha} = \mathbb{D} : \rho_0 \boldsymbol{\beta}_0 . \tag{6.49}$$

At the thermodynamic reference state $\mathcal{B}_0^*$ defined in Section 5.2, the specific Helmholtz free energy must vanish. Hence, from equation (5.25_2) one obtains

$$u_0^* = \Theta_0 s_0^* . \tag{6.50}$$

Using (6.43), substitution of (6.46) and (6.41) with (6.49) and (6.50) specifies the free energy function (6.33) of a single phase to

$$\begin{aligned} \psi = \frac{1}{2\rho_0} \mathbf{h}^e : \mathbb{C} : \mathbf{h}^e - (\Theta - \Theta_0) \frac{1}{\rho_0} \boldsymbol{\alpha} : \mathbb{C} : \mathbf{h}^e \\ + c_v \left(\Theta - \Theta_0 - \Theta \ln\left(\frac{\Theta}{\Theta_0} \right) \right) + u_0^* - s_0^* \Theta . \end{aligned} \tag{6.51}$$

It should be noted that the presumed independence of temperature attributed to c_v has no influence on the preceding derivations. Also, equation (6.51) must be complemented by an appropriate definition of the elastic strain measure $\mathbf{h}^e$ before the free energy of a single phase solid may actually be calculated. Such a definition will be provided below.

6.3.2 Internal interaction in constrained equilibria

The free energy of a two-phase solid as obtainable by combination of (6.22) and (6.51) is not able to account for the hysteresis observed in phase transformation from austenite to martensite. Hence, the above description has to be modified based on the underlying physical phenomena.
Müller (1989) and Müller & Xu (1991) attribute the hysteretic behavior of SMAs to the *interfacial energy* between martensitic and austenitic domains in the body. In their theory, the interfacial energy includes phenomena such as the elastic misfit of the individual phases and the energy of elastic interaction of neighboring domains. This is motivated by the argument that coherence between domains of different phases distorts the crystal lattice in the vicinity of the interface, and that the energy required may be ascribed to the interface. Hence, in the following the term *free energy of internal interaction* will be used. It will be denoted by ψ_{it}.
There is no unique approach to derive a free energy of internal interaction. Based on micromechanical considerations, interaction matrices accounting for the individual martensite variants may be defined (cf. Patoor et al. 1996, Niclaeys et al. 2002). Then, appropriate averaging procedures such as self-consistent polycrystalline models or numerical methods such as the finite element method must be applied to find the interaction energy of a polycrystal at the macroscale (cf. Gall et al. 2000).
In a phenomenological approach, Raniecki et al. (1992) introduce a *configurational internal energy* $\bar{u}(\xi)$ and a *configurational entropy* $\bar{s}(\xi)$ due to phase transformations to amend the internal energy and entropy in equation (6.51), u_0^* respectively s_0^*. Then, the internal energies and entropies accounting for the effects of internal interaction may be written as

$$\begin{aligned} u^A &= u_0^{*A} + \bar{u}(1-\xi) \\ u^M &= u_0^{*M} + \bar{u}(\xi) \end{aligned} \tag{6.52}$$

respectively

$$\begin{aligned} s^A &= s_0^{*A} + \bar{s}(1-\xi) \\ s^M &= s_0^{*M} + \bar{s}(\xi)\,. \end{aligned} \tag{6.53}$$

It is reasonable to assume that the configurational specific free energy of martensite attains its maximum at the beginning of the $A \to M$ transformation and decreases with increasing ξ, while the configurational specific free energy of austenite is maximal at the beginning of the reverse phase transformation. At the same time it is required that the configurational specific free energy (5.25_2) in terms of the configurational internal energy and entropy be non-negative for all admissible values of ξ, with the configurational internal

energy $\bar{u}(\xi)$ and entropy $\bar{s}(\xi)$ approaching zero as ξ tends to one (cf. Raniecki et al. 1992). These requirements are met by the linear functions

$$\begin{aligned} \bar{u}(x) &= \frac{1}{2}\,\bar{u}_0(1-x) \\ \bar{s}(x) &= \frac{1}{2}\,\bar{s}_0(1-x)\,, \end{aligned} \tag{6.54}$$

where the constants $\bar{u}_0$ and $\bar{s}_0$ must satisfy

$$\bar{u}_0 - \Theta\bar{s}_0 \geq 0\,. \tag{6.55}$$

Equations (6.52) and (6.53) define internal energies and entropies that are meant to replace their counterparts in the respective specification of equation (6.51) to austenite and martensite. However, instead of modifying the specific Helmholtz free energies of the individual phases, the free energy of internal interaction may be taken into account by modifying equation (6.22): Substitution of (6.52) and (6.53) into (5.25_2) gives the configurational specific free energies of austenite and martensite

$$\psi_{it}^{A} = u^{A} - \Theta s^{A} \qquad \psi_{it}^{M} = u^{M} - \Theta s^{M}\,. \tag{6.56}$$

Adopting the interrelation between both phases as given by (6.22), the contribution of these terms to the specific Helmholtz free energy of the two-phase solid is

$$\begin{aligned} (1-\xi)\psi_{it}^{A} + \xi\psi_{it}^{M} = (1-\xi)(u_0^{*A} - \Theta s_0^{*A}) + \xi(u_0^{*M} - \Theta s_0^{*M}) \\ + \xi(1-\xi)(\bar{u}_0 - \Theta\bar{s}_0)\,. \end{aligned} \tag{6.57}$$

The first two addenda on the right-hand side of (6.57) are contained in the specific Helmholtz free energy as defined by equation (6.22) when (6.51) is substituted for austenite and martensite, respectively. Thus, the third term incorporates the effects of internal interaction and may be used to define the free energy of internal interaction ψ_{it}

$$\psi_{it}(\Theta) = \bar{u}_0 - \Theta\bar{s}_0\,. \tag{6.58}$$

Then, equation (6.22) can be amended to yield

$$\psi = (1-\xi)\psi^{A} + \xi\psi^{M} + \xi(1-\xi)\psi_{it}\,. \tag{6.59}$$

The configurational internal energy $\bar{u}_0$ and entropy $\bar{s}_0$ due to transformation are to be determined experimentally.

6.3.3 Helmholtz free energy of a two-phase solid

Equation (6.59) defines the specific Helmholtz free energy of a two-phase solid from its constituents ψ^A and ψ^M, which represent the specific Helmholtz free energy of austenite and martensite, respectively. However, before ψ may be calculated from (6.51), where the individual free energies of the phases α are given in the form $\psi^\alpha = \psi^\alpha(\mathbf{h}^{e\alpha}, \Theta)$, the relationship between the phase-specific, *intrinsic* elastic strains $\mathbf{h}^{eA}$ and $\mathbf{h}^{eM}$ must be evaluated.
In the previous chapters, decompositions in elastic and inelastic, or — depending on the respective quantity — elastic-inelastic parts were introduced. In Section 6.2, the general term *inelastic deformation* was specified to include only deformation due to phase transformation. Other inelastic effects, such as plasticity or damage, are excluded.
The intrinsic elastic strains may then be obtained from the total and the elastic-phase transformation strains within the respective phases[19]

$$\mathbf{h}^{e\alpha} = \mathbf{h}^{\alpha} - \mathbf{h}^{etr\alpha}\,. \tag{6.60}$$

The intrinsic elastic-phase transformation strain within the austenitic *parent* phase is presumed to be zero

$$\mathbf{h}^{etrA} = \mathbf{0}\,. \tag{6.61}$$

To determine the intrinsic elastic-phase transformation strain of the martensitic product phase, the *intrinsic phase distortion* $\boldsymbol{\kappa}$ is introduced as a quantity possessing the properties of a measure of strain. $\boldsymbol{\kappa}$ is associated with the formation of martensite, which according to experimental observations on NiTi and other shape memory alloys is characterized by negligible changes in volume.[20] Hence, $\boldsymbol{\kappa}$ is required to be traceless. The intrinsic phase distortion may be interpreted as an average measure of the distortions due to phase transformation (cf. Raniecki & Bruhns 1991, Raniecki et al. 1992). It has the property

$$\boldsymbol{\kappa} : \boldsymbol{\kappa} = \eta^2 = const\,, \tag{6.62}$$

where the material parameter η is the *amplitude of pseudoelastic strain* or *pseudoelastic flow*. The intrinsic elastic-phase transformation strain of martensite may then be defined as

$$\mathbf{h}^{etrM} = \boldsymbol{\kappa} \qquad \mathrm{tr}\left(\mathbf{h}^{etrM}\right) = 0\,. \tag{6.63}$$

The strain of the two-phase solid B is postulated to obey the same mixture rule as ψ

$$\mathbf{h} = (1-\xi)\mathbf{h}^A + \xi\mathbf{h}^M\,. \tag{6.64}$$

[19] The decomposition into an elastic and an *elastic-phase transformation* part is motivated by the respective decomposition of the stretching $\mathbf{D}$ introduced in Section 3.7.
[20] For NiTi, the volumetric change is $-0.34\,\%$ from austenite to martensite (cf. Funakubo 1984).

Given the intrinsic elastic strains, the intrinsic stresses follow by virtue of equation (5.29_2)

$$\boldsymbol{\pi}^{\alpha} = \rho_0 \frac{\partial \psi^{\alpha}}{\partial \mathbf{h}^{e\alpha}} . \tag{6.65}$$

Equilibrium conditions

The intrinsic strains $\mathbf{h}^{\alpha}$ can be determined by analyzing states of equilibrium within the two-phase region. At equilibrium, the free energy function (6.59) attains its minimum. Hence, utilizing the method of Lagrange multipliers, (6.59) is minimized with respect to the mass fraction of martensite ξ and the intrinsic elastic strains $\mathbf{h}^{eA}$ respectively $\mathbf{h}^{eM}$ for fixed temperature and strain under constraint (6.64)

$$\begin{aligned} \mathcal{L} = (1-\xi)\psi^A + \xi\psi^M + \xi(1-\xi)\psi_{it} \\ + \boldsymbol{\Lambda} : (\mathbf{h} - (1-\xi)\mathbf{h}^A - \xi\mathbf{h}^M) \rightarrow \text{Min!} \end{aligned} \tag{6.66}$$

The appropriate Lagrange multiplier $\boldsymbol{\Lambda}$ is identified as the stress $\boldsymbol{\pi}$ as derivable from the thermal equation of state, weighted by the referential density ρ_0

$$\begin{aligned} \frac{\partial \mathcal{L}}{\partial \mathbf{h}^{eA}} &= (1-\xi)\frac{\partial \psi^A}{\partial \mathbf{h}^{eA}} - \boldsymbol{\Lambda}(1-\xi) \stackrel{!}{=} 0 \quad \Rightarrow \boldsymbol{\Lambda} = \frac{\partial \psi^A}{\partial \mathbf{h}^{eA}} = \frac{1}{\rho_0}\boldsymbol{\pi}^A \\ \frac{\partial \mathcal{L}}{\partial \mathbf{h}^{eM}} &= \xi\frac{\partial \psi^M}{\partial \mathbf{h}^{eM}} - \boldsymbol{\Lambda}\xi \stackrel{!}{=} 0 \quad \Rightarrow \boldsymbol{\Lambda} = \frac{\partial \psi^M}{\partial \mathbf{h}^{eM}} = \frac{1}{\rho_0}\boldsymbol{\pi}^M . \end{aligned} \tag{6.67}$$

Hence, the equilibrium stress is[21]

$$\boldsymbol{\pi} = \boldsymbol{\pi}^A = \boldsymbol{\pi}^M . \tag{6.68}$$

The partial derivative of (6.66) with respect to ξ gives

$$\psi^M - \psi^A + \frac{1}{\rho_0}\boldsymbol{\pi} : (\mathbf{h}^A - \mathbf{h}^M) + (1-2\xi)\psi_{it} = 0 . \tag{6.69}$$

Evidently, the Gibbs potentials of the phases α as defined by (5.30) must differ at equilibrium only by a term depending on ψ_{it}.
To determine the intrinsic strains, it is assumed that the thermoelastic properties of both phases are equal and approximately constant

$$\mathbb{C} = \mathbb{C}^A = \mathbb{C}^M = \mathbb{C}_0 \qquad \boldsymbol{\alpha} = \boldsymbol{\alpha}^A = \boldsymbol{\alpha}^M = \boldsymbol{\alpha}_0 . \tag{6.70}$$

[21] The phase distortion $\boldsymbol{\kappa}$ may be considered to be a function of a micromechanically motivated parameter h. Then, at equilibrium $\boldsymbol{\kappa}$ attains its maximum with respect to h, see Raniecki et al. (1992).

Considering this simplification, the *phase chemical potential* $\pi_0^f(\Theta)$ defined by

$$\pi_0^f(\Theta) = \psi^A - \psi^M \,, \tag{6.71}$$

by virtue of (6.51), (6.67) and (6.68) may be reduced to

$$\pi_0^f(\Theta) = \Delta u^* - \Theta \Delta s^* \,, \tag{6.72}$$

where

$$\Delta u^* = u_0^{*A} - u_0^{*M} \tag{6.73}$$

$$\Delta s^* = s_0^{*A} - s_0^{*M} \,. \tag{6.74}$$

Here, the specific internal energy of austenite (martensite) at stress free state is denoted by u_0^{*A} (u_0^{*M}), and the specific entropy of austenite (martensite) at stress free state is denoted by s_0^{*A} (s_0^{*M}). The phase chemical potential π_0^f represents the driving force for temperature induced phase transformation at stress-free state (cf. Raniecki et al. 1992). A graphical illustration is given subsequent to the derivation of equilibrium conditions.
Equating (6.67_1) and (6.67_2) based on (6.68) gives the intrinsic strains at equilibrium

$$\mathbf{h}^A = \mathbf{h} - \xi \boldsymbol{\kappa} \tag{6.75}$$

and

$$\mathbf{h}^M = \mathbf{h} + (1 - \xi)\boldsymbol{\kappa} \,. \tag{6.76}$$

Based on these equations, using (6.67) and (6.75) the stress $\boldsymbol{\pi}$ at equilibrium may be derived in terms of the total strain $\mathbf{h}$, the phase distortion $\boldsymbol{\kappa}$ and the absolute temperature Θ

$$\boldsymbol{\pi} = \mathbf{C}_0 : (\mathbf{h} - \xi\boldsymbol{\kappa} - \boldsymbol{\alpha}_0(\Theta - \Theta_0)) \,. \tag{6.77}$$

Then, the mass fraction of martensite ξ at equilibrium follows

$$\xi = \frac{\boldsymbol{\kappa} : \mathbf{C}_0 : (\mathbf{h} - (\Theta - \Theta_0)\boldsymbol{\alpha}_0) + \rho_0(\pi_0^f - \psi_{it})}{\boldsymbol{\kappa} : \mathbf{C}_0 : \boldsymbol{\kappa} - 2\rho_0\psi_{it}} \,. \tag{6.78}$$

Combining (6.77) and (6.78) gives an equilibrium condition for two-phase states in terms of the phase distortion $\boldsymbol{\kappa}$

$$\frac{1}{\rho_0}\boldsymbol{\pi} : \boldsymbol{\kappa} + \pi_0^f - (1 - 2\xi)\psi_{it} = 0 \,. \tag{6.79}$$

To eliminate the phase distortion $\boldsymbol{\kappa}$ from the foregoing relations, additional restrictions must be imposed that associate $\boldsymbol{\kappa}$ with $\mathbf{h}$ or $\boldsymbol{\pi}$. Raniecki et al. (1992) postulate that, after a change of the principal direction of stress and

subsequent proportional loading, the existing martensitic plates will rotate instantaneously. The new martensitic systems will then be formed in such a way that the overall phase distortion will have the same principal directions as the stress applied. Formally, this may be written as

$$\boldsymbol{\kappa} = \eta \frac{\boldsymbol{\pi}'}{\sqrt{\boldsymbol{\pi}' : \boldsymbol{\pi}'}} . \tag{6.80}$$

Adopting this concept, (6.80) and (6.79) may be combined to yield a stress-temperature relation in states of equilibrium. Graphically, this relation is represented by a circle with temperature-dependent radius in the π-plane. In addition, an equilibrium condition in stress-strain space is obtainable from (6.77) by substitution of (6.78) and subsequent elimination of the phase distortion by virtue of (6.80). However, these simplifications are deferred to Section 6.7. The notion of a driving force for temperature induced phase transformation at stress-free state π_0^f defined in (6.71) is illustrated graphically in Figure 6.2 (cf. Wollants et al. 1979, Otsuka & Wayman 1998a). Here, the temperature of coinciding chemical free energy of both phases is designated by T^0 and approximated by

$$T^0 = \frac{1}{2}(M_s^0 + A_s^0) . \tag{6.81}$$

Transformation will be initiated only when a thermodynamic driving force reaches a certain threshold value. At stress free state, supercooling to a suitably low temperature M_s^0 is required.

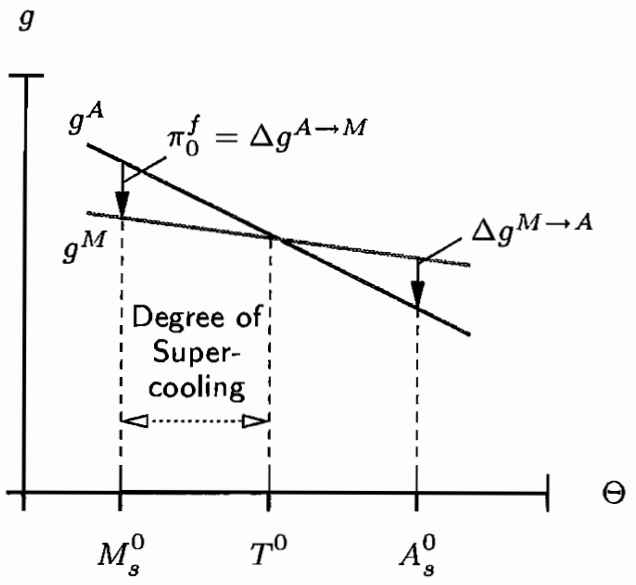

Figure 6.2: Phase chemical potential at stress free state

The definition of T^0 as depicted in Figure 6.2 generally holds only for non-thermoelastic martensitic transformations, characterized by an almost instantaneous growth of single martensite crystals to their final size, without further growth with decreasing temperature. When these martensite crystals undergo reverse transformation, austenite crystals are nucleated and grow within the martensitic phase (cf. Funakubo 1984).
However, most martensitic transformations associated with superelasticity or shape memory effect are thermoelastic. Here, the interface between austenitic and martensitic phases is very mobile upon cooling and heating, leading to a rate of growth of the nucleated martensite crystals proportional to the cooling rate. The driving force required to initiate phase transformation is comparatively low in thermoelastic martensitic transformations. Regarding Figure 6.2, the relation

$$M_s^0 < A_s^0 \tag{6.82}$$

does not hold necessarily in thermoelastic martensitic transformations. Hence, for alloys undergoing Type II thermoelastic martensitic transformation, characterized by

$$A_f^0 > M_s^0 > A_s^0 > M_f^0 , \tag{6.83}$$

it is more appropriate to approximate the equilibrium temperatures by (cf. Otsuka & Wayman 1998a, Funakubo 1984)

$$T^0 = \frac{1}{2}(M_s^0 + A_f^0) \qquad T^{0\prime} = \frac{1}{2}(A_s^0 + M_f^0) . \tag{6.84}$$

Constrained equilibria

The equilibrium states considered are unstable. No real process of phase transformation from $\xi = 0$ to $\xi = 1$ would proceed along a path defined by the equilibrium conditions derived above, which imply decreasing stresses in connection with the evolution of martensite and increasing strains (cf. Müller & Xu 1991). In fact, the description of deformation processes involving phase transformation relies on the idea of constrained equilibria presented in Chapter 5.
The specific Helmholtz free energy function of constrained equilibria is given by equation (6.59) derived in the previous section without regard to equilibrium states. Müller & Xu (1991) introduced the notion of so-called *uniform stress models* by proposing that both phases are subject to the same stresses

$$\boldsymbol{\pi}^A = \boldsymbol{\pi}^M = \boldsymbol{\pi} . \tag{6.85}$$

Hence, according to their theory, the intrinsic stresses of both phases are identical in states of *constrained* equilibrium as well. The latter equality in (6.85) implies that equilibrium strains (6.75) and (6.76)

$$\mathbf{h}^A = \mathbf{h} - \xi\boldsymbol{\kappa} \qquad \mathbf{h}^M = \mathbf{h} + (1-\xi)\boldsymbol{\kappa} \tag{6.86}$$

and the equilibrium stress given by equation (6.77) hold for states of constrained equilibria as well

$$\boldsymbol{\pi} = (\mathbf{h}^e - (\Theta - \Theta_0)\boldsymbol{\alpha}_0) : \mathbb{C}_0 \,. \tag{6.87}$$

Here, the elastic Hencky strain is defined as

$$\mathbf{h}^e = \mathbf{h} - \xi\boldsymbol{\kappa} \,. \tag{6.88}$$

This is motivated by the definition of the intrinsic phase distortion $\boldsymbol{\kappa}$ as an average measure of the distortions due to phase transformation in polycrystals. The intrinsic phase distortion weighted by the mass fraction of martensite may then be defined as the elastic-phase transformation part of the strain, which is denoted by $\mathbf{h}^{etr}$

$$\mathbf{h}^{etr} = \xi\boldsymbol{\kappa} \,. \tag{6.89}$$

Equivalent to (6.88) is the following decomposition

$$\mathbf{h}^e = \mathbf{h} - \mathbf{h}^{etr} \,. \tag{6.90}$$

From (6.63) it is readily seen that

$$\mathrm{tr}\left(\mathbf{h}^{etr}\right) = 0 \,. \tag{6.91}$$

Noting (6.86) and (6.88), equation (6.59) yields the specific Helmholtz free energy of constrained equilibria in the form

$$\begin{aligned} \psi(\mathbf{h}^e, \Theta, \xi) = {} & \frac{1}{2\rho_0}\, \mathbf{h}^e : \mathbb{C}_0 : \mathbf{h}^e - (\Theta - \Theta_0)\frac{1}{\rho_0}\, \boldsymbol{\alpha}_0 : \mathbb{C}_0 : \mathbf{h}^e \\ & + c_v \left(\Theta - \Theta_0 - \Theta \ln\left(\frac{\Theta}{\Theta_0} \right) \right) \\ & + u_0^{*A} - \Theta s_0^{*A} - \xi \pi_0^f(\Theta) + \xi(1-\xi)\psi_{it}(\Theta) \,. \end{aligned} \tag{6.92}$$

In deriving (6.92), identical thermomechanical properties for both phases were stipulated. The preceding derivations do not rely on this simplification. In fact, phase specific and temperature dependent stiffness tensors $\mathbb{C}^\alpha$ and tensors of thermal expansion coefficients $\boldsymbol{\alpha}^\alpha$ may be incorporated in the same fashion as outlined here. However, they naturally imply a more complicated free energy function than given by (6.92). For example, Bernardini (2001) derives a free energy function taking into account phase specific material properties based on a variational formulation, neglecting the energy of interaction. On the grounds of micromechanical considerations, Ziólkowski & Raniecki (1999) obtain a free energy function with phase-specific thermomechanical properties that includes (6.92) as a particular case.

Relation (6.87) for the stress was derived based on the intrinsic strains $\mathbf{h}^{e\alpha}$.

Adopting (6.92), the stress may be calculated by means of the thermal equation of state (5.74) instead

$$\begin{aligned} \boldsymbol{\pi} &= \rho_0 \frac{\partial \psi}{\partial \mathbf{h}^e} \\ &= (\mathbf{h}^e - (\Theta - \Theta_0)\boldsymbol{\alpha}_0) : \mathbb{C}_0 \,. \end{aligned} \tag{6.93}$$

Employing the caloric equation of state (5.75), the specific entropy of constrained equilibria is given by

$$\begin{aligned} s &= -\frac{\partial \psi}{\partial \Theta} \\ &= -\frac{1}{\rho_0}\, \boldsymbol{\alpha}_0 : \mathbb{C}_0 : \mathbf{h}^e + c_v \ln\left(\frac{\Theta}{\Theta_0}\right) - \xi \Delta s^* + \xi(1-\xi)\bar{s}_0 + s_0^{*A} \,. \end{aligned} \tag{6.94}$$

Internal loops of the hysteresis

Although during monotone loading of a pseudoelastic specimen the phase transformation will not follow the equilibrium conditions defined above, they are important to the description of internal loops of the hysteresis. Following Müller & Xu (1991), states within the bounding loop may be considered as *metastable*. The material behavior of a process originating from a metastable state depends on the position of this state relative to states of equilibrium and on the direction of the process, i.e. loading or unloading. This situation is depicted in Figure 6.3 in stress-strain-space in one dimension.
Here, states of equilibria are represented by a dotted line leading from the upper left to the lower right corner of the idealized pseudoelastic hysteresis. Considering the hysteresis on the left hand side first, it may be seen that elastic unloading from the transformation plateau first leads to metastable states

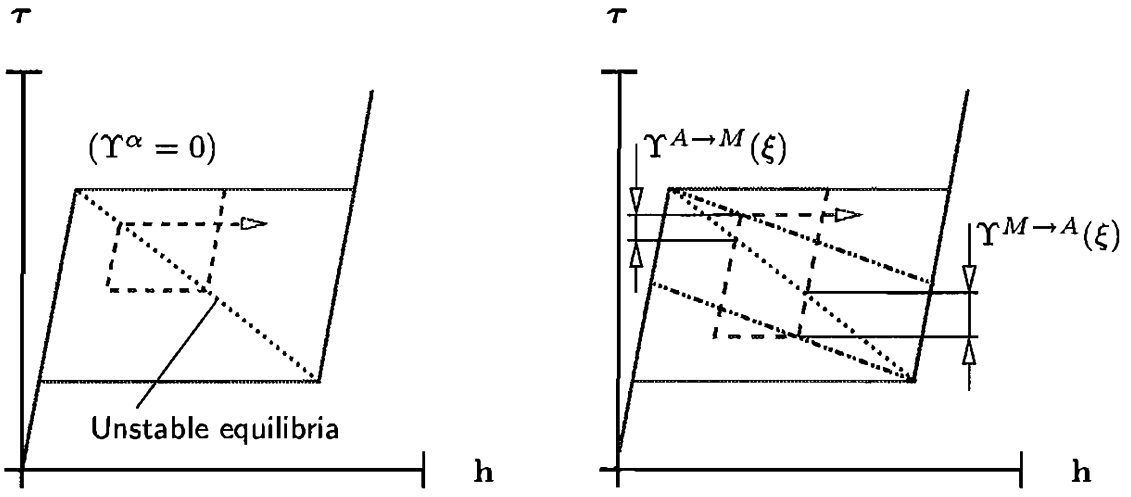

Figure 6.3: Criteria for internal loops

above the line of unstable equilibria. Decreasing the strain further will eventually lead to a state on the line of unstable equilibria. Disregarding possible threshold values Υ, i.e.

$$\Upsilon^{A\to M}(\xi) = \Upsilon^{M\to A}(\xi) = 0\,, \tag{6.95}$$

reverse phase transformation will initiate from here. Reversing the strain rate results in the same behavior, first elastic loading, followed by a process of phase transformation once the line of unstable equilibria is reached (cf. Müller & Xu 1991).
However, although assumption 6.95 is justified by isothermal, deformation-controlled experiments on a CuZnAl single crystal (cf. Müller & Xu 1991), there is some experimental evidence obtained on NiTi specimens suggesting the existence of threshold values that must be reached before phase transformation is initiated (cf. Pascal & Monasevich 1981, Tanaka et al. 1995b, Helm 2001). This is illustrated on the right-hand side of Figure 6.3, where it is assumed that the threshold value is a linear function of the mass fraction of martensite. Threshold values Υ will not be taken into account here. For a thorough study on this subject, see Raniecki & Lexcellent (1994).

6.4 Transformation kinetics

With the relations presented in the previous section, the state of a single- or two-phase material may be characterized. However, a kinetic equation describing the evolution of martensite remains to be specified. In this section, based on the notions and thermodynamic constraints discussed in Chapter 5, an appropriate kinetic law will be derived.

6.4.1 Thermodynamic driving force and corresponding flux

The Clausius-Duhem inequality in form of equation (5.76) requires the internal entropy production rate $\dot{\gamma}$ to be non-negative

$$\Theta\rho\dot{\gamma} = \frac{\rho}{\rho_0}\,\dot{w}^i - \rho\,\frac{\partial\psi}{\partial\mathbf{a}}\cdot\overset{\circ}{\mathbf{a}}{}^{\mathrm{Log}} - \Theta^{-1}\mathbf{q}\cdot\nabla\Theta \geq 0\,, \tag{6.96}$$

or, more strictly, that both the entropy production rate due to the dissipative power (5.84)

$$\Theta\rho\dot{\gamma}_{mech} = \frac{\rho}{\rho_0}\,\dot{w}^i - \rho\,\frac{\partial\psi}{\partial\mathbf{a}}\cdot\overset{\circ}{\mathbf{a}}{}^{\mathrm{Log}} \geq 0 \tag{6.97}$$

and the entropy production rate due to irreversible heat conduction in the presence of a thermal gradient (5.82)

$$\Theta\rho\dot{\gamma}_{th} = -\Theta^{-1}\mathbf{q}\cdot\nabla\Theta \geq 0 \tag{6.98}$$

are non-negative, separately. As stated in Section 5.6, *a priori* there is no reason to suppose that both (6.97) and (6.98) must hold singly. However, as (6.97) contains no terms depending on $\nabla\Theta$, the above decomposition is valid.
Recognizing that only inelastic deformations due to phase transformation are considered here and that the mass fraction of martensite ξ is the only internal state variable, substitution of the phase transformation part of the specific energy rate $\dot{w}^i$ given by (5.62) into equation (6.97) gives

$$\boldsymbol{\tau} : \overset{\circ}{\mathbf{h}}{}^{e\,tr\,\mathrm{Log}} - \rho_0 \frac{\partial \psi}{\partial \xi} \dot{\xi} \geq 0 . \tag{6.99}$$

In order to employ the concept of generalized irreversible forces and fluxes introduced in Section 5.6, the logarithmic rate of the elastic-phase transformation part of the strain is eliminated from (6.99) by means of definitions (6.89) and (6.62) to yield

$$\left(\frac{1}{\xi} \boldsymbol{\tau} : \mathbf{h}^{e\,tr} - \rho_0 \frac{\partial \psi}{\partial \xi} \right) \dot{\xi} \geq 0 . \tag{6.100}$$

Based on this inequality, the thermodynamic force π^f driving phase transformation

$$(\mathbf{X}^i)_{tr} = \pi^f = \frac{1}{\xi} \boldsymbol{\tau} : \mathbf{h}^{e\,tr} - \rho_0 \frac{\partial \psi}{\partial \xi} \tag{6.101}$$

and the corresponding thermodynamic flux

$$(\mathbf{J})_{tr} = \dot{\xi} \tag{6.102}$$

are defined.
On the grounds of these definitions, a kinetic law for phase transformation can be proposed to associate the thermodynamic flux $\dot{\xi}$ with a prescribed thermodynamic force π^f.[22] Relation (6.100) has to hold true to ensure thermodynamic consistency, implying the following requirement for the kinetic equation

$$\begin{aligned} &\dot{\xi} > 0 \quad \text{for} \quad \pi^f > 0 \\ &\dot{\xi} < 0 \quad \text{for} \quad \pi^f < 0 . \end{aligned} \tag{6.103}$$

[22] The thermodynamic driving force π^f is not to be mistaken for the phase chemical potential π_0^f.

6.4.2 Evolution of thermodynamic driving force

To describe the evolution of the thermodynamic driving force π^f, two functions $f^{A\to M}(\pi^f,\xi)$ for $A \to M$ and $f^{M\to A}(\pi^f,\xi)$ for $M \to A$ transformation are defined. Due to their dependence on π^f and ξ, and the requirement that f^α remain constant during processes of active phase transformation (cf. Raniecki et al. 1992), they link the thermodynamic driving force to the mass fraction of martensite

$$\begin{aligned} f^{A\to M} &= const \quad \text{for} \quad \dot{\xi} > 0 \\ f^{M\to A} &= const \quad \text{for} \quad \dot{\xi} < 0\,. \end{aligned} \tag{6.104}$$

A possible interpretation is available by considering the yield surface known from plasticity, which corresponds to (6.104) for $const = 0$. In fact, theories of plasticity have been extended to model the behavior of SMAs (cf. Bertram 1982, and in a Eulerian description adopting the logarithmic rate, Pethö 2000), and some authors refer to functions similar to relations (6.104) as *yield surfaces* (cf. Orgéas & Favier 1998, Helm & Haupt 2003).
It is assumed here that the association between π^f and ξ is of the type

$$f^{A\to M}(\pi^f,\xi) = \pi^f - \rho_0 k^{A\to M}(\xi) \le 0 \tag{6.105}$$

respectively

$$f^{M\to A}(\pi^f,\xi) = -\pi^f + \rho_0 k^{M\to A}(\xi) \le 0\,. \tag{6.106}$$

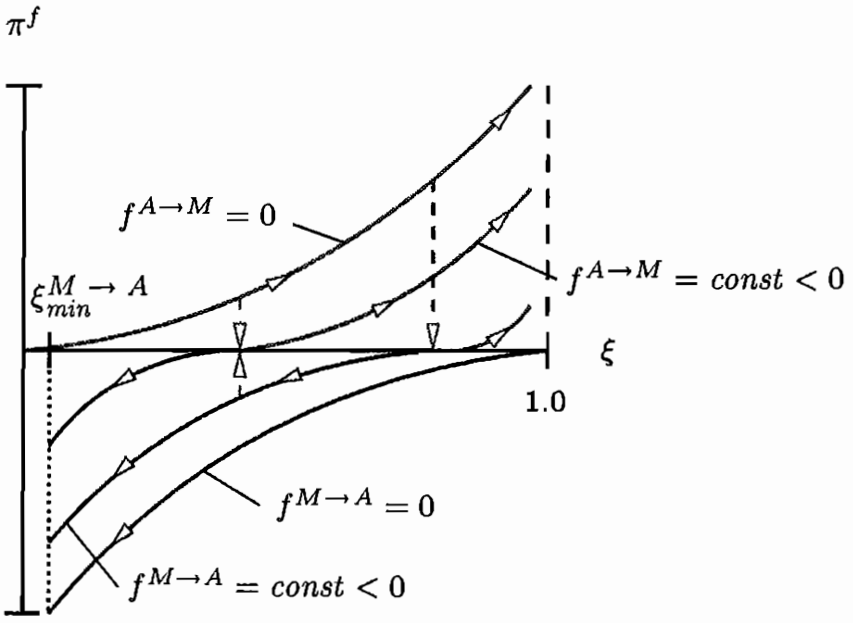

Figure 6.4: Thermodynamic driving force for admissible thermomechanical processes

Here, functions $k(\xi)$ are introduced which will prove to be crucial to the description of π^f. In fact, noting (6.104), the rate of the thermodynamic force $\dot{\pi}^f$ may be calculated using

$$\begin{aligned} \dot{\pi}^f &= \rho_0 \dot{k}^{A\to M} \quad \text{for} \quad \dot{\xi} > 0 \\ \dot{\pi}^f &= \rho_0 \dot{k}^{M\to A} \quad \text{for} \quad \dot{\xi} < 0\,. \end{aligned} \tag{6.107}$$

First, attention is restricted to the bounding loops of the hysteresis. It is observed that π^f is zero at the initiation of forward respectively reverse phase transformation. Motivated by the analogy to plasticity, this may be combined with the assumption that the isoquants $f(\pi^f, \xi)$ must vanish on the bounding loops. Hence, for $A \to M$ transformation initiating from states $\xi = 0$, and for processes of $M \to A$ transformation initiating from martensitic states ($\xi = 1$), the thermodynamic driving force equals the function $k^\alpha(\xi)$. Then, initial conditions must be

$$k^{A\to M}\big|_{\xi=0} = 0\,, \tag{6.108}$$

following from $f^{A\to M} = \pi^f\big|_{\xi=0}$, and

$$k^{M\to A}\big|_{\xi=1} = 0\,, \tag{6.109}$$

implied by $f^{M\to A} = -\,\pi^f\big|_{\xi=1}$.
Processes of phase transformation originating from states within the bounding loop are associated with $\pi^f = 0$ at the moment of their initiation as well. However, here it is postulated that $f^{A\to M} < 0$ and $f^{M\to A} < 0$ (see Figure 6.4 following Raniecki et al. 1992). Therefore, to obtain a positive respectively negative driving force for $A \to M$ and $M \to A$ transformations, respectively, it is required that

$$k^{A\to M} \geq 0 \qquad k^{M\to A} \leq 0\,. \tag{6.110}$$

To states of $\xi \neq 0$ and $\pi^f = 0$ within the bounding loops correspond positive $k^{A\to M}$ and negative $k^{M\to A}$.
As $f^{A\to M} \leq 0$ and $f^{M\to A} \leq 0$ and states of complete $A \to M$ transformation ($\xi = 1$) respectively complete $M \to A$ transformation ($\xi = 0$) are not observed experimentally on polycrystalline SMAs, the evolution of the thermodynamic driving force depending on the mass fraction of martensite

$$0 \leq \xi \leq 1 \tag{6.111}$$

is subject to additional constraints, namely

$$\begin{aligned} \lim_{\xi\to 1} k^{A\to M} &= \infty & \lim_{\xi\to 0} k^{M\to A} &= -\infty \\ \lim_{\xi\to 1} (1-\xi)k^{A\to M} &= 0 & \lim_{\xi\to 0} \xi k^{M\to A} &= 0 \\ \frac{\mathrm{d}k^{A\to M}}{\mathrm{d}\xi} &> 0 & \frac{\mathrm{d}k^{M\to A}}{\mathrm{d}\xi} &> 0\,. \end{aligned} \tag{6.112}$$

These constraints may be derived from (6.105) to (6.107), noting the implications of definition (6.101) of π^f in terms of the mass fraction of martensite ξ. There is an indefinite number of functions k^α that satisfy these constraints. Based on Tanaka (1990), who adopts the description of transformation kinetics proposed by Magee (1970), Raniecki et al. (1992) introduce the constants $A_i > 0$, B_i and $C_i \geq 0$ to propose the equations

$$k^{A\to M}(\xi) = -(A_1 + B_1\xi)\ln(1-\xi) + C_1\xi \geq 0 \tag{6.113}$$

for $A \to M$ and

$$k^{M\to A}(\xi) = (A_2 - B_2(1-\xi))\ln\xi - C_2(1-\xi) \leq 0 \tag{6.114}$$

for $M \to A$ transformation, which comply with (6.108) and (6.109) as well as (6.110) and (6.112). These functions are adopted here. Their evolution for forward respectively reverse phase transformation is illustrated in Figure 6.5 (see Section 7.4.1 for the material parameter set used).

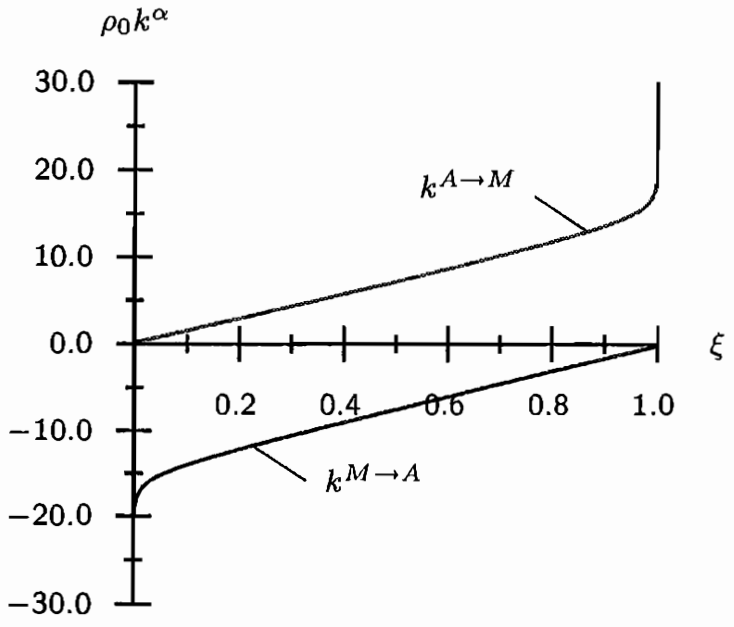

Figure 6.5: Evolution of functions k^α

The shape of the hysteresis as determined by the model is very sensitive to the functions k^α. Therefore, depending on the characteristics of the respective shape memory alloy under consideration, a different choice for k^α may be necessary to better represent the hysteresis experimentally observed.

6.4.3 Neutral processes

For active processes of phase transformation, the requirements

- A $\rightarrow$ M transformation: $\pi^f > 0$
- M $\rightarrow$ A transformation: $\pi^f < 0$

for the thermodynamic driving force were specified. However, these necessary criteria are not sufficient to determine whether a process initiating from a given state $(\mathbf{h}^e,\Theta,\xi)$ will be actively phase transforming or a so-called *neutral process* characterized by $\xi = const.$ Therefore, a criterion for neutral processes is needed.
By virtue of (6.92), definition (6.101) of the thermodynamic driving force for phase transformation

$$\pi^f = \frac{1}{\xi}\,\boldsymbol{\tau} : \mathbf{h}^{etr} - \rho_0 \frac{\partial \psi}{\partial \xi} \tag{6.115}$$

may be written in the form

$$\pi^f = \frac{1}{\xi}\,\boldsymbol{\tau} : \mathbf{h}^{etr} + \rho_0 \pi_0^f(\Theta) - \rho_0(1-2\xi)\psi_{it}(\Theta)\,. \tag{6.116}$$

With the definition of the phase chemical potential (6.72), the free energy of interaction (6.58), and the caloric equation of state (6.93), the driving force reads

$$\begin{aligned}\pi^f = \pi^f(\mathbf{h}^e,\Theta,\xi) = \frac{1}{\xi}\,(\mathbf{h}^e - (\Theta-\Theta_0)\boldsymbol{\alpha}_0) : \mathbb{C}_0 : \mathbf{h}^{etr} \\ + \rho_0(\Delta u^* - \Theta\Delta s^*) - \rho_0(1-2\xi)(\bar{u}_0 - \Theta\bar{s}_0)\,.\end{aligned} \tag{6.117}$$

To evaluate the total differential of (6.117)

$$\dot{\pi}^f = \frac{\partial \pi^f}{\partial \mathbf{h}^e} : \overset{\circ}{\mathbf{h}}{}^{e\,\mathrm{Log}} + \frac{\partial \pi^f}{\partial \Theta}\dot{\Theta} + \frac{\partial \pi^f}{\partial \xi}\dot{\xi}\,, \tag{6.118}$$

the partial derivatives

$$\frac{\partial \pi^f}{\partial \mathbf{h}^e} = \frac{1}{\xi}\,\boldsymbol{\tau} : \frac{\partial \mathbf{h}^{etr}}{\partial \mathbf{h}^e} + \frac{1}{\xi}\,\mathbb{C}_0 : \mathbf{h}^{etr} \tag{6.119}$$

$$\frac{\partial \pi^f}{\partial \Theta} = \frac{1}{\xi}\,\boldsymbol{\tau} : \frac{\partial \mathbf{h}^{etr}}{\partial \Theta} - \frac{1}{\xi}\,\boldsymbol{\alpha}_0 : \mathbb{C}_0 : \mathbf{h}^{etr} - \rho_0\Delta s^* + \rho_0(1-2\xi)\bar{s}_0 \tag{6.120}$$

$$\frac{\partial \pi^f}{\partial \xi} = \frac{1}{\xi}\,\boldsymbol{\tau} : \frac{\partial \mathbf{h}^{etr}}{\partial \xi} - \frac{1}{\xi^2}\,\boldsymbol{\tau} : \mathbf{h}^{etr} + 2\rho_0\psi_{it} \tag{6.121}$$

are calculated. For constant mass fraction of martensite

$$\dot{\xi} = 0\,, \tag{6.122}$$

the last term in (6.118) vanishes

$$\begin{aligned} \dot{\pi}^f\big|_\xi = \dot{\pi}^f\big|_{\xi=const} &= \frac{\partial \pi^f}{\partial \mathbf{h}^e} : \overset{\circ}{\mathbf{h}}{}^{e\,\mathrm{Log}} + \frac{\partial \pi^f}{\partial \Theta}\dot{\Theta} \\ &= \dot{\pi}^f - \frac{\partial \pi^f}{\partial \xi}\dot{\xi}\,. \end{aligned} \tag{6.123}$$

Noting (6.107)

$$\dot{\pi}^f = \rho_0 \dot{k}^\alpha \quad \text{for} \quad \dot{k}^\alpha \in \left\{ \dot{k}^{A\to M}, \dot{k}^{M\to A} \right\}, \tag{6.124}$$

substitution of the partial derivative (6.121) into (6.123_2) gives

$$\dot{\pi}^f\big|_\xi = \left(\rho_0 \frac{\partial k^\alpha}{\partial \xi} - \frac{1}{\xi}\boldsymbol{\tau} : \frac{\partial \mathbf{h}^{etr}}{\partial \xi} + \frac{1}{\xi^2}\boldsymbol{\tau} : \mathbf{h}^{etr} - 2\rho_0 \psi_{it} \right) \dot{\xi}\,. \tag{6.125}$$

Evidently, there will be no active phase transformation for arbitrary rates $\overset{\circ}{\mathbf{h}}{}^{e\,\mathrm{Log}}$ and $\dot{\Theta}$ from a given state ($\mathbf{h}^e$,Θ,ξ) if the criterion

$$\dot{\pi}^f\big|_\xi = 0 \tag{6.126}$$

is fulfilled. Raniecki et al. (1992) introduce the term *neutral process* for the resulting elastic material response.

6.4.4 Kinetic law

Inversion of equation (6.125) yields the required kinetic equation for processes of active $A \to M$ transformation proceeding for $\pi^f > 0$ and $\dot{\pi}^f\big|_\xi > 0$ as long as $\xi \leq 1$

$$\dot{\xi}^{A\to M} = \frac{\dot{\pi}^f\big|_\xi}{\left(\rho_0 \dfrac{\partial k^{A\to M}}{\partial \xi} - \dfrac{1}{\xi}\boldsymbol{\tau} : \dfrac{\partial \mathbf{h}^{etr}}{\partial \xi} + \dfrac{1}{\xi^2}\boldsymbol{\tau} : \mathbf{h}^{etr} - 2\rho_0 \psi_{it} \right)} \tag{6.127}$$

or $M \to A$ transformation subject to $\pi^f < 0$ and $\dot{\pi}^f\big|_\xi < 0$ as long as $\xi \geq 0$

$$\dot{\xi}^{M\to A} = \frac{\dot{\pi}^f\big|_\xi}{\left(\rho_0 \dfrac{\partial k^{M\to A}}{\partial \xi} - \dfrac{1}{\xi}\boldsymbol{\tau} : \dfrac{\partial \mathbf{h}^{etr}}{\partial \xi} + \dfrac{1}{\xi^2}\boldsymbol{\tau} : \mathbf{h}^{etr} - 2\rho_0 \psi_{it} \right)}\,, \tag{6.128}$$

where $\dot{\pi}^f\big|_\xi$ is given by (6.123_1) combined with (6.119) and (6.120).
Evaluation of the kinetic equation requires knowledge not only of the rates of

the elastic Hencky strain $\mathbf{h}^e$ and the mass fraction of martensite ξ, but also of the elastic-phase transformation part of the strain $\mathbf{h}^{etr}$ and its derivative with respect to ξ. Hence, additional specifications regarding the mechanical properties of the material under consideration are required. In Section 6.7, an isotropic material symmetry is postulated. Then, all quantities may be expressed explicitly in terms of the state variables $\mathbf{h}^e$, Θ, and ξ.

6.5 Fourier's law and heat conduction equation

At this stage, the thermomechanical description of the process is complemented by an appropriate heat transfer relation.
Heat transfer by diffusion or conduction refers to the transport of energy in a medium due to a temperature gradient. The underlying physical mechanism is that of random atomic or molecular activity. Conduction is the transfer of energy from the more energetic to the less energetic particles of a substance due to interactions between the particles (cf. Incropera & DeWitt 1996).
Fourier's law is a phenomenological rate equation stating that the heat transfer rate $\bar{q}_x$ in a direction x is directly proportional to the temperature gradient $\nabla\Theta$ and the cross-sectional area A normal to x, and that $\bar{q}_x$ varies inversely with the length of heat conduction Δx. The appropriate constant of proportionality is the *thermal conductivity* k. Dividing by A, the heat flux in x-direction is obtained

$$q_x = -k \frac{\partial \Theta}{\partial x} . \tag{6.129}$$

Here, the minus sign is necessary because heat is always transferred in the direction of decreasing temperature. The heat flux q_x is normal to the cross-sectional area A or, more generally, the direction of heat flow will always be normal to a surface of constant temperature, called an *isothermal surface.*
Recognizing that the heat flux $\mathbf{q}$ is a vector quantity, a more general statement of the conduction rate equation known as *Fourier's law*[23] is

$$\mathbf{q} = -k \nabla\Theta . \tag{6.130}$$

The energy conservation principle applied to an elemental volume as a closed system states that the rate at which energy is stored in the volume $\dot{Q}_{st}$ equals the sum of the heat transfer across the volume boundaries $\dot{Q}$ and the heat generated by energy sources

$$\dot{Q}_{st} = \rho c_p \dot{\Theta} dv = \dot{Q} + \dot{h}_{lat} dv . \tag{6.131}$$

[23] To account for the time dependence of heat conduction, a different heat conduction equation, i.e. the heat conduction equation attributed to Maxwell and Cattaneo, is required (cf. Kosiński 1975). Oberste-Brandenburg (1999) successfully employed *Maxwell-Cattaneo's relation* when considering martensitic phase transitions at a microscale, taking into account effects at the phase boundary.

The net inflow heat flux

$$\dot{Q} = -\nabla \cdot \mathbf{q} dv \tag{6.132}$$

is found from balancing the inflow and the outflow heat flux by application of the divergence theorem. This gives

$$\rho c_p \dot{\Theta} = -\nabla \cdot \mathbf{q} + \dot{h}_{lat}\,, \tag{6.133}$$

which is identical to equation (5.108).
Introducing Fourier's law for constant thermal conductivity, specifically assuming independence of temperature ($k \neq k(\Theta)$) and position ($k \neq k(\mathbf{x})$) yields the heat conduction equation known as *Fourier's equation*

$$\rho c_p \dot{\Theta} = k \nabla^2 \Theta + \dot{h}_{lat}\,. \tag{6.134}$$

Adopting Fourier's law, condition (5.82)

$$\Theta \rho \dot{\gamma}_{th} = -\Theta^{-1} \mathbf{q} \cdot \nabla \Theta \geq 0 \tag{6.135}$$

is satisfied automatically. This may be observed by substitution of (6.130), which gives

$$\Theta \rho \dot{\gamma}_{th} = \frac{k}{\rho \Theta^2} (\nabla \Theta)^2 > 0 \tag{6.136}$$

for non-negative thermal conductivity k. Hence, thermodynamic consistency is obtained since relation (6.100) is required to hold true.

6.6 Identification of model-specific material parameters

Instead of the constants Δu^*, Δs^*, $\bar{u}_0$ and $\bar{s}_0$ introduced in the definitions of the phase chemical potential (6.72) and the specific free energy of interaction (6.58), transformation temperatures are used to characterize shape memory alloys in engineering sciences. From the above, two such temperatures, the martensite start temperature M_s^0 and the austenite start temperature A_s^0 at stress free states, may be derived in terms of the constants used here.
Starting from the thermodynamic driving force for phase transformation in the form of (6.116)

$$\pi^f = \frac{1}{\xi} \boldsymbol{\tau} : \mathbf{h}^{etr} + \rho_0 \pi_0^f(\Theta) - \rho_0 (1 - 2\xi) \psi_{it}(\Theta)\,, \tag{6.137}$$

at stress-free states ($\boldsymbol{\tau} = \mathbf{0}$), the start temperatures are obtained using (6.72) and (6.58)

$$M_s^0 = \frac{\Delta u^* - \bar{u}_0}{\Delta s^* - \bar{s}_0} \tag{6.138}$$

$$A_s^0 = \frac{\Delta u^* + \bar{u}_0}{\Delta s^* + \bar{s}_0}\,. \tag{6.139}$$

In deriving these transformation temperatures, it is postulated that the threshold values for π^f are negligible and that π^f vanishes at the onset of $A \rightarrow M$ and $M \rightarrow A$ transformations, respectively (see Section 6.3.3).
Even though the definition of the thermodynamic driving force for phase transformation used here differs from the definition of Raniecki et al. (1992), the transformation temperatures derived from π^f correspond to those of the R_L-model. As the evolution of the thermodynamic driving force is described here using the same functions k^α as those adopted by Raniecki et al. (1992) from Tanaka (1990), the constants A_i, B_i and C_i are chosen in agreement with the R_L-model, taking into account subsequent modifications introduced by Ziólkowski (1993) and Raniecki & Lexcellent (1994)

$$A_1 = \frac{\Delta s^* - \bar{s}_0}{a_1} \qquad B_1 = \frac{2r_1\bar{s}_0}{a_1} \qquad C_1 = 2r_1\psi_{it}(M_s^0) \tag{6.140}$$

$$A_2 = \frac{\Delta s^* + \bar{s}_0}{a_2} \qquad B_2 = \frac{2r_2\bar{s}_0}{a_2} \qquad C_2 = 2r_2\psi_{it}(A_s^0)\,. \tag{6.141}$$

These constants can be calculated for given Δu^*, Δs^*, $\bar{u}_0$ and $\bar{s}_0$, provided that a_1 and a_2 as well as r_1 and r_2 are known. The latter two constants, i.e. the phenomenological constants r_1 and r_2, which are introduced to characterize the transformation kinetics, may be determined by studying the slope of the stress plateau during forward and reverse transformation under isothermal conditions. In Figure 6.6, the effect of r_1 on the forward and of r_2 on the reverse transformation is clearly visible. Depicted is an adiabatic test in tension, with the intermediate values of the parameters r_i obtained by calibrating a small strain version of the model to experimental data (cf. Müller & Bruhns 2002a).
To determine a_1 and a_2, the bounding loops $f^{A\rightarrow M} = 0$ yielding

$$\pi^f = \rho_0 k^{A\rightarrow M} \quad \text{for} \quad \dot{\xi} > 0\,, \tag{6.142}$$

and $f^{M\rightarrow A} = 0$ giving

$$\pi^f = \rho_0 k^{M\rightarrow A} \quad \text{for} \quad \dot{\xi} < 0 \tag{6.143}$$

are considered. However, an explicit solution for the mass fraction of martensite as first suggested by Koistinen & Marburger (1959) is available only for $r_i = 1$. Then, with definitions (6.140) and (6.141) and $\Delta s^* > |\bar{s}_0|$, the mass fraction of martensite during temperature induced phase transformation at stress free states ($\boldsymbol{\tau} = \mathbf{0}$) can be derived from (6.137), combined with (6.113) respectively (6.114). Noting (6.138) and (6.139) yields (cf. Raniecki et al. 1992)

$$\xi = 1 - e^{-a_1(M_s^0 - \Theta)} \quad \text{for} \quad \dot{\xi} > 0 \tag{6.144}$$

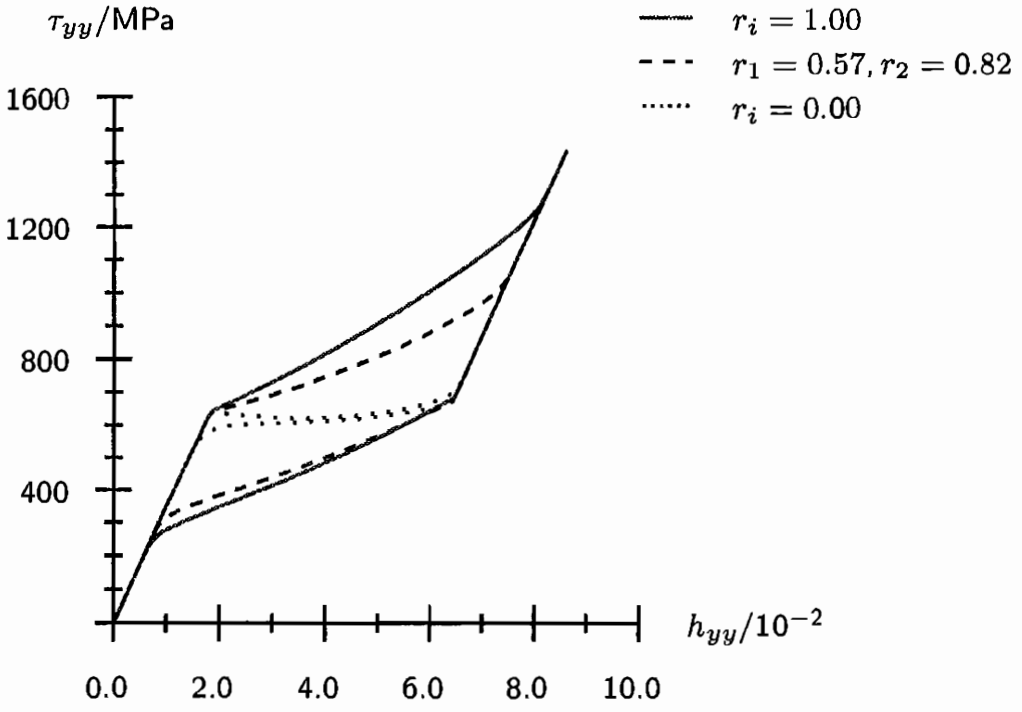

Figure 6.6: Effect of r_1 and r_2 on stress-strain hysteresis

and

$$\xi = e^{-a_2(\Theta - A_s^0)} \qquad \text{for} \quad \dot{\xi} < 0\,. \tag{6.145}$$

The functions k^α chosen above are singular at $\xi = 1$ and $\xi = 0$, respectively. However, according to experimental observations, neither states of complete $A \to M$ nor states of complete $M \to A$ transformations occur. Hence, limiting values $\xi_{max}^{A \to M}$ and $\xi_{min}^{M \to A}$ corresponding to the termination of forward respectively reverse phase transformation may be introduced. This gives

$$a_1 = -\frac{\ln(1 - \xi_{max}^{A \to M})}{M_s^0 - M_f^0} \tag{6.146}$$

and

$$a_2 = -\frac{\ln(\xi_{min}^{M \to A})}{A_f^0 - A_s^0}\,. \tag{6.147}$$

The limiting values are reached by temperature induced phase transformation at temperatures M_f^0 and A_f^0, respectively. Raniecki et al. (1992) propose to set $\xi_{max}^{A \to M}(M_f^0) = 0.99$ and $\xi_{min}^{M \to A}(A_f^0) = 0.01$.
As stated above, the explicit solutions (6.144) and (6.145) are subject to the condition $r_i = 0$. In general, $\xi(\Theta)$ can only be determined iteratively from

implicit equations. However, following the procedure described above, for a_1 and a_2 explicit equations may be obtained

$$a_1 = -\frac{(\Delta s^* - \bar{s}_0 + 2r_1\bar{s}_0\xi)\ln(1-\xi)}{2\xi(\bar{u}_0 - \Theta\bar{s}_0 + r_1(M_s^0\bar{s}_0 - \bar{u}_0)) + (\Delta s^* - \bar{s}_0)(M_s^0 - \Theta)},$$
$$a_2 = \frac{(\Delta s^* + \bar{s}_0 - 2r_2\bar{s}_0(1-\xi))\ln\xi}{2(1-\xi)(\bar{u}_0 + \Theta\bar{s}_0 - r_2(\bar{s}_0 A_s^0 + \bar{u}_0)) + (\Delta s^* + \bar{s}_0)(A_s^0 - \Theta)}. \tag{6.148}$$

Substitution of the respective finish temperatures M_f^0 and A_f^0 and limiting values $\xi_{max}^{A \to M}(M_f^0)$ and $\xi_{min}^{M \to A}(A_f^0)$ yields a_1 and a_2.
In addition to the elasticity constants E and ν represented by $\mathbf{C}_0$, the tensor of thermal expansion coefficients $\boldsymbol{\alpha}_0$, density ρ_0, specific heat c_v and reference temperature Θ_0, 19 model-specific constants Δu^*, Δs^*, $\bar{u}_0$, $\bar{s}_0$, η, A_1, A_2, B_1, B_2, C_1, C_2, a_1, a_2, r_1, r_2, A_s^0, M_s^0, A_f^0 and M_f^0 have been introduced. However, some of these constants are interrelated. Noting equations (6.138), (6.139), (6.140) and (6.141) in conjunction with relations (6.148) defining a_1 and a_2, and r_1 and r_2 already determined, for given transformation temperatures M_s^0, M_f^0, A_s^0 and A_f^0 only three constants remain to be specified. Raniecki et al. (1992) propose to use experimental data from isothermal, one-dimensional experiments to determine $\partial\boldsymbol{\tau}/\partial\mathbf{h}$, the value of $\boldsymbol{\tau}$ at the initiation of phase transformation, and $\pi^f = 0$ (cf. Figure 6.7 for isotropy). This procedure gives three relations for three unknown constants, i.e. η, Δu^* and Δs^*. Hence, in effect the model requires five additional material constants Δu^*, Δs^*, $\bar{u}_0$, $\bar{s}_0$ and η in comparison to common isotropic thermoelasticity theories, and four additional purely phenomenological parameters a_1, a_2, r_1 and r_2.

6.7 Isotropy

6.7.1 Constitutive equations under isotropy

There is some experimental evidence supporting the assumption that phase transformation of SMAs is approximately isotropic. Orgéas & Favier (1998) study the isothermal behavior of stress induced martensitic transformations in an equiatomic NiTi alloy. Their shear specimens exhibit completely isotropic behavior both during initial loading, which is stress-induced martensitic transformation, and during subsequent cycling, which is a martensite reorientation process as they conduct their experiments below the A_f-temperature. Sittner & Novák (2000) arrive at the same conclusion by employing a constant stress averaging approach to model polycrystalline SMAs. Their calculations are based on experimental data obtained on CuAlNi single crystals.
Hence restricting attention to isotropy, the relations derived in the previous sections may be specified to explicitly yield all quantities of interest in terms of the state variables $\mathbf{h}^e$, Θ, and ξ.

In definition (6.80) it was postulated that stress $\boldsymbol{\pi}$ and phase distortion may be considered as coaxial.[24] Hence, with $\boldsymbol{\pi} = \boldsymbol{\tau}$

$$\boldsymbol{\kappa} = \eta \frac{\boldsymbol{\tau}'}{\sqrt{\boldsymbol{\tau}' : \boldsymbol{\tau}'}} . \tag{6.149}$$

The denominator on the right-hand side is defined as an equivalent Kirchhoff stress

$$\tau = \sqrt{\boldsymbol{\tau}' : \boldsymbol{\tau}'} . \tag{6.150}$$

Simplifying further and assuming isotropy, the deviatoric intrinsic phase distortion $\boldsymbol{\kappa}$ due to phase transformation is presumed to be proportional to the deviator of the total strain $\mathbf{h}$

$$\frac{1}{\eta} \boldsymbol{\kappa} = \frac{1}{h} \mathbf{h}' . \tag{6.151}$$

Here, the quantity h is an equivalent Hencky strain defined from the deviatoric part of $\mathbf{h}$ by

$$h = \sqrt{\mathbf{h}' : \mathbf{h}'} . \tag{6.152}$$

Considering equation (6.89), which defines the elastic-phase transformation part of the strain $\mathbf{h}^{etr}$ as the phase distortion $\boldsymbol{\kappa}$ weighted by the mass fraction of martensite ξ

$$\mathbf{h}^{etr} = \xi \boldsymbol{\kappa} , \tag{6.153}$$

the isotropic relationship

$$\frac{1}{\eta\xi} \mathbf{h}^{etr} = \frac{1}{\eta} \boldsymbol{\kappa} = \frac{1}{h} \mathbf{h}' \tag{6.154}$$

is obtained. Noting that the elastic Hencky strain was introduced as one of three state variables in Section 5.6 motivates the derivation of an alternative relation. Using

$$\mathbf{h} = \mathbf{h}^{e} + \mathbf{h}^{etr} \tag{6.155}$$

to define the equivalent elastic strain

$$h^{e} = \sqrt{\mathbf{h}^{e\prime} : \mathbf{h}^{e\prime}} = h - \eta\xi , \tag{6.156}$$

[24] In both studies cited above, an asymmetry between tension and compression is observed. This phenomenon cannot be represented by the simplified model. For an extension of the theory, see Raniecki & Lexcellent 1998.

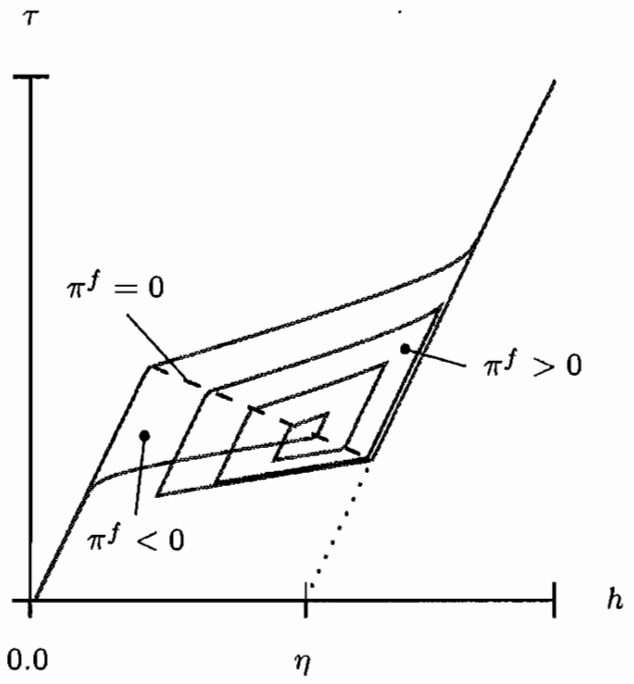

Figure 6.7: Hysteresis in equivalent Kirchhoff stress and equivalent Hencky strain plane

the elastic-phase transformation part of the strain may be expressed in terms of the elastic Hencky strain

$$\mathbf{h}^{etr} = \frac{\eta\xi}{h^e}\,\mathbf{h}^{e\prime}\,. \tag{6.157}$$

Postulating isotropy, the undetermined partial derivatives in equations (6.119) to (6.121), (6.125), and (6.127) as well as (6.128) are specified to yield

$$\frac{\partial \mathbf{h}^{etr}}{\partial \mathbf{h}^e} = \frac{\eta\xi}{h^e}\left(\mathbb{I} - \frac{1}{3}\,\mathbf{1}\otimes\mathbf{1} - \left(\frac{1}{h^e}\right)^2 \mathbf{h}^{e\prime}\otimes\mathbf{h}^{e\prime}\right) \tag{6.158}$$

$$\frac{\partial \mathbf{h}^{etr}}{\partial \Theta} = \mathbf{0} \tag{6.159}$$

$$\frac{\partial \mathbf{h}^{etr}}{\partial \xi} = \frac{\eta}{h^e}\,\mathbf{h}^{e\prime} = \frac{1}{\xi}\,\mathbf{h}^{etr}\,. \tag{6.160}$$

Combination with equation (6.127) respectively (6.128) gives $\dot{\xi}$ subject to the functional dependence

$$\dot{\xi} = \dot{\xi}(\mathbf{h}^e, \overset{\circ}{\mathbf{h}}{}^{e\,\mathrm{Log}}, \Theta, \dot{\Theta}, \xi)\,. \tag{6.161}$$

With regard to numerical solution procedures, e.g. the finite element method,

the dependency on the elastic part of the strain — which was introduced to obtain thermodynamically independent state variables — has to be replaced by a dependency on the total strain $\mathbf{h}$ and the stretching $\mathbf{D}$. With

$$\dot{h} = \frac{1}{h}\,\mathbf{h}' : \mathbf{D} \tag{6.162}$$

and (6.154), the logarithmic rate of the elastic-phase transformation part of the strain is

$$\overset{\circ}{\mathbf{h}}{}^{e^{tr}\,\mathrm{Log}} = \mathbf{D}^{e^{tr}} = \frac{\eta}{h}\left(\mathbf{h}'\dot{\xi} + \xi(\mathbb{I} - \frac{1}{3}\,\mathbf{1}\otimes\mathbf{1} - \frac{1}{h^2}(\mathbf{h}'\otimes\mathbf{h}')) : \mathbf{D}\right) . \tag{6.163}$$

Substitution of (6.160) into equations (6.127) for $A \rightarrow M$ respectively (6.128) for $M \rightarrow A$ transformation gives

$$\dot{\xi}^{\alpha} = \frac{\dot{\pi}^{f}\big|_{\xi}}{\left(\rho_0 \dfrac{\partial k^{\alpha}}{\partial \xi} - 2\rho_0\psi_{it}\right)}\,, \tag{6.164}$$

where $\dot{\pi}^{f}\big|_{\xi} = \dot{\pi}^{f}\big|_{\xi}(\dot{\xi}^{\alpha})$. In conjunction with equation (6.123_1)

$$\dot{\pi}^{f}\big|_{\xi} = \frac{\partial \pi^{f}}{\partial \mathbf{h}^{e}} : \mathbf{D}^{e} + \frac{\partial \pi^{f}}{\partial \Theta}\dot{\Theta} \tag{6.165}$$

and the partial derivatives (6.119) and (6.120) as well as (6.158) and (6.159), equation (6.164) can be solved for the rate of the mass fraction of martensite to eliminate the functional correspondence (6.161). Hence

$$\begin{aligned}\dot{\xi}^{\alpha} = \frac{1}{\left(\rho_0 \dfrac{\partial k^{\alpha}}{\partial \xi} - 2\rho_0\psi_{it} + \dfrac{\eta}{h}\left(\dfrac{\eta}{h-\eta\xi}\,\boldsymbol{\tau} : \mathbb{I}_h^{dev} + \dfrac{\eta}{h}\,\mathbb{C}_0 : \mathbf{h}'\right) : \mathbf{h}'\right)} \\ \cdot \left(\left(\frac{\eta}{h-\eta\xi}\,\boldsymbol{\tau} : \mathbb{I}_h^{dev} + \frac{\eta}{h}\,\mathbb{C}_0 : \mathbf{h}'\right) : \left(\mathbf{D} - \frac{\eta}{h}\,\xi\,\mathbb{I}_h^{dev} : \mathbf{D}\right)\right. \\ \left. + \left(-\frac{\eta}{h}\,\boldsymbol{\alpha}_0 : \mathbb{C}_0 : \mathbf{h}' - \rho_0\Delta s^{*} + \rho_0(1-2\xi)\bar{s}_0\right)\dot{\Theta}\right) .\end{aligned} \tag{6.166}$$

Here, the deviatoric unit tensor

$$\mathbb{I}_h^{dev} = \mathbb{I} - \frac{1}{3}\,\mathbf{1}\otimes\mathbf{1} - \frac{1}{h^2}\mathbf{h}'\otimes\mathbf{h}' \tag{6.167}$$

is introduced. Next, $\mathbf{h}^{e}$ is eliminated from (6.87) to yield

$$\boldsymbol{\tau} = ((\mathbf{h} - \frac{\eta\xi}{h}\,\mathbf{h}') - (\Theta - \Theta_0)\boldsymbol{\alpha}_0) : \mathbb{C}_0\,. \tag{6.168}$$

Now, the isotropic elasticity tensor $\mathbb{C}_0$ introduced in (6.18) is specified to be

$$\mathbb{C}_0 = \kappa \mathbf{1} \otimes \mathbf{1} + 2\mu \left(\mathbb{I} - \frac{1}{3} \mathbf{1} \otimes \mathbf{1} \right) . \tag{6.169}$$

Here, the bulk modulus κ is defined in terms of the *Lamé constants*[25] λ and μ

$$\kappa = \lambda + \frac{2}{3} \mu , \tag{6.170}$$

which in turn are related to *Young's modulus* E and *Poisson's ratio* ν by

$$\lambda = \frac{\nu E}{(1+\nu)(1-2\nu)} \qquad \mu = \frac{E}{2(1+\nu)} . \tag{6.171}$$

In addition, the tensor of thermal expansion $\boldsymbol{\alpha}_0$ is assumed to be isotropic

$$\boldsymbol{\alpha}_0 = \alpha_0 \mathbf{1} . \tag{6.172}$$

Using (6.169), elastic relation (6.18) may be expressed as (cf. Bruhns et al. 1999)

$$\boldsymbol{\tau} = \lambda \operatorname{tr} \left(\mathbf{h}^e \right) \mathbf{1} + 2\mu \mathbf{h}^e - 3\kappa (\Theta - \Theta_0) \alpha_0 \mathbf{1} , \tag{6.173}$$

or (cf. Bongmba 2001)

$$\boldsymbol{\tau} = \sum_{\sigma=1}^{n} \left((\kappa - \frac{2}{3}\mu) \ln J^e + \mu \ln \chi_\sigma^e - 3\kappa (\Theta - \Theta_0) \alpha_0 \right) \mathbf{B}_\sigma^e . \tag{6.174}$$

Based on the isotropic tensors of elasticity and thermal expansion, equation (6.166) can be simplified by substitution of equation (6.162) to yield a scalar equation for the rate of martensite $\dot{\xi}^\alpha$

$$\dot{\xi}^\alpha = \frac{2\mu\eta\dot{h} + \rho_0 \left(-\Delta s^* + (1-2\xi)\bar{s}_0 \right) \dot{\Theta}}{\rho_0 \dfrac{\partial k^\alpha}{\partial \xi} - 2\rho_0 \psi_{it} + 2\mu\eta^2} . \tag{6.175}$$

With this result, rate equation (6.163) for $\mathbf{h}^{etr}$ may be evaluated. Combination with the logarithmic rate of (6.90) yields the elastic part of the stretching. Then, the elastic Hencky strain may be obtained by corotational integration as defined in (3.143)

$$\mathbf{h}^e = (\mathbf{R}^{\mathrm{Log}})^{\mathrm{T}} \star \int_0^t \mathbf{R}^{\mathrm{Log}} \star \mathbf{D}^e \mathrm{d}s . \tag{6.176}$$

Hence, adopting the stated relations, the mass fraction of martensite, the elastic part of the strain, and consequently through equation (6.93) the stress $\boldsymbol{\tau}$ may be readily obtained for prescribed rate of deformation $\mathbf{D}$ and temperature Θ.

[25] Of course, λ and μ are *constant* only when $\mathbf{C}$ is considered to be independent of temperature.

6.7.2 Transformation start and finish lines

Under the assumption of isotropy, the thermodynamic driving force given by (6.117) may be specified using the isotropic elasticity and thermal expansion tensors $\mathbf{C}_0$ respectively $\boldsymbol{\alpha}_0$ to yield

$$\pi^f = \tau\eta + \rho_0(\Delta u^* - \Theta\Delta s^*) - \rho_0(1-2\xi)(\bar{u}_0 - \Theta\bar{s}_0)\,. \tag{6.177}$$

Equation (6.177) can be used to derive criteria for the initiation and conclusion of phase transformation. Phase transformation is initiated for $\pi^f = 0$, hence the equivalent Kirchhoff stress at the onset of $A \rightarrow M$ or $M \rightarrow A$ transformation is

$$\tau = -\frac{\rho_0}{\eta}\left(\Delta u^* - \Theta\Delta s^* - (1-2\xi)(\bar{u}_0 - \Theta\bar{s}_0)\right). \tag{6.178}$$

Taking the derivative with respect to time gives the slope of the transformation start and finish lines in the τ-Θ-plane

$$\frac{\mathrm{d}\tau}{\mathrm{d}\Theta} = \frac{\rho_0}{\eta}\left(\Delta s^* - (1-2\xi)\bar{s}_0\right). \tag{6.179}$$

Setting $\xi = 0$ for M_s^τ and A_f^τ, and $\xi = 1$ for A_s^τ and M_f^τ gives

$$\left.\frac{\mathrm{d}\tau}{\mathrm{d}\Theta}\right|_{M_s^\tau} = \left.\frac{\mathrm{d}\tau}{\mathrm{d}\Theta}\right|_{A_f^\tau} = \frac{\rho_0}{\eta}\left(\Delta s^* - \bar{s}_0\right) \tag{6.180}$$

and

$$\left.\frac{\mathrm{d}\tau}{\mathrm{d}\Theta}\right|_{A_s^\tau} = \left.\frac{\mathrm{d}\tau}{\mathrm{d}\Theta}\right|_{M_f^\tau} = \frac{\rho_0}{\eta}\left(\Delta s^* + \bar{s}_0\right). \tag{6.181}$$

Note that equation (6.178) holds only for M_s^τ and A_s^τ. Relations (6.180) and (6.181) for A_f^τ respectively M_f^τ imply that at the conclusion of transformation, the value of π^f must be independent of temperature.
Relations (6.180) and (6.181) show that the transformation temperatures are increased by the application of external stresses. This property of the model, which is in agreement with experimental observations (cf. Tanaka 1990), is illustrated graphically in Figure 6.8. Note the analogy to the *Clausius-Clapeyron equation*, which describes the effect of hydrostatic pressure and temperature on phase transition (cf. Wollants et al. 1979). In Figure 6.8, temperatures below A_f^0 are beyond the scope of the theory presented. Here, the calculated stress-temperature relations must be regarded as estimations since the reorientation of martensite plates and other effects which are relevant in this temperature range are not accounted for by the model (cf. Tanaka et al. 1986). Hence, the respective parts of the graphs are denoted by dashed lines.

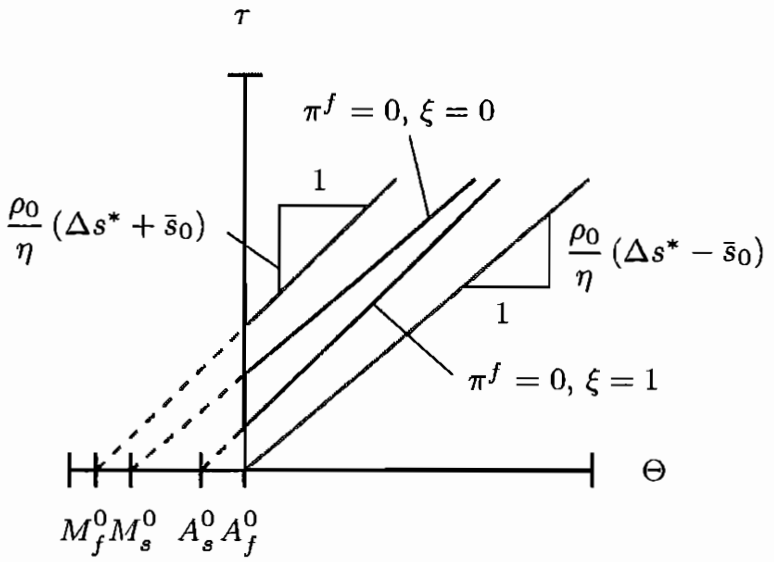

Figure 6.8: Transformation temperatures depending on equivalent Kirchhoff stress

6.7.3 Thermomechanical coupling

In Section 5.7, the rate at which energy is generated per unit mass was derived. Noting that only inelastic effects due to phase transformation are considered here, equation (5.107) may be specified to the single internal variable ξ of the theory presented. Neglecting heat sources such as radiation ($r = 0$), (5.107) yields

$$\frac{1}{\rho}\dot{h}_{lat} = \frac{1}{\rho_0}\boldsymbol{\tau} : \mathbf{D}^{etr} - \frac{\partial g}{\partial \xi}\dot{\xi} + \Theta\frac{\partial^2 g}{\partial \Theta \partial \boldsymbol{\tau}} : \overset{\circ}{\boldsymbol{\tau}}{}^{\mathrm{Log}} + \Theta\frac{\partial^2 g}{\partial \Theta \partial \xi}\dot{\xi}\,. \tag{6.182}$$

This relation may be evaluated using (6.93)

$$\boldsymbol{\tau} = (\mathbf{h}^e - (\Theta - \Theta_0)\boldsymbol{\alpha}_0) : \mathbb{C}_0 \tag{6.183}$$

and Legendre transformation (5.30) from the specific Helmholtz free energy to the specific Gibbs energy, which is a function of stress, temperature and mass fraction of martensite

$$g(\boldsymbol{\tau}, \Theta, \xi) = \psi - \frac{1}{\rho_0}\boldsymbol{\tau} : \mathbf{h}^e\,. \tag{6.184}$$

Noting the specific Helmholtz free energy as given in (6.92)

$$\begin{aligned}\psi(\mathbf{h}^e, \Theta, \xi) = {} & \frac{1}{2\rho_0}\mathbf{h}^e : \mathbb{C}_0 : \mathbf{h}^e - (\Theta - \Theta_0)\frac{1}{\rho_0}\boldsymbol{\alpha}_0 : \mathbb{C}_0 : \mathbf{h}^e \\ & + c_v\left(\Theta - \Theta_0 - \Theta\ln\left(\frac{\Theta}{\Theta_0}\right)\right) \\ & + u_0^{*A} - \Theta s_0^{*A} - \xi\pi_0^f(\Theta) + \xi(1-\xi)\psi_{it}(\Theta)\,,\end{aligned} \tag{6.185}$$

the derivatives of the specific Gibbs energy with respect to ξ

$$\frac{\partial g}{\partial \xi} = \frac{\partial \psi}{\partial \xi} = -\pi_0^f(\Theta) + (1-2\xi)\psi_{it}(\Theta) \tag{6.186}$$

and Θ

$$\frac{\partial g}{\partial \Theta} = \frac{\partial \psi}{\partial \Theta} = -\frac{1}{\rho_0}\boldsymbol{\alpha}_0 : \mathbb{C}_0 : \mathbf{h}^e - c_v \ln\left(\frac{\Theta}{\Theta_0}\right) + \xi\Delta s^* - \xi(1-\xi)\bar{s}_0 - s_0^{*A} \tag{6.187}$$

are obtained. Hence

$$\frac{\partial^2 g}{\partial \Theta \partial \boldsymbol{\tau}} = -\frac{1}{\rho_0}\,\boldsymbol{\alpha}_0 \tag{6.188}$$

and

$$\frac{\partial^2 g}{\partial \Theta \partial \xi} = \Delta s^* - (1-2\xi)\bar{s}_0\,. \tag{6.189}$$

Defining the logarithmic rate of the Kirchhoff stress from (6.93)

$$\overset{\circ}{\boldsymbol{\tau}}{}^{\mathrm{Log}} = (\mathbf{D}^e - \dot{\Theta}\boldsymbol{\alpha}_0) : \mathbb{C}_0\,, \tag{6.190}$$

the energy generation per unit mass is obtained in its final form, which may directly be implemented into a finite element code

$$\frac{1}{\rho}\,\dot{h}_{lat} = \frac{1}{\rho_0}\,\boldsymbol{\tau} : \mathbf{D}^{etr} + (\Delta u^* - \bar{u}_0(1-2\xi))\dot{\xi} - \frac{1}{\rho_0}\,\Theta\boldsymbol{\alpha}_0 : \overset{\circ}{\boldsymbol{\tau}}{}^{\mathrm{Log}}\,. \tag{6.191}$$

7 Implementation and numerical results

Finite element analysis is an essential component in design and development of structures and parts. The presented thermomechanically coupled material law is implemented into the commercial finite element code MSC.Marc. The implemented model may be used to assist in the process of design and analysis of pseudoelastic structures.
In this chapter, adaptions necessary for applying the model in numerical analyses and the implementation of the pseudoelastic material law are presented. The finite element method is not reviewed here. Instead, references to the relevant literature are given when appropriate. Comprehensive monographs on linear and non-linear finite element analysis are those written by Bathe (1986), Crisfield (1991), Zienkiewicz & Taylor (2000) and Belytschko et al. (2000). Parts of this chapter are based on these books.
This chapter is structured as follows. First, the finite element formulation chosen and the structure of the material law to be implemented are defined. As numeric analysis is based on discrete time steps, incremental kinematical quantities must be derived. To retain objectivity, the definitions introduced in the previous chapters have to be complemented or substituted by appropriate discretized relations. Some remarks concerning the continuum and consistent tangent stiffness are given in Section 7.3, as they may be used to increase numerical efficiency during equilibrium iterations. Next, it is shown how the model can be calibrated to experimental data. The properties of the model are illustrated in stress-strain and temperature-strain diagrams, among others. The chapter is concluded by presenting the finite element analysis of a more complex pseudoelastic structure.

7.1 Introduction

The balance and constitutive equations presented in the previous sections in conjunction with well posed initial and boundary conditions define a nonlinear initial boundary value problem. Its solution gives the Kirchhoff stress $\boldsymbol{\tau}$, the temperature Θ as well as all kinematical quantities such as the elastic and phase transformation parts of the deformation gradient $\mathbf{F}$ and the elastic and elastic-phase transformation parts of the stretching $\mathbf{D}$.
In a finite element analysis, the problem is decomposed into discrete time steps. For each time step, first incremental displacements are calculated based on the discretized balance of momentum equation. From these, the deformation gradient is obtained, which is passed on to a — possibly user-defined — material law. Primarily, stresses and tangent moduli are calculated here, but depending on the respective material law, decomposed strains, temperature rate and the set of internal variables may be determined as well. This second step is the part of the solution process that will be considered in more detail below. Finally, given the stresses, the balance laws can be evaluated to yield

a new set of incremental displacements. The process is then repeated until a pre-defined tolerance is met or exceeded.
For the model summarized in Figure 7.1, based on the total and incremental deformation gradients, the stresses, strains, and internal variables have to be computed. As the finite element code MSC.Marc chosen for the implementation does not permit fully thermomechanically-coupled analyses, equilibrium iterations are performed for the mechanical problem only (cf. MSC.Marc 2001a to 2001e). The error made by not directly accounting for temperature effects is minimized by using short time steps. Nevertheless, greater accuracy and efficiency can be expected from algorithms solving the thermomechanical problem as a whole.
The discretization of the material law is performed based on the monographs by Simo & Hughes (1998) and Belytschko et al. (2000) and adapted to the particular environment provided by the user subroutine `hypela2` of MSC.Marc. The finite element procedure used will be the so-called *updated Lagrangian formulation*, which is well-suited for the constitutive law tabularized in Figure 7.1. In an updated Lagrangian formulation, Eulerian measures of stress and strain are used in conjunction with a Lagrangian mesh. Derivatives and integrals are taken with respect to the Eulerian (or spatial) coordinates.

Thermoelasticity:	$\mathbf{h}^e = \dfrac{\partial \Sigma}{\partial \boldsymbol{\tau}}_{\circ} + \boldsymbol{\alpha}(\Theta - \Theta_0)$
	$\mathbf{D}^e = \overline{\partial \Sigma / \partial \boldsymbol{\tau}}^{\,\mathrm{Log}}$
Pseudoelasticity:	$\mathbf{D}^{etr} = \dfrac{\eta}{h}\left(\mathbf{h}'\dot{\xi} + \xi(\mathbb{I} - \dfrac{1}{3}\mathbf{1}\otimes\mathbf{1} - \dfrac{1}{h^2}(\mathbf{h}'\otimes\mathbf{h}')) : \mathbf{D}\right)$
Evolution equation:	$\dot{\xi} = \dot{\xi}(\mathbf{h}^e, \overset{\circ}{\mathbf{h}}{}^{e\,\mathrm{Log}}, \Theta, \dot{\Theta}, \xi)$
Thermodynamic force:	$\pi^f = \dfrac{1}{\xi}\,\boldsymbol{\tau} : \mathbf{h}^{etr} + \rho_0 \pi_0^f(\Theta) - \rho_0(1-2\xi)\psi_{it}(\Theta)$
Criteria for active processes:	$A \to M: \quad \pi^f > 0 \quad \wedge \quad \dot{\pi}^f\big\vert_{\xi} > 0$
	$M \to A: \quad \pi^f < 0 \quad \wedge \quad \dot{\pi}^f\big\vert_{\xi} < 0$
	$\dot{\pi}^f\big\vert_{\xi} = \dfrac{\partial \pi^f}{\partial \mathbf{h}^e} : \overset{\circ}{\mathbf{h}}{}^{e\,\mathrm{Log}} + \dfrac{\partial \pi^f}{\partial \Theta}\dot{\Theta}$
	$\dot{\pi}^f = \rho_0 \dot{k}^{\alpha}$

Figure 7.1: Model for pseudoelasticity

7.2 Objective discretization

The considerations in this section aim at the integration of the constitutive equation for given stretching and rate of temperature. The Eulerian material law is to be integrated in a way that satisfies the requirement of frame indifference. Algorithms complying with this requirement are said to be *incrementally objective* (cf. Simo & Hughes 1998). Objectivity is preserved by following three steps in the integration process: First, the given objective rate quantity, e.g. the stretching $\mathbf{D}$ or the stress rate $\overset{\circ}{\boldsymbol{\tau}}{}^{\mathrm{Log}}$, are tensorially transformed to the reference configuration. Here, in the *convected description*, arbitrary integration algorithms may be applied to determine the values of the respective quantities at the end of the time step. Thirdly, the result has to be transformed to the Eulerian description again.
Hence, discretized kinematic relations are required to describe the motion and deformation within the time step. In addition, the aforementioned tensorial transformation can be performed for known incremental rotation only.

7.2.1 Kinematics

It is assumed that the configuration is known at time $t = t_n$. To determine the state at the end of the time step, i.e. at $t = t_{n+1}$, incrementally objective approximations for the relevant Eulerian rate-like objects, such as the stretching and vorticity tensors, will be needed. However, first the relations describing the kinematics of the time step must be discretized.
The incremental displacement $\mathbf{u}$ relates the motion at the end of the time step $t_{n+1} = t_n + \Delta t$ to the motion at the beginning of the time step

$$\boldsymbol{\chi}_{n+1} = \boldsymbol{\chi}_n + \mathbf{u} \tag{7.1}$$

and defines the deformation gradient at the end of the time step

$$\mathbf{F}_{n+1} = \mathbf{F}_n + \nabla_0 \otimes \mathbf{u}\,. \tag{7.2}$$

Introducing the parameter α, intermediate stages in the motion are given by

$$\boldsymbol{\chi}_{n+\alpha} = \alpha\boldsymbol{\chi}_{n+1} + (1-\alpha)\boldsymbol{\chi}_n \quad \text{for} \quad \alpha \in [0,1]\,, \tag{7.3}$$

yielding the deformation gradient

$$\mathbf{F}_{n+\alpha} = \alpha\mathbf{F}_{n+1} + (1-\alpha)\mathbf{F}_n\,. \tag{7.4}$$

This relation may be used to define the incremental or *relative deformation gradient* of the increment $\mathbf{f}$

$$\mathbf{f}_{n+\alpha} = \mathbf{F}_{n+\alpha}\mathbf{F}_n^{-1} = \mathbf{1} + \alpha\nabla_n \otimes \mathbf{u}\,, \tag{7.5}$$

where the gradient with respect to the configuration $\mathcal{B}_n$ is denoted by ∇_n. Specifically, the incremental deformation gradient is

$$\mathbf{f}_{n+1} = \mathbf{F}_{n+1}\mathbf{F}_n^{-1} = \mathbf{1} + \nabla_n \otimes \mathbf{u}\,. \tag{7.6}$$

The deformation gradient $\mathbf{F}_{n+1}$ determines left Cauchy-Green tensor

$$\mathbf{B}_{n+1} = \mathbf{F}_{n+1}\mathbf{F}_{n+1}^{\mathrm{T}} \tag{7.7}$$

and Hencky strain at the end of the increment

$$\mathbf{h}_{n+1} = \frac{1}{2}\ln\mathbf{B}_{n+1}\,. \tag{7.8}$$

The procedure employed in the numerical computation of (7.8) is outlined in Appendix B.3.

7.2.2 Integration of logarithmic spin

Transformations between current and reference configurations require the discretized logarithmic rotation tensor $\mathbf{R}^{\mathrm{Log}}_{n+\alpha}$. The logarithmic rotation is given by the linear tensorial differential equation (3.140) in conjunction with the initial value $\mathbf{R}^{\mathrm{Log}}_n$ at the beginning t_n of the time step

$$\dot{\mathbf{R}}^{\mathrm{Log}} = \boldsymbol{\Omega}^{\mathrm{Log}}(\mathbf{R}^{\mathrm{Log}})^{\mathrm{T}}, \qquad \mathbf{R}^{\mathrm{Log}}\big|_{t=t_n} = \mathbf{R}^{\mathrm{Log}}_n\,. \tag{7.9}$$

An algorithm for the objective integration of $\boldsymbol{\Omega}^{\mathrm{Log}}$ will be given at the end of this section.
First, the stretching tensor $\mathbf{D}$ and the vorticity tensor $\mathbf{W}$ must be calculated in terms of the discretized deformation gradient in order to determine the logarithmic spin $\boldsymbol{\Omega}^{\mathrm{Log}}$. Note that to preserve incremental objectivity, these quantities *cannot* be obtained from (3.114) and (3.116), respectively. In fact, an incrementally objective approximation for the rate of deformation tensor is given by (cf. Simo & Hughes 1998)

$$\mathbf{D}_{n+\alpha} = \frac{1}{2\Delta t}\,\mathbf{f}^{-\mathrm{T}}_{n+\alpha}(\mathbf{f}^{\mathrm{T}}_{n+1}\mathbf{f}_{n+1} - \mathbf{1})\mathbf{f}^{-1}_{n+\alpha}\,, \tag{7.10}$$

hence

$$\mathbf{D}_n = \frac{1}{2\Delta t}(\mathbf{f}^{\mathrm{T}}_{n+1}\mathbf{f}_{n+1} - \mathbf{1}) \qquad \mathbf{D}_{n+1} = \frac{1}{2\Delta t}(\mathbf{1} - \mathbf{f}^{-\mathrm{T}}_{n+1}\mathbf{f}^{-1}_{n+1})\,. \tag{7.11}$$

The vorticity may be calculated from

$$\mathbf{W}_{n+\alpha} = \frac{1}{2\Delta t}\left((\mathbf{f}_{n+1} - \mathbf{1})\mathbf{f}^{-1}_{n+\alpha} - \mathbf{f}^{-\mathrm{T}}_{n+\alpha}(\mathbf{f}^{\mathrm{T}}_{n+1} - \mathbf{1})\right)\,, \tag{7.12}$$

yielding

$$\mathbf{W}_n = \frac{1}{2\Delta t}(\mathbf{f}_{n+1} - \mathbf{f}_{n+1}^{\mathrm{T}}) \qquad \mathbf{W}_{n+1} = \frac{1}{2\Delta t}(\mathbf{f}_{n+1}^{-\mathrm{T}} - \mathbf{f}_{n+1}^{-1}). \tag{7.13}$$

By virtue of equation (3.12), for a rigid body motion the incremental deformation gradient is

$$\mathbf{f}_{n+1} = \mathbf{Q}, \tag{7.14}$$

where $\mathbf{Q}$ is an orthogonal rotation tensor. Hence, it is readily observed that the stretching, as given by (7.10), vanishes identically for incremental rigid body motions

$$\mathbf{D}_{n+\alpha} = \mathbf{0}. \tag{7.15}$$

The logarithmic spin is then calculated from the left Cauchy-Green, stretching and vorticity tensors using eigenprojections, see Appendix A.2. Differential equation (7.9) for the logarithmic rotation may be solved by an extension of the generalized midpoint rule to yield the incremental logarithmic rotation (cf. Simo & Hughes 1998). For arbitrary α within the time step it follows

$$\mathbf{R}_{n+\alpha}^{\mathrm{Log}} = \mathbf{R}_n^{\mathrm{Log}}(\exp(\alpha\Delta t\boldsymbol{\Omega}_{n+\alpha}^{\mathrm{Log}}))^{\mathrm{T}}. \tag{7.16}$$

The *exponential map* of orthogonal tensors can be parameterized in different ways. Following Simo & Hughes (1998), a parameterization in terms of quaternion parameters q_0 and q^* is adopted. It is based on the fact that for arbitrary vectors $\boldsymbol{\alpha}$, there is a unique vector $\boldsymbol{\omega}$ defined by

$$\hat{\boldsymbol{\Omega}}\boldsymbol{\alpha} = \boldsymbol{\omega} \times \boldsymbol{\alpha} \quad \forall\, \boldsymbol{\alpha} \in \mathbb{E} \tag{7.17}$$

called the axial vector of the skew-symmetric spin $\hat{\boldsymbol{\Omega}}$ (cf. Ogden 1984). Then, the optimal evaluation of the exponential map is given by the algorithm in Figure 7.2 (see Simo & Hughes 1998)[26].
In particular, the logarithmic rotation at the end of the time step is given by

$$\mathbf{R}_{n+1}^{\mathrm{Log}} = \mathbf{R}_n^{\mathrm{Log}}(\exp(\Delta t\boldsymbol{\Omega}_{n+1}^{\mathrm{Log}}))^{\mathrm{T}}. \tag{7.18}$$

Hence, the incremental or *relative* rotation of the time step $\mathbf{R}^{\mathrm{Log}}$ may be defined as

$$\mathbf{r}_{n+1}^{\mathrm{Log}} = (\mathbf{R}_n^{\mathrm{Log}})^{\mathrm{T}}\mathbf{R}_{n+1}^{\mathrm{Log}} = (\exp(\Delta t\boldsymbol{\Omega}_{n+1}^{\mathrm{Log}}))^{\mathrm{T}}. \tag{7.19}$$

[26] There seems to be a mistake in formula (2_1) of Box 8.3 in Simo & Hughes (1998). Hence, the formulation in Belytschko et al. (2000) is adopted here.

1. Given the spin $\hat{\boldsymbol{\Omega}}$, compute quaternion parameters

$$q_0 = \cos(\|\boldsymbol{\omega}\|/2)$$
$$q^* = \sin(\|\boldsymbol{\omega}\|/2)$$

if $|q^*| > tol$ then

$$q^* = \frac{1}{2}\frac{\sin(\|\boldsymbol{\omega}\|2)}{(\|\boldsymbol{\omega}\|2)}$$

else

$$q^* = \frac{1}{2}\left[1 - \|\boldsymbol{\omega}\|^2/24 + \|\boldsymbol{\omega}\|^4/1920 + \dots\right]$$

end if

$$\mathbf{q} = q^*\boldsymbol{\omega}$$

2. Compute the exponential by the formula

$$\exp(\hat{\boldsymbol{\Omega}}) = 2\left(q_0^2 - \frac{1}{2}\right)\mathbf{1} + 2q_0\hat{\boldsymbol{\Omega}} + 2\mathbf{q}\mathbf{q}^{\mathrm{T}}$$
$$= 2\begin{bmatrix} q_0^2 + q_1^2 - \frac{1}{2} & q_1q_2 - q_3q_0 & q_1q_3 + q_2q_0 \\ q_2q_1 + q_3q_0 & q_0^2 + q_2^2 - \frac{1}{2} & q_2q_3 - q_1q_0 \\ q_3q_1 - q_2q_0 & q_3q_2 + q_1q_0 & q_0^2 + q_3^2 - \frac{1}{2} \end{bmatrix}$$

Figure 7.2: Optimal evaluation of the exponential map

7.2.3 Objective integration of constitutive equations

The key to preserving objectivity of the discrete equations is to formulate the integration algorithm in a local rotated representation. In the rotated description, the rotated objects remain unaltered under superposed spatial rigid body motions. Subsequently to the corotational integration, the discrete equations are transformed back to the Eulerian configuration (cf. Khan & Huang 1995, Simo & Hughes 1998, Bruhns et al. 2001). This methodology is well-suited for corotational objective stress rates such as the logarithmic rate of the Kirchhoff stress considered here.
By virtue of (3.141), the logarithmic rate of the Kirchhoff stress can be written in the form

$$\overline{\mathbf{R}^{\mathrm{Log}} \star \boldsymbol{\tau}}^{\cdot} = \mathbf{R}^{\mathrm{Log}} \star \overset{\circ}{\boldsymbol{\tau}}{}^{\mathrm{Log}} \tag{7.20}$$

and integrated as indicated in equation (3.143)

$$\boldsymbol{\tau} = \left(\mathbf{R}^{\mathrm{Log}}\right)^{\mathrm{T}} \star \int_0^t \mathbf{R}^{\mathrm{Log}} \star \overset{\circ}{\boldsymbol{\tau}}{}^{\mathrm{Log}} \mathrm{d}s \,. \tag{7.21}$$

Hence, for known state at t_n,

$$\boldsymbol{\tau}_{n+1} = (\mathbf{R}_{n+1}^{\mathrm{Log}})^{\mathrm{T}} \star \left[\mathbf{R}_n^{\mathrm{Log}} \star \boldsymbol{\tau}_n + \int_{t_n}^{t_{n+1}} \mathbf{R}^{\mathrm{Log}} \star \overset{\circ}{\boldsymbol{\tau}}{}^{\mathrm{Log}} \mathrm{d}s \right] \tag{7.22}$$

$$= (\mathbf{r}_{n+1}^{\mathrm{Log}})^{\mathrm{T}} \star \boldsymbol{\tau}_n + (\mathbf{R}_{n+1}^{\mathrm{Log}})^{\mathrm{T}} \star \int_{t_n}^{t_{n+1}} \mathbf{R}^{\mathrm{Log}} \star \overset{\circ}{\boldsymbol{\tau}}{}^{\mathrm{Log}} \mathrm{d}s \,. \tag{7.23}$$

The remaining integral on the right-hand side may either be solved by direct integration of the constitutive equations, or by applying an iterative scheme comprising an implicit Eulerian integration algorithm and a subsequent Newton-iteration. Here, integration is performed using a software package based on *Gear's method* (cf. Kahaner et al. 1989). Using this software package, no further derivations except for the tangent stiffness (see Section 7.3) are required. The relevant equations of the model for the case of isotropic material symmetry are summarized in Appendix B.1.
However, more insight is to be gained by alternatively considering the generalized midpoint rule

$$\int_{t_n}^{t_{n+1}} \mathbf{R}^{\mathrm{Log}} \star \overset{\circ}{\boldsymbol{\tau}}{}^{\mathrm{Log}} \mathrm{d}s = \Delta t \left(\alpha \mathbf{R}_{n+1}^{\mathrm{Log}} \star \overset{\circ}{\boldsymbol{\tau}}{}_{n+1}^{\mathrm{Log}} + (1-\alpha) \mathbf{R}_n^{\mathrm{Log}} \star \overset{\circ}{\boldsymbol{\tau}}{}_n^{\mathrm{Log}} \right) \tag{7.24}$$

to give

$$\boldsymbol{\tau}_{n+1} = (\mathbf{r}_{n+1}^{\mathrm{Log}})^{\mathrm{T}} \star \boldsymbol{\tau}_n + \Delta t \left(\alpha \overset{\circ}{\boldsymbol{\tau}}{}_{n+1}^{\mathrm{Log}} + (1-\alpha) (\mathbf{r}_{n+1}^{\mathrm{Log}})^{\mathrm{T}} \star \overset{\circ}{\boldsymbol{\tau}}{}_n^{\mathrm{Log}} \right) . \tag{7.25}$$

Choosing $\alpha = 1$ yields the implicit (backward) Euler scheme

$$\boldsymbol{\tau}_{n+1} = (\mathbf{r}_{n+1}^{\mathrm{Log}})^{\mathrm{T}} \star \boldsymbol{\tau}_n + \Delta t \overset{\circ}{\boldsymbol{\tau}}{}_{n+1}^{\mathrm{Log}} \,. \tag{7.26}$$

Obviously, this algorithm is incrementally objective for arbitrary $\alpha \in [0,1]$. This may be observed by considering the rate-constitutive equation

$$\overset{\circ}{\boldsymbol{\tau}}{}^{\mathrm{Log}} = \mathbb{A} : \mathbf{D} \,, \tag{7.27}$$

subject to the rigid body motion $\mathbf{f}_{n+1} = \mathbf{Q}$ as discussed above. For a rigid body motion, the stretching vanishes. On the other hand, the incremental logarithmic rotation is obtained as

$$\mathbf{r}_{n+1}^{\mathrm{Log}} = \mathbf{Q}^{\mathrm{T}} \,. \tag{7.28}$$

Hence the integration is objective

$$\boldsymbol{\tau}_{n+1} = \mathbf{Q} \star \boldsymbol{\tau}_n \,. \tag{7.29}$$

The discretized constitutive equations for the backward Euler scheme (7.26) are given in Appendix B.5.

7.2.4 Validation

Before the pseudoelastic model is implemented, the implementation of the kinematic relations and the objective integration algorithm are verified based on the hypoelastic rate-constitutive law obtained by inverting (6.14), neglecting temperature effects

$$\overset{\circ}{\boldsymbol{\tau}}{}^{\mathrm{Log}} = \mathbf{D}^e : \mathbb{C} \,. \tag{7.30}$$

To this end, a test in simple shear is considered. The analytical solution derived by Xiao et al. (1997a, 1997b) is as follows.
A deformation of simple shear in the $\mathbf{e}_1$-$\mathbf{e}_2$-plane in a fixed orthonormal basis ($\mathbf{e}_1$,$\mathbf{e}_2$,$\mathbf{e}_3$) has the representation

$$\mathbf{x} = (X_1 + \gamma X_2)\mathbf{e}_1 + X_2\mathbf{e}_2 + X_3\mathbf{e}_3 \,. \tag{7.31}$$

From the deformation gradient

$$\mathbf{F} = \mathbf{e}_1 \otimes \mathbf{e}_1 + \gamma \mathbf{e}_1 \otimes \mathbf{e}_2 + \mathbf{e}_2 \otimes \mathbf{e}_2 + \mathbf{e}_3 \otimes \mathbf{e}_3 \,, \tag{7.32}$$

the left Cauchy-Green tensor is obtained

$$\mathbf{B} = (1+\gamma^2)\mathbf{e}_1 \otimes \mathbf{e}_1 + \gamma(\mathbf{e}_1 \otimes \mathbf{e}_2 + \mathbf{e}_2 \otimes \mathbf{e}_1) + \mathbf{e}_2 \otimes \mathbf{e}_2 + \mathbf{e}_3 \otimes \mathbf{e}_3 \,. \tag{7.33}$$

Its eigenvalues are calculated to be

$$\chi_1 = (2 + \gamma^2 + \gamma\sqrt{4+\gamma^2})/2 \tag{7.34}$$

$$\chi_2 = (2 + \gamma^2 - \gamma\sqrt{4+\gamma^2})/2 \tag{7.35}$$

$$\chi_3 = 1 \,, \tag{7.36}$$

and, introducing $\bar{\mathbf{1}} = (\mathbf{1} - \mathbf{e}_3 \otimes \mathbf{e}_3)$, its eigenprojections are

$$\mathbf{B}_1 = \frac{1}{\chi_1 - \chi_2}(\mathbf{B} - \chi_2\bar{\mathbf{1}} - \mathbf{e}_3 \otimes \mathbf{e}_3) \tag{7.37}$$

$$\mathbf{B}_2 = \frac{1}{\chi_2 - \chi_1}(\mathbf{B} - \chi_1\bar{\mathbf{1}} - \mathbf{e}_3 \otimes \mathbf{e}_3) \tag{7.38}$$

$$\mathbf{B}_3 = \mathbf{e}_3 \otimes \mathbf{e}_3 \,. \tag{7.39}$$

Hence, by virtue of definition (3.91), the Hencky strain tensor is computed

$$\mathbf{h} = \frac{\ln\chi_1 - \ln\chi_2}{2(\chi_1 - \chi_2)}(\mathbf{B} - \mathbf{e}_3 \otimes \mathbf{e}_3) + \frac{\chi_1 \ln\chi_2 - \chi_2 \ln\chi_1}{2(\chi_1 - \chi_2)}\,\bar{\mathbf{1}}\,, \tag{7.40}$$

which, using (6.7.1), yields the stress components in the $\mathbf{e}_1$-$\mathbf{e}_2$-plane

$$\tau_{12} = \frac{2\mu}{\sqrt{4+\gamma^2}} \ln\left[1 + \frac{\gamma^2}{2} + \gamma\sqrt{1+\frac{\gamma^2}{4}}\right] \qquad \tau_{11} = -\tau_{22} = \frac{1}{2}\gamma\tau_{12}\,. \tag{7.41}$$

Note that $J = 1$ gives $\boldsymbol{\sigma} = \boldsymbol{\tau}$ in simple shear. With increasing shear γ, the corresponding shear stress τ_{12} is strongly nonlinear, with a maximum at the so-called *hypoelastic yield point* ($\gamma_m = 3.0177171$, $\tau_m/\mu = 1.3254868$) (cf. Xiao et al. 1997a).
The same problem is solved numerically by considering a simple shear deformation of a single finite element. The corresponding stress response is depicted in Figure 7.3. Evidently, the agreement between analytical solution and finite element analysis is very good. Hence, the implementation of the elastic law is regarded as successful.

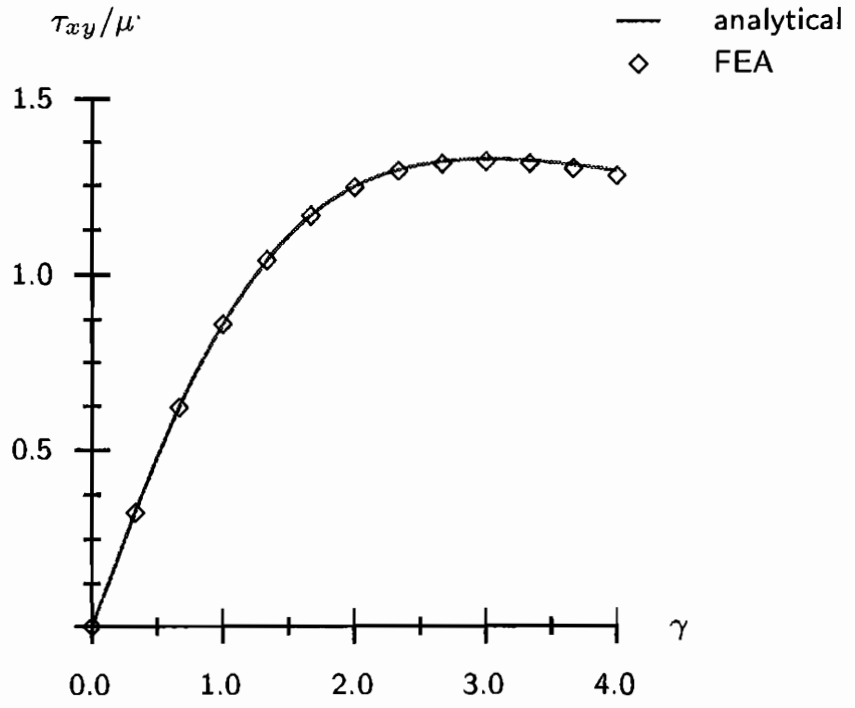

Figure 7.3: Simple shear: hypoelastic yield point

7.3 Tangent stiffness

The linearization of the constitutive equation may be carried out in two ways. Using continuum tangent moduli, the so-called *tangent stiffness matrix* is ob-

tained as the resulting material tangent stiffness matrix. Alternatively, the constitutive equation may be linearized based on the algorithmic tangent moduli, which gives rise to the so-called *consistent tangent stiffness* (cf. Simo & Taylor 1985, Wriggers 1986).
The appropriate tangent stiffness for the particular problem depends on issues regarding ease of implementation and on the smoothness of the problem. While the continuum tangent modulus is often implemented without difficulty, it may be subject to convergence problems at discontinuities of the derivatives of the constitutive equation. On the other hand, the consistent tangent stiffness, required for optimal convergence, may be harder or impossible to derive. Without loss of generality, attention is restricted here to isothermal processes. For an extension of the concept outlined below to thermomechanical processes, see Miehe (1988).
Adopting the hypoelastic constitutive equation

$$\overset{\circ}{\boldsymbol{\tau}}{}^{\mathrm{Log}} = \mathbb{C} : \mathbf{D}^e \tag{7.42}$$

and recognizing the additive decomposition (3.147) of the stretching $\mathbf{D}$ into its elastic part and elastic-inelastic parts, the continuum tangent stiffness may be derived. To this end, it is postulated that the elastic-inelastic part of the stretching is expressible in terms of the total stretching and possibly other independent variables, i.e. $\mathbf{D}^{ei} = \mathbf{D}^{ei}(\mathbf{D})$ for the material law under consideration, which yields

$$\overset{\circ}{\boldsymbol{\tau}}{}^{\mathrm{Log}} = \mathbb{C}^{ei} : \mathbf{D} \,. \tag{7.43}$$

The weak form of the balance of momentum equation (4.101) consists of two parts contributing to the internal nodal forces in a finite element discretization. The first part involves the current state of stress $\boldsymbol{\tau}$. Due to its dependence on the velocity gradient $\mathbf{L}$, it accounts for geometric effects of deformation, including rotation and stretching. Hence, the respective stiffness matrix denoted by $\mathbb{C}^{geo}$ is referred to as *geometric* stiffness.
Through the rate of stress $\overset{\circ}{\boldsymbol{\tau}}{}^{\mathrm{Log}}$ given by (7.43), the second part of (4.101) contributing to the internal nodal forces depends on the material response. It leads to the so-called *material* tangent stiffness matrix $\mathbb{C}^{mat}$, which relates the rates of the internal nodal forces to the rate of the displacements due to the material response. In equation (4.101), the Lie derivative of the Kirchhoff stress is substituted by the logarithmic rate of $\boldsymbol{\tau}$

$$\overset{\circ}{\boldsymbol{\tau}}{}^{\mathrm{L}} = \overset{\circ}{\boldsymbol{\tau}}{}^{\mathrm{Log}} + \mathbb{G} : \mathbf{D} \,. \tag{7.44}$$

Here, the tensor $\mathbb{G}$ given in Appendix A.3 is defined by the logarithmic rate and independent of the respective material response. Hence, by virtue of (7.43), the material tangent is obtained

$$\mathbb{C}^{mat} = J^{-1}(\mathbb{C}^{ei} + \mathbb{G}) \,. \tag{7.45}$$

For numerical efficiency, the *consistent tangent* is required (cf. MSC.Marc 2001a, MSC.Marc 2001d)

$$\mathbb{C}^{c}_{n+1} = \frac{\partial \overset{\circ}{\boldsymbol{\tau}}{}^{\mathrm{Log}}_{n+1}}{\partial \mathbf{D}_{n+1}} \,. \tag{7.46}$$

The accuracy of computational results does not depend on the accuracy of the stiffness matrix. However, convergence will be quadratic for a fully consistent stiffness matrix only. Due to its formulation in strain space, for the model under consideration the derivation of the consistent tangent proceeds in a similar manner to that of the continuum stiffness matrix.
The continuum tangent stiffness $\mathbb{C}^{etr}$ of the model discussed in Chapter 6 is derived in Appendix B.4.

7.4 Calibration of the model to experimental data

7.4.1 Identification of parameters

In order to be applied to the simulation of pseudoelastic structures, the model has to be calibrated. This is done based on experimental data obtained from a specimen of chemical composition and thermomechanical treatment similar to that of the respective structure whose behavior is to be analyzed. Accurate predictions of the structural behavior can be expected only if the agreement between the thermomechanical properties of the specimen the model is calibrated to and the structure under consideration is very good.
Referring to Sections 6.6 and 6.7, six constants governing the thermoelastic and thermal material behavior, and nine model-specific parameters are to be identified. With only experimental data on isothermal tests available, the value of the coefficient of thermal expansion $\alpha_0 = 8.8 \cdot 10^{-6}\,{}^{1}/_{\mathrm{K}}$ and the specific heat at constant pressure $c_p = 837.36\,{}^{\mathrm{J}}/_{\mathrm{kg\,K}}$ for the reference temperature $\Theta_0 = 0\,\mathrm{K}$ are adopted from Hodgson & Brown (2000). Note that the value chosen for α_0 is in fact the average of the phase specific properties given by these authors. Hodgson & Brown (2000) specify a density of $\rho_0 = 0.0065\,{}^{\mathrm{kg}}/_{\mathrm{m\,mm^2}}$ and a Poisson's ratio of $\nu = 0.33$. Young's modulus is identified as $E = 35\,000\,\mathrm{MPa}$ based on experimental data, which is obtained by subjecting a specimen of near equiatomic NiTi (50.7 at % Nickel) as depicted in Figure 7.4 to simple tension (cf. Wurzel 2001).
The parameters of the model relevant to the description of pseudoelasticity are determined based on the same isothermal test in tension. Ideally, all parameters should follow from the respective relations specified in Section 6.6. However, defining the optimal parameter set as the one which minimizes the deviations in stress-strain-space between calculated hysteresis and experimental results, in general these parameters can be regarded as initial values only, subject to subsequent optimization.

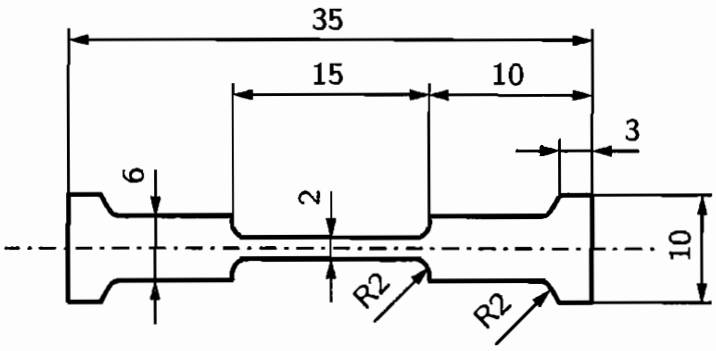

Figure 7.4: Specimen 44-1-F

The optimal parameter set is the one which best fits the calculated curve to the measured data. It is found by employing an appropriate optimization procedure such as the *method of least squares*. Here, it is assumed that the best-fit curve of a given type is the curve that has the minimal sum of the deviations squared, i.e. the least square error, from a given set of data. Denoting the vector of parameters by $\mathbf{x}$, according to the method of least squares the best fitting curve has the property

$$f(\mathbf{x}) = \sum_i (\bar{y}_i - y_i(\mathbf{x}))^2 \rightarrow \text{Min!} \quad \forall \mathbf{x} \in \mathrm{D}_{\mathbf{x}}\,. \tag{7.47}$$

Here, $\bar{y}_i$ are the values experimentally observed, and y_i are the corresponding values of the calculation, computed based on the parameter set $\mathbf{x}$ of the domain $\mathrm{D}_{\mathbf{x}}$.
In general, no analytical solution to the foregoing minimization problem is available. Hence, numerical optimization procedures need to be applied. They are classified according to their complexity into methods of zeroth, first and second order. While procedures of order zero are limited to functional evaluations, implying both low convergence ratio and low computational cost, higher order methods employing the gradient ∇f converge faster, but are computationally more expensive (cf. Vogelsang 2001). Here, a method of order zero is applied.
The parameters summarized in Table 7.1 are obtained by regarding the transformation temperatures of the specimen depicted above as initial values of the respective parameters of the model (cf. Wurzel 2001)

$$M_f^0 = 212\,\mathrm{K}$$
$$M_s^0 = 243\,\mathrm{K}$$
$$A_s^0 = 243\,\mathrm{K}$$
$$A_f^0 = 268\,\mathrm{K}.$$

Initially, the phenomenological parameters r_i are chosen to be equal to one. From the pseudoelastic hysteresis, the amplitude of pseudoelastic flow η is esti-

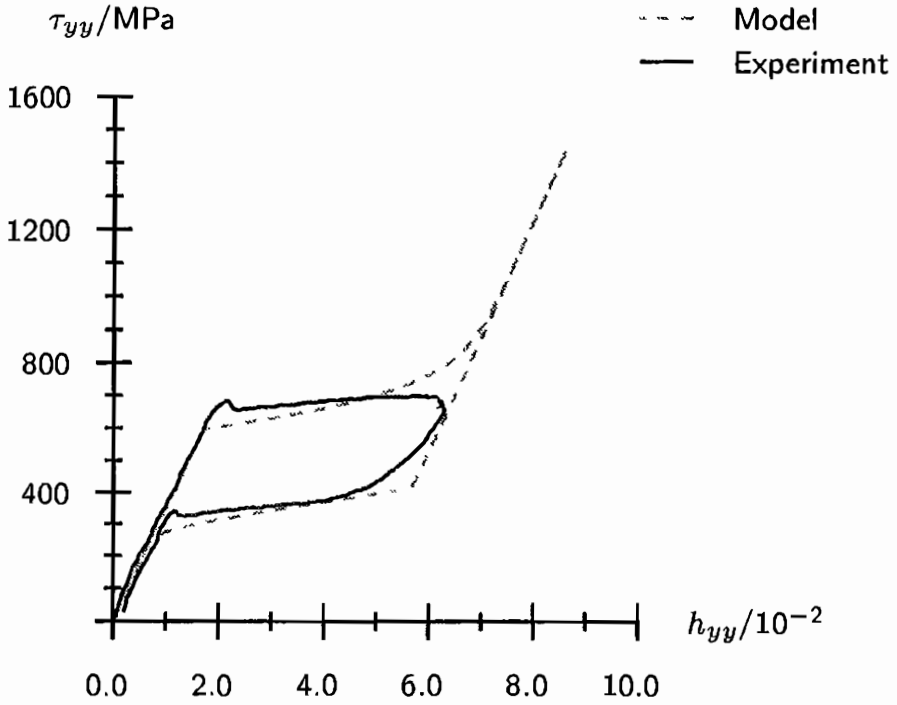

Figure 7.5: Calibrated model

mated as illustrated in Figure 6.7. In addition, initial values of Δu^* and Δs^* are adopted from Ziólkowski (2001).

Based on this information, by virtue of (6.138) and (6.139), from the transformation temperatures initial values of the configurational internal energy $\bar{u}_0$ and entropy $\bar{s}_0$ are calculated. The phenomenological constants a_1 and a_2 are obtained from relations (6.146) and (6.147), noting that $r_i = 1$, initially. The tabulated parameters then follow by a minimization procedure using a linear, small strain version of the model.

Evidently, the isothermal behavior experimentally observed can be simulated very well (see Figure 7.5). However, although the agreement between measured and calculated hystereses is very good, it should be noted that the parameter set strongly relies on the assumption that the mass fraction of martensite is equal to or at least close to one ($\xi = 1$) at the reversal of the loading direction in the experiment. However, this information is not to be gained from a stress-strain curve alone, and η can be determined accurately only by in-situ measurement of the phase composition of the specimen. It remains to be examined if the parameter set of Table 7.1 yields good results in tests in torsion and in non-isothermal tests as well. Due to its geometric specifications, the specimen cut from sheet metal could not be subjected to simple torsion or shear loading. As the transformation behavior of NiTi SMAs is very sensitive even to minor changes in composition and thermomechanical treatment, a comparison to experimental data available in the literature is of little use. With regard to the latter issue, i.e. non-isothermal tests, reliable ex-

Parameter	Value
E/ MPa	35000.0
ν	0.33
α_0/ ^{1}/K	$8.8 \cdot 10^{-6}$
ρ_0/ kg/m mm^2	$6.45 \cdot 10^{-3}$
c_p/ J/kg K	837.36
Δu^*/ J/kg	16800.0
Δs^*/ J/kg K	64.50
$\bar{u}_0$/ J/kg	4264.5
$\bar{s}_0$/ J/kg K	11.5
η	0.055
a_1	0.15
a_2	0.70
r_1	0.55
r_2	0.95

Table 7.1: Parameter set of specimen 44-1-F

perimental data with well defined thermal boundary conditions and accurate measurement of temperature remains to be obtained. The model predictions in non-isothermal calculations will, of course, be strongly influenced by the thermal parameters adopted from the cited literature.

7.4.2 Transformation temperatures

From the parameter set given in Table 7.1, relations for the transformation temperatures of Clausius-Clapeyron type, schematically illustrated in Figure 6.8 above, may be specified. The slopes of the transformation start and finish temperatures, presumed to be identical for M_s^τ and A_f^τ as well as for A_s^τ and M_f^τ, respectively, follow from (6.180)

$$\left.\frac{\mathrm{d}\tau}{\mathrm{d}\Theta}\right|_{M_s^\tau} = \left.\frac{\mathrm{d}\tau}{\mathrm{d}\Theta}\right|_{A_f^\tau} = \frac{\rho_0}{\eta}\,(\Delta s^* - \bar{s}_0) = 6.21\ ^{\mathrm{MPa}}/_{\mathrm{K}} \tag{7.48}$$

respectively (6.181)

$$\left.\frac{\mathrm{d}\tau}{\mathrm{d}\Theta}\right|_{A_s^\tau} = \left.\frac{\mathrm{d}\tau}{\mathrm{d}\Theta}\right|_{M_f^\tau} = \frac{\rho_0}{\eta}\,(\Delta s^* + \bar{s}_0) = 8.91\ ^{\mathrm{MPa}}/_{\mathrm{K}}\,. \tag{7.49}$$

To plot the equivalent Kirchhoff stress in terms of the transformation temperatures, their initial values at stress free state ($\tau = 0$) are required. The start

temperatures follow from (6.138) and (6.139)

$$M_s^0 = \frac{\Delta u^* - \bar{u}_0}{\Delta s^* - \bar{s}_0} = 236.52\,\mathrm{K} \tag{7.50}$$

respectively

$$A_s^0 = \frac{\Delta u^* + \bar{u}_0}{\Delta s^* + \bar{s}_0} = 277.16\,\mathrm{K}\,. \tag{7.51}$$

Rearranging (6.148) and substituting the limiting values corresponding to the temperatures M_f^0 and A_f^0, chosen as $\xi_{max}^{A \to M}(M_f^0) = 0.99$ respectively $\xi_{min}^{M \to A}(A_f^0) = 0.01$, yields the finish temperatures

$$M_f^0 = \frac{1}{(2\xi - 1)\bar{s}_0 + \Delta s^*} \Big(a_1^{-1}(\Delta s^* - \bar{s}_0 + 2r_1\bar{s}_0\xi)\ln(1-\xi) + 2\xi((1-r_1)\bar{u}_0 + r_1\bar{s}_0 M_s^0) + \Delta u^* - \bar{u}_0 \Big)\Big|_{\xi^{A\to M}} = 228.13\,\mathrm{K} \tag{7.52}$$

and

$$A_f^0 = \frac{1}{(1-2\xi)\bar{s}_0 - \Delta s^*} \Big(a_2^{-1}(\Delta s^* + \bar{s}_0 - 2r_2\bar{s}_0(1-\xi))\ln\xi - 2(1-\xi)((1-r_2)\bar{u}_0 - r_2\bar{s}_0 A_s^0) - (\Delta u^* + \bar{u}_0) \Big)\Big|_{\xi^{M\to A}} = 297.74\,\mathrm{K}\,. \tag{7.53}$$

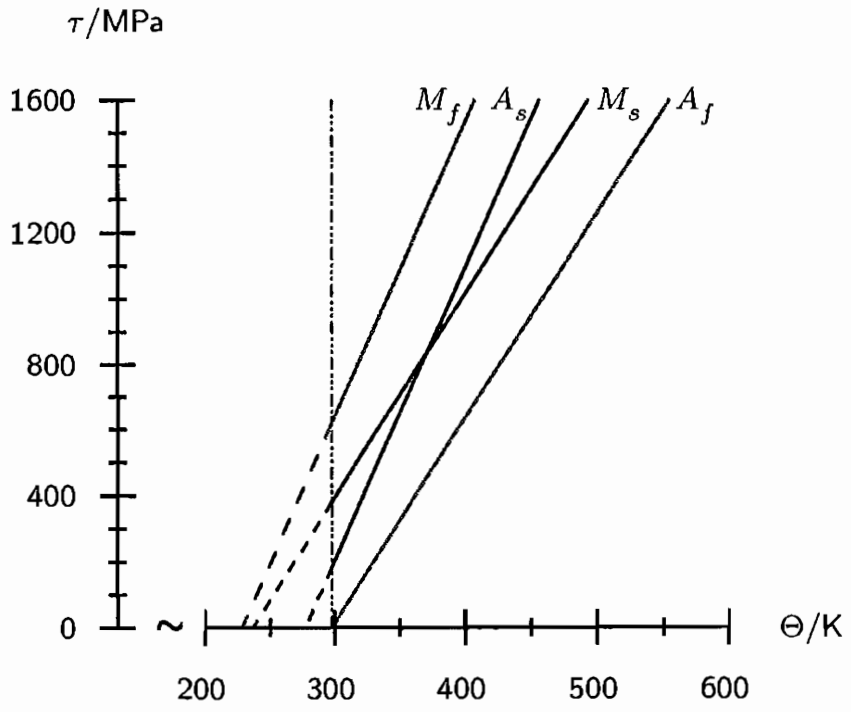

Figure 7.6: Transformation temperatures of the calibrated model

Note that at the point ($\Theta_s = 370.83\,\mathrm{K}$, $\tau_s = 834.78\,\mathrm{MPa}$), M_s^τ and A_s^τ curves intersect. While parallelism of these curves is not required by the model (cf. Raniecki et al. 1992), experimental data on TiNi and Fe-based alloys indicate that an intersection is not to be expected within the temperature range under consideration (cf. Tanaka et al. 1995b). Hence, the intersection depicted in Figure 7.6 is regarded as a non-physical effect attributable to the manner in which the parameters of the model were calibrated. Calculations in the vicinity of or above Θ_s are therefore not admissible. Concerning the process of parameter identification, appropriate constraints should be introduced to ensure that only valid parameter sets are generated.

7.5 Finite element analysis

7.5.1 Visualization of model properties

Based on the parameters summarized in Table 7.1, the characteristic properties of the model can be illustrated graphically by considering tests in simple tension and simple shear. In the diagrams below, thermal boundary conditions were either adiabatic or isothermal. Hence, the actual material behavior subject to realistic boundary conditions is expected to correspond to some intermediate curve.
First, isothermal and adiabatic curves in simple tension and simple shear are depicted for a single cycle, see Figure 7.7. By definition, in a diagram show-

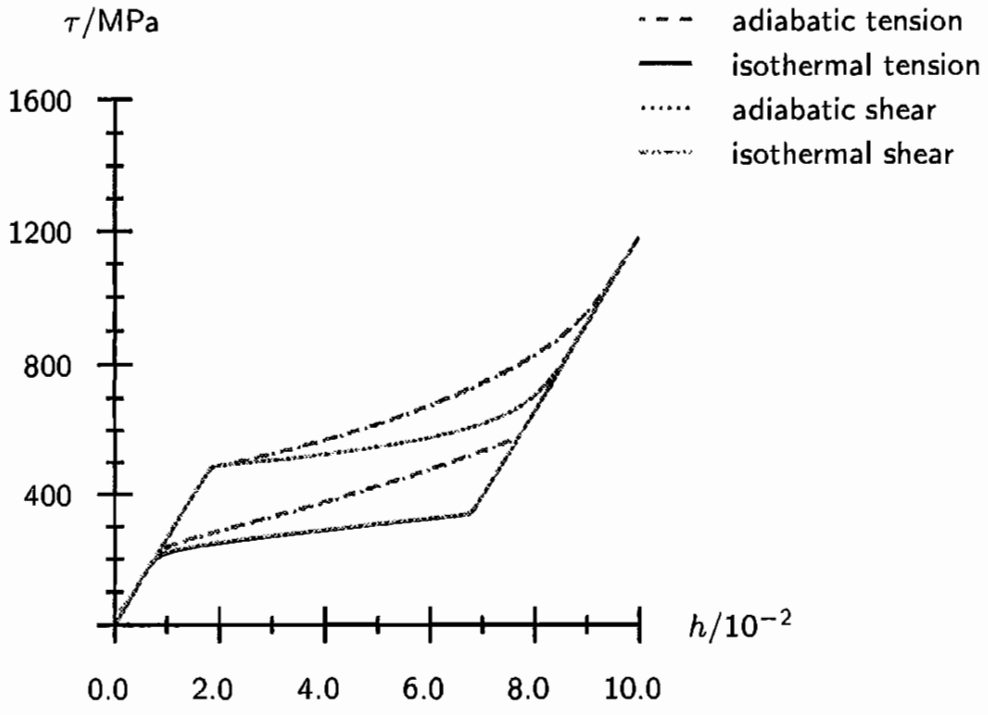

Figure 7.7: Equivalent stress response: simple shear and simple tension

ing the evolution of equivalent Kirchhoff stress in terms of equivalent Hencky strain, the hystereses of tension and shear loading coincide. Noticeable, but less pronounced than in some of the diagrams below, is the difference between isothermal and adiabatic boundary conditions. The experimentally observed fact that transformation stress increases with temperature is reproduced quite well.

The dependence of phase transformation on temperature is indicated in Figure 7.8. Here, adiabatic tests in tension at $\Theta = 315\,\mathrm{K}$ and at $\Theta = 335\,\mathrm{K}$ are depicted. Evidently, with increasing temperature the hysteresis shifts to higher stresses. However, its size is unaffected by temperature.

In Figure 7.9, the stress response during ten loading cycles under simple tension is depicted for an adiabatic and an isothermal specimen. The influence of the thermomechanical coupling almost doubles the martensite finish stress after ten cycles. The corresponding temperatures are depicted in Figure 7.10. As the adiabatic specimen heats due to energy dissipated irreversibly, the stress (or strain) required to induce phase transformation increases and the upper branch of the hysteresis shifts upwards. At the same time, the $M \rightarrow A$ transformation stress increases in parallel as the reverse transformation to austenite is initiated at higher stress levels, since stable martensite exists at increasing levels of stress only. Apparently, the adiabatic process is not characterized by a constant *plateau* stress. Note that the reversible piezocaloric effect as depicted in Figure 7.10 is negligible in comparison to the heat generated due to dissipation of mechanical work, which is responsible for the increase in temperature from one cycle to the next in the adiabatic test, and especially in comparison to the reversible heat due to phase transformation, causing approximately 90 % of the temperature effect.

The evolution of martensite is depicted in Figure 7.11. As the specimen heats in the adiabatic test, the hystereses shift to higher strains in a manner consistent with the stress response in Figure 7.9. As before, the hysteresis in the ξ-h_{yy}-plane remains constant during cycling for isothermal boundary conditions.

The relationship between mass fraction of martensite ξ and thermodynamic driving force π^f defined by the functions k^α is unaffected by thermal effects, see Figure 7.12. It can be observed here that in the last two adiabatic cycles, the specimen is unloaded before the $A \rightarrow M$ transformation is concluded.

The characterization of the model would not be complete without a description of the behavior of processes within the bounding loop. In Figures 7.13 to 7.16, stress response and evolution of martensite are depicted for adiabatic and isothermal processes. In the first two figures, the loading process is interrupted repeatedly. Upon reaching the line of unstable equilibria ($\pi^f = 0$), processes of elastic unloading turn active until reversal of the loading direction. Subsequently, when the line of equilibria is reached, active $A \rightarrow M$ processes are initiated. Note that the transformation stress is lower now than before.

This is not in agreement with experimental observations. In fact, in actual specimens the stress remains at this lower level only initially. Once the point of maximum strain in the history of the specimens is reached, the stress quickly climbs to a level close to that of the original $A \rightarrow M$ process, where it remains during further loading (cf. Lin et al. 1994).
In Figures 7.15 and 7.16, inner cycles are obtained by reversing the loading direction repeatedly during unloading the specimen from its martensitic state. Again, the diagonal corresponding to states of unstable equilibria is clearly identifiable as the criterion for the initiation of active processes. Strictly speaking, this observation is true for the isothermal test only, since during adiabatic processes, the line of unstable equilibria is not a straight line due to the increasing slope of the hysteresis.
Finally, the stress-strain-diagrams pertaining to simple shear are plotted as well, see Figures 7.17 and 7.18. Based on the definition of equivalent strain adopted here, the shear stress required to induce martensite is significantly lower than the corresponding tensile stress.

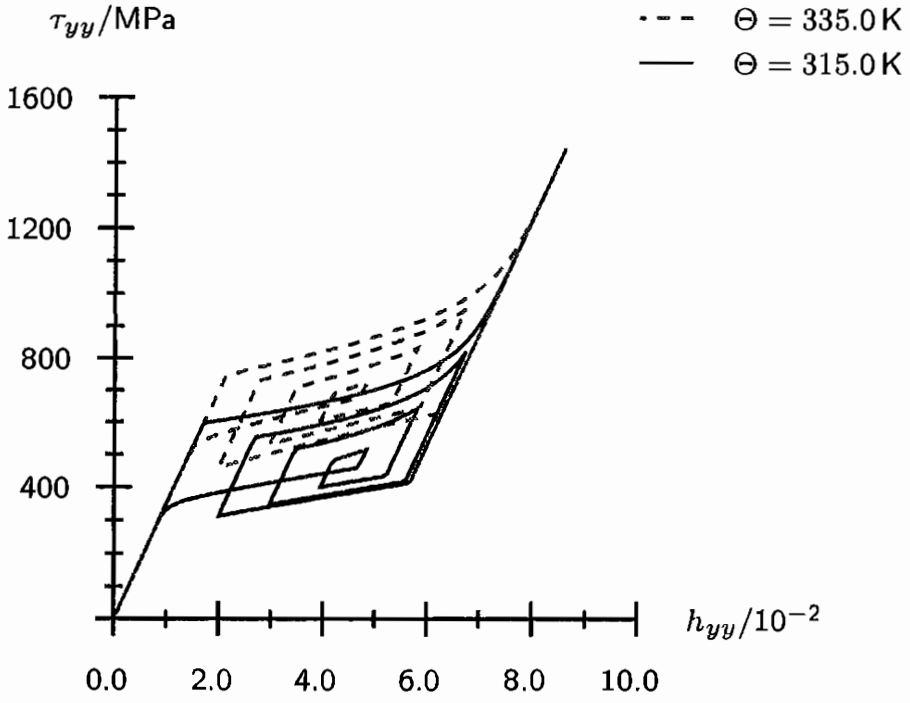

Figure 7.8: Temperature dependence of hysteresis

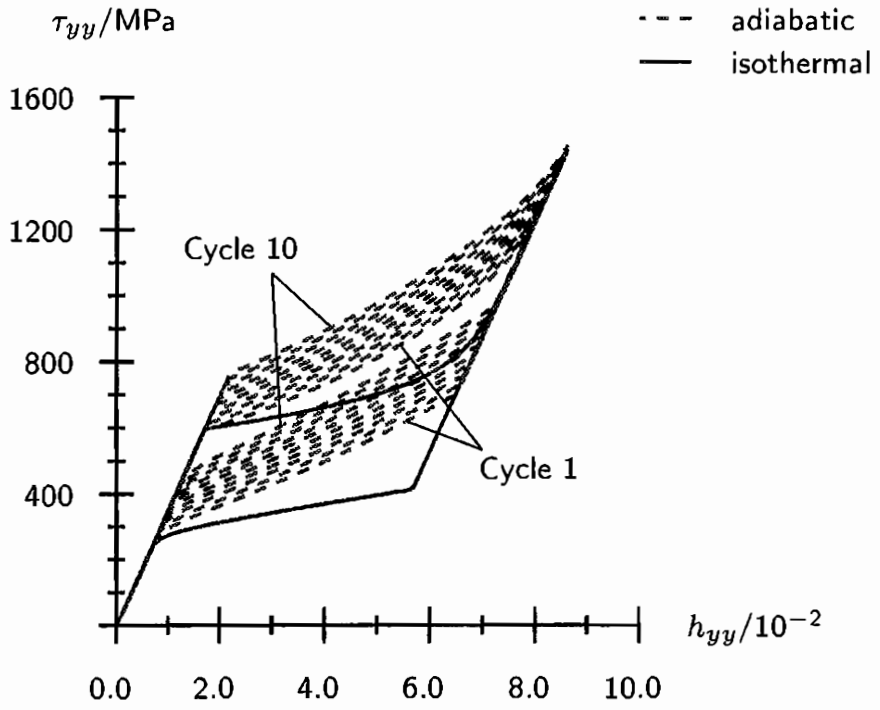

Figure 7.9: Stress response: 10 cycles in simple tension

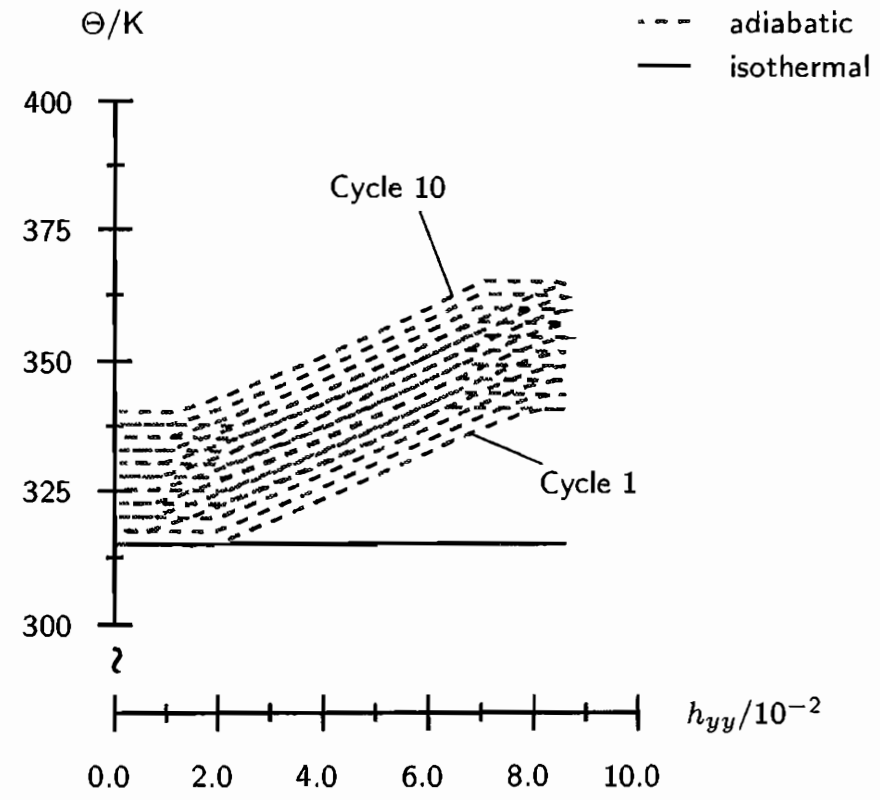

Figure 7.10: Temperature evolution: 10 cycles in simple tension

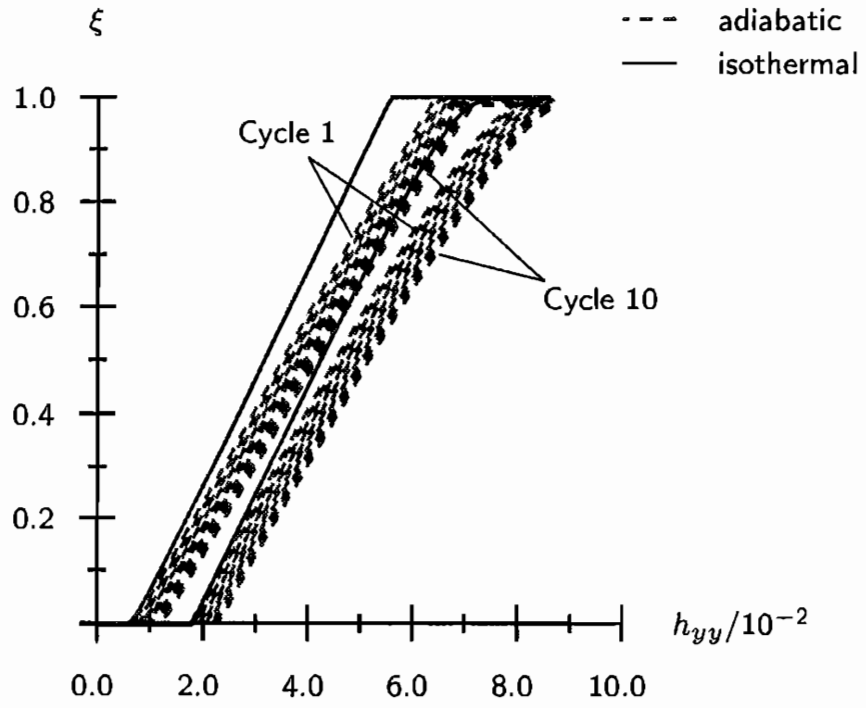

Figure 7.11: Evolution of martensite: 10 cycles in simple tension

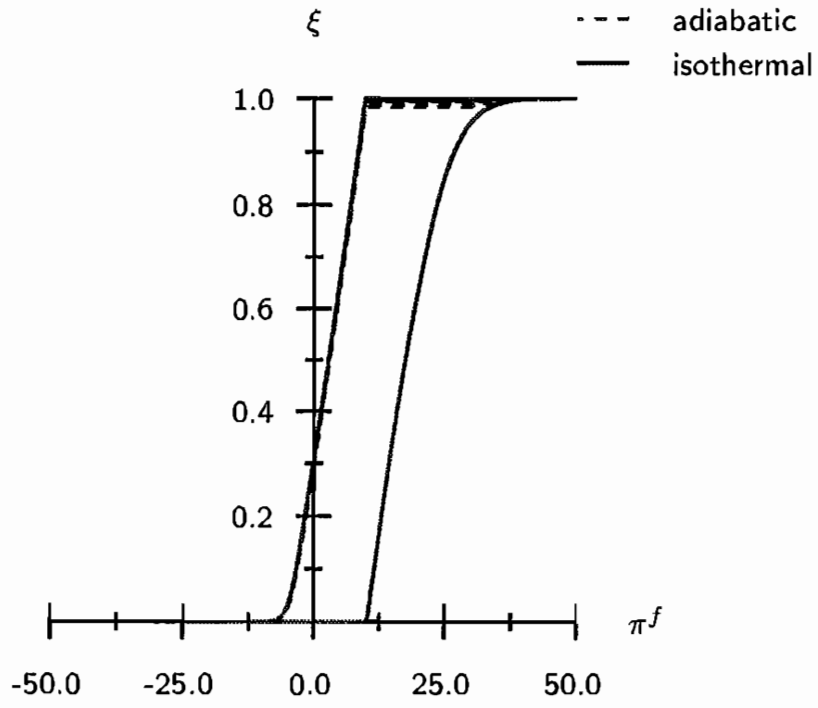

Figure 7.12: Martensite and thermodynamic driving force: 10 cycles in simple tension

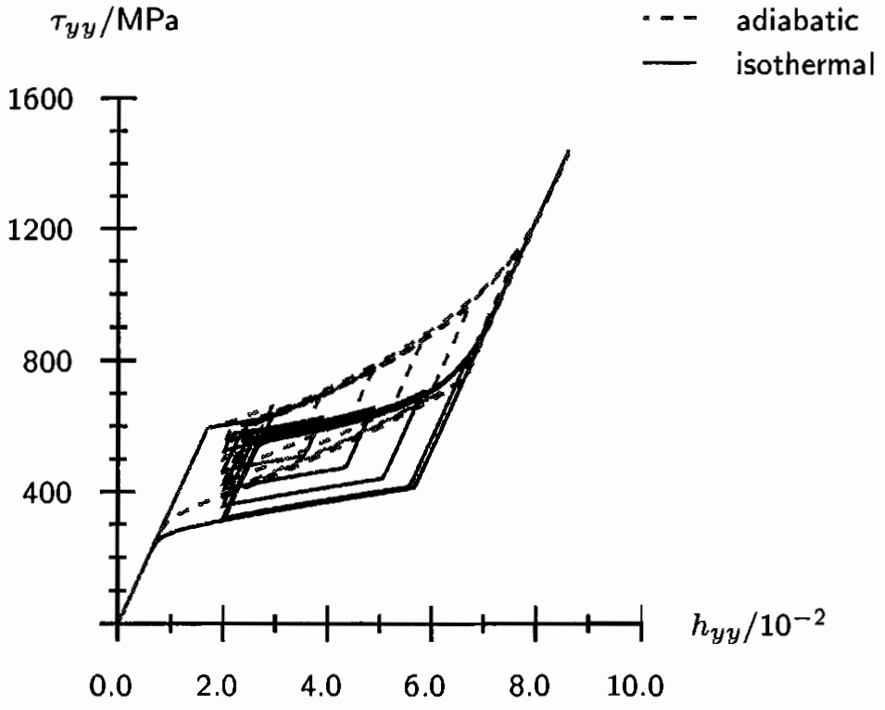

Figure 7.13: Stress response: inner cycles during loading in simple tension

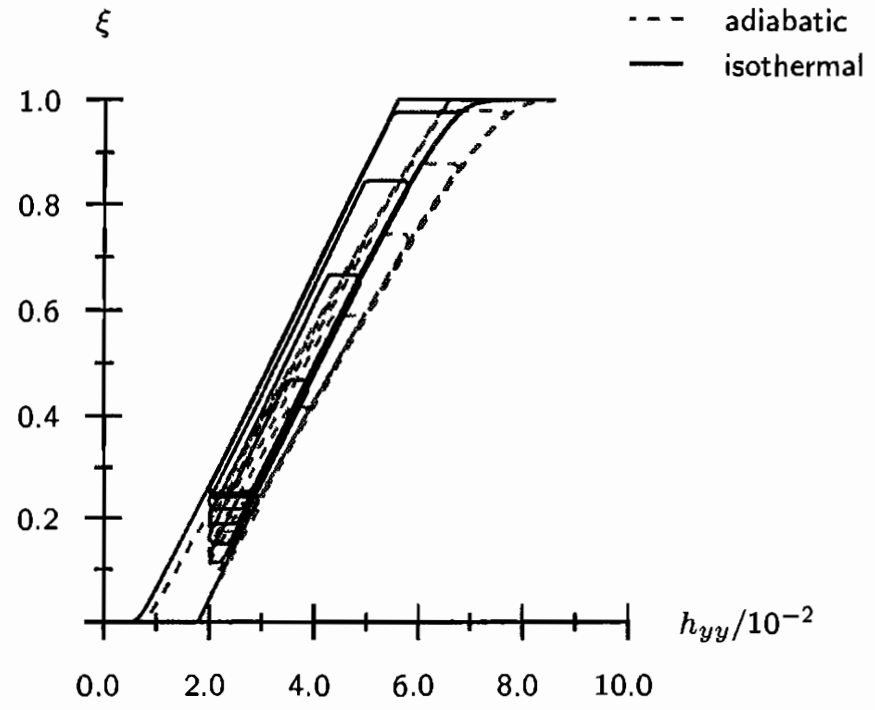

Figure 7.14: Evolution of martensite: inner cycles during loading in simple tension

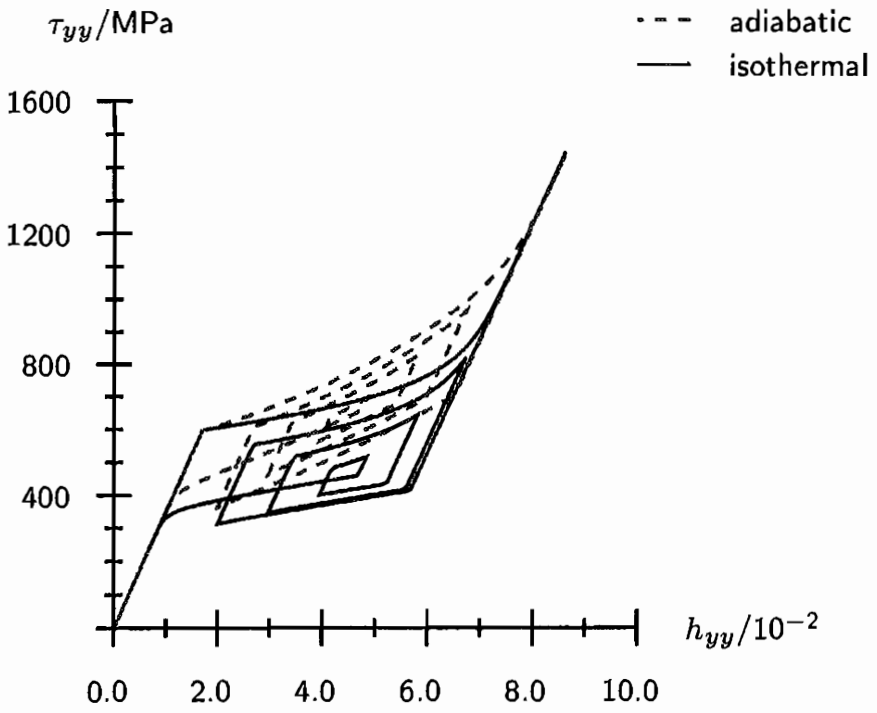

Figure 7.15: Stress response: inner cycles during unloading in simple tension

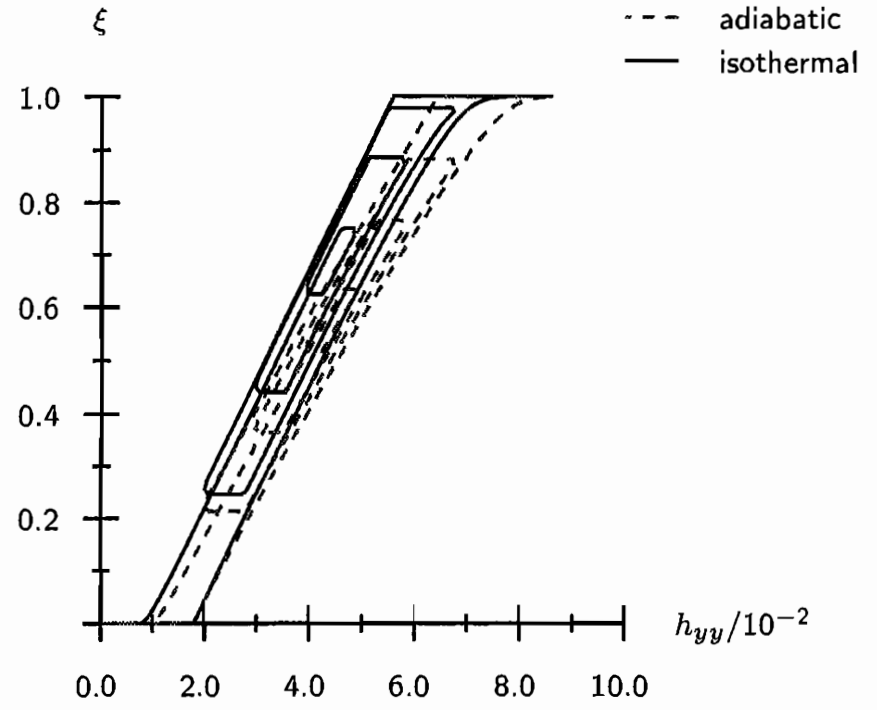

Figure 7.16: Evolution of martensite: inner cycles during unloading in simple tension

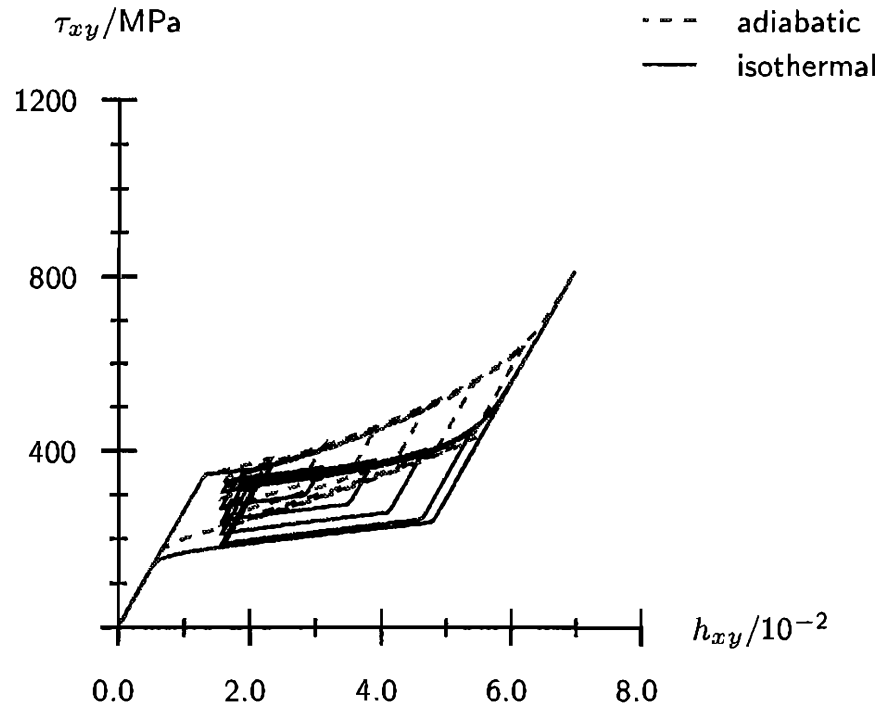

Figure 7.17: Stress response: inner cycles during loading in simple shear

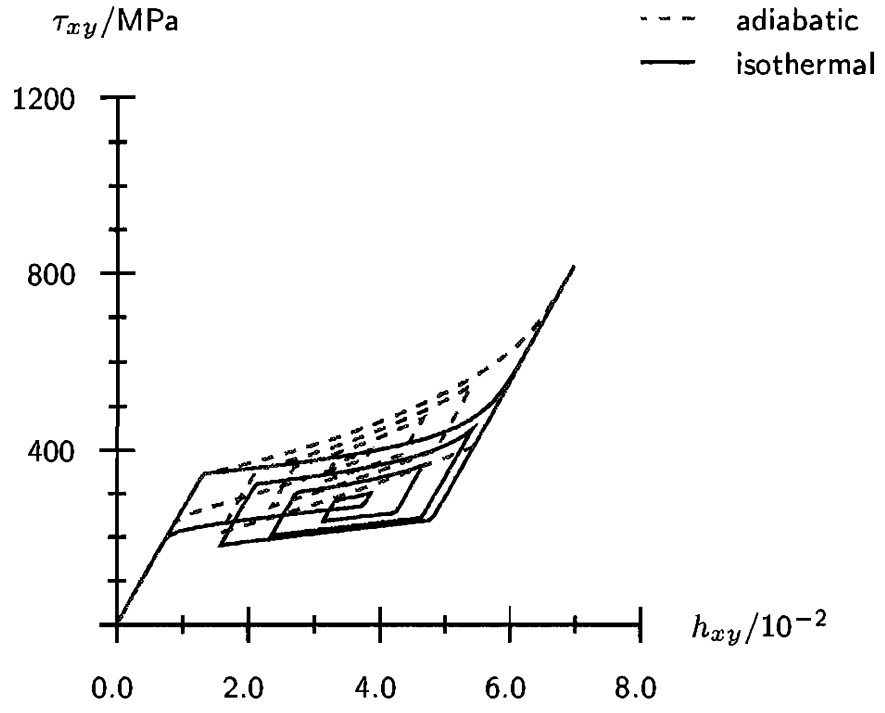

Figure 7.18: Stress response: inner cycles during unloading in simple shear

7.5.2 Structural behavior

To validate the implementation of the material law into the finite element code MSC.Marc, two fairly complex structures are considered. Both are design concepts developed by El Hawary (2003) intended to be used as damping devices or for load limitation purposes. The design concepts are depicted in Figures 7.19 and 7.21; they are not to be evaluated here, but to be used merely as examples of realistic pseudoelastic structures. The parts are to be inserted within a drive shaft to keep external vibrations or excessive loads from damaging sensitive components.

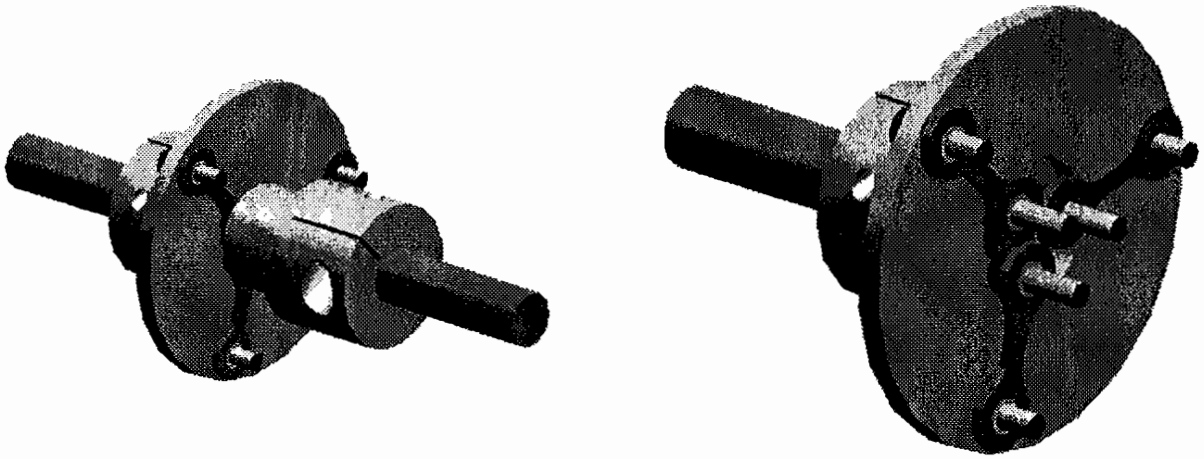

Figure 7.19: Flexible coupling: damping device using tension as active principle

The first design concept considered is specified in Figure 7.20. It is loaded by bolts attached to a drive shaft. The other side of the bolts is inserted into

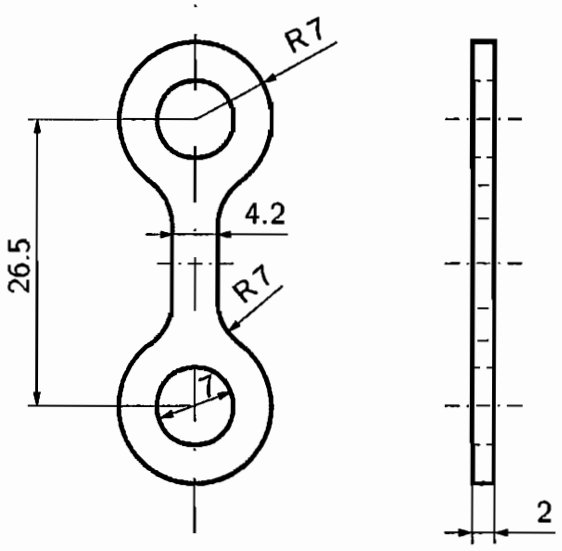

Figure 7.20: Damping device: Tension

the eyelets at the upper and lower ends of the part. If the opposing ends of the drive shaft are subjected to relative rotations, the device will be loaded in tension.
The second design concept is intended for the same purpose, with bending as active principle. This will naturally lead to a less efficient use of the pseudoelastic damping material, as the centers of the "arms" of the star-shaped structure will always remain elastic and only the outer regions transform. The star-shaped structure in Figure 7.21 is to be used in a similar manner. The bolts attached to a drive shaft are inserted into every other eyelet of the pseudoelastic star-shaped part. The load is then transmitted by the part to bolts inserted into the remaining three eyelets, which are attached to a drive shaft opposite to the first one. The dimensioned drawing used to model the structure is shown in Figure 7.22.
Initially, the first structure, i.e. the device with tension as active principle, is considered. Only half of the symmetry is made use of to obtain more illustrative graphical results. The structure is subjected to a continuously growing force until parts of the structure are becoming unrealistically high stressed as the model does not account for plasticity in stress induced martensite. Thermal boundary conditions are chosen to be adiabatic. This is expected to be the realistic case in an application area of load limitation, where the load is expected to be applied quickly, not leaving enough time for heat conduction or convection.
Figures 7.23, 7.24 and 7.25 show the distribution of martensite, equivalent Kirchhoff stress and temperature, respectively, at maximum load. The obvi-

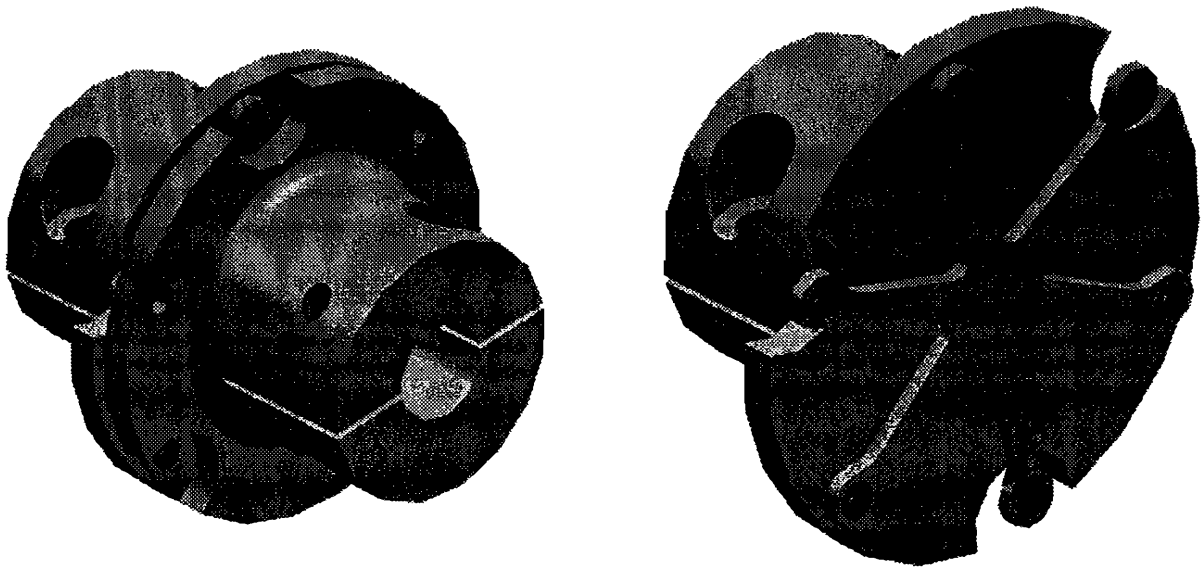

Figure 7.21: Flexible coupling: damping device using bending as active principle

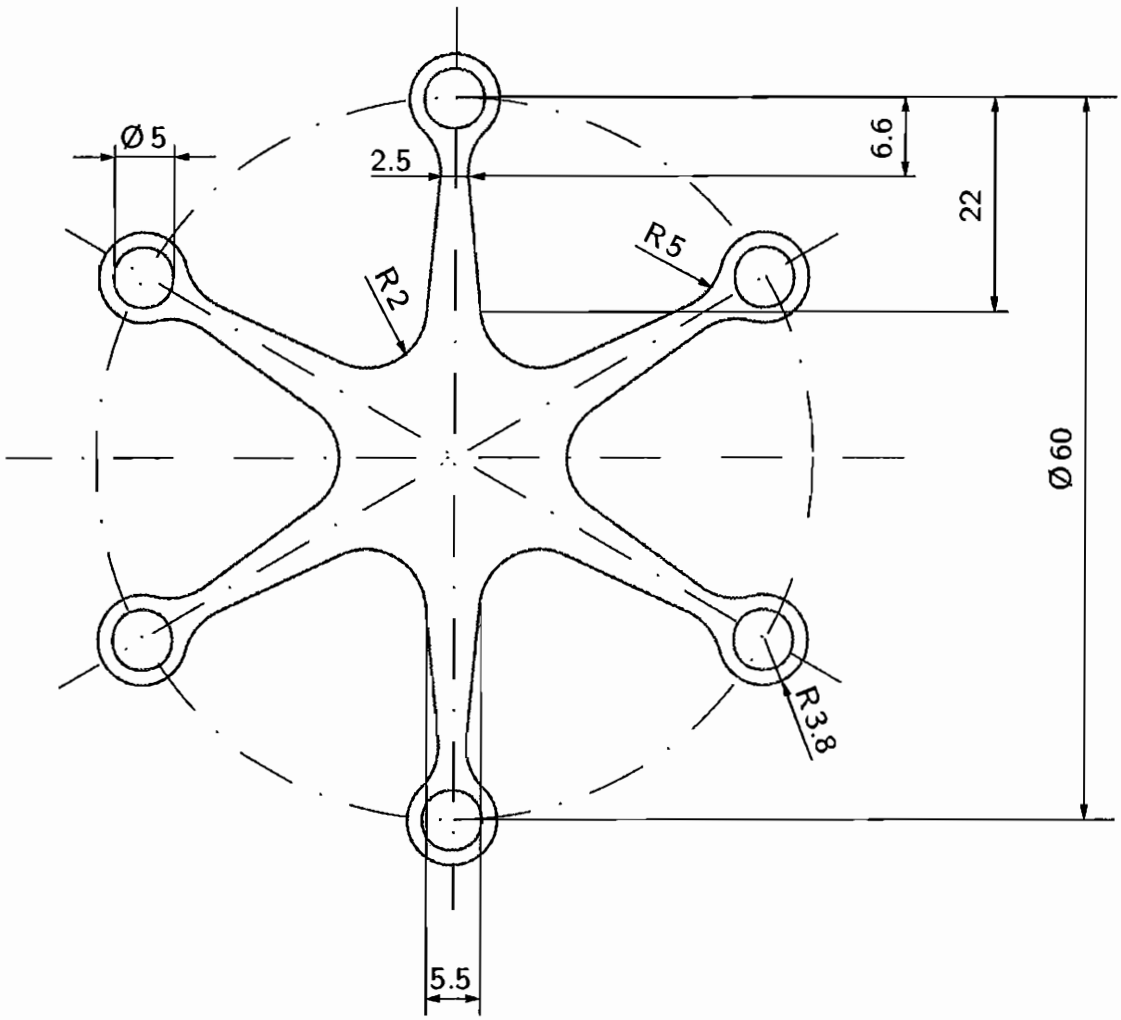

Figure 7.22: Damping device: Bending

ous result that stresses are higher in the eyelet than in the bar-shaped part of the structure is clearly visible. Deformations are depicted at full size, i.e. the scale is 1:1. Note that due to narrowing of the eyelet, in reality interactions between bolt and eyelet would be observed. From Figure 7.24 it is seen that at maximum load, parts of the structure have reached stresses exceeding 1000 MPa. The simulation is stopped here as the model is not expected to yield good results for stresses far higher than the plateau stress.
In Figure 7.26, the distribution of martensite, equivalent Kirchhoff stress and temperature of the second structure are plotted at maximum load. The respective contour bands are of the same range as those in Figures 7.23, 7.24 and 7.25, respectively. For this specimen, only the sixth part of the structure is modeled for symmetry reasons. However, simulation of the part proved to be computationally expensive, as the gradients along the cross section increase with increasing load (see Figure 7.27).

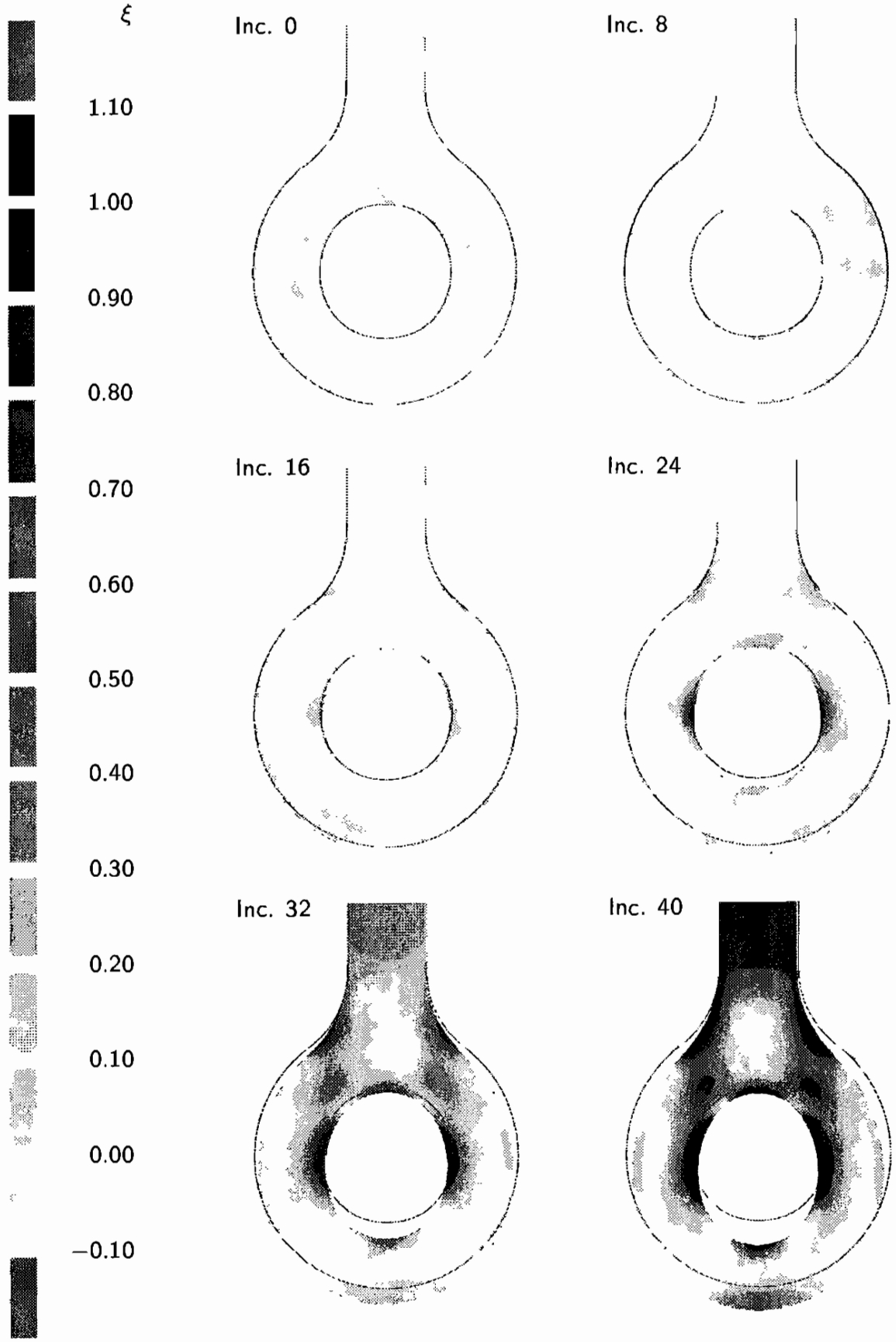

Figure 7.23: Evolution of martensite

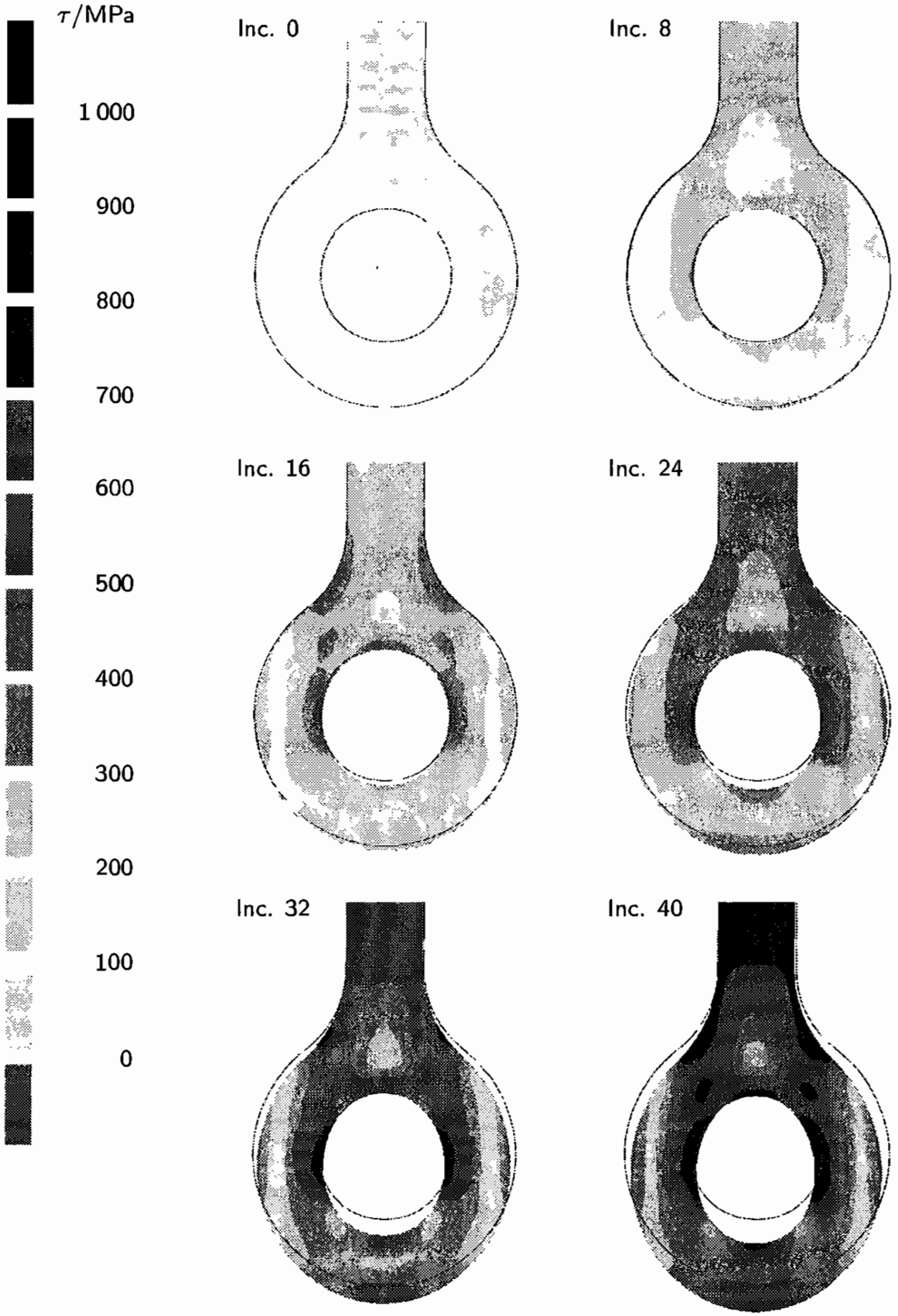

Figure 7.24: Evolution of equivalent Kirchhoff stress

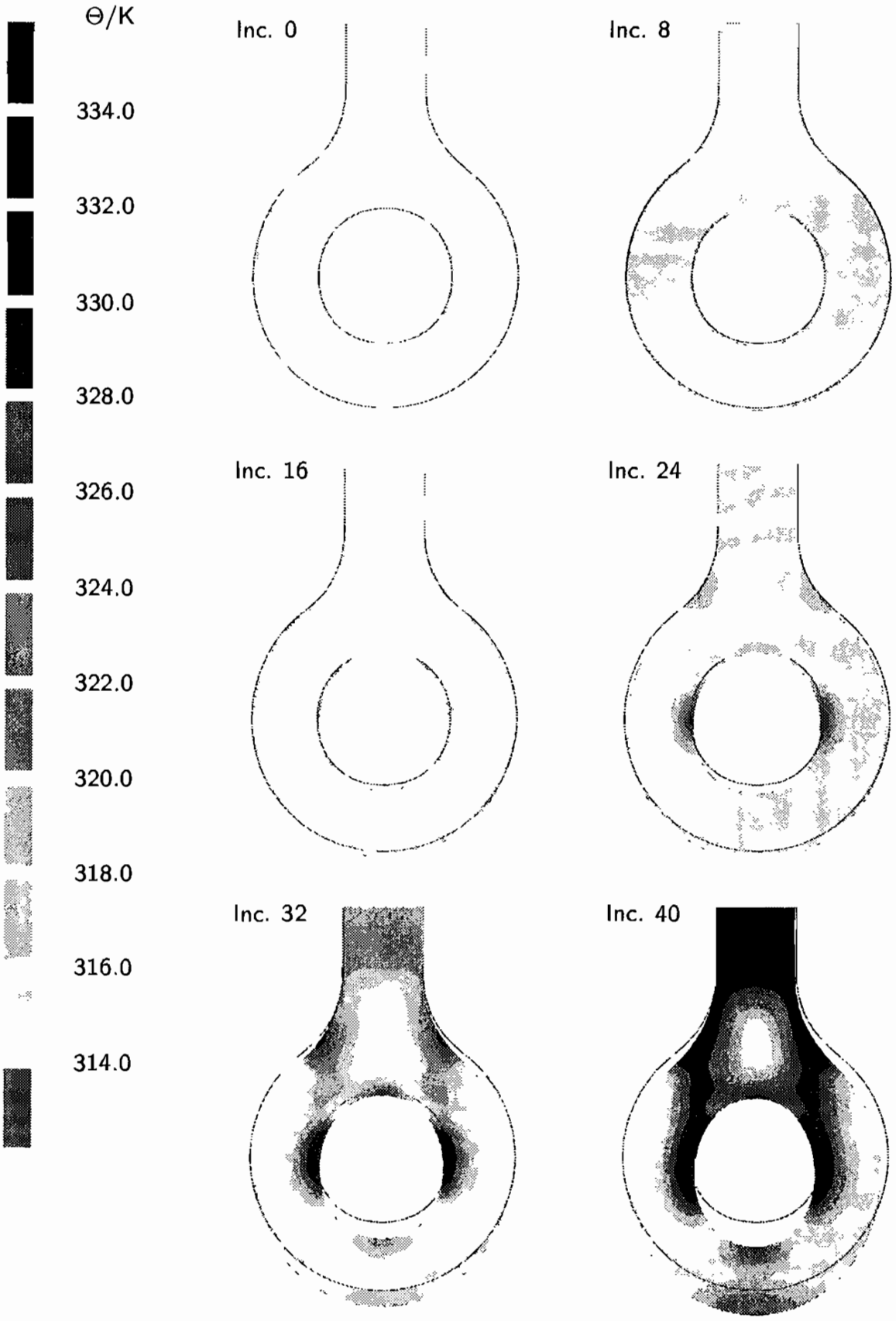

Figure 7.25: Evolution of temperature

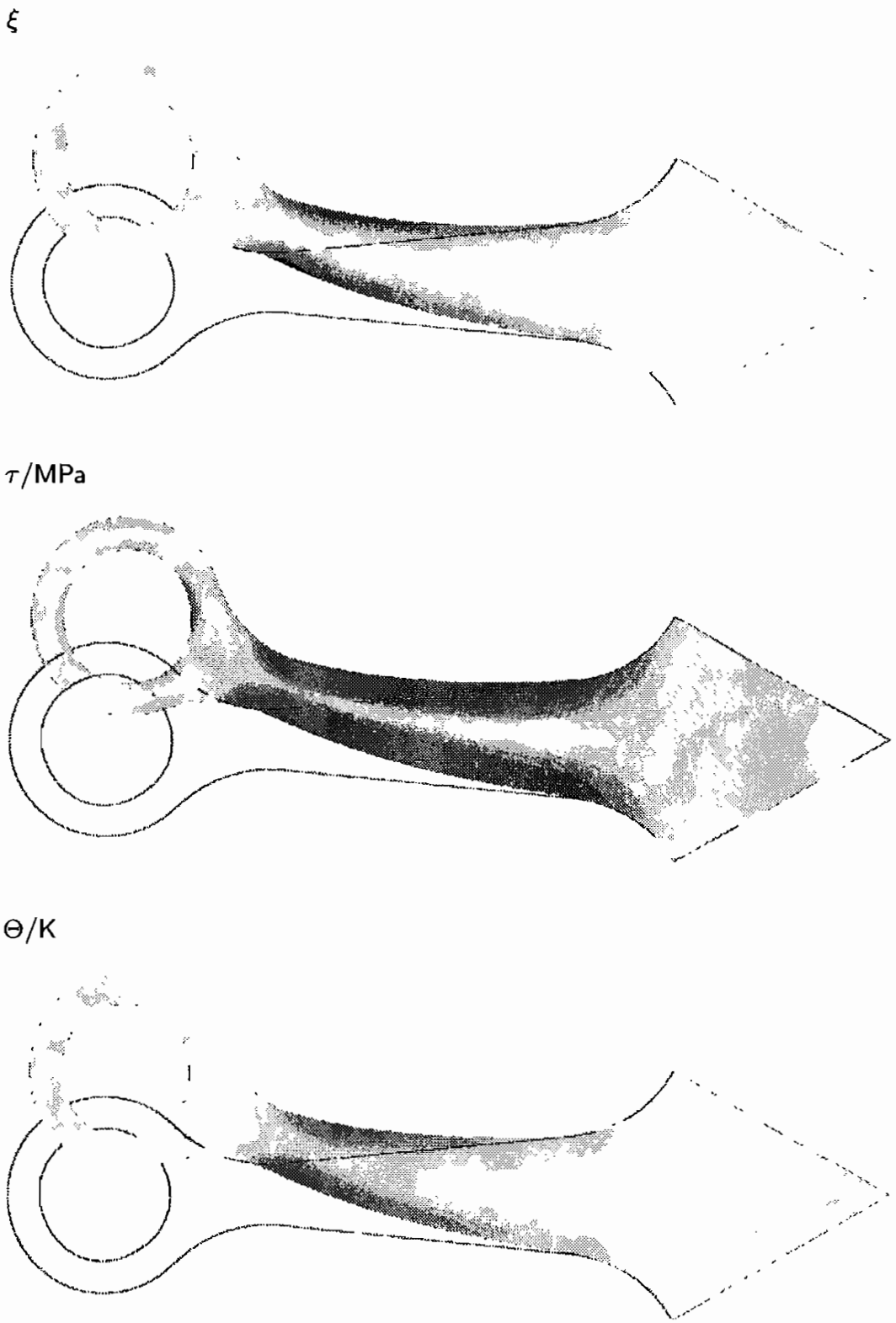

Figure 7.26: Distribution of martensite, equivalent Kirchhoff stress and temperature (Note: Contour bands are of the same range as their respective counterparts in Figures 7.23, 7.24 and 7.25)

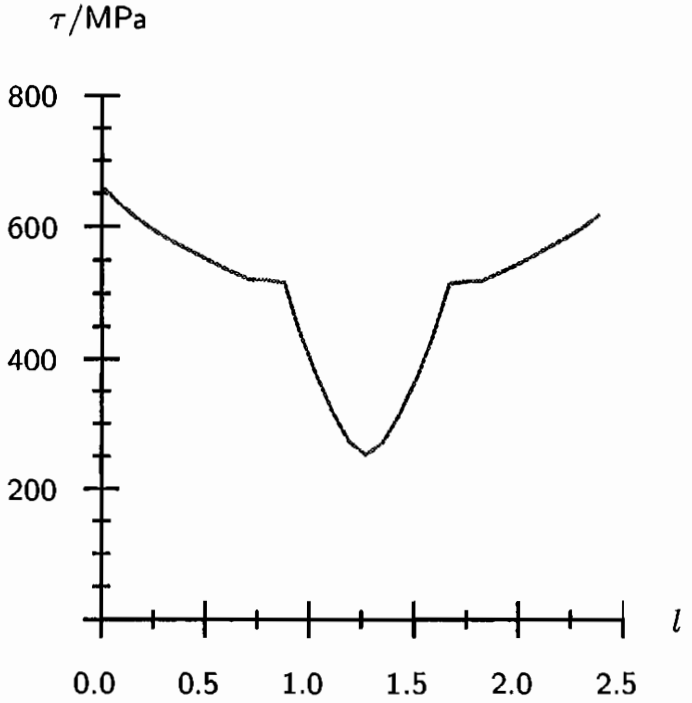

Figure 7.27: Equivalent stress over arc length close to an eyelet of the star-shaped structure

In the preceding computations, a relative/absolute strain energy criterion of $\varepsilon_{tol} = 10^{-10}$ was used as global convergence criterion. The results show that the implemented material law is suitable for the simulation of the behavior of complex structures. The effects of thermomechanical coupling are clearly visible.

8 Conclusion and possible extensions

8.1 Results

In this treatise a thermodynamic model capable of the description of pseudoelasticity is proposed based on a Eulerian finite deformation theory. Adopting a thermodynamic theory with internal variables, the mass fraction of martensite is defined as an internal state variable. The state of the two-phase solid is uniquely determined by temperature, elastic Hencky strain and mass fraction of martensite.

Based on the concept of irreversible forces, an evolution equation for the mass fraction of martensite ξ is derived. Thus, by expressing the elastic-phase transformation part of the stretching in terms of the rate of martensite, a constitutive equation for the Kirchhoff stress is obtained.

The model is calibrated to experimental data obtained on a NiTi specimen. While computational results obtained with this parameter set are in very good agreement to the experimental data, it should be noted that an important quantity, i.e. the value of ξ at maximum strain, was not known in the process of parameter identification.

For isotropy, the model is implemented into a finite element code in an updated Lagrangian formulation. The constitutive equation is integrated by corotational integration to preserve objectivity.

Using the parameter set referred to above, the stress-strain behavior predicted by the model is analyzed. The stress response exhibits a strong dependence on temperature, reflected both by isothermal tests at different temperatures and by the comparison of isothermal and adiabatic simulations. This is in agreement with experimental observations.

The implementation is successfully applied to the simulation of complex structures, predicting the heating of the structures due to thermomechanical coupling. With regard to the damping devices simulated, the distribution of martensite within the structure may be used to judge the suitability of the devices for their intended purpose.

However, while the simulations endorse the applicability of the material model to pseudoelastic structures in general, there are some drawbacks to the theory as well that could be addressed in future extensions of the model. Some suggestions in this regard are given next. For example, the model does not account for the tension-compression asymmetry that is well-established in literature. To adequately model one-way shape memory effect, the reorientation of martensite has to be considered. Also, for a continuum model it is hard to account for effects such as the macroscopic transformation band observed on NiTi specimens under certain conditions. During mechanical cycling with increasing strain amplitude, Lin et al. (1994) observe a sudden increase in transformation stress at the point where the processes had been reversed before. While the transformation stress of inner cycles is lower than that of

the bounding loop initially, the old value of stress is attained at the point of maximum strain in the loading history.

8.2 Possible extensions

The presented model may be extended in a number of ways to account for

- phase-specific thermoelastic constants
- tension-compression asymmetry
- one-way (shape memory) effect
- plasticity and two-way effect
- fatigue.

As the model has been formulated in a very general way, adopting the assumption of isotropy at the latest possible moment, modifications should be readily incorporated. For example, the model may be extended to include phase-specific Young's moduli in a straight-forward manner by following the procedure presented, omitting some of the simplifications adopted here.
To take into account the tension-compression asymmetry, an extension of their original R_L-model is proposed by Raniecki & Lexcellent (1998). Their modifications lead to an amended free energy function. Bouvet et al. (2002) propose a J_2-J_3 theory based on experimental data obtained on a CuAlBe specimen. Qidwai & Lagoudas (2000) adopt the same type of criterion in their theory to take into account volumetric changes as well, which are disregarded here. Auricchio & Taylor (1999) propose an efficient integration algorithm for isotropic J_2-J_3 plasticity which could be adopted as well.
Concerning the one-way effect, different concepts are introduced in the literature (cf. Section 2.2.4): Either, the mass (or volume) fraction of martensite is decomposed into a twinned, thermally induced and an untwinned, stress induced part, or in addition to a scalar fraction of martensite, a tensorial quantity describing the orientation of martensite is introduced. The concept presented here may be extended either way.
To model the two-way shape memory effect, a plasticity-type extension to the presented theory may be considered. It seems to be reasonable to suppose that the number of dislocations grows with the number of pseudoelastic cycles as proposed by Bo & Lagoudas (1999a). A history variable that evolves with the absolute value of the increments of the mass fraction of martensite could be used to capture this behavior. The experimentally observed increase in permanent set with growing number of cycles supports this notion. However, the theory developed by Bo & Lagoudas (1999a) in this context does not fulfill the requirement of implementability into numerical procedures such as finite element methods.

Finally, functional and mechanical fatigue are unsolved problems in the characterization and modeling of shape memory alloys. When specimens are loaded to almost completely martensitic state, mechanical fatigue gives rise to short lifetimes. Functional fatigue results in a continuous decrease in the size of the hysteresis. In fact, the maximal pseudoelastic hysteresis is generally observed in the first loading cycle only. Both characteristics may be described phenomenologically by combining the presented model with a damage theory such as the anisotropic damage model developed by Bongmba (2001) based on the kinematical framework underlying the presented theory.

A Relations regarding logarithmic spin and logarithmic rate

The following relations are based on Xiao et al. (1997b) and Xiao et al. (1998b). They are helpful in implementing material laws based on their theory into finite element codes.

A.1 Eigenprojections

Spectral decomposition gives

$$\mathbf{B} = \sum_{\sigma=1}^{n} \chi_\sigma \mathbf{B}_\sigma \tag{A.1}$$

where χ_σ – eigenvalues of $\mathbf{B}$
$\mathbf{B}_\sigma$ – corresponding orthonormal eigenprojections
m – number of distinct eigenvalues of $\mathbf{B}$.

To calculate the eigenprojections, Sylvester's formula may be used

$$\mathbf{B}_\alpha = \delta_{n1}\mathbf{1} + \prod_{\beta\neq\alpha}^{n} \frac{\mathbf{B} - \chi_\beta \mathbf{1}}{\chi_\alpha - \chi_\beta}\,. \tag{A.2}$$

The following relations hold

$$\sum_{\alpha=1}^{n} \mathbf{B}_\alpha = \mathbf{1}\,, \tag{A.3}$$

$$\mathbf{B}_\alpha \mathbf{B}_\beta = \delta_{\alpha\beta}\mathbf{B}_\beta\,, \tag{A.4}$$

$$\mathbf{B}_\alpha \mathbf{B} = \chi_\alpha \mathbf{B}_\alpha\,. \tag{A.5}$$

A Eulerian strain measure may be written in terms of a scale function

$$\mathbf{e} = \sum_{\sigma=1}^{n} g(\chi_\sigma)\mathbf{B}_\sigma \tag{A.6}$$

with

$$\mathbf{e}^i \mathbf{B}_\alpha = \mathbf{B}_\alpha \mathbf{e}^i = g(\chi_\sigma)^i \mathbf{B}_\alpha \qquad \mathrm{i} \in \mathbb{N}\,. \tag{A.7}$$

A.2 Calculation of logarithmic spin

In this section, relations for $\boldsymbol{\Omega}^{\mathrm{Log}}$, $\mathbf{N}^{\mathrm{Log}}$ and $\mathbb{B}$ are derived.

$$\boldsymbol{\Omega}^{\mathrm{Log}} = \mathbf{W} + \sum_{\alpha\neq\beta}^{n} \left(\frac{\chi_\alpha + \chi_\beta}{\chi_\beta - \chi_\alpha} + \frac{1}{g(\chi_\alpha) - g(\chi_\beta)} \right) \mathbf{B}_\alpha \mathbf{D} \mathbf{B}_\beta \tag{A.8}$$

$$\text{with} \quad g = \frac{1}{2}\ln\chi \tag{A.9}$$

$$\boldsymbol{\Omega}^{\mathrm{Log}} = \mathbf{W} + \sum_{\alpha\neq\beta}^{n} \left(\frac{1 + (\chi_\alpha/\chi_\beta)}{1 - (\chi_\alpha/\chi_\beta)} + \frac{2}{\ln(\chi_\alpha/\chi_\beta)} \right) \mathbf{B}_\alpha \mathbf{D} \mathbf{B}_\beta \tag{A.10}$$

Calculation of eigenprojections depending on the number of distinct eigenvalues:

- $n = 1$

$$\mathbf{B}_1 = \mathbf{1} \tag{A.11}$$

- $n = 2$

$$\begin{aligned} \mathbf{B}_1 &= \frac{1}{\chi_1 - \chi_2}(\mathbf{B} - \chi_2\mathbf{1}) \\ \mathbf{B}_2 &= \frac{1}{\chi_2 - \chi_1}(\mathbf{B} - \chi_1\mathbf{1}) \end{aligned} \tag{A.12}$$

- $n = 3$

$$\begin{aligned} \mathbf{B}_1 &= \frac{\chi_3 - \chi_2}{\Delta}\left[\mathbf{B}^2 - (\chi_2 + \chi_3)\mathbf{B} + \chi_2\chi_3\mathbf{1}\right] \\ \mathbf{B}_2 &= \frac{\chi_1 - \chi_3}{\Delta}\left[\mathbf{B}^2 - (\chi_1 + \chi_3)\mathbf{B} + \chi_1\chi_3\mathbf{1}\right] \\ \mathbf{B}_3 &= \frac{\chi_2 - \chi_1}{\Delta}\left[\mathbf{B}^2 - (\chi_1 + \chi_2)\mathbf{B} + \chi_1\chi_2\mathbf{1}\right] \end{aligned} \tag{A.13}$$

where

$$\Delta = (\chi_1 - \chi_2)(\chi_2 - \chi_3)(\chi_3 - \chi_1)\,. \tag{A.14}$$

The definition of $\boldsymbol{\Omega}^{\mathrm{Log}}$ in terms of $\mathbf{W}$ and $\mathbf{N}^{\mathrm{Log}}$ is

$$\boldsymbol{\Omega}^{\mathrm{Log}} = \mathbf{W} + \mathbf{N}^{\mathrm{Log}}, \tag{A.15}$$

where

$$\mathbf{N}^{\mathrm{Log}} = \begin{cases} \mathbf{0} & \chi_1 = \chi_2 = \chi_3 \\ \nu[\mathbf{BD}] & \chi_1 \neq \chi_2 = \chi_3 \\ \nu_1[\mathbf{BD}] + \nu_2[\mathbf{B}^2\mathbf{D}] + \nu_3[\mathbf{B}^2\mathbf{DB}] & \chi_1 \neq \chi_2 \neq \chi_3 \neq \chi_1 \end{cases} \tag{A.16}$$

with[27]

$$\nu = \frac{1}{\chi_1 - \chi_2}\left(\frac{1 + (\chi_1/\chi_2)}{1 - (\chi_1/\chi_2)} + \frac{2}{\ln(\chi_1/\chi_2)}\right), \tag{A.17}$$

$$\nu_k = -\frac{1}{\Delta}\sum_{i=1}^{3}(-\chi_i)^{3-k}\left(\frac{1+\epsilon_i}{1-\epsilon_i} + \frac{2}{\ln\epsilon_i}\right), \qquad k = 1,2,3 \tag{A.18}$$

$$\epsilon_1 = \chi_2/\chi_3 \qquad \epsilon_2 = \chi_3/\chi_1 \qquad \epsilon_3 = \chi_1/\chi_2$$

$$\left[\mathbf{B}^r\mathbf{DB}^s\right] = \mathbf{B}^r\mathbf{DB}^s - \mathbf{B}^s\mathbf{DB}^r \qquad \text{mit} \quad r,s = 0,1,2\,. \tag{A.19}$$

The eigenvalues of $\mathbf{B}$ follow from its principal invariants (3.53) to (3.55).

$$\chi_i = \frac{1}{3}\left(I + 2\sqrt{I^2 - 3II}\cos\left(\frac{1}{3}(\varphi - 2\pi i)\right)\right)$$

$$\varphi = \cos^{-1}\left(\frac{2I^3 - 9I\cdot II + 27III}{2(I^2 - 3II)^{\frac{3}{2}}}\right) \tag{A.20}$$

$$i = 1,2,3\,.$$

Hence, for $n = 2$

$$\begin{aligned} N_{ij}^{\mathrm{Log}} &= \nu(B_{iq}D_{qj} - D_{iq}B_{qj}) \\ &= \nu(B_{iq}\delta_{qk}\delta_{jl} - \delta_{ik}\delta_{ql}B_{qj})D_{kl} \\ &= \mathbb{B}_{ijkl}D_{kl} \end{aligned} \tag{A.21}$$

$$\mathbb{B}_{ijkl} = \nu(B_{ik}\delta_{jl} - \delta_{ik}B_{jl}) \tag{A.22}$$

and for $n = 3$

$$N_{ij}^{\mathrm{Log}} = \mathbb{B}_{ijkl}D_{kl} \tag{A.23}$$

$$\mathbb{B}_{ijkl} = \nu_3(B_{ik}^2B_{jl} - B_{ik}B_{jl}^2) + \nu_2(B_{ik}^2\delta_{jl} - \delta_{ik}B_{jl}^2) + \nu_1(B_{ik}\delta_{jl} - \delta_{ik}B_{jl})\,. \tag{A.24}$$

[27] Regarding (A.18$_1$), cf. Bruhns et al. (1999).

A.3 Tensors $\mathbb{G}$ and $\mathbb{X}$

Tensors $\mathbf{G}$ and $\mathbf{X}$ are defined by

$$\mathbb{G}_{ijkl} = \mathbb{X}_{ijkl} - \delta_{ik}\tau_{jl} - \delta_{jl}\tau_{ik} \tag{A.25}$$

respectively

$$\mathbb{X}_{ijkl} = \mathbb{B}_{irkl}\tau_{rj} - \mathbb{B}_{rjkl}\tau_{ri}\,. \tag{A.26}$$

A.4 Basis-free expressions for t and $\boldsymbol{\tau}$

The stress tensors $\mathbf{t}$ and $\boldsymbol{\tau}$ are expressible in basis-free form as

$$\mathbf{t} = \sum_{i,j=0}^{r-1} \varrho_{ij}\mathbf{B}^i\boldsymbol{\tau}\mathbf{B}^j \tag{A.27}$$

respectively

$$\boldsymbol{\tau} = \sum_{i,j=0}^{r-1} \eta_{ij}\mathbf{B}^i\mathbf{t}\mathbf{B}^j\,. \tag{A.28}$$

η_{ij} is obtained from the formulas for ϱ_{ij} by replacing ρ_{ij}^{-1} by ρ_{ij}. In the following, $\sum_{(ijk)}$ is the sum for $(ijk) = (123)$, (231), and (312), $\bar{\chi}_{jk} = \chi_j - \chi_k$, $\chi_{jk} = \chi_j + \chi_k$, $\chi_j^k = \chi_j\chi_k$, $\rho_{ij} = \rho(\chi_i, \chi_j)$, and $\rho_{ii} = \lim_{\chi_i \to \chi_j} \rho(\chi_i, \chi_j)$. Δ is defined in (A.14).

1. r = 1: $\chi_1 = \chi_2 = \chi_3$

$$\varrho_{00} = {\rho_{11}}^{-1} \tag{A.29}$$

2. r = 2: $\chi_1 \neq \chi_2 = \chi_3$

$$\begin{aligned}
\varrho_{00} &= (\chi_1 - \chi_2)^{-2}\left[\chi_2^2{\rho_{11}}^{-1} + \chi_1^2{\rho_{22}}^{-1} - 2\chi_1\chi_2{\rho_{12}}^{-1}\right] \\
-\varrho_{01} &= (\chi_1 - \chi_2)^{-2}\left[\chi_2{\rho_{11}}^{-1} + \chi_1{\rho_{22}}^{-1} - (\chi_1 + \chi_2){\rho_{12}}^{-1}\right] \\
\varrho_{11} &= (\chi_1 - \chi_2)^{-2}\left[{\rho_{11}}^{-1} + {\rho_{22}}^{-1} - 2{\rho_{12}}^{-1}\right]
\end{aligned} \tag{A.30}$$

3. r = 3: $\chi_1 \neq \chi_2 \neq \chi_3$

$$\varrho_{00} = \frac{1}{\Delta^2} \sum_{(ijk)} (\rho_{ii}{}^{-1} \bar{\chi}_{jk}^2 \chi_j^2 \chi_k^2 + 2\rho_{ij}{}^{-1} \bar{\chi}_{jk} \bar{\chi}_{ki} \chi_j^k \chi_k^i)$$

$$\varrho_{11} = \frac{1}{\Delta^2} \sum_{(ijk)} (\rho_{ii}{}^{-1} \bar{\chi}_{jk}^2 \chi_{jk}^2 + 2\rho_{ij}{}^{-1} \bar{\chi}_{jk} \bar{\chi}_{ki} \chi_{jk} \chi_{ki})$$

$$\varrho_{22} = \frac{1}{\Delta^2} \sum_{(ijk)} (\rho_{ii}{}^{-1} \bar{\chi}_{jk}^2 + 2\rho_{ij}{}^{-1} \bar{\chi}_{jk} \bar{\chi}_{ki})$$

$$\varrho_{01} = -\frac{1}{\Delta^2} \sum_{(ijk)} (\rho_{ii}{}^{-1} \bar{\chi}_{jk}^2 \chi_{jk} \chi_j^k + \rho_{ij}{}^{-1} \bar{\chi}_{jk} \bar{\chi}_{ki} (III + 2II\chi_k))$$

$$\varrho_{02} = \frac{1}{\Delta^2} \sum_{(ijk)} (\rho_{ii}{}^{-1} \bar{\chi}_{jk}^2 \chi_j^k + \rho_{ij}{}^{-1} \bar{\chi}_{jk} \bar{\chi}_{ki} \chi_k \chi_{ij})$$

$$\varrho_{12} = -\frac{1}{\Delta^2} \sum_{(ijk)} (\rho_{ii}{}^{-1} \bar{\chi}_{jk}^2 \chi_{jk} + \rho_{ij}{}^{-1} \bar{\chi}_{jk} \bar{\chi}_{ki} (I + \chi_k)) \tag{A.31}$$

Function ρ is given by

$$\rho^{-1}(\chi_\alpha, \chi_\beta) = (2\sqrt{\chi_\alpha \chi_\beta})^{-1} \left(\frac{\chi_\alpha - \chi_\beta}{g(\chi_\alpha) - g(\chi_\beta)} \right) . \tag{A.32}$$

The principal invariants of $\mathbf{B}$ in terms of its eigenvalues are

$$\begin{aligned} I &= \chi_1 + \chi_2 + \chi_3 \\ II &= \chi_1\chi_2 + \chi_2\chi_3 + \chi_3\chi_1 \\ III &= \chi_1\chi_2\chi_3 . \end{aligned} \tag{A.33}$$

B Implementation

B.1 Summary of equations

Transformation temperatures:

$$M_s^0 = \frac{\Delta u^* - \bar{u}_0}{\Delta s^* - \bar{s}_0} \tag{B.1}$$

$$A_s^0 = \frac{\Delta u^* + \bar{u}_0}{\Delta s^* + \bar{s}_0} \tag{B.2}$$

Elastic tangent:

$$\mathbb{C} \tag{B.3}$$

Lame constant:

$$\mu = \frac{E}{2(1+\nu)} \tag{B.4}$$

Strain deviator:

$$\mathbf{h}' \tag{B.5}$$

Equivalent strain:

$$h = \sqrt{\mathbf{h}' : \mathbf{h}'} \tag{B.6}$$

Rate of equivalent strain:

$$\dot{h} = \frac{1}{h}\,\mathbf{h}' : \overset{\circ}{\mathbf{h}}{}^{\mathrm{Log}} \tag{B.7}$$

Phase chemical potential:

$$\pi_0^f(\Theta) = \Delta u^* - \Theta \Delta s^* \tag{B.8}$$

with

$$\Delta u^* = u_0^{*A} - u_0^{*M} \tag{B.9}$$

$$\Delta s^* = s_0^{*A} - s_0^{*M} \tag{B.10}$$

Specific free energy of interaction:

$$\psi_{it}(\Theta) = \bar{u}_0 - \Theta \bar{s}_0 \tag{B.11}$$

Thermodynamic driving force:

$$\pi^f = \frac{1}{\xi}\,\boldsymbol{\tau} : \mathbf{h}^{etr} + \rho_0 \pi_0^f(\Theta) - \rho_0(1-2\xi)\psi_{it}(\Theta) \tag{B.12}$$

Criterion for neutral processes for isotropy in terms of $\dot{h}$ and $\dot{\Theta}$:

$$\dot{\pi}^f\big|_\xi = 2\mu\eta\dot{h} + \rho_0\left(-\Delta s^* + (1-2\xi)\bar{s}_0\right)\dot{\Theta} \tag{B.13}$$

Rate equation for ξ for isotropy:

$$\dot{\xi}^\alpha = \frac{2\mu\eta\dot{h} + \rho_0\left(-\Delta s^* + (1-2\xi)\bar{s}_0\right)\dot{\Theta}}{\rho_0\dfrac{\partial k^\alpha}{\partial\xi} - 2\rho_0\psi_{it} + 2\mu\eta^2} \tag{B.14}$$

with

$$\frac{\partial k^{A\to M}}{\partial\xi} = -\frac{2\bar{s}_0}{a_1}\ln(1-\xi) + \frac{\Delta s^* - \bar{s}_0(1-2\xi)}{a_1(1-\xi)} + 2\psi_{it}(M_s^0) \tag{B.15}$$

$$\frac{\partial k^{M\to A}}{\partial\xi} = \frac{2\bar{s}_0}{a_2}\ln\xi + \frac{\Delta s^* - \bar{s}_0(1-2\xi)}{a_2\xi} + 2\psi_{it}(A_s^0) \tag{B.16}$$

Logarithmic rate of the elastic-phase transformation part of the strain:

$$\overset{\circ}{\mathbf{h}}{}^{etr\,\mathrm{Log}} = \mathbf{D}^{etr} = \frac{\eta}{h}\left(\mathbf{h}'\dot{\xi} + \xi(\mathbb{I} - \frac{1}{3}\,\mathbf{1}\otimes\mathbf{1} - \frac{1}{h^2}(\mathbf{h}'\otimes\mathbf{h}')) : \mathbf{D}\right) \tag{B.17}$$

Elastic stretching:

$$\mathbf{D}^e = \mathbf{D} - \mathbf{D}^{etr} \tag{B.18}$$

Stress rate:

$$\overset{\circ}{\boldsymbol{\tau}}{}^{\mathrm{Log}} = (\mathbf{D}^e - \dot{\Theta}\boldsymbol{\alpha}_0) : \mathbb{C} \tag{B.19}$$

Stress via corotational integration:

$$\boldsymbol{\tau} = (\mathbf{R}^{\mathrm{Log}})^{\mathrm{T}} \star \int_0^t \mathbf{R}^{\mathrm{Log}} \star \overset{\circ}{\boldsymbol{\tau}}{}^{\mathrm{Log}} \mathrm{d}s \tag{B.20}$$

Energy generation per unit mass:

$$\frac{1}{\rho}\,\dot{h}_{lat} = \frac{1}{\rho_0}\,\boldsymbol{\tau} : \mathbf{D}^{etr} + (\Delta u^* - \bar{u}_0(1-2\xi))\dot{\xi} - \frac{1}{\rho_0}\,\Theta\boldsymbol{\alpha}_0 : \overset{\circ}{\boldsymbol{\tau}}{}^{\mathrm{Log}} \tag{B.21}$$

B.2 Intermediate configuration

It was pointed out above that the kinematic framework used in this treatise is kinematically consistent, i.e. the elastic and inelastic parts of the deformation gradient, $\mathbf{F}^e$ respectively $\mathbf{F}^i = \mathbf{F}^{tr}$, as well as all related kinematic quantities, can be uniquely determined without any assumptions regarding $\mathbf{F}^e$. This may be illustrated as follows.
Starting from the $\boldsymbol{\tau}_{n+1}$ obtained from corotational integration of the constitutive equation, the elastic left stretch tensor is given by

$$\mathbf{V}^e_{n+1} = \exp\left(\partial\Sigma/\partial\boldsymbol{\tau}_{n+1}\right) . \tag{B.22}$$

The elastic rotation follows from integration of the linear tensorial differential equation

$$\dot{\mathbf{R}}^e = \boldsymbol{\Omega}^e\mathbf{R}^e \qquad \mathbf{R}^e\big|_{t=t_n} = \mathbf{R}_n\,, \tag{B.23}$$

where the elastic spin is given by

$$\boldsymbol{\Omega}^e = \boldsymbol{\Omega}^{\mathrm{Log}} - \mathbf{N}^e\,. \tag{B.24}$$

Using the eigenvalues λ^e_σ and eigenprojections $\mathbf{B}^e_\sigma$ of $\mathbf{V}^e$, the tensor $\mathbf{N}^e$ may be expressed as

$$\mathbf{N}^e = \sum_{\sigma\neq\tau}^{n}\left(\frac{2\lambda^e_\sigma\lambda^e_\tau}{\lambda^{e2}_\tau - \lambda^{e2}_\sigma} + \frac{1}{\ln\lambda^e_\sigma - \ln\lambda^e_\tau}\right)\mathbf{B}^e_\sigma\mathbf{D}^e\mathbf{B}^e_\tau\,. \tag{B.25}$$

Alternatively, a basis-free expression may be derived, see (A.16). Note that by virtue of (3.145), the last two equations yield

$$\boldsymbol{\Omega}^e = \boldsymbol{\Omega}^{\mathrm{R}} \tag{B.26}$$

for processes of purely elastic deformation, where $\mathbf{V} = \mathbf{V}^e$ and $\mathbf{R} = \mathbf{R}^e$.
Equation (B.23) is integrated as described in Section 7.2.2

$$\mathbf{R}^e_{n+1} = \exp(\Delta t\boldsymbol{\Omega}^e)\mathbf{R}^e_n\,. \tag{B.27}$$

Hence, the elastic part of the deformation gradient

$$\mathbf{F}^e_{n+1} = \mathbf{V}^e_{n+1}\mathbf{R}^e_{n+1}\,, \tag{B.28}$$

and with it the inelastic part

$$\mathbf{F}^i_{n+1} = \mathbf{F}^{-e}_{n+1}\mathbf{F}_{n+1} \tag{B.29}$$

are readily obtained without any assumptions regarding $\mathbf{F}^e$.

B.3 Calculation of $\mathbf{h}_n$ and $\mathbf{h}_{n+1}$

To determine the time-discrete Hencky strains $\mathbf{h}_n$ and $\mathbf{h}_{n+1}$, the left Cauchy-Green tensor is calculated using (3.48) at the times $t = t_n$ and $t = t_{n+1}$

$$\mathbf{B}_{n+\alpha\Delta t} = \mathbf{F}_{n+\alpha\Delta t}\mathbf{F}^{\mathrm{T}}_{n+\alpha\Delta t}\,. \tag{B.30}$$

The eigenvalues and eigenprojections of the left Cauchy-Green tensor are obtained by virtue of (A.11) to (A.13) and (A.20). Then, the Hencky strain at $t = t_n$ respectively $t = t_{n+1}$ is obtained from (A.6) for $\alpha = 0$ respectively $\alpha = 1$ using the natural logarithmic scale function $g(\chi) = \frac{1}{2}\ln\chi$ given in (A.9)

$$\mathbf{h}_{n+\alpha\Delta t} = \mathbf{h}_{n+\alpha\Delta t}(\chi_\sigma, \mathbf{B}_\sigma)\big|_{n+\alpha\Delta t}\,. \tag{B.31}$$

B.4 Tangent stiffness matrix

Given the relations of the material law proposed in Chapter 6, the tangent stiffness matrix is derived. The elastic-phase transformation part of the stretching is

$$\mathbf{D}^{etr} = \frac{\eta}{h}\mathbf{h}'\dot{\xi} + \mathbf{D} : \mathbb{Z}_1(\xi, h, \mathbf{h}') \tag{B.32}$$

with

$$\mathbb{Z}_1(\xi, h, \mathbf{h}') = \frac{\eta\xi}{h}\left(\mathbb{I} - \frac{1}{3}\mathbf{1}\otimes\mathbf{1} - \frac{1}{h^2}(\mathbf{h}'\otimes\mathbf{h}')\right) \tag{B.33}$$

having the symmetries

$$(\mathbb{Z}_1)_{ijkl} = (\mathbb{Z}_1)_{klij} = (\mathbb{Z}_1)_{jikl} = (\mathbb{Z}_1)_{jilk}\,. \tag{B.34}$$

The rate of the equivalent Hencky strain is given by

$$\dot{h} = \frac{1}{h}\mathbf{h}' : \mathbf{D}\,. \tag{B.35}$$

Defining the function

$$Z_2(\xi) = \left(\Delta s^* + (1 - 2\xi)\,\bar{s}_0\right)\,, \tag{B.36}$$

the rate of the mass fraction of martensite is

$$\dot{\xi} = \frac{1}{H_h^{(k)}}\left(\frac{2\mu\eta}{\rho_0 h}\mathbf{D} : \mathbf{h}' - Z_2(\xi)\dot{\Theta}\right)\,. \tag{B.37}$$

Here

$$H_h^{(k)} = \frac{\partial k^\alpha}{\partial\xi} - 2\psi_{it} + \frac{2\mu\eta^2}{\rho_0}\,. \tag{B.38}$$

The thermomechanical coupling is given by

$$\begin{aligned}\frac{1}{\rho c_p}\nabla\cdot\mathbf{q}+\dot{\Theta} &= -\frac{k}{\rho c_p}\nabla^2\Theta+\dot{\Theta}=\frac{\dot{h}_{lat}}{c_p}\\ &= \frac{\rho}{\rho_0 c_p}\mathbf{D}^{etr}:\boldsymbol{\tau}+Z_3(\xi)\dot{\xi}-\frac{\rho}{\rho_0 c_p}\Theta\boldsymbol{\alpha}_0:\overset{\circ}{\boldsymbol{\tau}}{}^{\mathrm{Log}}\end{aligned} \tag{B.39}$$

where

$$Z_3(\xi)=\frac{\rho}{c_p}(\Delta u^*-\bar{u}_0(1-2\xi))\,, \tag{B.40}$$

and the logarithmic rate of the Kirchhoff stress is

$$\overset{\circ}{\boldsymbol{\tau}}{}^{\mathrm{Log}}=(\mathbf{D}-\mathbf{D}^{etr}-\dot{\Theta}\boldsymbol{\alpha}_0):\mathbb{C}^e\,. \tag{B.41}$$

Now, the rate of temperature $\dot{\Theta}$ is to be expressed in terms of the stretching $\mathbf{D}$. Hence, (B.41) is substituted in (B.39)

$$\begin{aligned}-\frac{k}{\rho c_p}\nabla^2\Theta+\dot{\Theta} &= \frac{\rho}{\rho_0 c_p}\mathbf{D}^{etr}:\boldsymbol{\tau}+Z_3\dot{\xi}\\ &\quad -\frac{\rho}{\rho_0 c_p}\Theta(\mathbf{D}-\mathbf{D}^{etr}-\dot{\Theta}\boldsymbol{\alpha}_0):\mathbb{C}^e:\boldsymbol{\alpha}_0\\ &= \mathbf{D}^{etr}:\mathbf{Z}_4(\boldsymbol{\tau},\Theta)+Z_3\dot{\xi}-\frac{\rho\Theta}{\rho_0 c_p}(\mathbf{D}-\dot{\Theta}\boldsymbol{\alpha}_0):\mathbb{C}^e:\boldsymbol{\alpha}_0\,,\end{aligned} \tag{B.42}$$

where

$$\text{with}\quad \mathbf{Z}_4(\boldsymbol{\tau},\Theta)=\frac{\rho}{\rho_0 c_p}(\boldsymbol{\tau}+\Theta\mathbb{C}^e:\boldsymbol{\alpha}_0)\,. \tag{B.43}$$

Then, substituting (B.32) into (B.42) yields

$$\begin{aligned}&-\frac{k}{\rho c_p}\nabla^2\Theta+\dot{\Theta}\left(1-\frac{\rho\Theta}{\rho_0 c_p}\boldsymbol{\alpha}_0:\mathbb{C}^e:\boldsymbol{\alpha}_0\right)\\ &=\frac{\eta}{h}\dot{\xi}\mathbf{h}':\mathbf{Z}_4+(\mathbb{Z}_1:\mathbf{D}):\mathbf{Z}_4+Z_3\dot{\xi}-\frac{\rho\Theta}{\rho_0 c_p}\mathbf{D}:\mathbb{C}^e:\boldsymbol{\alpha}_0\\ &=\dot{\xi}H_h^{(k)}\cdot Z_5(h,\mathbf{h}',\xi,\Theta,\boldsymbol{\tau})+\mathbf{D}:\left(\mathbb{Z}_1:\mathbf{Z}_4-\frac{\rho\Theta}{\rho_0 c_p}\mathbb{C}^e:\boldsymbol{\alpha}_0\right)\,.\end{aligned} \tag{B.44}$$

where

$$H_h^{(k)}\cdot Z_5(h,\mathbf{h}',\xi,\Theta,\boldsymbol{\tau})=\left(\frac{\eta}{h}\mathbf{h}':\mathbf{Z}_4+Z_3\right)\,. \tag{B.45}$$

Using

$$\mathbf{Z}_1 : \mathbf{D} = \mathbf{D} : \mathbf{Z}_1 \,, \tag{B.46}$$

substituting (B.36) into (B.44) gives

$$\begin{aligned}
&-\frac{k}{\rho c_p}\nabla^2\Theta + \dot{\Theta}\left(1 - \frac{\rho\Theta}{\rho_0 c_p}\boldsymbol{\alpha}_0 : \mathbb{C}^e : \boldsymbol{\alpha}_0\right) \\
&= \left(\frac{2\mu\eta}{\rho_0 h}\mathbf{D} : \mathbf{h}' - Z_2\dot{\Theta}\right) Z_5 + \mathbf{D} : \left(\mathbf{Z}_1 : \mathbf{Z}_4 - \frac{\rho\Theta}{\rho_0 c_p}\mathbb{C}^e : \boldsymbol{\alpha}_0\right) \\
\Rightarrow \quad &\dot{\Theta} Z_6(h, \mathbf{h}', \xi, \Theta, \boldsymbol{\tau}) = \mathbf{D} : \left(\frac{2\mu\eta}{\rho_0 h} Z_5 \mathbf{h}' + \mathbf{Z}_1 : \mathbf{Z}_4 - \frac{\rho\Theta}{\rho_0 c_p}\mathbb{C}^e : \boldsymbol{\alpha}_0\right) \\
&\qquad\qquad + \frac{k}{\rho c_p}\nabla^2\Theta \\
\Rightarrow \quad &\dot{\Theta} = \mathbf{D} : \mathbf{Z}_7(h, \mathbf{h}', \xi, \Theta, \boldsymbol{\tau}) + \frac{1}{Z_6}\frac{k}{\rho c_p}\nabla^2\Theta \,,
\end{aligned} \tag{B.47}$$

with

$$Z_6(h, \mathbf{h}', \xi, \Theta, \boldsymbol{\tau}) = \left(1 - \frac{\rho\Theta}{\rho_0 c_p}\boldsymbol{\alpha}_0 : \mathbb{C}^e : \boldsymbol{\alpha}_0 + Z_2 Z_5\right) \tag{B.48}$$

and

$$\mathbf{Z}_7(h, \mathbf{h}', \xi, \Theta, \boldsymbol{\tau}) = \left(\frac{2\mu\eta}{\rho_0 h}\frac{Z_5}{Z_6}\mathbf{h}' + \frac{1}{Z_6}\mathbf{Z}_1 : \mathbf{Z}_4 - \frac{1}{Z_6}\frac{\rho\Theta}{\rho_0 c_p}\mathbb{C}^e : \boldsymbol{\alpha}_0\right) . \tag{B.49}$$

Substitution of $\dot{\Theta}$ in $\dot{\xi}$ yields

$$\begin{aligned}
\dot{\xi} &= \frac{1}{H_h^{(k)}}\left(\frac{2\mu\eta}{\rho_0 h}\mathbf{D} : \mathbf{h}' - Z_2\mathbf{D} : \mathbf{Z}_7 - \frac{Z_2}{Z_6}\frac{k}{\rho c_p}\nabla^2\Theta\right) \\
&= \mathbf{D} : \left[\frac{1}{H_h^{(k)}}\left(\frac{2\mu\eta}{\rho_0 h}\mathbf{h}' - Z_2\mathbf{Z}_7\right)\right] - \frac{1}{H_h^{(k)}}\frac{Z_2}{Z_6}\frac{k}{\rho c_p}\nabla^2\Theta \,.
\end{aligned} \tag{B.50}$$

Finally, substituting $\dot{\Theta}$ and $\dot{\xi}$ into (B.32) and (B.41), neglecting heat conduction leads to

$$\overset{\circ}{\boldsymbol{\tau}}{}^{\mathrm{Log}} = \mathbf{D} : \mathbb{C}^{ei} \,, \tag{B.51}$$

with

$$\mathbb{C}^{ei} = \left(\mathbb{I} - \frac{\eta}{h}\frac{1}{H_h^{(k)}}\left(\frac{2\mu\eta}{\rho_0 h}\mathbf{h}' - Z_2\mathbf{Z}_7\right) \otimes \mathbf{h}' - \mathbf{Z}_1 - \mathbf{Z}_7 \otimes \boldsymbol{\alpha}_0\right) : \mathbb{C}^e \,. \tag{B.52}$$

B.5 Linearization

In this section, the material law is linearized with regard to an implementation within a backward-Euler scheme. First,

$$\mathbb{Z}_1(\xi) = \frac{\eta}{h}\,\xi\left(\mathbb{I} - \frac{1}{3}\,\mathbf{1}\otimes\mathbf{1} - \frac{1}{h^2}(\mathbf{h}'\otimes\mathbf{h}')\right) \tag{B.53}$$

is defined. The partial derivatives of this relation

$$\frac{\partial \mathbf{Z}_1}{\partial \xi} = \frac{1}{\xi}\mathbf{Z}_1 \tag{B.54}$$

and of Z_2 from above are

$$\frac{\partial Z_2}{\partial \xi} = -2\bar{s}_0\,. \tag{B.55}$$

For the transformation to martensite the following relation hold

$$\begin{aligned} H_h^{(1)}(\xi,\Theta) = &-\frac{2\bar{s}_0}{a_1}\ln(1-\xi) + \frac{\Delta s^* - \bar{s}_0\,(1-2\xi)}{a_1(1-\xi)} \\ &+2\psi_{it}\left(M_s^0\right) - 2\psi_{it}(\Theta) + \frac{2\mu\eta^2}{\rho_0} \end{aligned} \tag{B.56}$$

with

$$\psi_{it}(\Theta) = \bar{u}_0 - \Theta\bar{s}_0\,. \tag{B.57}$$

This gives the partial derivatives

$$\frac{\partial H_h^{(1)}}{\partial \Theta} = 2\bar{s}_0 \tag{B.58}$$

and

$$\begin{aligned} \frac{\partial H_h^{(1)}}{\partial \xi} &= \frac{2\bar{s}_0}{a_1\,(1-\xi)} + \frac{2\bar{s}_0\,(1-\xi) + \Delta s^* - \bar{s}_0\,(1-2\xi)}{a_1(1-\xi)^2} \\ &= \frac{4\bar{s}_0}{a_1(1-\xi)} + \frac{Z_2}{a_1(1-\xi)^2}\,. \end{aligned} \tag{B.59}$$

For the transformation to austenite the following relation holds

$$\begin{aligned} H_h^{(2)}(\xi,\Theta) = &\frac{2\bar{s}_0}{a_2}\ln(\xi) + \frac{\Delta s^* - \bar{s}_0(1-2\xi)}{a_2\xi} \\ &+2\psi_{it}(A_s^0) - 2\bar{u}_0 + 2\Theta\bar{s}_0 + \frac{2\mu\eta^2}{\rho_0}\,. \end{aligned} \tag{B.60}$$

This gives the partial derivatives

$$\frac{\partial H_h^{(2)}}{\partial \Theta} = 2\bar{s}_0 \tag{B.61}$$

and

$$\frac{\partial H_h^{(2)}}{\partial \xi} = \frac{2\bar{s}_0}{a_2\xi} + \frac{2\bar{s}_0\xi - \left(\Delta s^* - \bar{s}_0\left(1-2\xi\right)\right)}{a_2\xi^2} = \frac{4\bar{s}_0}{a_2\xi} - \frac{Z_2}{a_2\xi^2}\,. \tag{B.62}$$

The evolution of martensite is governed by

$$\dot{\xi} = \frac{1}{H_h^{(k)}}\left(\frac{2\mu\eta}{\rho_0 h}\mathbf{D} : \mathbf{h}' - Z_2\dot{\Theta}\right) = \frac{\dot{\pi}^f}{\rho_0 H_h^{(k)}}\,, \tag{B.63}$$

leading to the logarithmic rate of the stress

$$\overset{\circ}{\boldsymbol{\tau}}{}^{\mathrm{Log}} = \left(\mathbf{D} - \frac{\eta}{h}\mathbf{h}'\dot{\xi} - \mathbf{D} : \mathbb{Z}_1 - \dot{\Theta}\boldsymbol{\alpha}_0\right) : \mathbb{C}^e\,. \tag{B.64}$$

Discretization gives

$$h_{n+1} = \sqrt{\mathbf{h}'_{n+1} : \mathbf{h}'_{n+1}}\,, \tag{B.65}$$

and

$$\rho_{n+1} = \frac{\rho_0}{\det(\mathbf{F}_{n+1})}\,. \tag{B.66}$$

The residual of the linearization with respect to ξ is

$$X_{n+1} = -\xi_{n+1} + \xi_n + \Delta t\dot{\xi}_{n+1} = -\xi_{n+1} + \xi_n + \Delta\xi_{n+1} = 0\,, \tag{B.67}$$

with

$$\begin{aligned}\Delta\xi_{n+1} &= \frac{1}{H_{h\,n+1}^{(k)}}\left(\frac{2\mu\eta}{\rho_0 h_{n+1}}\left(\Delta t\mathbf{D}_{n+1}\right)\mathbf{h}'_{n+1} - Z_{2n+1}\Delta\Theta_{n+1}\right)\\ &= \frac{\Delta\pi^f{}_{n+1}}{\rho_0 H_{h\,n+1}^{(k)}}\,.\end{aligned} \tag{B.68}$$

The residual of the linearization with respect to $\boldsymbol{\tau}$ is

$$\mathbf{S}_{n+1} = -\boldsymbol{\tau}_{n+1} + \widetilde{\mathbf{R}}_{n+1}^{\mathrm{Log}} \star \boldsymbol{\tau}_n + \Delta t\overset{\circ}{\boldsymbol{\tau}}{}^{\mathrm{Log}}{}_{n+1} = \mathbf{0}\,. \tag{B.69}$$

Substitution of the logarithmic rate of $\boldsymbol{\tau}$ yields

$$\begin{aligned}\mathbf{S}_{n+1} = -\boldsymbol{\tau}_{n+1} + \widetilde{\mathbf{R}}_{n+1}^{\mathrm{Log}} \star \boldsymbol{\tau}_n + \Bigg(&\left(\Delta t\mathbf{D}_{n+1}\right) - \frac{\eta}{h_{n+1}}\mathbf{h}'_{n+1}\Delta\xi_{n+1}\\ &- \left(\Delta t\mathbf{D}_{n+1}\right) : \mathbb{Z}_{1\,n+1} - \Delta\Theta_{n+1}\boldsymbol{\alpha}_0\Bigg) : \mathbb{C}^e\,.\end{aligned} \tag{B.70}$$

Here, it must be noted that

$$\Delta t\mathbf{D}_{n+1} \neq \mathbf{h}_{n+1} - \mathbf{h}_n \,. \tag{B.71}$$

The independent variables are τ_{n+1}, ξ_{n+1}, and Θ_{n+1}. However, the latter is given by the finite element code.
The partial derivatives are

$$\frac{\partial X_{n+1}}{\partial \xi_{n+1}} = \frac{\partial \Delta\xi_{n+1}}{\partial \xi_{n+1}} - 1 \,, \tag{B.72}$$

$$\frac{\partial X_{n+1}}{\partial \tau_{n+1}} = \frac{\partial \Delta\xi_{n+1}}{\partial \tau_{n+1}} \,, \tag{B.73}$$

and

$$\begin{aligned}\frac{\partial \mathbf{S}_{n+1}}{\partial \xi_{n+1}} = \Bigg(&- \frac{\eta}{h_{n+1}} \mathbf{h'}_{n+1} \frac{\partial \Delta\xi_{n+1}}{\partial \xi_{n+1}} - (\Delta t\mathbf{D}_{n+1}) : \frac{\partial \mathbf{Z}_{1\,n+1}}{\partial \xi_{n+1}} \\ &- \frac{\partial \Delta\Theta_{n+1}}{\partial \xi_{n+1}} \boldsymbol{\alpha}_0 \Bigg) : \mathbb{C}^e \,,\end{aligned} \tag{B.74}$$

$$\frac{\partial \mathbf{S}_{n+1}}{\partial \tau_{n+1}} = -\mathbb{I} + \left(-\frac{\eta}{h_{n+1}} \mathbf{h'}_{n+1} \otimes \frac{\partial \Delta\xi_{n+1}}{\partial \tau_{n+1}} - \frac{\partial \Delta\Theta_{n+1}}{\partial \tau_{n+1}} \otimes \boldsymbol{\alpha}_0 \right) : \mathbb{C}^e \,. \tag{B.75}$$

The derivatives of $\Delta\xi_{n+1}$ are

$$\begin{aligned}\frac{\partial \Delta\xi_{n+1}}{\partial \Theta_{n+1}} = &\left(-\frac{1}{(H^{(k)}_{h\,n+1})^2} \frac{\partial H^{(k)}_{h\,n+1}}{\partial \Theta_{n+1}} \right) \Delta\xi_{n+1} H^{(k)}_{h\,n+1} \\ &+ \frac{1}{H^{(k)}_{h\,n+1}} \left(-Z_{2\,n+1} \frac{\partial \Delta\Theta_{n+1}}{\partial \Theta_{n+1}} \right) \\ = &\frac{1}{H^{(k)}_{h\,n+1}} \left(-\frac{\partial H^{(k)}_{h\,n+1}}{\partial \Theta_{n+1}} \Delta\xi_{n+1} - Z_{2\,n+1} \frac{\partial \Delta\Theta_{n+1}}{\partial \Theta_{n+1}} \right) \,,\end{aligned} \tag{B.76}$$

$$\begin{aligned}\frac{\partial \Delta\xi_{n+1}}{\partial \xi_{n+1}} = & \left(-\frac{1}{(H^{(k)}_{h\,n+1})^2}\frac{\partial H^{(k)}_{h\,n+1}}{\partial \xi_{n+1}}\right)\Delta\xi_{n+1}H^{(k)}_{h\,n+1} \\ & + \frac{1}{H^{(k)}_{h\,n+1}}\left(-\frac{\partial Z_{2\,n+1}}{\partial \xi_{n+1}}\Delta\Theta_{n+1} - Z_{2\,n+1}\frac{\partial \Delta\Theta_{n+1}}{\partial \xi_{n+1}}\right) \\ = & \frac{1}{H^{(k)}_{h\,n+1}}\left[-\frac{\partial H^{(k)}_{h\,n+1}}{\partial \xi_{n+1}}\Delta\xi_{n+1} - \frac{\partial Z_{2\,n+1}}{\partial \xi_{n+1}}\Delta\Theta_{n+1}\right. \\ & \left. - Z_{2\,n+1}\frac{\partial \Delta\Theta_{n+1}}{\partial \xi_{n+1}}\right]\end{aligned} \tag{B.77}$$

and

$$\frac{\partial \Delta\xi_{n+1}}{\partial \tau_{n+1}} = \frac{1}{H^{(k)}_{h\,n+1}}\left(-Z_{2\,n+1}\frac{\partial \Delta\Theta_{n+1}}{\partial \tau_{n+1}}\right) = -\frac{Z_{2\,n+1}}{H^{(k)}_{h\,n+1}}\frac{\partial \Delta\Theta_{n+1}}{\partial \tau_{n+1}}\,. \tag{B.78}$$

References

ACHENBACH, M. (1989): *A model for an alloy with shape memory*, in: Int. J. Plast., Volume 5, 371–395.

ALTENBACH, J. & ALTENBACH, H. (1994): *Einführung in die Kontinuumsmechanik*, Teubner Studienbücher 1994.

AURICCHIO, F. (2001): *A robust integration-algorithm for a finite-strain shape-memory-alloy superelastic model*, in: Int. J. Plast., Volume 17, 971–990.

AURICCHIO, F. & LUBLINER, J. (1995): *A uniaxial model for shape-memory alloys*, Technical report, Dipartamiento di Ingegneria Civile, 1995.

AURICCHIO, F. & TAYLOR, R. L. (1997): *Shape-memory alloys: modelling and numerical simulations of the finite-strain superelastic behavior*, in: Comput. Methods Appl. Mech. Engrg., Volume 143, 175–194.

AURICCHIO, F. & TAYLOR, R. L. (1999): *A return-map algorithm for general associative isotropic elasto-plastic materials in large deformation regimes*, in: Int. J. Plast., Volume 15, 1359–1378.

AURICCHIO, F., TAYLOR, R. L. & LUBLINER, J. (1997): *Shape-memory alloys: macromodelling and numerical simulations of the superelastic behavior*, in: Comput. Methods Appl. Mech. Engrg., Volume 146, 281–312.

BASAR, Y. & WEICHERT, D. (2000): *Nonlinear continuum mechanics of solids. Fundamental mathematical and physical concepts*, Springer-Verlag 2000.

BATHE, K.-J. (1986): *Finite Elemente Methoden*, Springer-Verlag 1986.

BELYTSCHKO, T., LIU, W. K. & MORAN, B. (2000): *Nonlinear finite elements for continua and structures*, John Wiley & Sons, Ltd. 2000.

BERNARDINI, D. (2001): *On the macroscopic free energy functions for shape memory alloys*, in: J. Mech. Phys. Solids, Volume 49, 813–837.

BERTRAM, A. (1982): *Thermo-mechanical constitutive equations for the description of shape memory effects in alloys*, in: Nucl. Eng. Des., Volume 74, 173–182.

BHATTACHARYA, K. & DOLZMANN, G. (2000): *Relaxed constitutive relations for phase transforming materials*, in: J. Mech. Phys. Solids, Volume 48, 1493–1517.

Bo, Z. & Lagoudas, D. C. (1999a): *Thermomechanical modeling of polycrystalline SMAs under cyclic loading, part I: theoretical derivations*, in: Int. J. Engng. Sci., Volume 37, 1089–1140.

Bo, Z. & Lagoudas, D. C. (1999b): *Thermomechanical modeling of polycrystalline SMAs under cyclic loading, part II: material characterization and experimental results for a stable transformation cycle*, in: Int. J. Engng. Sci., Volume 37, 1141–1173.

Bo, Z. & Lagoudas, D. C. (1999c): *Thermomechanical modeling of polycrystalline SMAs under cyclic loading, part III: evolution of plastic strains and twoway shape memory effect*, in: Int. J. Engng. Sci., Volume 37, 1175–1203.

Bo, Z. & Lagoudas, D. C. (1999d): *Thermomechanical modeling of polycrystalline SMAs under cyclic loading, part IV: modeling of minor hysteresis loops*, in: Int. J. Engng. Sci., Volume 37, 1205–1249.

Bongmba, C. N. & Bruhns, O. T. (2001): *On the numerical implementation of a finite strain anisotropic damage model based upon the logarithmic rate*, in: Eur. J. Finite Elements, Volume 10, 385–400.

Bongmba, N. C. (2001): *Ein finites anisotropes Materialmodell auf der Basis der Hencky-Dehnung und der logarithmischen Rate zur Beschreibung duktiler Schädigung* 2001, Dissertation, Ruhr-Universität Bochum.

Bouvet, C., Calloch, S. & Lexcellent, C. (2002): *Mechanical behavior of a Cu-Al-Be shape memory alloy under multiaxial proportional and nonproportional loadings*, in: ASME, Volume 124, 112–124.

Boyd, J. G. & Lagoudas, D. C. (1996a): *A thermodynamical constitutive model for shape memory materials. Part I. The monolithic shape memory alloy*, in: Int. J. Plast., Volume 12, 6, 805–842.

Boyd, J. G. & Lagoudas, D. C. (1996b): *A thermodynamical constitutive model for shape memory materials. Part II. The SMA composite material*, in: Int. J. Plast., Volume 12, 7, 843–873.

Brewster, D. (1965): *Memoirs of the Life, Writings, and Discoveries of Sir Isaac Newton*, Volume 2 of *The Sources of Science*, Johnson Reprint Corporation New York and London 1965.

Bruhns, O. T. (2003): *Objective rates in finite elastoplasticity*, IUTAM-Symposium Stuttgart 2001, Kluwer Academic Publ., Dordrecht 2003, Computational mechanics of solid materials at large strains.

BRUHNS, O. T., XIAO, H. & MEYERS, A. (1999): *Self-consistent Eulerian rate type elasto-plasticity models based upon the logarithmic stress rate*, in: Int. J. Plast., Volume 15, 479–520.

BRUHNS, O. T., XIAO, H. & MEYERS, A. (2001): *A self-consistent Eulerian rate type model for finite deformation elastoplasticity with isotropic damage*, in: Int. J. Solids Structures, Volume 38, 657–683.

BRUHNS, O. T., XIAO, H. & MEYERS, A. (2002): *New results for the spin of the Eulerian triad and the logarithmic spin and rate*, in: Acta Mech., Volume 155, 95–109.

BUBNER, N. (1996): *Landau-Ginzburg model for a deformation-driven experiment on shape memory alloys*, in: Continuum Mech. Thermodyn., Volume 8, 293–308.

CALLEN, H. B. (1970): *Thermodynamics: an introduction to the physical theories of equilibrium thermostatics and irreversible thermodynamics*, John Wiley & Sons, Inc., New York 1970.

CARLSON, D. E. & HOGER, A. (1986): *The derivative of a tensor-valued function of a tensor*, in: Q. Appl. Math., Volume 44, 3, 409–423.

CASEY, J. & NAGHDI, P. M. (1981): *A correct definition of elastic and plastic deformation and its computational significance*, in: J. Appl. Mech., Volume 48, 983–984.

CHADWICK, P. (1976): *Continuum mechanics: Concise theory and problems*, Dover Publications, Inc., Mineola, New York 1976.

CHIRANI, S. A., ALEONG, D., DUMONT, C., MCDOWELL, D. & PATOOR, E. (2003): *Superelastic behavior modeling in shape memory alloys*, in: J. Phys. IV, Volume (to appear).

COLEMAN, B. D. & GURTIN, M. E. (1967): *Thermodynamics with internal state variables*, in: J. Chem. Phys., Volume 47, 2, 597–613.

COLEMAN, B. D. & NOLL, W. (1960): *An approximation theorem for functionals, with applications in continuum mechanics*, in: Arch. Rational Mech. Analysis, Volume 6, 355–370.

COLEMAN, B. D. & NOLL, W. (1961): *Foundations of linear viscoelasticity*, in: Rev. Mod. Phys., Volume 33, 2, 239–249.

COLEMAN, B. D. & NOLL, W. (1963): *The thermodynamics of elastic materials with heat conduction and viscosity*, in: Arch. Rational Mech. Analysis, Volume 13, 167–178.

COLEMAN, B. D. & NOLL, W. (1964): *Erratum: Foundations of linear viscoelasticity*, in: Rev. Mod. Phys., Volume 33, 439, 1103.

CRISFIELD, M. (1991): *Non-linear finite element analysis of solids and structures - Volume 1: Essentials*, John Wiley & Sons Limited, Chichester 1991.

DELOBELLE, P. & LEXCELLENT, C. (1996): *A phenomenological three dimensional model for pseudoelastic behavior of shape memory alloys*, in: Journal de Physique IV, supplément au Journal de Physique III, Volume 6, C1–293 – C1–300.

DIENES, J. K. (1979): *On the analysis of rotation and stress rate in deforming bodies*, in: Acta Mech., Volume 32, 217–232.

DIENES, J. K. (1986): *A discussion of material rotation and stress rate*, in: Acta Mech., Volume 65, 1–11.

DRUCKER, D. C. (1988): *Conventional and unconventional plastic response and representation*, in: Appl. Mech. Rev., Volume 41, 4, 151–167.

EL HAWARY, T. (2003): *Berechnung und Konstruktion drehelastischer, dämpfender Kupplungen auf Basis von NiTi-Formgedächtnislegierungen*, Technical report, Ruhr-Universität Bochum, Bochum, 2003.

FALK, F. (1983): *One-dimensional model of shape memory alloys*, in: Arch. Mech., Volume 35, 1, 63–84.

FALK, F. & KONOPKA, P. (1990): *Three-dimensional Landau theory describing the martensitic phase transformation of shape-memory alloys*, in: Journal of physics, Volume 2, 61–77.

FISCHER, F. D., BERVEILLER, M., TANAKA, K. & OBERAIGNER, E. R. (1994): *Continuum mechanical aspects of phase transformations in solids*, in: Arch. Appl. Mech., Volume 64, 54–85.

FISCHER, F. D. & OBERAIGNER, E. R. (2001): *A micromechanical model of phase boundary movement during solid-solid phase transformations*, in: Arch. Appl. Mech., Volume 71, 193–205.

FISCHER, F. D. & TANAKA, K. (1992): *A micromechanical model for the kinetics of martensitic transformation*, in: Int. J. Solids Structures, Volume 29, 14/15, 1723–1728.

FU, S., HUO, Y. & MÜLLER, I. (1993): *Thermodynamics of pseudoelasticity - an analytical approach*, in: Acta Mech., Volume 99, 1–19.

FUNAKUBO, H. (Ed.) (1984): *Shape Memory Alloys*, Gordon and Breach Science Publishers 1984.

GADAJ, S. P., NOWACKI, W. K. & TOBUSHI, H. (1999): *Temperature evolution during tensile test of TiNi shape memory alloy*, in: Arch. Mech., Volume 51, 6, 649–663.

GALL, K., LIM, T. J., MCDOWELL, D. L., SEHITOGLU, H. & CHUMLYAKOV, Y. I. (2000): *The role of intergranular constraint on the stress-induced martensitic transformation in textured polycrystalline NiTi*, in: Int. J. Plast., Volume 16, 1189–1214.

GAO, X., HUANG, M. & BRINSON, L. C. (2000): *A multivariant micromechanical model for SMAs, Part 1. Crystallographic issues for single crystal model*, in: Int. J. Plast., Volume 16, 1345–1369.

GIBKES, J., KAACK, M., DELGADILLO HOLTFORT, I., DIETZEL, D., BEIN, B. K., PELZL, J., BUSCHKA, M., WEINERT, K., BRAM, M., BUCHKREMER, H. P. & STÖVER, D. (2002): *Photothermal Characterisation of Local and Depth Dependent Thermal Properties of NiTi Shape Memory Alloys*, in: *Shape Memory Materials and Its Applications: Proceedings of the International Conference on Shape Memory Superelastic Technologies and Shape Memory Materials 2001, Kunming, China*, 2002, pp. 345–348.

GOVINDJEE, S. & HALL, G. J. (2000): *A computational model for shape memory alloys*, in: Int. J. Solids Structures, Volume 37, 735–760.

GOVINDJEE, S., MIELKE, A. & HALL, G. J. (2002): *The free energy of mixing for n-variant martensitic phase transformations using quasi-convex analysis*, in: J. Mech. Phys. Solids, Volume 50, 1897–1922.

GREEN, A. E. & NAGHDI, P. M. (1971): *Some remarks on elastic-plastic deformation at finite strain*, in: Int. J. Engng. Sci., Volume 9, 1219–1229.

GUO, Z.-H. (1984): *Rates of stretch tensors*, in: J. Elast., Volume 14, 263–267.

GUO, Z.-H., LEHMANN, T., HAOYUN, L. & MAN, C.-S. (1992): *Twirl tensors and the tensor equation $AX - XA = C$*, in: J. Elast., Volume 27, 227–245.

HELM, D. (2001): *Formgedächtnislegierungen - Experimentelle Untersuchung, phänomenologische Modellierung und numerische Simulation der thermomechanischen Materialeigenschaften* 2001, Universität Gesamthochschule Kassel.

HELM, D. & HAUPT, P. (2001): *Geometrisch nichtlineare Modellierung und numerische Simulation von Formgedächtnislegierungen*, in: ZAMM · Z. Angew. Math. Mech., Volume 81, S2, 339–340.

HELM, D. & HAUPT, P. (2003): *Shape memory behaviour: modelling within continuum thermomechanics*, in: Int. J. Solids Structures, Volume 40, 827–849.

HENCKY, H. (1928): *Über die Form des Elastizitätsgesetzes bei ideal elastischen Stoffen*, in: Z. Techn. Phys., Volume 9, 214–220.

HILL, R. (1968): *On constitutive inequalities for simple materials - I*, in: J. Mech. Phys. Solids, Volume 16, 229–242.

HILL, R. (1978): *Aspects of invariance in solid mechanics*, in: Adv. Appl. Mech., Volume 18, 1–75.

HODGSON, D. E. & BROWN, J. W. (2000): *Using Nitinol Alloys*, Technical report, Shape Memory Applications, Inc., San Jose, CA, USA, 2000.

HOGER, A. (1986): *The material time derivative of logarithmic strain*, in: Int. J. Solids Structures, Volume 22, 9, 1019–1032.

HOGER, A. (1987): *The stress conjugate to logarithmic strain*, in: Int. J. Solids Structures, Volume 23, 12, 1645–1656.

HOGER, A. & CARLSON, D. E. (1984): *Determination of the stretch and rotation in the polar decomposition of the deformation gradient*, in: Q. Appl. Math., Volume 42, 113–117.

HORNBOGEN, E. (1987): *Legierungen mit Formgedächtnis - Neue Werkstoffe für die Technik der Zukunft?*, in: Metall, Volume 41, 5, 488–493.

HUANG, M., GAO, X. & BRINSON, L. C. (2000): *A multivariant micromechanical model for SMAs - Part 2. Polycrystal model*, in: Int. J. Plast., Volume 16, 1371–1390.

HUET, C. (1999): *On non-equilibrium entropy in continuum thermodynamics of materials with memory*, in: Arch. Mech., Volume 51, 2, 123–154.

HUO, Y. & MÜLLER, I. (1993): *Nonequilibrium thermodynamics of pseudoelasticity*, in: Continuum Mech. Thermodyn., Volume 5, 163–204.

INCROPERA, F. P. & DEWITT, D. P. (1996): *Fundamentals of heat and mass transfer*, 4th Edition, John Wiley & Sons 1996.

ITSKOV, M. (2002): *The derivative with respect to a tensor: some theoretical aspects and applications*, in: Z. Angew. Math. Mech., Volume 82, 8, 535–544.

KAACK, M. (2002): *Elastische Eigenschaften von NiTi-Formgedächtnis-Legierungen* 2002, Dissertation, Ruhr-Universität Bochum.

KAACK, M., YOHANNES, T., GIBKES, J., PELZL, J., HECKMANN, A., SITEPU, H., SCHMAHL, W. & TANKOVSKY, N. (2002): *Elastic bulk and surface properties of thermally and mechanically cycled NiTi shape memory alloys*, in: *Shape Memory Materials and Its Applications: Proceedings of the International Conference on Shape Memory Superelastic Technologies and Shape Memory Materials 2001, Kunming, China*, 2002, pp. 341–344.

KAHANER, D., MOLER, C., NASH, S. & MALCOLM, M. A. (1989): *Numerical Methods and Software*, Prentice Hall 1989.

KAKESHITA, T., SHIMIZU, K., NAKAMICHI, S., TANAKA, R., ENDO, S. & ONO, F. (1992): *Effect of hydrostatic pressures on thermoelastic martensitic transformations in aged TiNi and ausaged Fe-Ni-Co-Ti shape memory alloys*, in: Materials Transactions, JIM, Volume 33, 1, 1–6.

KAWAI, M., OGAWA, H. & KOGA, T. (1999): *Multiaxial constitutive modelling for R-phase and M-phase transformations of TiNi shape memory alloys*, in: Arch. Mech., Volume 51, 6, 665–692.

KESTIN, J. & RICE, J. R. (1970): *A critical review of thermodynamics*, Mono Book Corp., Baltimore 1970, Paradoxes in the application of thermodynamics to strained solids, pp. 275–298.

KHAN, A. S. & HUANG, S. (1995): *Continuum theory of plasticity*, John Wiley & Sons, Inc. 1995.

KLEIBER, M. & RANIECKI, B. (1985): *Elastic-plastic materials at finite strains*, in: SAWCZUK, A. & BIANCHI, G. (Eds.): *Plasticity Today*, Elsevier Applied Science Publishers 1985, pp. 3–46.

KLUITENBERG, G. (1962): *Thermodynamical theory of elasticity and plasticity*, in: Physica, Volume 28, 217–232.

KOISTINEN, D. P. & MARBURGER, R. E. (1959): *A general equation prescribing the extent of the austenite-martensite transformation in pure iron-carbon alloys and plain carbon steels*, in: Acta Met., Volume 7, 59–60, letters to the editor.

KOSIŃSKI, W. (1975): *Thermal waves in inelastic bodies*, in: Arch. Mech., Volume 27, 5-6, 733–748.

KRÖNER, E. (1960): *Allgemeine Kontinuumstheorie der Versetzungen und Eigenspannungen*, in: Arch. Rational Mech. Anal., Volume 4, 273–334.

KUENTZLER, R. (1992): *Electronic and lattice properties of martensitic compounds: off-stoichiometric TiNi and doped TiNi*, in: Solid State Comm., Volume 82, 12, 989–992.

LEE, E. (1969): *Elastic-plastic deformation at finite strains*, in: J. Appl. Mech., Volume 36, 1–6.

LEE, J. Y., MCINTOSH, G. C., KAISER, A. B., PARK, Y. W., KAACK, M., PELZL, J., KIM, C. K. & NAHM, K. (2001): *Thermopower behavior for the shape memory alloy NiTi*, in: J. Appl. Phys., Volume 89, 11, 6223–6227.

LEHMANN, T. (1972): *Einige Bemerkungen zu einer allgemeinen Klasse von Stoffgesetzen für große elasto-plastische Formänderungen*, in: Ing.-Arch., Volume 41, 297–310.

LEHMANN, T. (1974): *Einige Betrachtungen zur Thermodynamik großer elasto-plastischer Formänderungen*, in: Acta Mech., Volume 20, 187–207.

LEHMANN, T. (1984): *General frame for the definition of constitutive laws for large non-isothermic elastic-plastic and elastic-visco-plastic deformations*, in: LEHMANN, T. (Ed.): *Constitutive law in thermoplasticity*, Springer Verlag 1984, pp. 379–463.

LEHMANN, T. (1989a): *On dissipation connected with plastic deformations*, in: ZAMM, Volume 69, 5, 511–513.

LEHMANN, T. (1989b): *On the balance of energy and entropy at inelastic deformations of solid bodies*, in: Eur. J. Mech. A/Solids, Volume 8, 3, 235–251.

LEHMANN, T. (1989c): *Some thermodynamical considerations on inelastic deformations including damage processes*, in: Acta Mech., Volume 79, 1–24.

LEXCELLENT, C., BOUVET, C., CALLOCH, S. & VIVET, A. (2001): *A general macroscopic description of the thermomechanical behavior of SMA materials*, in: *Workshop on memory alloy materials*, Institute of Fundamental Technological Research Polish Academy of Sciences and Center of Excellence for Advanced Materials and Structures 2001.

LEXCELLENT, C., LECLERCQ, S., GABRY, B. & BOURBON, G. (2000): *The two way shape memory effect of shape memory alloys: an experimental study and a phenomenological model*, in: Int. J. Plast., Volume 16, 1155–1168.

LEXCELLENT, C., TOBUSHI, H., ZIOLKOWSKI, A. & TANAKA, K. (1994): *Thermodynamical model of reversible R-phase transformation in TiNi shape memory alloy*, in: Int. J. Pres. Ves. and Piping, Volume 58, 51–57.

LI, Z. Q. & SUN, Q. P. (2002): *The initiation and growth of macroscopic martensite band in nano-grained NiTi microtube under tension*, in: Int. J. Plast., Volume 18, 1481–1498.

LI, Z. Q. & YANG, L. (2002): *The application of the Eshelby equivalent inclusion method for unifying modulus and transformation toughening*, in: Int. J. Solids Structures, Volume 39, 5225–5240.

LIN, P. H., TOBUSHI, H., TANAKA, K., HATTORI, T. & MAKITA, M. (1994): *Pseudoelastic behaviour of TiNi shape memory alloy subjected to strain variations*, in: J. of Intell. Mater. Syst. and Struct., Volume 5, 694–701.

LUBLINER, J. (1984): *A maximum-dissipation principle in generalized plasticity*, in: Acta Mech., Volume 52, 225–237.

LUBLINER, J. & AURICCHIO, F. (1996): *Generalized plasticity and shape-memory alloys*, in: Int. J. Solids Structures, Volume 33, 7, 991–1003.

MACVEAN, D. B. (1968): *Die Elementararbeit in einem Kontinuum und die Zuordnung von Spannungs- und Verzerrungstensoren*, in: ZAMP, Volume 19, 157–185.

MAGEE, C. L. (1970): *The nucleation of martensite*, in: *Papers presented at a seminar of the American Society for Metals*, American Society for Metals, Metals Park, Ohio 1970, pp. 115–156.

MALVERN, L. E. (1969): *Introduction to the mechanics of a continuous medium*, Prentice-Hall, Inc., Englewood Cliffs, New Jersey 1969.

MARSDEN, J. E. & HUGHES, T. J. R. (1983): *Mathematical formulations of elasticity*, Dover Publications, Inc., Mineola, New York 1983.

MASUDA, A. & NOORI, M. (2002): *Optimization of hysteretic characteristics of damping devices based on pseudoelastic shape memory alloys*, in: Int. J. Non-Lin. Mech., Volume 37, 1375–1386.

MELTON, K. N. (1998): *General applications of SMA's and smart materials*, in: OTSUKA, K. & WAYMAN, C. M. (Eds.): *Shape memory materials*, Cambridge University Press 1998, pp. 220–239.

MEMRY (2003): `http://www.memry.com/tn_stent.jpg`, 3 Berkshire Boulevard.

MEYERS, A. (1996): *Zur objektiven Verzerrungsrate*, private communication, 1996.

MEYERS, A., SCHIESSE, P. & BRUHNS, O. T. (2000): *Some comments on objective rates of symmetric Eulerian tensors with application to Eulerian strain rates*, in: Acta Mech., Volume 139, 91–103.

MIEHE, C. (1988): *Zur numerischen Behandlung thermomechanischer Prozesse* 1988, Dissertation, Universität Hannover.

MIYAZAKI, S. (1998): *Medical and dental applications of shape memory alloys*, in: OTSUKA, K. & WAYMAN, C. M. (Eds.): *Shape memory materials*, Cambridge University Press 1998, pp. 267–281.

MIYAZAKI, S., IMAI, T., IGO, Y. & OTSUKA, K. (1986): *Effect of cyclic deformation on the pseudoelasticity characteristics of Ti-Ni alloys*, in: Metallurg. Trans., Volume 17A, 115–120.

MIYAZAKI, S., KIMURA, S., OTSUKA, K. & SUZUKI, Y. (1984): *The habit plane and transformation strains associated with the martensitic transformation in Ti-Ni single crystals*, in: Scr. Metall., Volume 18, 883–888.

MIYAZAKI, S. & OTSUKA, K. (1986): *Deformation and transition behavior associated with the R-phase in Ti-Ni alloys*, in: Metallurg. Trans., Volume 17A, 53–63.

MIYAZAKI, S., OTSUKA, K. & SUZUKI, Y. (1981): *Transformation pseudoelasticity and deformation behavior in a Ti-50.6at%Ni alloy*, in: Scr. Metall., Volume 15, 287–292.

MORI, T. & TANAKA, K. (1973): *Average stress in matrix and average elastic energy of materials with misfitting inclusions*, in: Acta Metall., Volume 21, 571–574.

MORRILL, B. (1972): *An Introduction to Equilibrium Thermodynamics*, Pergamon Press Inc. 1972.

MSC.MARC (2001a): *Volume A: Theory and user information*, Marc Analysis Research Corporation, 260 Sheridan Avenue, Suite 309, Palo Alto, CA 94306 USA.

MSC.MARC (2001b): *Volume B: Element library*, Marc Analysis Research Corporation, 260 Sheridan Avenue, Suite 309, Palo Alto, CA 94306 USA.

MSC.MARC (2001c): *Volume C: Program input*, Marc Analysis Research Corporation, 260 Sheridan Avenue, Suite 309, Palo Alto, CA 94306 USA.

MSC.MARC (2001d): *Volume D: User subroutines and special routines*, Marc Analysis Research Corporation, 260 Sheridan Avenue, Suite 309, Palo Alto, CA 94306 USA.

MSC.MARC (2001e): *Volume E: Demonstration problems*, Marc Analysis Research Corporation, 260 Sheridan Avenue, Suite 309, Palo Alto, CA 94306 USA.

MÜLLER, C. & BRUHNS, O. T. (2002a): *A Consistent Eulerian Rate Type Model of Polycrystalline Shape Memory Alloys Based Upon the Logarithmic Stress Rate*, in: MANG, H., RAMMERSTORFER, F. & EBERHARDSTEINER, J. (Eds.): *Proceedings of the Fifth World Congress on Computational Mechanics (WCCM V), July 7-12, 2002*, Vienna University of Technology, Austria http://wccm.tuwien.ac.at 2002.

MÜLLER, C. & BRUHNS, O. T. (2002b): *Modeling of Polycrystalline Shape Memory Alloys at Finite Strains based upon the Logarithmic Stress Rate*, in: J. Phys. IV, Volume (to appear).

MÜLLER, C. & BRUHNS, O. T. (2003): *Numerical simulation of shape memory alloys at finite strains*, in: *Proceedings of SMST 2003, Pacific Grove, USA (to appear)*, SMST 2003.

MÜLLER, I. (1989): *On the size of the hysteresis in pseudelasticity*, in: Continuum Mech. Thermodyn., Volume 1, 125–142.

MÜLLER, I. (2001): *Thermodynamics of mixtures and phase field theory*, in: Int. J. Solids Structures, Volume 38, 1105–1113.

MÜLLER, I. & XU, H. (1991): *On the pseudoelastic hysteresis*, in: Acta Metall. Mater., Volume 39, 3, 263–271.

NAGHDI, P. (1990): *A critical review of the state of finite plasticity*, in: Journal of applied mathematics and physics, Volume 41, 316–394.

NEMAT-NASSER, S. (1983): *On finite plastic flow of crystalline solids and geomaterials*, in: J. Appl. Mech., Volume 50, 1114–1126.

NEMAT-NASSER, S. (1992): *Phenomenological theories of elastoplasticity and strain localization at high strain rates*, in: Appl. Mech. Rev., Volume 45, 3, 19–45.

NICLAEYS, C., ZINEB, T. B., ARBAB-CHIRANI, S. & PATOOR, E. (2002): *Determination of the interaction energy in the martensitic state*, in: Int. J. Plast., Volume 18, 1619–1647.

OBATA, M., GOTO, Y. & MATSUURA, S. (1990): *Micromechanical consideration on the theory of elasto-plasticity at finite deformations*, in: Int. J. Engng. Sci., Volume 28, 3, 241–252.

OBERSTE-BRANDENBURG, C. (1999): *Ein Materialmodell zur Beschreibung der Austenit-Martensit Phasentransformation unter Berücksichtigung der transformationsinduzierten Plastizität* 1999, Dissertation, Ruhr-Universität Bochum.

OGDEN, R. W. (1984): *Non-linear elastic deformations*, Dover Publications, Inc. Mineola, New York 1984.

ORGÉAS, L. & FAVIER, D. (1998): *Stress-induced martensitic transformation of a NiTi alloy in isothermal shear, tension and compression*, in: Acta Mater., Volume 46, 15, 5579–5591.

ORTÍN, J. & PLANES, A. (1988): *Thermodynamic analysis of thermal measurements in thermoelastic martensitic transformations*, in: Acta Metall., Volume 36, 8, 1873–1889.

ORTÍN, J. & PLANES, A. (1989): *Thermodynamics of thermoelastic martensitic transformations*, in: Acta Metall., Volume 37, 5, 1433–1441.

OTSUKA, K., SAWAMURA, T. & SHIMIZU, K. (1971): *Crystal structure and internal defects of equiatomic TiNi martensite*, in: Phys. Stat. Sol., Volume 5, 457–470.

OTSUKA, K. & WAYMAN, C. M. (1998a): *Introduction*, in: OTSUKA, K. & WAYMAN, C. M. (Eds.): *Shape memory materials*, Cambridge University Press 1998, pp. 1–26.

OTSUKA, K. & WAYMAN, C. M. (1998b): *Mechanism of shape memory effect and superelasticity*, in: OTSUKA, K. & WAYMAN, C. M. (Eds.): *Shape memory materials*, Cambridge University Press 1998, pp. 27–48.

PASCAL, Y. & MONASEVICH, L. (1981): *Hysteresis features of the martensitic transformation of Titanium Nickelide*, in: Phys. Met. Metall., Volume 52, 5, 95–99.

PATOOR, E. (2001): *Scale transition modelling of the SMA behavior: Texture effects and microstructural evolutions*, in: *Workshop on memory alloy materials*, Institute of Fundamental Technological Research Polish Academy of Sciences and Center of Excellence for Advanced Materials and Structures 2001.

PATOOR, E., EBERHARDT, A. & BERVEILLER, M. (1988): *Thermomechanical behaviour of shape memory alloys*, in: Arch. Mech., Volume 40, 5-6, 775–794.

PATOOR, E., EBERHARDT, A. & BERVEILLER, M. (1996): *Micromechanical modelling of superelasticity in shape memory alloys*, in: Journal de Physique IV, supplément au Journal de Physique III, Volume 6, C1–277 – C1–292.

PETHÖ, A. (2000): *Constitutive modelling of shape memory alloys based on a finite strain description*, in: Periodica Polytechnica Ser. Mech. Eng., Volume 44, 1, 115–126.

PETHÖ, A. (2001): *Constitutive modelling of shape memory alloys at finite strain*, in: ZAMM · Z. Angew. Math. Mech., Volume 81, S2, 355–356.

PEYROUX, R., CHRYSOCHOOS, A., LICHT, C. & LÖBEL, M. (1998): *Thermomechanical couplings and pseudoelasticity of shape memory alloys*, in: Int. J. Engng. Sci., Volume 36, 4, 489–509.

QIDWAI, M. A. & LAGOUDAS, D. C. (2000): *On thermomechanics and transformation surfaces of polycrystalline NiTi shape memory alloy material*, in: Int. J. Plast., Volume 16, 1309–1343.

RANIECKI, B. & BRUHNS, O. T. (1991): *Thermodynamic reference model for elastic-plastic solids undergoing phase transformations*, in: Arch. Mech., Volume 43, 2-3, 343–376.

RANIECKI, B. & LEXCELLENT, C. (1994): *R_L-models of pseudoelasticity and their specification for some shape memory solids*, in: Eur. J. Mech. A/Solids, Volume 13, 1, 21–50.

RANIECKI, B. & LEXCELLENT, C. (1998): *Thermodynamics of isotropic pseudoelasticity in shape memory alloys*, in: Eur. J. Mech. A/Solids, Volume 17, 2, 185–205.

RANIECKI, B., LEXCELLENT, C. & TANAKA, K. (1992): *Thermodynamic models of pseudoelastic behaviour of shape memory alloys*, in: Arch. Mech., Volume 44, 3, 261–284.

RANIECKI, B. & TANAKA, K. (1994): *On the thermodynamic driving force for coherent phase transformations*, in: Int. J. Engng. Sci., Volume 32, 12, 1845–1858.

REBELO, N., WALKER, N. & FOADIAN, H. (2001a): *Modeling Superelastic Material Devices in a Commercial Environment*, in: SCHNACK, E., BRINSON, L. & BERVEILLER, M. (Eds.): *SMA Workshop in Karlsruhe*, Institute of Solide Mechanics, TU Karsruhe 2001.

REBELO, N., WALKER, N. & FOADIAN, H. (2001b): *Simulation of Implantable Nitinol Stents*, in: *ABAQUS Users' Conference Papers*, Hibbitt, Karlsson & Sorensen, Inc. http://www.hks.com/ 2001.

REINHARDT, W. & DUBEY, R. (1996): *Coordinate-independent representation of spins in continuum mechanics*, in: J. Elast., Volume 42, 133–144.

REINHARDT, W. D. & DUBEY, R. N. (1995): *Eulerian strain-rate as a rate of logarithmic strain*, in: Mech. Res. Comm., Volume 22, 2, 165–170.

RICE, J. R. (1971): *Inelastic constitutive relations for solids: An internal-variable theory and its application to metal plasticity*, in: J. Mech. Phys. Solids, Volume 19, 433–455.

RICHTER, H. (1952): *Zur Elastizitätstheorie endlicher Verformungen*, in: Math. Nachr., Volume 8, 65–73.

SABURI, T. (1998): *Ti-Ni shape memory alloys*, in: OTSUKA, K. & WAYMAN, C. M. (Eds.): *Shape memory materials*, Cambridge University Press 1998, pp. 49–96.

SABURI, T., YOSHIDA, M. & NENNO, S. (1984): *Deformation behavior of shape memory Ti-Ni alloy crystals*, in: Scr. Metall., Volume 18, 363–366.

SAWYERS, K. (1986): *Comments on the paper determination of the stretch and rotation in the polar decomposition of the deformation gradient by A. Hoger and D. E. Carlson*, in: Q. Appl. Math, Volume 44, 2, 309–311.

SCHMIDT, E., STEPHAN, K. & MAYINGER, F. (1984): *Technische Thermodynamik*, 11th Edition, Springer-Verlag 1984.

SEELECKE, S. (1997): *Torsional vibration of a shape memory wire*, in: Continuum Mech. Thermodyn., Volume 9, 165–173.

SEELECKE, S. (2002): *Modeling the dynamic behavior of shape memory alloys*, in: Int. J. Non-Lin. Mech., Volume 37, 1363–1374.

SHAW, J. A. (2000): *Simulations of localized thermo-mechanical behavior in a TiNi shape memory alloy*, in: Int. J. Plast., Volume 16, 541–562.

SHAW, J. A. & KYRIAKIDES, S. (1995): *Thermomechanical aspects of NiTi*, in: J. Mech. Phys. Solids, Volume 43, 8, 1243–1281.

SHAW, J. A. & KYRIAKIDES, S. (1997): *On the nucleation and propagation of phase transformation fronts in a NiTi alloy*, in: Acta Mater., Volume 45, 2, 683–700.

SIMO, J. C. & HUGHES, T. J. R. (1998): *Computational inelasticity*, in: Interdisciplinary applied mathematics, Volume 7.

SIMO, J. C. & PISTER, K. S. (1984): *Remarks on rate constitutive equations for finite deformation problems: computational implications*, in: Comput. Meths. Appl. Mech. Engrg., Volume 46, 201–215.

SIMO, J. C. & TAYLOR, R. L. (1985): *Consistent tangent operators for rate-independent elastoplasticity*, in: Comput. Methods Appl. Mech. Eng., Volume 48, 101–118.

SITTNER, P. & NOVÁK, V. (2000): *Anisotropy of martensitic transformations in modeling of shape memory alloy polycrystals*, in: Int. J. Plast., Volume 16, 1243–1268.

SNYDER, M. D. & BATHE, K.-J. (1981): *A solution procedure for thermo-elastic-plastic and creep problems*, in: Nucl. Eng. Des., Volume 64, 49–80.

STÖCKEL, D. (1987): *Formgedächtnis und Pseudoelastizität von Nickel-Titan-Legierungen*, in: Metall, Volume 41, 5, 494–500.

STÖCKEL, D. (1993): *Superelastische Nickel-Titan-Legierungen - Eigenschaften und Anwendung*, in: Metall, Volume 47, 8, 728–733.

SUN, Q. P. & HWANG, K. C. (1993): *Micromechanics modelling for the constitutive behavior of polycrystalline shape memory alloys - I. Derivation of general relations*, in: J. Mech. Phys. Solids, Volume 41, 1, 1–17.

SUN, Q. P. & LEXCELLENT, C. (1996): *On the unified micromechanics constitutive description of one-way and two-way shape memory effects*, in: Journal de Physique IV, supplément au Journal de Physique III, Volume 6, C1–367 – C1–375.

SUN, Q.-P. & LI, Z.-Q. (2002): *Phase transformation in superelastic NiTi polycrystalline micro-tubes under tension and torsion - from localization to homogeneous deformation*, in: Int. J. Solids Structures, Volume 39, 3797–3809.

SUN, Q. P., LI, Z. Q. & TSE, K. K. (2001): *On superelastic deformation of NiTi shape memory alloy micro-tubes and wires - band nucleation and propagation*, in: GABBERT, U. & TZOU, H. S. (Eds.): *IUTAM Symposium on Smart Structures and Structonic Systems*, Kluwer Academic Publishers 2001, pp. 113–120.

TANAKA, K. (1990): *A phenomenological description on thermomechanical behavior of shape memory alloys*, in: J. Pres. Ves. Technol., Volume 112, 158–163.

TANAKA, K., KOBAYASHI, S. & SATO, Y. (1986): *Thermomechanics of transformation pseudoelasticity and shape memory effect in alloys*, in: Int. J. Plast., Volume 2, 59–72.

TANAKA, K., NISHIMURA, F., HAYASHI, T., TOBUSHI, H. & LEXCELLENT, C. (1995a): *Phenomenological analysis on subloops and cyclic behaviour in shape memory alloys under mechanical and/or thermal loads*, in: Mech. Mater., Volume 19, 281–292.

TANAKA, K., NISHIMURA, F. & TOBUSHI, H. (1995b): *Transformation start lines in TiNi and Fe-based shape memory alloys after incomplete transformations induced by mechanical and/or thermal loads*, in: Mech. Mater., Volume 19, 271–280.

TANAKA, K., NISHIMURA, F., TOBUSHI, H. & LIN, P.-H. (1996): *Phenomenological analysis of plateaus on stress-strain hysteresis in TiNi shape memory alloy wires*, in: Mech. Mater., Volume 24, 19–30.

TRUESDELL, C. (1951): *A new definition of a fluid. II. The Maxwellian fluid*, in: J. de Math., Volume 30, 111–158.

TRUESDELL, C. (1959): *The rational mechanics of materials - past, present, future*, in: Appl. Mech. Rev., Volume 12, 2, 75–80.

TRUESDELL, C. & NOLL, W. (1992): *The non-linear field theories of mechanics*, 2nd Edition, Springer Verlag 1992.

TRUESDELL, C. & TOUPIN, R. A. (1960): *The classical field theories*, in: FLÜGGE, S. (Ed.): *Handbuch der Physik*, Springer-Verlag, Berlin 1960, Volume III/1.

VOGELSANG, H. (2001): *Parameteridentifikation für ein selbstkonsistentes Stoffmodell unter Berücksichtigung von Phasentransformationen* 2001, Dissertation, Ruhr-Universität Bochum.

WAYMAN, C. M. & DUERIG, T. W. (1990): *An introduction to martensite and shape memory*, Technical report, Department of Materials of Science and Engineering, University of Illinois at Urbana, 1990.

WOLLANTS, P., DE BONTE, M. & ROOS, J. R. (1979): *A thermodynamic analysis of the stress-induced martensitic transformation in a single crystal*, in: Z. Metallkde., Volume 70, 2, 113–117.

WRIGGERS, P. (1986): *Konsistente Linearisierungen in der Kontinuumsmechanik und ihre Anwendung auf die Finite-Element-Methode*, Habilitationsschrift 1986.

WURZEL, D. (2001): *Mikrostruktur und funktionelle sowie mechanische Eigenschaften von NiTi-Formgedächtnislegierungen*, Reihe 5, Fortschritt-Berichte VDI 2001, also: Bochum, Univ., Diss.

XIAO, H. (1995): *Unified explicit basis-free expressions for time rate and conjugate stress of an arbitrary Hill's strain*, in: Int. J. Solids Structures, Volume 32, 22, 3327–3340.

XIAO, H. (2002): *Hencky strain and Hencky model: Extending history and ongoing tradition*, Dedicated to my mentor, Prof. Dr.- Ing. Otto T. Bruhns, on his 60th birthday, Lehrstuhl für Technische Mechanik, Ruhr-Universität Bochum, 2002.

XIAO, H., BRUHNS, O. T. & MEYERS, A. (1996): *A new aspect in the kinematics of large deformations*, in: GUPTA, N. K. (Ed.): *Plasticity and impact mechanics*, New Age Intern Publ. Ltd., New Delhi 1996, pp. 100–109.

XIAO, H., BRUHNS, O. T. & MEYERS, A. (1997a): *Hypo-elasticity model based upon the logarithmic stress rate*, in: J. Elast., Volume 47, 51–68.

XIAO, H., BRUHNS, O. T. & MEYERS, A. (1997b): *Logarithmic strain, logarithmic spin and logarithmic rate*, in: Acta Mech., Volume 124, 89–105.

XIAO, H., BRUHNS, O. T. & MEYERS, A. (1998a): *Direct relationship between the Lagrangean logarithmic strain and the Lagrangean stretching and the Lagrangean Kirchhoff stress*, in: Mech. Res. Comm., Volume 25, 1, 59–67.

XIAO, H., BRUHNS, O. T. & MEYERS, A. (1998b): *Objective corotational rates and unified work-conjugacy relation between Eulerian and Lagrangean strain and stress measures*, in: Arch. Mech., Volume 50, 6, 1015–1045.

XIAO, H., BRUHNS, O. T. & MEYERS, A. (1998c): *On objective corotational rates and their defining spin tensors*, in: Int. J. Solids Structures, Volume 35, 30, 4001–4014.

XIAO, H., BRUHNS, O. T. & MEYERS, A. (1998d): *Strain rates and material spins*, in: J. Elast., Volume 52, 1–41.

XIAO, H., BRUHNS, O. T. & MEYERS, A. (1999a): *Existence and uniqueness of the integrable-exactly hypoelastic equation* $\overset{\circ}{\tau}{}^{*} = \lambda(trD)I + 2\mu D$ *and its significance to finite inelasticity*, in: Acta Mech., Volume 138, 31–50.

XIAO, H., BRUHNS, O. T. & MEYERS, A. (1999b): *A natural generalization of hypoelasticity and Eulerian rate type formulation of hyperelasticity*, in: J. Elast., Volume 56, 59–93.

XIAO, H., BRUHNS, O. T. & MEYERS, A. (2000a): *The choice of objective rates in finite elastoplasticity: general results on the uniqueness of the logarithmic rate*, in: Proc. R. Soc. Lond. A, Volume 456, 1865–1882.

XIAO, H., BRUHNS, O. T. & MEYERS, A. (2000b): *A consistent finite elastoplasticity theory combining additive and multiplicative decomposition of the stretching and the deformation gradient*, in: Int. J. Plast., Volume 16, 143–177.

XIAO, H. & CHEN, L.-S. (2002): *Hencky's elasticity model and linear stress-strain relations in isotropic finite hyperelasticity*, in: Acta Mech., Volume 157, 51–60.

XIAO, H. & CHEN, L.-S. (2003): *Hencky's logarithmic strain and dual stress-strain and strain-stress relations in isotropic finite hyperelasticity*, in: Int. J. Solids Structures, Volume 40, 1455–1463.

ZIEGLER, H. (1970): *Plastizität ohne Thermodynamik?*, in: ZAMP, Volume 21, 798–805.

ZIENKIEWICZ, O. & TAYLOR, R. (1987): *The finite element method - Volume 1: Basic formulation and linear problems*, 4th Edition, McGraw-Hill Book Company 1987.

ZIENKIEWICZ, O. & TAYLOR, R. (2000): *The finite element method - Volume 1: The basis*, 5th Edition, Butterworth-Heinemann 2000.

ZIÓLKOWSKI, A. (1993): *Theoretical analysis of efficiency of shape memory alloy heat engines (based on constitutive models of pseudoelasticity)*, in: Mech. Mater., Volume 16, 365–377.

ZIÓLKOWSKI, A. (2001): *Finite element modelling of SMA structures*, in: RANIECKI, B. & ZIOLKOWSKI, A. (Eds.): *Workshop on Shape Memory Alloy Materials*, Institute of Fundamental Technological Research, Polish Academy of Sciences, Warsaw 2001.

ZIÓLKOWSKI, A. & RANIECKI, B. (1996): *FEM-analysis of the one-dimensional coupled thermomechanical problem of TiNi SMA*, in: Journal de Physique IV, supplément au Journal de Physique III, Volume 6, 395–403.

ZIÓLKOWSKI, A. & RANIECKI, B. (1999): *On the macroscopic free energy potential for shape memory alloys treated as a two-phase continuum*, in: Arch. Mech., Volume 51, 6, 885–911.

Mitteilungen aus dem Institut für Mechanik

Nr. 1 Theodor Lehmann:
Große elasto-plastische Formänderungen (Dezember 1976)

Nr. 2 Bogdan Raniecki/Klaus Thermann:
Infinitesimal Thermoplasticity and Kinematics of Finite Elastic-Plastic Deformations. Basic Concepts (Juni 1978)

Nr. 3 Wolfgang Krings:
Beitrag zur Finiten Element Methode bei linearem, viskoelastischem Stoffverhalten (Januar 1976)

Nr. 4 Burkhard Lücke:
Theoretische und experimentelle Untersuchung der zyklischen elastoplastischen Blechbiegung bei endlichen Verzerrungen (Januar 1976)

Nr. 5 Knut Schwarze:
Einfluß von Querschnittsverformungen bei dünnwandigen Stäben mit stetig gekrümmter Profilmittellinie (Februar 1976)

Nr. 6 Hubert Sommer:
Ein Beitrag zur Theorie des ebenen elastischen Verzerrungszustandes bei endlichen Formänderungen (Januar 1977)

Nr. 7 H. Stumpf/F. J. Biehl:
Die Methode der orthogonalen Projektionen und ihre Anwendung zur Berechnung orthotroper Platten (März 1977)

Nr. 8 Albert Meyers:
Ein Beitrag zum optimalen Entwurf von schnellaufenden Zentrifugenschalen (April 1977)

Nr. 9 Berend Fischer:
Zur zyklischen, elastoplastischen Beanspruchung eines dickwandigen Zylinders bei endlichen Verzerrungen (April 1977)

Nr. 10 Wojciech Pietraszkiewicz:
Introduction to the Non-Linear Theory of Shells (Mai 1977)

Nr. 11 Wilfried Ullenboom:
Optimierung von Stäben unter nichtperiodischer dynamischer Belastung (Juni 1977)

Nr. 12 Jürgen Güldenpfennig:
Anwendung eines Modells der Vielkristallplastizität auf ein Problem gekoppelter elastoplastischer Wellen (Juli 1977)

Nr. 13 Pawel Rafalski:
Minimum Principles in Plasticity (März 1978)

Nr. 14 Peter Hilgers:
Der Einsatz eines Mikrorechners zur hybriden Optimierung und Schwingungsanalyse (Juli 1978)

Nr. 15 Hans-Albert Lauert:
Optimierung von Stäben unter dynamischer periodischer Beanspruchung bei Beachtung von Spannungsrestriktionen (August 1979)

Nr. 16 Martin Fritz:
Berechnung der Auflagerkräfte und der Muskelkräfte des Menschen bei ebenen Bewegungen aufgrund von kinematographischen Aufnahmen (Juli 1979)

Nr. 17 H. Stumpf/F. J. Biehl:
Approximations and Error Estimates in Eigenvalue Problems of Elastic Systems with Application to Eigenvibrations of Orthotropic Plates (Dezember 1979)

Nr. 18 Uwe Kohlberg:
Variational Principles and their Numerical Application to Geometrically Nonlinear v. Karman Plates (Juli 1979)

Nr. 19 Heinz Antes:
Über Fehler und Möglichkeiten ihrer Abschätzung bei numerischen Berechnungen von Schalentragwerken (Januar 1980)

Nr. 20 Czeslaw Wozniak:
Large Deformations of Elastic and Non-Elastic Plates, Shells and Rods (März 1980)

Nr. 21 Maria K. Duszek:
Problems of Geometrically Non-Linear Theory of Plasticity (Juni 1980)

Nr. 22 Burkhard von Bredow:
Optimierung von Stäben unter stochastischer Erregung (Dezember 1980)

Nr. 23 Jürgen Preuss:
Optimaler Entwurf von Tragwerken mit Hilfe der Mehrzielmethode (Februar 1981)

Nr. 24 Ekkehard Großmann:
Kovarianzanalyse mechanischer Zufallsschwingungen bei Darstellung der mehrfachkorrelierten Erregungen durch stochastische Differentialgleichungen (Februar 1981)

Nr. 25 Dieter Weichert:
Variational Formulation and Solution of Boundary-Value Problems in the Theory of Plasticity and Application to Plate Problems (März 1981)

Nr. 26 Wojciech Pietraszkiewicz:
On Consistent Approximations in the Geometrically Non-Linear Theory of Shells (Juni 1981)

Nr. 27 Georg Zander:
Zur Bestimmung von Verzweigungslasten dünnwandiger Kreiszylinder unter kombinierter Längs- und Torsionslast (September 1981)

Nr. 28 Pawel Rafalski:
An Alternative Approach to the Elastic-Viscoplastic Initial-Boundary Value Problem (September 1981)

Nr. 29 Heinrich Oeynhausen:
Verzweigungslasten elastoplastisch deformierter, dickwandiger Kreiszylinder unter Innendruck und Axialkraft (November 1981)

Nr. 30 F.-J. Biehl:
Zweiseitige Eingrenzung von Feldgrößen beim einseitigen Kontaktproblem (Dezember 1981)

Nr. 31 Maria K. Duszek:
Foundations of the Non-Linear Plastic Shell Theory (Juni 1982)

Nr. 32 Reinhard Piltner:
Spezielle finite Elemente mit Löchern, Ecken und Rissen unter Verwendung von analytischen Teillösungen (Juli 1982)

Nr. 33 Petrisor Mazilu:
Variationsprinzipe der Thermoplastizität
I. Wärmeausbreitung und Plastizität (Dezember 1982)

Nr. 34 Helmut Stumpf:
Unified Operator Description, Nonlinear Buckling and Post-Buckling Analysis of Thin Elastic Shells (Dezember 1982)

Nr. 35 Bernd Kaempf:
Ein Exremal-Variationsprinzip für die instationäre Wärmeleitung mit einer Anwendung auf thermoelastische Probleme unter Verwendung der finiten Elemente (März 1983)

Nr. 36 Alfred Kraft:
Zum methodischen Entwurf mechanischer Systeme im Hinblick auf optimales Schwingungsverhalten (Juli 1983)

Nr. 37 Petrisor Mazilu:
Variationsprinzipe der Thermoplastizität
II. Gekoppelte thermomechanische Prozesse (August 1983)

Nr. 38 Klaus-Detlef Mickley:
Punktweise Eingrenzung von Feldgrößen in der Elastomechanik und ihre numerische Realisierung mit Fundamental-Splinefuntionen (November 1983)

Nr. 39 Lutz-Peter Nolte:
Beitrag zur Herleitung und vergleichende Untersuchung geometrisch nichtlinearer Schalentheorien unter Berücksichtigung großer Rotationen (Dezember 1983)

Nr. 40 Ulrich Blix:
Zur Berechnung der Einschnürung von Zugstäben unter Berücksichtigung thermischer Einflüsse mit Hilfe der Finite-Element-Methode (Dezember 1983)

Nr. 41 Peter Becker:
Zur Berechnung von Schallfeldern mit Elementmethoden (Februar 1984)

Nr. 42 Dietmar Bouchard:
Entwicklung und Anwendung eines an die Diskrete-Fourier-Transformation angepaßten direkten Algorithmus zur Bestimmung der modalen Parameter linearer Schwingungssysteme (Februar 1984)

Nr. 43 Uwe Zdebel:
Theoretische und experimentelle Untersuchungen zu einem thermoplastischen Stoffgesetz (Dezember 1984)

Nr. 44 Jan Kubik:
Thermodiffusion Flows in a Solid with a Dominant Constituent (April 1985)

Nr. 45 Horst J. Klepp:
Über die Gleichgewichtslagen und Gleichgewichtsbereiche nichtlinearer autonomer Systeme (Juni 1985)

Nr. 46 J. Makowsky/L.-P. Nolte/H. Stumpf:
Finite In-Plane Deformations of Flexible Rods - Insight into Nonlinear Shell Problems (Juli 1985)

Nr. 47 Franz Karl Labisch:
Grundlagen einer Analyse mehrdeutiger Lösungen nichtlinearer Randwertprobleme der Elastostatik mit Hilfe von Variationsverfahren (August 1985)

Nr. 48 J. Chroscielewski/L.-P. Nolte:
Strategien zur Lösung nichtlinearer Probleme der Strukturmechanik und ihre modulare Aufbereitung im Konzept MESY (Oktober 1985)

Nr. 49 Karl-Heinz Bürger:
Gewichtsoptimierung rotationssymmetrischer Platten unter instationärer Erregung (Dezember 1985)

Nr. 50 Ulrich Schmid:
Zur Berechnung des plastischen Setzens von Schraubenfedern (Februar 1987)

Nr. 51 Jörg Frischbier:
Theorie der Stoßbelastung orthotroper Platten und ihr experimentelle Überprüfung am Beispiel einer unidirektional verstärkten CFK-Verbundplatte (März 1987)

Nr. 52 W. Tampczynski:
Strain history effect in cyclic plasticity (Juli 1987)

Nr. 53 Dieter Weichert:
Zum Problem geometrischer Nichtlinearitäten in der Plastizitätstheorie (Dezember 1987)

Nr. 54 Heinz Antes/Thomas Meise/Thomas Wiebe:
Wellenausbreitung in akustischen Medien
Randelement-Prozeduren im 2-D Frequenzraum und im 3-D Zeitbereich (Januar 1988)

Nr. 55 Wojciech Pietraszkiewicz:
Geometrically non-linear theories of thin elastic shells (März 1988)

Nr. 56 Jerzy Makowski/Helmut Stumpf:
Finite strain theory of rods (April 1988)

Nr. 57 Andreas Pape:
Zur Beschreibung des transienten und stationären Verfestigungsverhaltens von Stahl mit Hilfe eines nichtlinearen Grenzflächenmodells (Mai 1988)

Nr. 58 Johannes Groß-Weege:
Zum Einspielverhalten von Flächentragwerken (Juni 1988)

Nr. 59 Peihua Liu:
Optimierung von Kreisplatten unter dynamischer nicht rotationssymmetrischer Last (Juli 1988)

Nr. 60 Reinhard Schmidt:
Die Anwendung von Zustandsbeobachtern zur Schwingungsüberwachung und Schadensfrüherkennung auf mechanische Konstruktionen (August 1988)

Nr. 61 Martin Pitzer:
Vergleich einiger FE-Formulierungen auf der Basis eines inelastischen Stoffgesetzes (Juli 1988)

Nr. 62 Jerzy Makowski/Helmut Stumpf:
Geometric structure of fully nonlinear and linearized Cosserat type shell theory (Dezember 1988)

Nr. 63 O. T. Bruhns:
Große plastische Formänderungen – Bad Honnef 1988 (Januar 1989)

Nr. 64 Khanh Chau Le/Helmut Stumpf/Dieter Weichert:
Variational principles of fracture mechanics (Juli 1989)

Nr. 65 Guido Obermüller:
Ein Beitrag zur Strukturoptimierung unter stochastischen Lasten (Juni 1989)

Nr. 66 Herbert Diehl:
Ein Materialmodell zur Berechnung von Hochgeschwindigkeitsdeformationen metallischer Werkstoffe unter besonderer Berücksichtigung der Schädigung durch Scherbänder (Juni 1989)

Nr. 67 Michael Geis:
Zur Berechnung ebener, elastodynamischer Rißprobleme mit der Randelementmethode (November 1989)

Nr. 68 Günter Renker:
Zur Identifikation nichtlinearer strukturmechanischer Systeme (November 1989)

Nr. 69 Berthold Schieck:
Große elastische Dehnungen in Schalen aus hyperelastischen inkompressiblen Materialien (November 1989)

Nr. 70 Frank Szepan:
Ein elastisch-viskoplastisches Stoffgesetz zur Beschreibung großer Formänderungen unter Berücksichtigung der thermomechanischen Kopplung (Dezember 1989)

Nr. 71 Christian Scholz:
Ein Beitrag zur Gestaltsoptimierung druckbelasteter Rotationsschalen (Dezember 1989)

Nr. 72 J. Badur/H. Stumpf:
On the influence of E. and F. Cosserat on modern continuum mechanics and field theory (Dezember 1989)

Nr. 73 Werner Fornefeld:
Zur Parameteridentifikation und Berechnung von Hochgeschwindigkeitsdeformationen metallischer Werkstoffe anhand eines Kontinuums-Damage-Modells (Januar 1990)

Nr. 74 J. Saczuk/H. Stumpf:
On statical shakedown theorems for non-linear problems (April 1990)

Nr. 75 Andreas Feldmüller:
Ein thermoplastisches Stoffgesetz isotrop geschädigter Kontinua (April 1991)

Nr. 76 Ulfert Rott:
Ein neues Konzept zur Berechnung viskoplastischer Strukturen (April 1991)

Nr. 77 Thomas Heinrich Pingel:
Beitrag zur Herleitung und numerischen Realisierung eines mathematischen Modells der menschlichen Wirbelsäule (Juli 1991)

Nr. 78 O. T. Bruhns:
Große plastische Formänderungen – Bad Honnef 1991 (Dezember 1991)

Nr. 79 J. Makowski/J. Chroscielewski/H. Stumpf:
Computational Analysis of Shells Undergoing Large Elastic Deformation Part I: Theoretical Foundations

Nr. 80 J. Chroscielewski/J. Makowski/H. Stumpf:
Computational Analysis of Shells Undergoing Large Elastic Deformation Part II: Finite Element Implementation

Nr. 81 R. H. Frania/H. Waller:
Entwicklung und Anwendung spezieller finiter Elemente für Kerbspannungsprobleme im Maschinenbau (Mai 1992)

Nr. 82 B. Bischoff-Beiermann:
Zur selbstkonsistenten Berechnung von Eigenspannungen in polykristallinem Eis unter Berücksichtigung der Monokristallanisotropie (Juli 1992)

Nr. 83 J. Pohé:
Ein Beitrag zur Stoffgesetzentwicklung für polykristallines Eis (Februar 1993)

Nr. 84 U. Kikillus:
Ein Beitrag zum zyklischen Kiechverhalten von Ck 15 (Mai 1993)

Nr. 85 T. Guo:
Untersuchung des singulären Rißspitzenfeldes bei stationärem Rißwachstum in verfestigendem Material (Juni 1993)

Nr. 86 Achim Menne:
Identifikation der dynamischen Eigenschaften von hydrodynamischen Wandlern (Januar 1994)

Nr. 87 Uwe Folchert:
Identifikation der dynamischen Eigenschaften hydrodynamischer Kupplungen (Januar 1994)

Nr. 88 Jörg Körber:
Ein verallgemeinertes Finite-Element-Verfahren mit asymptotischer Stabilisierung angewendet auf viskoplastische Materialmodelle (April 1994)

Nr. 89 Peer Schieße:
Ein Beitag zur Berechnung des Deformationsverhaltens anisotrop geschädigter Kontinua unter Berücksichtigung der thermoplastischen Kopplung (April 1994)

Nr. 90 Egbert Schopphoff:
Dreidimensionale mechanische Analyse der menschlichen Wirbelsäule (Juli 1994)

Nr. 91 Christoph Beerens:
Zur Modellierung nichtlinearer Dämpfungsphänomene in der Strukturmechanik (Juli 1994)

Nr. 92 K. C. Le/H. Stumpf:
Finte elastoplasticity with microstructure (November 1994)

Nr. 93 O. T. Bruhns:
Große plastische Formänderungen – Bad Honnef 1994 (Dezember 1994)

Nr. 94 Armin Lenzen:
Untersuchung von dynamischen Systemen mit der Singulärwertzerlegung – Erfassung von Strukturveränderungen (Dezember 1994)

Nr. 95 J. Makowski/H. Stumpf:
Mechanics of Irregular Shell Structures (Dezember 1994)

Nr. 96 J. Chroscielewski/J. Makowski/H. Stumpf:
Finte Elements for Irregular Nonlinear Shells (Dezember 1994)

Nr. 97 W. Krings/A. Lenzen/u. a.:
Festschrift zum 60. Geburtstag von Heinz Waller (Februar 1995)

Nr. 98 Ralf Podleschny:
Untersuchung zum Instabilitätsverhalten scherbeanspruchter Risse (April 1995)

Nr. 99 Bernd Westerhoff:
Eine Untersuchung zum geschwindigkeitsabhängigen Verhalten von Stahl (Juli 1995)

Nr. 100 Marc Mittelbach:
Simulation des Deformations- und Schädigungsverhaltens beim Stoßversuch mit einem Kontinuums-Damage-Modell (Dezember 1995)

Nr. 101 Ulrich Hoppe:
Über grundlegende Konzepte der nichtlinearen Kontinuumsmechanik und Schalentheorie (Mai 1996)

Nr. 102 Marcus Otto:
Erweiterung des Kaustikenverfahrens zur Analyse räumlicher Spannungskonzentrationen (Juni 1996)

Nr. 103 Horst Lanzerath:
Zur Modalanalyse unter Verwendung der Randelementemethode (Juli 1996)

Nr. 104 Andreas Wichtmann:
Entwicklung eines thermodynamisch konsistenten Stoffgesetzes zur Beschreibung der Reckalterung (August 1996)

Nr. 105 Bjarne Fosså:
Ein Beitrag zur Fließflächenmessung bei vorgedehnten Stählen (Oktober 1996)

Nr. 106 Khanh Cha Le:
Kontinuumsmechanisches Modellieren von Medien mit veränderlicher Mikrostruktur (Dezember 1996)

Nr. 107 Holger Behrens:
Nichtlineare Modellierung und Identifikation hydrodynamischer Kupplungen mit allgemeinen diskreten Modellansätzen (Januar 1997)

Nr. 108 Johannes Moosheimer:
Gesteuerte Schwingungsdämpfung mit Elektrorheologischen Fluiden (Juli 1997)

Nr. 109 Dirk Klaus Anding:
Zur simultanen Bestimmung materialabhängiger Koeffizienten inelastischer Stoffgesetze (Oktober 1997)

Nr. 110 Stephan Weng:
Ein Evolutionsmodell zur mechanischen Analyse biologischer Strukturen (Dezember 1997)

Nr. 111 Michael Strassberger:
Aktive Schallreduktion durch digitale Zustandsregelung der Strukturschwingungen mit Hilfe piezo-keramischer Aktoren (Dezember 1997)

Nr. 112 Hans-Jörg Becker:
Simultation des Deformationsverhaltens polykristallinen Eises auf der Basis eines monokristallinen Stoffgesetzes (Dezember 1997)

Nr. 113 Thomas Nerzak:
Modellierung und Simulation der Ausbreitung adiabatischer Scherbänder in metallischen Werkstoffen bei Hochgeschwindigkeitsdeformationen (Dezember 1997)

Nr. 114 O. T. Bruhns:
Große plastische Formänderungen (März 1998)

Nr. 115 Jan Steinhausen:
Die Beschreibung der Dynamik von Antriebssträngen durch Black-Box-Modelle hydrodynamischer Kupplungen (August 1998)

Nr. 116 Thomas Pandorf:
Experimentelle und numerische Untersuchungen zur Kerbspitzenbeanspruchung bei schlagbelasteten Biegeproben (August 1998)

Nr. 117 Claus Oberste-Brandenburg:
Ein Materialmodell zur Beschreibung der Austenit-Martensit Phasentransformation unter Berücksichtigung der transformationsinduzierten Plastizität (Juni 1999)

Nr. 118 Michael Märtens:
Regelung mechanischer Strukturen mit Hilfe piezokeramischer Stapelaktoren (Dezember 1999)

Nr. 119 Dirk Kamarys:
Detektion von Strukturveränderungen durch neue Identifikationsverfahren in der experimentellen Modalanalyse (Dezember 1999)

Nr. 120 Wolfgang Hiese:
Gültigkeitskriterien zur Bestimmung von Scherbruchzähigkeiten (Januar 2000)

Nr. 121 Peter Jaschke:
Mathematische Modellierung des Betriebsverhaltens hydrodynamischer Kupplungen mit hybriden Modellansätzen (Februar 2000)

Nr. 122 Stefan Müller:
Zum Einsatz von semi-aktiven Aktoren zur optimalen Schwingungsreduktion in Tragwerken (Februar 2000)

Nr. 123 Dirk Eichel:
Zur Kondensation strukturdynamischer Aufgaben mit Hilfe von Polynommatrizen (Juni 2000)

Nr. 124 Andreas Bürgel:
Bruchmechanische Kennwerte beim Wechsel im Versagensverhalten dynamisch scherbeanspruchter Risse (August 2000)

Nr. 125 Daniela Lürding:
Modellierung großer Deformationen in orthotropen, hyperelastischen Schalenstrukturen (März 2001)

Nr. 126 Thorsten Quent:
Ein mikromechanisch begründetes Modell zur Beschreibung des duktilen Verhaltens metallischer Werkstoffe bei endlichen Deformationen unter Berücksichtigung von Porenschädigung (Mai 2001)

Nr. 127 Ndzi C. Bongmba:
Ein finites anisotropes Materialmodell auf der Basis der Hencky-Dehnung und der logarithmischen Rate zur Beschreibung duktiler Schädigung (Mai 2001)

Nr. 128 Henning Schütte:
Ein finites Modell für spröde Schädigung basierend auf der Ausbreitung von Mikrorissen (August 2001)

Nr. 129 Henner Vogelsang:
Parameteridentifikation für ein selbstkonsistentes Stoffmodell unter Berücksichtigung von Phasentransformationen (Dezember 2001)

Nr. 130 Jörn Mosler:
Finite Elemente mit sprungstetigen Abbildungen des Verschiebungsfeldes für numerische Analysen lokalisierter Versagenszustände (Dezember 2002)

Nr. 131 Karin Preusch:
Hierarchische Schalenmodelle für nichtlineare Kontinua mit der p-Version der Finite-Element Methode (Mai 2003)

Nr. 132 Christoph Müller:
Thermodynamic modeling of polycrystalline shape memory alloys at finite strains (August 2003)

Mitteilungen aus dem Institut für Mechanik
RUHR-UNIVERSITÄT BOCHUM
Nr. 132

978-3-935892-7-0